



University of L'Aquila
Department of Information Engineering, Computer Science and
Mathematics

PhD in Information and Communication Technologies (ICT)
Curriculum: System Engineering, Telecommunications and HW/SW platforms
XXXV Cycle

**Structural properties and privacy guarantees of
control systems over Markov wireless
communication channels**

SSD ING-INF/04

Anastasia Impicciatore

Anastasia Impicciatore

Coordinator:
Professor Vittorio Cortellessa

Handwritten signature of Vittorio Cortellessa in black ink, positioned above a horizontal line.

Tutor:
Professor Alessandro D'Innocenzo

Handwritten signature of Alessandro D'Innocenzo in black ink, positioned above a horizontal line.

Co-Tutor:
Professor Pierdomenico Pepe

Handwritten signature of Pierdomenico Pepe in black ink, positioned above a horizontal line.

A thesis submitted for the degree of

Doctor of Philosophy

L'Aquila, A.Y. 2022/2023

To my father,
I would love to pass to my children his optimism

“Success is not final, failure is not fatal: it is the
courage to continue that counts.”

Sir Winston Churchill

Acknowledgements

This thesis is the final outcome of my academic path that has been very challenging and stimulating. The work could not be accomplished without great support and contribution of many people.

First, I would like to thank Alessandro D’Innocenzo and Pierdomenico Pepe, my advisors, for giving me the opportunity to work under their supervision. I greatly appreciate their priceless suggestions and timely feedback.

I am incredibly grateful to Alessandro D’Innocenzo, for all the support, invaluable ideas and opportunities he has always provided me with.

I would like to express my deep gratitude to Pierdomenico Pepe for his constant support and also for his great intuition in investigating challenging research directions.

I would like to thank Yuriy Zacchia Lun for his contribution in supporting me across challenging research directions.

I was honored to be hosted by Profesoor George Pappas at University of Pennsylvania, in a stimulating, interesting, and fun research environment, where I had a privilege to meet some of the most remarkable researchers and DPhil students.

I am utterly grateful to Vittorio Cortellessa, coordinator of the ICT Doctoral Program at University of L’Aquila, for creating a compelling work environment, and for great availability and support in all sort of matters during these first years of our young PhD school.

As last, but certainly not least, I would like to express my deepest gratitude to my family. In particular I thank my parents Annamaria and Sauro, for their love and support in all the important moments of my life.

Declaration

I hereby declare that except where specific reference is made to the work of others, the contents of this dissertation are original and have not been submitted in whole or in part for consideration of any other degree or qualification in this, or any other university.

The results presented in this thesis have been obtained during the author's candidature under the supervision of Professor Alessandro D'Innocenzo and Professor Pierdomenico Pepe (University of L'Aquila). Some results have been obtained in collaboration with researcher Yuriy Zacchia Lun (University of L'Aquila). Finally, other results on privacy guarantees over wireless communication channels have been obtained during the visiting period at the University of Pennsylvania, Philadelphia, United states under the supervision of Professor George J. Pappas and through the collaboration with Dr. Anastasios Tsiamis.

The conference contributions are listed in the following.

- A. Impicciatore, A. D'Innocenzo, and P. Pepe, "Sufficient Lyapunov conditions for pth moment ISS of discrete-time Markovian Switching Systems", in Proceedings of the IEEE 59th Conference on Decision and Control (CDC). IEEE, Dec. 2020.
- A. Impicciatore, Y. Zacchia Lun, P. Pepe and A. D'Innocenzo, "Optimal output-feedback control and separation principle for Markov jump linear systems modeling wireless networked control scenarios", in Proceedings of the American Control Conference (ACC), May 2021.
- A. Impicciatore, M.T. Grifa, P. Pepe and A. D'Innocenzo, "Sufficient Lyapunov conditions for exponential mean square stability of discrete-time systems with markovian delays", 29th Mediterranean Conference on Control and Automation (MED), June 2021.
- A. Impicciatore, A. Tsiamis, Y. Zacchia Lun, A. D'Innocenzo, and G.J. Pappas, "Secure state estimation over Markov wireless communication channels", in Proceedings of the IEEE 61st Conference on Decision and Control (CDC). IEEE, Dec. 2022.

The journal contributions are listed in the following.

- A. Impicciatore, P. Pepe, A. D’Innocenzo, "Lyapunov Characterizations of Exponential Mean Square Input-to-State Stability for Discrete-Time Markovian Switching Nonlinear Systems", IEEE Transactions on Automatic Control, Full Paper. Early Access, Article DOI: 10.1109/TAC.2022.3211777, August 2023.
- A. Impicciatore, Y. Zacchia Lun, P. Pepe, A. D’Innocenzo, "Optimal output-feedback control over Markov wireless communication channels", IEEE Transactions on Automatic Control. Conditionally Accepted as Full Paper.

Anastasia Impicciatore

Abstract

The aim of this thesis is presenting the structural properties and privacy guarantees of control systems connected via wireless communication channels, that are modeled through the finite-state Markov channel abstraction. Spatially distributed systems connected via wireless medium, also known as wireless control networks, are here investigated. The aforementioned structural properties are properly exploited to develop a stability analysis specific for wireless control network scenarios.

As explained in the following chapters, there is a wide literature focusing on stability analysis, structural properties, and privacy guarantees of wireless control networks. Most of these works adopt Bernoulli random variables to model packet loss occurrences over wireless channels.

However, this strategy does not allow to model the occurrence of bursts of packet losses, as Markov chain theory does. The improvement with respect to the previous works is modeling the wireless channel as finite-state Markov channel, that allows for modeling the occurrence of bursts of packet losses, as well as the current mode of the channel. As a consequence of the Markovian characterization of the wireless channel, Markov jump system theory provides good mathematical approximations of wireless control network scenarios.

The contribution achieved by the research presented in this thesis is threefold. Firstly, this work investigates wireless control network scenarios with double sided packet-loss links modeled via finite-state Markov channels. Under the assumption of a TCP-like communication scheme and the mathematical framework of Markov jump linear systems, the separation principle holds also in this case with finite-state Markov channels. Secondly, the research here reported provides conditions guaranteeing secrecy against eavesdropping over finite-state Markov wireless links. Finally, the case of nonlinear discrete-time Markov jump systems is investigated with the aim of the generalization of Markov jump linear system framework, so that nonlinear plants may be involved in wireless control network analysis. Proper stability notions and Lyapunov conditions are presented for nonlinear discrete-time Markov jump systems in the case without any delay, as well as in the case of nonlinear discrete-time systems with Markovian delays.

Keywords: Markov Jump Systems, Lyapunov theorems, Wireless control networks,
Finite-state Markov channels

Contents

List of Figures	iv
1 Introduction	1
1.1 Chapter outline	2
1.2 Wireless control network: modeling strategies and significant challenges	2
1.2.1 Markov jump linear system theory applied to double-sided packet loss scenarios	4
1.2.2 The separation principle over finite-state Markov channels	6
1.2.3 Privacy guarantees against eavesdropping	7
1.2.4 Markovian switching nonlinear systems	8
1.2.5 Stability notions	9
1.2.6 Markovian delays	11
1.3 Main contributions	12
1.3.1 The output-feedback control over finite-state Markov channels: the separation principle	14
1.3.2 Privacy guarantees over finite-state Markov channels	17
1.3.3 Lyapunov characterizations for discrete-time Markov jump systems	18
1.3.4 Lyapunov conditions for discrete-time nonlinear systems subject to Markovian delays	19
1.4 Notation and mathematical background	20
1.5 Thesis organization	21
1.6 List of acronyms	22
2 Wireless control networks over finite-state Markov Channels: the separation principle	24
2.1 Chapter outline	25
2.2 Problem formulation	27
2.2.1 The wireless control network architecture	27
2.2.1.1 Communication between plant and controller: sensing link and actuation link	27

2.2.1.2	The discrete-time equivalent system	28
2.3	Bernoulli wireless channel model and its limitations	29
2.4	The finite-state Markov channel	30
2.4.1	Finite-state Markov channel historical background	30
2.4.2	Wireless link	33
2.5	The information set	37
2.6	Wireless control network model	40
2.6.1	Assumptions on wireless control network model	41
2.7	Output-feedback controller	42
2.7.1	Control synthesis based on next-step predictor	42
2.7.2	Output-feedback controller with current estimator	42
2.7.3	The Linear Quadratic Regulator	43
2.8	Estimation techniques	44
2.8.1	The Markovian next-step predictor	45
2.8.2	The Markovian current estimator	46
2.8.3	Computational complexity	47
2.9	Observer stability analysis	48
2.9.1	The operators	48
2.9.2	Next-step predictor stability analysis	50
2.9.3	Current estimator stability analysis	51
2.9.4	The next-step predictor filtering coupled algebraic Riccati equations	53
2.9.5	The current estimator filtering coupled algebraic Riccati equations	55
2.10	The separation principle	57
2.10.1	The next-step predictor separation principle	57
2.10.2	The current estimator separation principle	58
2.11	Mode-independent output-feedback	60
2.12	Numerical case study	64
2.12.1	The inverted pendulum on a cart	64
2.12.2	Detectability analysis	65
2.12.3	Stabilizability analysis	71
2.12.4	Performance analysis and comparison	73

3 Privacy guarantees	76
3.1 Chapter outline	77
3.2 Problem formulation	77
3.2.1 Secrecy mechanism	79
3.2.2 Wireless link	79
3.2.3 Probabilistic framework	82
3.3 Optimal mean square expected secrecy	83
3.4 Main result	86
3.5 Eavesdropper characterization	87
3.6 Example	88
3.6.1 Finite-state Markov channel scenario	89
4 On discrete-time Markovian switching nonlinear systems	93
4.1 Chapter outline	94
4.2 The probabilistic space	95
4.3 Problem Formulation	97
4.4 Exponential mean square stability characterization	100
4.5 Exponential mean square ISS characterization	101
4.6 The p th moment ISS	103
4.7 Sufficient conditions for p th moment ISS	104
4.8 Illustrative examples	105
4.8.1 Example 2	106
4.8.2 Application to wireless control network scenarios	110
4.8.2.1 Example 3	111
4.8.2.2 Example 4	115
4.8.3 Statistical results	121
5 Discrete-time systems with Markovian delays	126
5.1 Chapter outline	127
5.2 Notation and basic definitions	128
5.3 Problem formulation	128
5.4 Main result	132
5.5 Example	133
5.5.1 Statistical results	137
6 Conclusions	140
References	219

List of Figures

2.1	Wireless control network architecture.	27
2.2	FSMC model for sensing link: the Markov chain η_k represents the evolution of the channel, while successful packet delivery and PER come from $\hat{\gamma}_m, m \in \mathbb{S}_\eta$.	36
2.3	FSMC model for actuation link: the Markov chain θ_k represents the evolution of the channel, while successful packet delivery and PER come from $\hat{\nu}_i, i \in \mathbb{S}_\theta$.	37
2.4	Information flow timing between the plant and the controller used for the next-step predictor (a) and the current estimator (b).	38
2.5	Inverted pendulum on a cart	64
2.6	Closed-loop mean square state trajectories in configuration (i) • blue obtained with the Markovian next-step predictor; • red obtained with the Markovian current estimator; • dashed blue obtained with the Bernoullian next-step predictor; • dashed red obtained with the Bernoullian current estimator.	67
2.7	Closed-loop mean square state trajectories in configuration (ii) • blue obtained with the Markovian next-step predictor; • red obtained with the Markovian current estimator; • dashed blue obtained with the Bernoullian next-step predictor; • dashed red obtained with the Bernoullian current estimator.	69
2.8	Closed-loop average state trajectories in configuration (ii) • blue obtained with the Markovian next-step predictor; • red obtained with the Markovian current estimator; • dashed blue obtained with the Bernoullian next-step predictor; • dashed red obtained with the Bernoullian current estimator.	70
2.9	The charts report: • estimation error on cart position obtained by Monte Carlo simulations in yellow; • the average error trajectory in red; • the maximum error trajectory in blue; • the minimum error trajectory in green, concerning the next-step predictor (a) and the current estimator (b). The top right of each panel reports a zoom in for each plot.	73

2.10	Mean square state trajectories in closed-loop in • blue obtained with the Markovian next-step predictor; • red obtained with the Markovian current estimator; • dashed blue obtained with the Bernoullian next-step predictor; • dashed red obtained with the Bernoullian current estimator.	75
3.1	Remote estimation architecture.	78
3.2	User MSE obtained with FSMC model resulting from user parameters $d_u = 17$ m, $\bar{d}_u = 15$ m, and with secrecy parameter $\lambda = 1$	90
3.3	Error trajectories on cart's position obtained with $\lambda = 0.3$. • The figure at the top shows error trajectories on cart's position for the user in blue. • The figure at the bottom shows error trajectories on cart's position for the eavesdropper in red.	91
3.4	The figure reports the MSE on cart's position for the user (blue line) and for the eavesdropper (red line) with $\lambda = 0.3$	92
3.5	The figure reports the MSE on cart's position for the user (blue line) and for the eavesdropper (red line) with $\lambda = 1$	92
4.1	State diagram of the Markov chain considered in Example 1.	96
4.2	State diagram of the Markov chain $r(k)$ in Example 2.	107
4.3	Block diagram showing a wireless control network architecture.	110
4.4	State diagram of the Markov chain $r(k)$ modeling the wireless channel in Example 3: p is the probability of having two consecutive correct packet deliveries, while q is the probability of having two consecutive packet losses.	111
4.5	Traces obtained in Example 2 with $p = 0.98$, $q_1 = q_2 = 0.039$	122
4.6	Traces obtained in Example 3 with $p = 0.43$, $q = 0.099$	122
4.7	Pairs $(1 - p, q)$: EMS-ISS holds in Example 2, with $q_1 = q_2 = q$	123
4.8	Pairs $(1 - p, q)$: EMS-ISS holds in Example 3.	123
4.9	Traces of system state obtained in Case 1 and in Case 2, respectively.	124
4.10	Traces of 90th percentile obtained in CASE 1 and in CASE 2, respectively.	125
5.1	The Figure depicts the state diagram of the Markov chain $\eta(k)$ modeling the switching delay: p stands for the probability of having a delay $d(k + 1) = 0$, provided that the previous delay is $d(k) = 0$, while q stands for the probability of having a delay $d(k + 1) = 2$, provided that the previous delay is $d(k) = 2$	134
5.2	Traces of system state obtained with $\gamma = 1.2$, $p = 0.992$, and $q = 0.007$	138

5.3	The figure shows the region of couples $(p, q) \in (0, 1) \times (0, 1)$ such that conditions of Theorem 10 are satisfied with $\gamma = 1$.	139
5.4	The figure shows the region of couples $(p, q) \in (0, 1) \times (0, 1)$ such that conditions of Theorem 10 are satisfied with $\gamma = 1.1$.	139
5.5	The figure shows the regions of couples $(p, q) \in (0, 1) \times (0, 1)$ such that conditions of Theorem 10 are satisfied with $\gamma = 1.2$.	139

1

Introduction

Contents

1.1 Chapter outline	2
1.2 Wireless control network: modeling strategies and significant challenges	2
1.2.1 Markov jump linear system theory applied to double-sided packet loss scenarios	4
1.2.2 The separation principle over finite-state Markov channels	6
1.2.3 Privacy guarantees against eavesdropping	7
1.2.4 Markovian switching nonlinear systems	8
1.2.5 Stability notions	9
1.2.6 Markovian delays	11
1.3 Main contributions	12
1.3.1 The output-feedback control over finite-state Markov channels: the separation principle	14
1.3.2 Privacy guarantees over finite-state Markov channels	17
1.3.3 Lyapunov characterizations for discrete-time Markov jump systems	18
1.3.4 Lyapunov conditions for discrete-time nonlinear systems subject to Markovian delays	19
1.4 Notation and mathematical background	20
1.5 Thesis organization	21
1.6 List of acronyms	22

This thesis illustrates the results obtained during the development of author's

PhD project at University of L'Aquila under the supervision of Professor Alessandro D'Innocenzo and Professor Pierdomenico Pepe.

This chapter starts with an introduction of the scenario investigated in this thesis that concerns wireless control networks.

A brief description of the main features of wireless control networks is here reported. The following sections present an overview of the main challenges and contributions addressed by the PhD project here illustrated.

1.1 Chapter outline

This chapter is organized in two main parts.

- The first part of the chapter illustrates the main topic of this thesis, that is, the study of the impact of the Markov modeling [1] on structural properties and privacy guarantees for wireless control networks [2].

This topic is the motivation that links all the following chapters. The impact of the Markov modeling on wireless control network properties can be analyzed by exploiting Markovian switching systems [3], also known as Markov jump systems (see [4] for the linear case): the most important challenges are presented in Section 1.2.

- The second part of this first chapter illustrates the contributions achieved during this research work on the two modeling classes: Markov jump linear systems [4] and Markov jump nonlinear systems [3]. The main contributions are described in Section 1.3.

Moreover, Section 1.4 introduces notation and mathematical background, Section 1.5 illustrates the thesis organization to the reader, and finally, Section 1.6 provides a list of acronyms.

1.2 Wireless control network: modeling strategies and significant challenges

Wireless control networks [2,5] consist of spatially distributed [6] components such as computational units, actuators, and sensors [7] connected via wireless communication

links [8]: in this scenario the closed-loop control is provided over wireless links [9]. Wireless control networks have a large variety of application fields, such as industrial automation [10–14], building management [15], automotive, intelligent transportation [16], avionics and smart grids [17], receiving considerable attention from industry and academia [2, 18–21]. Moreover, they offer many advantages such as the ease of installation and maintenance, large flexibility, and increased safety [22].

Conventional control system design [23] relies on the assumption of instantaneous delivery of sensor measurements and control inputs with high reliabilities. The usage of wireless channels in the transmission of information [24] causes delays, packet losses and message error probabilities [2, 25]. For this reason, the significant challenges in control over wireless communication channels [26, 27] lie within the time-varying, unreliable [28] and shared nature [29] of this communication medium.

The presence and motion of people and objects in the propagation environment induces the shadow and small-scale fading that, paired with interference from other transmitters, causes information loss leading to performance and stability degradation [30–33]. Furthermore, due to the shared nature of the wireless medium, other agents in the vicinity can overhear the content of transmissions, and there is often a need to protect systems from eavesdroppers [34], [35]. This scenario leads for instance to privacy problems [36–41].

In wireless control system literature problems related to the packet loss occurrences [42–45] have been widely investigated and discussed. The packet dropouts have been modeled either as deterministic (in terms of time averages or worst case bounds on the number of consecutive packet losses, see, e.g., [25, 26, 46, 47]) or stochastic phenomena.

In the stochastic framework, many works in the literature assume memoryless packet drops, and thus dropouts are realizations of a Bernoulli process (see [24, 48–51]). Other works consider more general correlated (bursty) packet losses and use a transition probability matrix of a finite-state stationary Markov chain (see, e.g., [52–54] and references therein) to describe the stochastic process governing packet dropouts (see [52, 55]). In these works, wireless control networks with missing packets are modeled via time-homogeneous Markov jump linear systems [4, 56–60]. However, a simple Markov chain model for packet losses on wireless channels used in wireless control networks literature is not exhaustive since the occurrence of packet losses also depends on the operational mode of the communication channel [1], this dependence is well captured by

the mathematical abstraction provided by the finite-state stationary Markov channel model [1]. This thesis focuses on the finite-state Markov channel modeling framework.

The finite-state stationary Markov channel model approximates the channel mode transitions through a Markov chain and incorporates a specific packet error distribution information into each mode [1]. The finite-state Markov channel [1] is an essential model because wireless communication system designers traditionally use this mathematical abstraction of the wireless channel for modeling error bursts in fading channels to analyze and improve performance measures in the physical or media access control layers.

Moreover, several receivers' channel state estimation [61] and decoding algorithms rely upon finite-state Markov channel models [1].

Bursts of packet losses cannot be modeled by Bernoulli processes, which is the main limit of the control strategies based on Bernoulli channel [48]. Indeed, the Bernoullian model is less accurate than the finite-state Markov channel model, and thus bursts of packet losses may cause unstable behavior without the possibility of recovery, as illustrated in Chapter 2.

Works such as the one by *Lun et al.* [62] illustrate how the adoption of the finite-state Markov channel model [1] in the design of wireless control networks impacts the control performance in a positive way. This modeling strategy of the wireless channel provides a consistent improvement [62] in stabilizing control synthesis. This is the reason why the research work adopts the finite-state Markov channel, for the control design strategy that accounts for bursts of packet losses occurrence, as well as the current state of the wireless communication channel. See Chapter 2 for more details.

As the reader will observe in the following, the most important challenges concerning wireless control networks related to wireless connectivity can be grouped considering the two main features of the wireless communication medium:

- the unreliability [2] (addressed by Chapter 2),
- the shared nature of the wireless medium [40] (addressed by Chapter 3).

1.2.1 Markov jump linear system theory applied to double-sided packet loss scenarios

Markov jump linear system theory has been frequently used in literature [63–65] to model the challenges in analysis and design of wireless control networks [66, 67].

Specifically, Markov jump linear systems are linear switching systems [68–73] where the switching rule is a Markov chain exploited for wireless link modeling [1, 8, 74].

This thesis exploits Markov jump linear system theory [4] to model and analyze the impact of finite-state Markov channel modeling [1] of double-sided packet loss links in wireless control network scenarios [48].

Double-sided packet losses have been already investigated for instance in [25, 47], with arbitrary packet loss process [25], or Markovian [47]. These works summarize the packet losses on both links.

Let us consider a wireless control network scenario where the plant and the controller are connected via wireless links [48]: the link concerning the communication from the controller to the actuators and the link concerning the communication from the sensor to the controller. Let us call actuation link the link concerning the communication from the controller to the actuators. Let us call sensing link the link concerning the communication from the sensor to the controller.

The significant difficulty of the setting presented in this thesis arises from a combined effect of two link packet losses possibly resulting in long periods in which the controller and actuator cannot simultaneously receive new data (see also Remark 1 in Chapter 2). However, a simple Markov chain model for packet losses on wireless channels [2] used in wireless control networks literature is not exhaustive since the occurrence of packet losses also depends on the operational mode of the communication channel [1] (obtained via channel state estimation [61]). Thus, the channel model exploited in this PhD thesis is the finite-state Markov channel [1].

Consequently, the existing stabilizability and detectability notions [48, 49, 75] are not suitable for the general finite-state Markov channel scenario, as illustrated in the following chapters.

This research work overcomes this limitation by addressing the output-feedback control problem [76] over finite-state Markov channels and characterizing novel stabilizability and detectability conditions [77]. The investigated wireless control network infrastructure relies on a TCP-like architecture [48], implying that the communication between the controller and the actuators is characterized by acknowledgement messages.

Messages of acknowledgement are crucial messages for this research setting: without them the separation [48] between estimation and control is impossible even in Bernoullian setting.

Concerning the actuation link, the controller is the transmitter: specifically, the transmitter is not able to know the outcome of the transmission before sending the message [78]. This is the reason why the controller receives the acknowledgement message only after a time-step delay [48, 79], while this delay does not affect the sensing link.

In modern communication systems the channel state estimation [61] is always performed through the receiver. Therefore, on the sensing link, the controller (i.e., the receiver) is able to know the outcome of the transmission and the mode of the channel without delay.

1.2.2 The separation principle over finite-state Markov channels

As highlighted in the previous paragraph, in contrast to traditional control and estimation problems, wireless control networks are unreliable [24, 50]: this means that the observation and control packets may be lost or delayed due to the wireless transmission features [76]. Thus, the underlying communication network with double-sided packet losses is modeled stochastically [80] by assigning probabilities to the successful transmission of packets [43, 44, 49]. One of the challenges addressed by this PhD thesis is the separation principle for estimation and control problems in wireless control networks over finite-state Markov channels. This challenge aims at the generalization of the results in [48]. In traditional control theory there is a large amount of works investigating the separation principle [81].

As it is well known, in traditional control schemes [23], the separation principle is guaranteed by structural properties, i.e., stabilizability and detectability [75].

Many works in the field of control theory investigate problems of estimation and control over wireless lossy networks [43–46, 48, 49].

There are important research lines (such as the one that has led to the work titled “*Foundations of Control and Estimation Over Lossy Networks*”, by Schenato et al. [48]) that investigate the separation principle in wireless control network architectures with double-sided packet losses. The aforementioned paper by Schenato et al. provides the proof of the separation principle for wireless transmissions with TCP-like protocols. Moreover, the same work shows that when considering UDP-like protocols separation cannot hold. Specifically, in [48, Theorem 5.6], the separation principle is guaranteed by the structural properties of stabilizability and detectability, that are exploited in

the analyzed scenario considering the Bernoulli probabilities of packet losses over the sensing link and the actuation link [48, Lemma 5.4, Theorem 5.5].

This manuscript addresses the analysis of a TCP-like remote control architecture (that is analogous to the one in [48]) with a more accurate channel model for the wireless link, i.e., the finite-state Markov channel model [1].

As deeply explained in the following chapters (see Chapter [2]), the problem of the separation principle over finite-state Markov channels is here investigated by exploiting the notions of mean square detectability and mean square stabilizability [4], i.e., structural properties in the mean square sense.

The mean square stabilizability with delay, introduced in the work by Lun *et al.* [79], accounts for the one time-step delay due to the presence of acknowledgement messages (see Chapter [2] for more details).

Mean square detectability and mean square stabilizability with delay (presented in Chapter [2] for the considered wireless control network scenario) report formally the classical structural properties in control theory (stabilizability and detectability [75]) in the finite-state Markov channel framework, providing the basis for development of solid conditions guaranteeing the separation principle over finite-state Markov channels [77].

1.2.3 Privacy guarantees against eavesdropping

The previous sections focus on the unreliable nature of the wireless medium (mentioned above), that may cause packet losses and other non ideal behaviors in wireless control networks. Another important feature of the wireless channel is the shared nature of the wireless medium [82], that makes other agents in the vicinity able to overhear the content of transmissions [83]. This risk has an impact on the privacy of the transmission [84].

Consequently, this problem leads to the necessity of protecting system data from eavesdroppers [34, 35], for instance by adopting encryption-based tools [40] or physical-layer security methods [85], and control-theoretic approaches [37, 39, 86].

The privacy scenario [37, 38] here investigated concerns a wireless estimation problem [49] over a finite-state Markov channel [1].

This research line focuses on state estimation [49] in wireless control networks with secrecy against eavesdropping [38].

Specifically, in the remote architecture scenario here considered [87], a sensor transmits a system state information to the estimator over a legitimate user link, and an eavesdropper overhears these data over its link independent on the user link. Each

connection may be affected by packet losses and is modeled by the finite-state Markov channel that has been briefly introduced before [1].

The part of the PhD thesis concerning privacy guarantees moves from the paper titled “*State Estimation with Secrecy against Eavesdroppers*”, by Tsiamis et al. [38]: the secrecy mechanism and the remote architecture here illustrated are the same as the ones in [38].

Certainly, problems concerning estimation techniques [88,89] and privacy guarantees [34] over wireless channels have been already addressed in literature.

However, the wireless link [8] has been modeled either exploiting the Bernoulli processes [48], or exploiting two-mode Markov chains [34].

As explained in Section 1.3.2 and also in Chapter 3, a significant difference with respect to the previous literature is the development of privacy guarantees over finite-state Markov channels [87] (which is an improvement with respect to Bernoulli processes and the two-mode Markov chains).

1.2.4 Markovian switching nonlinear systems

The challenges presented above are typically addressed by adopting a linear modeling strategy [4], that is widely used in wireless control network literature [2].

Markov jump linear systems [4,90] provide very good approximations for wireless control networks [77,91,92] as long as the plant to control can be modeled as a linear system.

However, when the dynamics are nonlinear, the general mathematical model with nonlinear functions is needed [81,93-96].

The main modeling strategies and mathematical tools exploited to analyze wireless control networks [2] and their structural properties can be grouped as follows:

- the discrete-time Markov jump linear systems [4,90] (investigated in Chapter 2 and Chapter 3),
- the discrete-time Markovian switching nonlinear systems [3] (investigated in Chapter 4 and Chapter 5).

This section introduces the discussion on discrete-time Markovian switching systems, where the function can also be nonlinear [3], so that this class of systems is able to provide a good approximation for wireless control networks with nonlinear plants [97].

Discrete-time Markovian switching systems, also known as *Markov jump systems* [4, 67, 98], are particularly useful for modeling systems subject to abrupt changes [99], such as wireless control networks, that may suffer from packet losses [49].

Markovian switching nonlinear systems [3, 100] are good approximations of wireless control networks when the plant is characterized by nonlinear dynamics [94].

This thesis investigates the class of discrete-time Markov jump linear systems, as well as the general class of discrete-time Markovian switching nonlinear systems. Particularly, the investigations concerning the stability properties [101, 102] focus on exponential mean square stability [3] and exponential mean square input-to-state stability [97], that are stability notions involving the second moment of the state [3, 4].

1.2.5 Stability notions

The investigations on the formal guarantees for stability properties of wireless control networks [2, 72, 80] play a key role in this thesis.

The classical stability notions traditionally used in control theory [81] are not suitable for a wireless control network scenario modeled through a stochastic framework [80], as the one studied in this work.

Thus, the main challenge concerning stability notions addressed by this work is the construction of a suitable mathematical setting [3, 4, 97] providing the best mathematical approximation of the considered wireless control network scenario for the formal description of the stability problems [48].

The stability notions here investigated are the mean square sense stability notions [4].

Stability notions in the mean square sense are the most suitable ones because they involve the stochastic features existing in the stochastic mathematical environment describing the wireless channel [1, 74]. Specifically, this thesis deals with mean square stability and mean square input-to-state stability [103–105] notions [3, 4].

Mean square stability (i.e., a stability notion in the mean square sense) of discrete-time Markovian switching systems has been extensively analysed in the linear case [4], but there are also some works such as [3] investigating this stability notion in the nonlinear framework.

The input-to-state stability [106, 107] property has been widely investigated in the literature [108–111]: the corresponding notion was originally proposed by Sontag for continuous-time nonlinear systems (see for instance [105, 112–118]). Intuitively, when a system is input-to-state stable, every state trajectory corresponding to a bounded

control remains bounded and tends to the equilibrium when inputs tend to zero.

In the last decades, a great effort has been spent studying some variants of the original notion and related applications [103, 111, 119–127]. In [128], a network of integral input-to-state stable [109, 110] retarded systems is considered and a small-gain methodology for constructing a Lyapunov-Krasovskii functional of such a network is developed. Following the same research line, [129] and [130] present input-to-state stability and integral input-to-state stable feedback control design strategies facing actuators disturbances. Relevant works expressing the significance of exponential input-to-state stability property are [131, 132].

Together with the increasing attention given to switching nonlinear systems, particularly in the last decades, Lyapunov characterizations of stability and input-to-state stability for this kind of systems has played an important role: the reader can refer to [133–136]. The methodology presented in [137] for the discrete-time case is based on the one provided by [133, 134] for the continuous-time case. A converse Lyapunov result for the global asymptotic stability is established in [137] for discrete-time switching systems. However, the procedure presented there is developed for an arbitrary switching framework and it is based on common Lyapunov functions, while the approach provided in this manuscript (particularly in Chapter 4) concerns the use of multiple Lyapunov functions [136] in the Markovian switching domain [3], where the switching rule is a Markov chain [138]. More details on the aforementioned approach are provided in Chapter 4.

The deterministic counterpart of the considered stochastic mathematical scenario is provided by [136], where discrete-time switching nonlinear systems [68], whose switching rule is constrained by a digraph, are investigated.

With respect to [136, 139, 140], this research focuses on the scenario in which the state of the system is a random variable [141], and therefore, the main interest of this investigation is the behavior of its second moment [4, 141], i.e., the mean square. Consequently, the considered stability notions [4] (i.e., the mean square stability, the exponential mean square stability [3], the mean square input-to-state stability, and the exponential mean square input-to-state stability [97, 142]) are different with respect to the ones considered by *Pepe* in [136, 140] and by *Goebel* in [139].

As far as the Markovian switching domain is concerned, the notions of p th moment stability and p th moment input-to-state stability are investigated in [143] and [144], respectively. In [144] continuous-time stochastic retarded systems are analysed and a

Razumikhin-type theorem is developed for p th moment input-to-state stability. The Razumikhin stability approach is also exploited in [124], where some novel criteria for p th moment input-to-state stability and integral input-to-state stability are derived, considering impulsive stochastic functional differential equations.

In the discrete-time framework, impulsive stochastic delay systems are studied in [125], where p th moment exponential input-to-state stability is investigated. Works concerning discrete-time Markovian switching nonlinear systems are [3] and [145]. In particular, in [145] a complete proof of the Markov property of the state of a class of discrete-time hybrid systems is given, and a mean square stability analysis is carried out in [3].

This research line moves from the work titled “*Stochastic model predictive control for constrained discrete-time Markovian switching systems*” [3], that provides a mean square stability analysis for discrete-time nonlinear Markovian switching systems.

This thesis provides a novel input-to-state stability analysis in the mean square sense for discrete-time nonlinear Markovian switching systems [97, 142].

1.2.6 Markovian delays

Time-delays [33, 46, 146] often lead to complex behaviors in the dynamics of wireless control networks [2] and may lead to the failure of stability [76].

Discrete-time systems subject to Markovian delays provide a good mathematical approximation of wireless control networks with random delays [147] modeled by Markov chains [148].

This part of the research work investigates bounded variations of Markovian delays (see [148] and the references therein).

These problems can be mathematically formalized by studying discrete-time systems [149, 150] with Markovian delays [148]. Discrete time-delay systems [151–155] have received renewed attention in recent years because of their important applications in engineering fields (see for instance [151, 153, 156–160]).

In recent years, the graph theory [161, 162] approach has been satisfactorily used in the development of stability theory for discrete-time switching systems with constrained switching signals (see [136, 163–168] and the references therein). Constraints on time-delays can be described by means of the delay digraphs notion (see [160, 169]) as a natural counterpart for time-delay systems of the switches digraphs approach for switching systems. See also [169, 170] for motivations of modeling the constraints

through a digraph, and for the impact of this choice in establishing the stability results. Constraints provided by bounded delay variations are studied in [148, 171, 172].

In [172] the problem of disturbance rejection control for Markovian jump linear systems is investigated, while [148] presents the regulation problem for discrete-time linear systems with bounded unknown random state delay. In [171], the constraints due to bounded delay variations can be described by a delay digraph as well.

The modeling framework for systems subject to Markovian switching is given by discrete-time Markovian switching systems, also known as *Markov jump systems* [3, 4]. There is a wide literature investigating this class of systems. Indeed, they are particularly useful in the modeling of systems subject to abrupt changes, such as wireless control networks [2].

This is because, the wireless channel may suffer from packet-losses that are the cause of abrupt changes and delays (see [4, 67, 98, 99]). There are two main reasons why Markovian switching systems are good approximations of wireless control networks that have been widely illustrated in Section 1.2 and are briefly recalled in the following.

- Markov chains allow to model bursts of packet losses, which is not possible using Bernoulli random variables (see [1] and the references therein).
- The Markov modelling of the wireless channel [1, 66, 79] in analysis and co-design of wireless control networks [54, 62, 66, 79] allows performance improvement in stabilizing control synthesis [62].

Given the arguments presented above, the aim of this part of PhD project is studying the discrete-time delay systems with Markovian delays. Thus, this part of the work focuses on stability notions concerning the second moment of the state [141] of the system, that is the exponential mean square stability [4].

1.3 Main contributions

The most significant contributions of this thesis can be found along the main research lines of the PhD project introduced in the previous paragraphs of this Chapter.

The reader can find here a list containing the main contributions achieved by the research work addressed by this thesis.

- (i) The main contributions concerning the separation principle over finite-state Markov channels [77, 92] (introduced with more details in Section 1.3.1) can be summarized as follows.

- The communication timing (between plant and controller in the wireless control network scenario) are explicitly considered, as well as computation and transmission delays. This leads to two different estimation strategies. The first estimation strategy proposed will be called next-step predictor, the second one will be called current estimator. Each estimation strategy will be presented with its feasibility conditions in Chapter 2.
 - The separation principle validity is proved for both the considered estimators in the general finite-state Markov channel setting.
 - Four different detectability notions (presented from the weakest to the strongest one) are introduced in Chapter 2 with the aim of providing a suitable theoretical basis for the formal description of the filtering problems. The aforementioned detectability notions are instrumental for the guarantees of the separation principle in the general finite-state Markov channel scenario.
- (ii) The contribution concerning privacy guarantees over the finite-state Markov channel is the applications of the modeling approach based on the finite-state Markov channel and Markov jump linear system theory for the development of privacy guarantees [87] (summarized in Section 1.3.2).
- (iii) The contributions concerning the modeling framework of discrete-time Markov jump systems [97] (introduced with more details in Section 1.3.3) can be summarized as follows.
- Lyapunov characterizations of exponential mean square stability and exponential mean square input-to-state stability based on multiple Lyapunov functions for discrete-time Markovian switching nonlinear systems [3].
 - Necessary and sufficient conditions for the exponential mean square input-to-state stability are proposed for discrete-time Markovian switching systems.
 - Sufficient conditions for p -th moment input-to-state stability.
- (iv) The application of the theory developed for exponential mean square stability and exponential mean square input-to-state stability to the case of discrete-time nonlinear systems subject to Markovian delays [173] (summarized in Section 1.3.4).

1.3.1 The output-feedback control over finite-state Markov channels: the separation principle

The considered wireless control network scenario is composed by a plant and a controller connected via wireless links and communicating by TCP-like protocols [48].

The closed-loop system composed by plant and controller exchanging information via wireless links can be modeled as a Markov jump linear system. This work addresses (as one of the contributions) the output-feedback control design for the described wireless control network scenario.

The output-feedback control for Markov jump linear systems has been investigated in [4] and [174]. This work focuses on the output-feedback control for Markov jump linear systems on a TCP-like scenario [48]. In the considered output-feedback control architecture [77,91,92], the controller is able to receive the information on the sensing link, i.e., the output of the system, the outcome of the transmission and the channel mode [61] without any delay. Instead, on the actuation link the controller sends the control law and it is able to receive the information concerning the outcome of the transmission and the channel mode with one time-step delay with respect to the time instant of the control law transmission [79]. This situation is summarized by saying that one time-step delay affects the actuation link mode observation [79]. The channel mode observation on the sensing link occurs without any delay because the acknowledgement message is not necessary for the receiver, as it is explained with more details in Chapter 2, Remark 2.

Previous works such as [48,49] do not consider the communication channel mode, but actually the receiver has access to this information, by performing a channel state estimation [61].

The novelty of this work lies within the output-feedback control in the FSMC setting [1].

Optimal linear quadratic regulation [175] with one time-step delay on actuation link mode has been already investigated in [79]. Specifically, the work by *Lun et al.* presented in [79] introduces an optimal linear quadratic regulator for a control system where the control law is sent over a TCP-like wireless actuation link. Consequently, the TCP-like communication is characterized by acknowledgement messages that provide one time step delay in the observation of the actuation link mode.

Thus, the optimal linear quadratic regulator has to account for the delay [79] in the observation of the actuation link mode [52].

In [176], the Kalman filter is adopted for a single simplified Gilbert channel modeled by a Markov chain with two Markov modes. This result cannot be applied to the general Markov channel scenarios that require $2N$ modes with $N > 2$: N channel modes result, e.g., from the signal-to-interference-plus-noise-ratio partitioning, and each mode is associated with a binary symmetric channel, see [1]. Thus, $2N$ modes derive from the general Markov channel mathematical model. Other estimation techniques are \mathcal{H}_2 and \mathcal{H}_∞ estimation: in [55], sub-optimal filters are obtained for the case of cluster availability of the operational modes.

It is well known that for the case in which the information on the output of the system and on the Markov chain are available at each time-step, the best linear estimator of the state is the Kalman filter [177–179] (see [176] and [4, Remark 5.2]).

An offline computation of the Kalman filter is inadvisable [180], as discussed more in detail in Chapter [2]. Indeed, the solution of the difference Riccati equation and the time varying Kalman gain are sample path dependent and the number of sample paths grows exponentially in time. On the other hand, an online computation of the Kalman filter requires online matrix inversions which might be inadvisable for the significant computational complexity.

For this reason, this work provides a different class of estimators, for which the filtering gains can be pre-computed offline. Specifically, two infinite horizon minimum mean square Markov jump filters [4, Chapter 5.3] are presented:

- the first one with a next-step predictor [181, Chapter 8.2.1],
- the second one using the current estimator [181, Chapter 8.2.4].

These estimators use different communication and computation timing sequences and offer different performance levels, as explained more in detail in Chapter [2]. This research line involves the contributions presented in two conference papers and one work submitted for possible publication as journal contribution.

- The conference paper presented at the 58th IEEE Conference on Decision and Control [79] illustrates the design over finite-state Markov channels,
- The conference paper presented at the 2021 American Control Conference illustrates optimal output-feedback over finite-state Markov channels [92].

- The article [77] provides the design of an optimal output-feedback controller over finite-state Markov channels, with two infinite horizon minimum mean square Markov jump filters [4, Chapter 5.3] (the next-step predictor and the current estimator).

Specifically, these two works focus on control design and structural properties (stabilizability and detectability) [182] for wireless control networks over finite-state Markov channels.

The paper by *Lun et al.* [79] has introduced the controllability notion over one step delayed actuation link mode observation, while the results in [92] concern the output-feedback control with double-sided packet losses and detectability notions for the next-step predictor.

Concerning the Markov jump linear system theory modeling wireless control network scenarios, the research leading to this thesis moves from the results in [79].

Particularly, this research work has added the double-sided packet losses to the wireless control network scenario in [79] and the results obtained concerning the next-step predictor have been presented in the conference paper [92].

An improvement with respect to [92] consists in the introduction of the current estimator together with a comparison between the two methodologies. This improvement achieved in the research has been presented in the paper submitted as possible journal contribution [77].

The current estimator provides better performance but it requires more restrictive constraints to be satisfied. Different computation timing sequences are used by the two estimators: the one concerning the current estimator presents more restrictive physical constraints (see Chapter 2 for more details).

The theoretical existence of these two estimators is a problem addressed using different detectability notions that have been introduced for the finite-state Markov channel scenario and that are presented in this work with the aim of finding suitable conditions guaranteeing the existence of an observer (either next-step predictor or current estimator).

Particularly, conditions guaranteeing the weakest detectability are necessary and sufficient, while requirements ensuring the strongest detectability are only sufficient.

Moreover, this thesis contains the detailed proofs of the separation principle for next-step predictor and current estimator. Finally, the reader can find a more general

case study with respect to the one in [92], providing several propagation environments showing in which cases it is possible to conclude the existence of one of the two observers. The main contributions concerning the output-feedback control briefly illustrated in this chapter can be summarized as follows.

- (i) The finite-state Markov channel is introduced into the TCP-like double-sided packet loss wireless control network scenario.
- (ii) The communication timing, as well as computation and transmission delays, are explicitly considered, as explained above.
- (iii) The separation principle validity is proved for both the considered estimators in the general finite-state Markov channel setting.
- (iv) Four different detectability notions (presented from the weakest to the strongest one) are introduced in Chapter 2.
- (v) The presented results are illustrated in a case study concerning an inverted pendulum on a cart described in Chapter 2.

1.3.2 Privacy guarantees over finite-state Markov channels

The research line concerning privacy over finite-state Markov channels moves from the work by *Tsiamis et al.* [38] and applies the modeling approach based on the finite-state Markov channel [1] and Markov jump system theory [4] to study the problem of secure state estimation [36] over wireless communication channels [74].

Specifically, *Tsiamis et al.* [38] model wireless links as independent and identically distributed (i.i.d.) Bernoulli random variables. Other works, such as *Leong et al.* [34], provide privacy guarantees over wireless links modeled as time-homogeneous two-state Markov chain models [138].

Differently from previous works that exploit either the Bernoulli model [30, 38] or two mode Markov chains for the wireless link, this work focuses on privacy guarantees over a finite-state Markov channel [1, 62].

In this research work each agent [87] (user or eavesdropper) estimates the process evolution of the signal-to-interference-plus-noise ratio on its link, independently from the other. A finite-state Markov chain (with more than two modes) approximates the signal-to-interference-plus-noise-ratio process over each link. A binary random variable

standing for the outcome of the transmission is associated to each Markov mode, which determines the distribution of the binary random variable [1].

The resulting finite-state Markov channel model [1] allows for a tighter integration in the coupled design of the communication and estimation components of the wireless control networks. Some procedures for control and estimation over packet dropping wireless links modeled by finite-state Markov channels can be related to the Markov jump linear system theory [79, 92, 183–185] generalizing the fundamental results based on i.i.d. Bernoullian assumptions [48]. Nevertheless, most of the contributions on estimation and control over fading channels consider the two-state Markov chain modeling a bursty packet erasure channel [176].

The secrecy problem addressed by [38] provides a secrecy notion which is suitable for wireless estimation problems solved by Kalman filtering: *perfect expected secrecy* [38, Definition 1], based on covariance matrices of the user and of the eavesdropper, respectively.

This work exploits a minimum mean square Markov jump filter instead of Kalman filter (see [38, 176]), because the filter dynamics depends just on the current mode of the wireless sensing link (rather than on the entire past history of modes). This implies that the filtering gains can be pre-computed offline [4].

The work by *Impicciatore et al.* [87] introduces a novel secrecy notion (reported in Chapter 3), which is suitable for minimum mean square Markov jump filter: *optimal mean square expected secrecy over finite-state Markov channels* that requires the user mean square error to be bounded and the eavesdropper mean square error unbounded. The reader can find more details in Chapter 3.

1.3.3 Lyapunov characterizations for discrete-time Markov jump systems

The contribution concerning Lyapunov characterizations for discrete-time Markov jump systems is based on the journal article by *Impicciatore et al.* titled “*Lyapunov characterizations of exponential mean square input-to-state stability for discrete-time Markovian switching nonlinear systems*” [97].

A preliminary version of the aforementioned article was the conference paper “*Sufficient Lyapunov conditions for p th moment ISS of discrete-time Markovian Switching Systems*” by the same authors [142], where a p th moment input-to-state stability analysis for discrete-time Markovian switching nonlinear systems has been presented.

In this conference contribution the p th moment input-to-state stability notion (introduced in [144]) is conveyed to the discrete-time Markovian switching nonlinear domain and sufficient Lyapunov conditions guaranteeing this property are provided. The contributions concerning the investigations in the discrete-time nonlinear Markovian switching framework are listed in the following.

- (i) Discrete-time Markovian switching nonlinear systems [3] are investigated in this work with the aim of providing Lyapunov characterizations of exponential mean square stability and exponential mean square input-to-state stability based on multiple Lyapunov functions.
- (ii) A converse result for discrete-time Markovian switching nonlinear systems is provided: a reverse implication for the Lyapunov conditions for exponential mean square stability, given in [3].
- (iii) Necessary and sufficient conditions for the exponential mean square input-to-state stability are proposed for discrete-time Markovian switching systems.
- (iv) Sufficient conditions for p -th moment input-to-state stability are illustrated in Chapter 4.

The contributions summarized above will be illustrated with all the necessary details and explanations in Chapter 4.

1.3.4 Lyapunov conditions for discrete-time nonlinear systems subject to Markovian delays

The mean square stability has been extensively analyzed for discrete-time Markovian switching linear systems without delays [4]. Only few works presented in the literature investigate this stability notion in the nonlinear framework [3, 145]. However, when considering discrete-time nonlinear systems with Markovian delays, the mean square stability notion results to be particularly useful for investigating the behavior of the mean square of the system state.

The contribution on this research line is twofold.

- Firstly, this work shows that when considering discrete-time delay systems with delay signals constrained to follow a delay digraph [160, 169, 170], the discrete-time

delay system can be rewritten as a discrete-time Markov jump system [3,4] if the delay switching rule [160,169] satisfies the Markov property.

- Secondly, this part of the thesis extends sufficient Lyapunov conditions existing for the global asymptotic stability property of discrete-time delay systems with delays digraphs [169,170] to the study of mean square stability.

The reader can find more explanations and details on this part in Chapter 5.

1.4 Notation and mathematical background

This section provides the main notation adopted throughout this thesis.

Let \mathbb{R} , \mathbb{R}^+ and \mathbb{N} denote the sets of real numbers, nonnegative real numbers and nonnegative integers, respectively.

Given a finite set \mathcal{A} , $|\mathcal{A}|$ denotes the cardinality of \mathcal{A} .

For $k_1, k_2 \in \mathbb{N}$, $\mathbb{N}_{[k_1, k_2]} \triangleq \{k \in \mathbb{N} \mid k_1 \leq k \leq k_2\}$.

The symbol \mathbb{F} indicates the set of either real or complex numbers. The absolute value of a number is denoted by $|\cdot|$. Let us recall that every finite-dimensional normed space over \mathbb{F} is a Banach space [186]. Let us denote the Banach space of all bounded linear operators of Banach space \mathbb{X} into Banach space \mathbb{Y} , by $\mathbb{B}(\mathbb{X}, \mathbb{Y})$. Let us set $\mathbb{B}(\mathbb{X}, \mathbb{X}) \triangleq \mathbb{B}(\mathbb{X})$.

Let the symbol \mathbf{O}_n denote the vector containing all zeros of length n and let the symbol \mathbb{I}_n indicate the identity matrix of size n .

The symbol \mathbb{O}_n represents the matrix of zeros of size $n \times n$.

The transposition is denoted by the apostrophe, the complex conjugation by an overbar, the conjugate transposition by superscript $*$. $\mathbb{F}_*^{n \times n}$ and $\mathbb{F}_+^{n \times n}$ represent the sets of Hermitian and positive semi-definite matrices, respectively.

For any positive integers C, r, n , and m , let us define the following sets:

- $\mathbb{H}^{Cr, n}$ is the set of all $\mathbf{K} = [K_m]_{m=1}^C$, K_m in $\mathbb{F}^{r \times n}$,
- $\mathbb{H}^{Cn, *}$ is the set of all $\mathbf{K} = [K_m]_{m=1}^C$, K_m in $\mathbb{F}_*^{n \times n}$,
- $\mathbb{H}^{Cn, +}$ the set of all \mathbf{K} in $\mathbb{H}^{Cn, *}$, with $K_m \in \mathbb{F}_+^{n \times n}$.

Let us set $\mathbb{H}^{Cn} = \mathbb{H}^{Cn,n}$.

Let the symbol $\rho(\cdot)$ denote the spectral radius of a square matrix (or a bounded linear operator), i.e., the largest absolute value of its eigenvalues, and let $\|\cdot\|$ be either any vector norm or any matrix norm.

Let us denote by \otimes the Kronecker product defined in the usual way, see, e.g., [187], and \oplus the direct sum. Notably, the direct sum of a sequence of square matrices $(\Phi_i)_{i=1}^C$ produces a block diagonal matrix having its elements, Φ_i , on the main diagonal blocks. Then, $\text{tr}(\cdot)$ indicates the trace of a square matrix.

For two Hermitian matrices of the same dimensions, Φ_1 and Φ_2 , $\Phi_1 \succeq \Phi_2$ (respectively $\Phi_1 \succ \Phi_2$) means that $\Phi_1 - \Phi_2$ is positive semi-definite (respectively positive definite).

Finally, $\mathbb{E}[\cdot]$ stands for the mathematical expectation of the underlying scalar-valued random variable, and $\Re(\cdot)$ indicates the real part of the elements of a complex matrix. For a positive real δ , a positive integer m , and $x \in \mathbb{R}^m$, $B_\delta^m(x) \triangleq \{y \in \mathbb{R}^m : \|y - x\| \leq \delta\}$.

For $x \in \mathbb{R}^+$, $[x]$ is the largest integer smaller or equal to x . The symbol \circ denotes composition (of functions).

Let us here recall that a continuous function $\sigma : \mathbb{R}^+ \rightarrow \mathbb{R}^+$ is

- of class \mathcal{K} if it is zero at zero and strictly increasing,
- of class \mathcal{K}_∞ if it is of class \mathcal{K} and unbounded,
- of class \mathcal{L} if it is decreasing and converging to zero as the argument tends to $+\infty$.

A continuous function $\beta : \mathbb{R}^+ \times \mathbb{R}^+ \rightarrow \mathbb{R}^+$ is said to be of class \mathcal{KL} if, for each fixed $t \in \mathbb{R}^+$, the function $s \rightarrow \beta(s, t)$, $s \in \mathbb{R}^+$, is of class \mathcal{K} , and, for each fixed $s \in \mathbb{R}^+$, the function $t \rightarrow \beta(s, t)$, $t \in \mathbb{R}^+$, is of class \mathcal{L} .

1.5 Thesis organization

The thesis is organized as follows.

- Chapter [1] provides an introduction to the main topics and contributions addressed by this research work.
- Chapter [2] provides the main challenges and solution strategies for the optimal output-feedback control problem over finite-state Markov channels with double-sided packet losses.

Specifically, Chapter 2 addresses the problem of the separation principle for wireless control network scenarios with analogous remote architecture as [48] and the finite-state Markov channel modeling the wireless link.

- Chapter 3 illustrates the privacy guarantees over finite-state Markov channels based on the results in [87].
- Chapter 4 addresses the general case of discrete-time Markov jump systems with Lyapunov characterizations of exponential mean square stability and exponential mean square input-to-state stability.
- Chapter 5 provides Lyapunov conditions for exponential mean square stability of discrete-time systems with Markovian delays.

Finally, some concluding remarks and future research directions are provided in Chapter 6.

1.6 List of acronyms

Consider the following abbreviation list that contains all the abbreviations and acronyms used throughout this work.

Acronyms	Description
WCN	wireless control network
TPM	transition probability matrix
FSMC	finite-state Markov channel
MJLS	Markov Jump Linear System
<i>MS</i>	Mean square
<i>MSS</i>	Mean square stability
<i>MSD</i>	Mean square detectable
<i>EMSS</i>	Exponential Mean square stability
<i>EMS-ISS</i>	Exponential Mean square input-to-state stability
<i>SINR</i>	Signal-to-nterference-plus-noise-ratio
<i>i.i.d.</i>	independent and identically distributed
GEC	Gilbert and Elliott channel
ISI	intersymbol-interference
UHF	ultrahigh frequency
HMM	hidden Markov model
PED	packet error distribution
PER	packet error rate
BER	bit error rate
PEP	packet error probability
LMI	Linear Matrix Inequality

2

Wireless control networks over finite-state Markov Channels: the separation principle

Contents

2.1 Chapter outline	25
2.2 Problem formulation	27
2.2.1 The wireless control network architecture	27
2.3 Bernoulli wireless channel model and its limitations	29
2.4 The finite-state Markov channel	30
2.4.1 Finite-state Markov channel historical background	30
2.4.2 Wireless link	33
2.5 The information set	37
2.6 Wireless control network model	40
2.6.1 Assumptions on wireless control network model	41
2.7 Output-feedback controller	42
2.7.1 Control synthesis based on next-step predictor	42
2.7.2 Output-feedback controller with current estimator	42
2.7.3 The Linear Quadratic Regulator	43
2.8 Estimation techniques	44
2.8.1 The Markovian next-step predictor	45
2.8.2 The Markovian current estimator	46
2.8.3 Computational complexity	47
2.9 Observer stability analysis	48
2.9.1 The operators	48
2.9.2 Next-step predictor stability analysis	50
2.9.3 Current estimator stability analysis	51

2.9.4 The next-step predictor filtering coupled algebraic Riccati equations	53
2.9.5 The current estimator filtering coupled algebraic Riccati equations	55
2.10 The separation principle	57
2.10.1 The next-step predictor separation principle	57
2.10.2 The current estimator separation principle	58
2.11 Mode-independent output-feedback	60
2.12 Numerical case study	64
2.12.1 The inverted pendulum on a cart	64
2.12.2 Detectability analysis	65
2.12.3 Stabilizability analysis	71
2.12.4 Performance analysis and comparison	73

This Chapter is based on the paper by *Impicciatore et al.* [77] submitted for possible journal publication and on the conference paper [92] (preliminary version of [77]).

The aim of the Chapter is providing an accurate problem formulation concerning the WCN scenario here illustrated by means of the notation introduced in Chapter 1. There are different stochastic models used to formally describe the wireless communication links [74] in WCN literature [188, 189] and they are widely discussed in this Chapter. As deeply explained in the following, a very interesting insight concerning the wireless link mathematical formalization is the impact of the adopted FSMC model over the performance of the controller in WCN design. Indeed, as deeply explained in the following, previous works in the Telecommunications field have already illustrated this insight of WCNs [62]. Following the research line by *Lun et al.* [62], this Chapter illustrates one of the most significant thesis contributions, i.e., the statement of the separation principle over FSMCs with double-sided packet losses.

2.1 Chapter outline

This section provides a short summary of the organization of this Chapter.

- Section 2.2 introduces the problem formulation concerning the specific challenges investigated for a WCN scenario, whose remote architecture control scheme is shown in Fig. 2.1.
- Section 2.3 describes the Bernoulli mathematical model [1, 48] of the wireless channel and highlights the limitations of the Bernoulli model.

- Section 2.4 describes the mathematical model given by the finite-state Markov channel and points out the performance impacts [62] and its advantages [77,91,92] with respect to the Bernoulli model.
- Section 2.5 takes into account two different timing diagrams reported in Fig. 2.4 concerning the transmission from the sensor to the controller (sensing link) and the communication from the controller to the actuators (actuation link). This leads to the adoption of two different estimation techniques:
 - the next-step predictor [4],
 - the current estimator [181].
- Section 2.6 provides the complete model of the wireless control network resulting from the architecture in Fig. 2.1 and from the finite-state Markov channel model.
- Section 2.7 describes the design of the output-feedback controller, that exploits the aforementioned estimation techniques.
- Section 2.8 provides the analysis of the estimation techniques and highlights the existing differences.
- Section 2.9 provides the instruments for the stability analysis in the mean square sense of the WCN scenario modeled as a MJLS.
- Section 2.10 illustrates the core of this Chapter, that is, the separation principle over FSMCs.
- Section 2.11 describes the mode-independent output-feedback control, that is compared to the mode-dependent output-feedback control.
- Section 2.12 provides the numerical example validating the results presented in this Chapter.
- Proofs of Lemmas and Theorems concerning the results presented in this Chapter are reported in Appendix A.

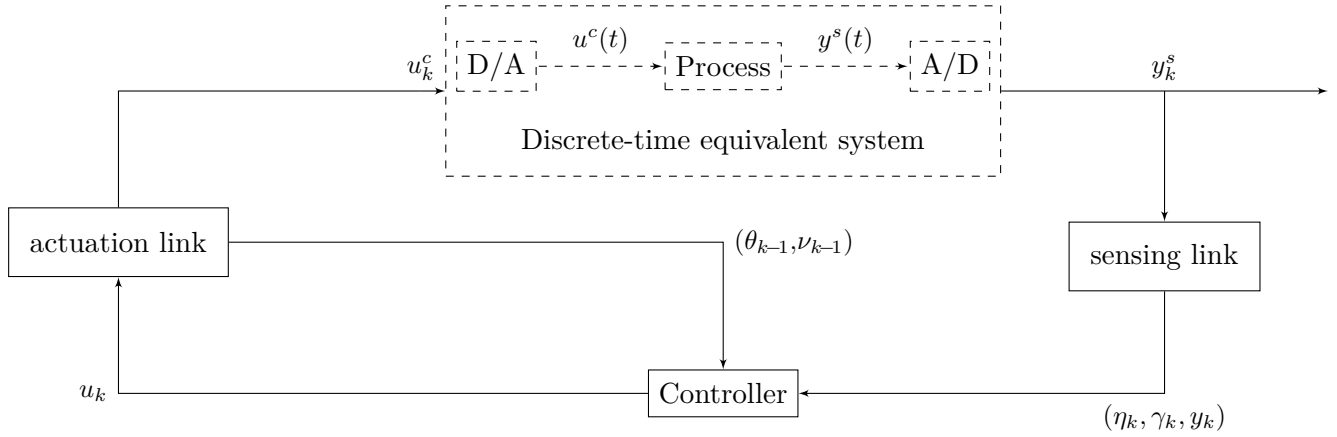


Figure 2.1: Wireless control network architecture.

2.2 Problem formulation

This section illustrates the problem formulation concerning the optimal output-feedback control of WCNs over FSMCs.

2.2.1 The wireless control network architecture

Fig. 2.1 shows the WCN architecture considered throughout this work. The remote control scheme is based on a TCP-like protocol and it is made up of four elements:

- the discrete-time equivalent system,
- the controller,
- the wireless links connecting the plant to the controller
 - wireless sensing link,
 - wireless actuation link.

2.2.1.1 Communication between plant and controller: sensing link and actuation link

The communication between the plant and the controller happens according to a TCP-like protocol [48]. In this thesis, the link responsible for the communication from the plant to the controller is called sensing link, while the link responsible for the communication from the controller to the plant is the actuation link. This implies

that the controller is the receiver on the sensing link and it is the transmitter on the actuation link.

As it is well known, the main feature of the TCP-like protocol is the presence of acknowledgement messages [48], that are received from the transmitter (in this case the controller) and that bring the information on the outcome of the transmission. Consequently, it is straightforward that the acknowledgement messages are received after the control law transmission. Specifically, the acknowledgement message is received one time-step after the control law transmission.

The mathematical description of the wireless links accounts for both the mode of the wireless channel [61], as well as the outcome of the transmission on the considered link. The random variables θ_{k-1} and η_k are the modes of actuation link and sensing link, respectively. The binary variables ν_{k-1} and γ_k model the transmission outcome on the actuation link and sensing link, respectively (as the reader will see in paragraph 2.4.2). The actuation link data θ_{k-1} and ν_{k-1} are received with one time-step delay, due to the features of the acknowledgement message discussed above. Analogously, η_k and γ_k are data concerning the sensing link. The quantities η_k and γ_k are not affected by any delay, because on the sensing link the controller is the receiver of the transmission. A complete description of θ_{k-1} , ν_{k-1} , η_k , and γ_k is illustrated in Section 2.4.2.

2.2.1.2 The discrete-time equivalent system

The discrete-time equivalent system is composed by the plant, the Analog to Digital Converter (A/D block in Fig. 2.1) with sampling period T , and Digital to Analog Converter (D/A block in Fig. 2.1) based for instance on Zero-Order Hold (ZOH), so that the analog control input, denoted by $u^c(t)$, can be applied to the continuous-time process. The output of the continuous-time process is denoted by $y^s(t)$ and it goes in input to the block A/D that produces as output the discrete-time output measurement $y_k^s \in \mathbb{F}^{n_y}$, $k \in \mathbb{N}$. The output of the controller, denoted by u_k , is sent through the actuation link to the actuators, that receive u_k^c . The variable u_k^c denotes the information received by the D/A block, that provides $u^c(t)$ as an output. Consider the remote architecture depicted in Fig. 2.1.

The discrete-time equivalent system is formally described by the system \mathcal{G} , defined as fol-

lows,

$$\mathcal{G} : \begin{cases} x_{k+1} = Ax_k + Bu_k^c + Gw_k, \\ y_k^s = Lx_k + Hw_k, \end{cases} \quad (2.1)$$

where $x_k \in \mathbb{F}^{n_x}$ is the system state and $y_k^s \in \mathbb{F}^{n_y}$ is the system output, $k \in \mathbb{N}$. For $k \in \mathbb{N}$, $w_k \in \mathbb{R}^{n_w}$ is a sequence of i.i.d. Gaussian random variables with zero mean. The matrices A , B , G , L , and H are system matrices of appropriate sizes. An unstable system matrix is considered, as in [48]. Otherwise, a stabilizing output-feedback control would not be required. As explained above, \mathcal{G} is controlled remotely by a digital output-feedback controller, which receives the measurements y_k^s on the wireless sensing link and sends the control inputs over the wireless actuation link.

Remark 1 Fig. [2.1] reports the scheme of a WCN infrastructure with possible packet loss occurrence on both the sensing link and actuation link.

The main challenge of this scenario arises from a combined effect of two link packet losses possibly resulting in long periods in which the controller and actuator cannot simultaneously receive new data. The scheme is a TCP-like communication [48] based on acknowledgement messages. Specifically, the controller receives the acknowledgement of the transmission on the connection actuators-controller (see Fig. [2.1]).

Packet losses over this connection are negligible since the probability of a packet loss for acknowledgement messages is very small in practical applications.

There are two main strategies concerning the wireless channel model:

- the Bernoulli channel model,
- the finite-state Markov channel model (the model adopted in the presented research line).

2.3 Bernoulli wireless channel model and its limitations

A vast amount of research assumes memoryless packet drops, so that dropouts are realizations of a Bernoulli process [24, 48, 50]. The research illustrated in [48] provides foundations of control and estimation over lossy networks by adopting the Bernoulli model of the communication links. Specifically, the processes of arrival of both

observations and control packets are modeled as random processes whose parameters are related to the characteristics of the communication channel. Two independent Bernoulli processes are considered, that govern packet losses between the sensor and the controller, and between the latter and the actuation points, see [48, Fig. 1]. As pointed out in [48], the Bernoullian abstraction of the transmission outcome (an idealization chosen for mathematical tractability) reveals useful design guidelines in the WCN design problem addressed by *Schenato et al.* [48].

However, the networking component (SINR, path loss, shadow fading, and interference [1, 74]) obviously has an additional impact on the performance of the closed-loop systems that is not considered by the Bernoulli model. Moreover, the catch affecting the Bernoulli model is that the presence of correlations in the packet loss process cannot be taken into account. Indeed, the occurrence of bursts of packet losses cannot be modeled by Bernoulli random variables.

The adoption of FSMC provides a more accurate model for the radio link [62]: specifically, a relevant theoretical outcome obtained via the adoption of the FSMC framework consists in designing a controller that guarantees stability and improves control performance of the closed-loop system, where other approaches based on a simplified channel model fail. Indeed, many works consider more general correlated (bursty) packet losses and use a TPM of a finite-state stationary Markov channel (see e.g. the finite-state Markov modelling of Rayleigh, Rician and Nakagami fading channels in [1, 190–192]) to describe the stochastic process that rules packet dropouts.

2.4 The finite-state Markov channel

This section provides details on the model and motivation of finite-state Markov channel, or FSMC [1]. Specifically, after the part concerning some historical backgrounds, this section reports an accurate description of the wireless link model considered for this research line.

2.4.1 Finite-state Markov channel historical background

The study of finite-state communication channels with memory dates back to the work by Shannon in 1957 [193]. In [193], Shannon proved coding theorems for finite-state channels with discrete channel input and output symbols, where the channel state could be calculated at the transmitter, but not necessarily at the receiver. In 1958, Blackwell

et al. [194] proved that for a practical class of finite-state channels with memory, reliable transmission is possible at rates below the channel capacity. In 1960, Gilbert introduced a new type of finite-state channel model to determine the information capacity of wireline telephone circuits with burst-noise [195]. One main distinction between Gilbert's model and Blackwell's model [194] was in the way channel output was defined to depend on channel states and inputs. In Blackwell's model, channel output was a deterministic function of the current channel state, which, in turn, stochastically depended on current channel input and previous channel state. Whereas in Gilbert's model, channel output was a probabilistic function of the current channel input and the current channel state. In particular, each channel state in Gilbert's model was associated with a discrete memoryless channel. Despite its simplicity, Gilbert's model was the first nontrivial example of channel models with memory, where the channel state is statistically independent of channel input symbols and is unknown to the transmitter or the receiver. Soon after the work of Gilbert [195], Elliott used this model to evaluate and compare the error rate performance of error correcting and error detecting codes over burst-noise channels [196]. This channel model is known as the GEC.

Researchers in the late 1960s extended the model proposed by Gilbert and Elliott to improve their representations of channels with memory. In 1968, McCullough [197] introduced more channel states in the model, each with a different error rate. State transitions in [197] were allowed only immediately following an error in the state. In another work in 1967, Fritchman [198] proposed a finite-state channel with J error free and $K - J$ error states. However, the model was complicated in terms of deriving channel error statistics, unless there was a single error state or $K - J = 1$, which effectively made the Fritchman model similar to the GEC model. In 1968, Gallager further developed the information theory of FSMCs [199], making it a classical subject in advanced information theory. Originally, Gallager used the term finite-state channel, where channel states are assumed to be the output of a Markov chain. FSMC is more clarifying and will be used throughout this work. In [199], pp. 97–111, 176–187], Gallager provides rigorous definitions, coding theorems, error exponents, and several examples of FSMCs with memory. Gallager also mentions fading channels in wireless radiotelephony as physical channels with memory that can be represented by FSMCs. Gallager's definition of FSMCs is the standard definition used by researchers today. This model accommodates for both cases where the channel state transition is driven and controlled by the channel input (such as ISI channels), as well as the case where the channel state

is statistically independent of the channel input (such as fading channels). From 1969 to the mid 1970s, research activity on applications of FSMCs was limited to modeling error bursts in digital wireline telephone circuits. The proposed models were mainly variations of earlier ones developed up to 1968, such as the Fritchman model [198].

From 1978 to 1989, research activity for finding new applications of FSMCs in digital communications was more or less dormant. During this period, theory and techniques for mobile radio communications were in early stages of development and cellular digital telephone networks did not emerge (were not commercially available) until the early 1990s. This explains why research activity on applications of FSMC for digital mobile communication systems did not receive impetus until the early to mid 1990s. There are many research works from 1989 to the present focusing on mobile radio fading channels.

Fading channels with memory are common in mobile radio communications [200]. With the advent and commercial success of digital cellular networks in the early 1990s, there was an immediate need for accurate modeling of fading channels with memory. The channel models helped system designers analyze and improve system performance measures, such as the error correcting capability of channel codes or the packet throughput. But more importantly, the use of channel models with memory for decoding at the receiver would potentially result in higher information rates than those achieved by assuming a memoryless channel [201].

In 1991, Semmar et al. [202] used the Fritchman model [198] with a single error state and two to four error-free states to characterize error sequences in UHF digital mobile radio channels at 910 MHz. In their work, the Fritchman model was fitted to measured data by determining suitable values for transition probabilities between channel states. In 1991, Vucetic [203] used a finite-state model for adaptive coding over time-varying radio channels: each state in the model represented a Rician fading channel with different Rician factors. The paper by Sivaprakasam and Shanmugan [204] developed a modified Baum-Welch algorithm [205] to estimate the parameters of a HMM based on the observation of actual error burst sequences in fading channels.

FSMC modeling of fading channels in mobile radio communications was improved by Wang and Moayeri in 1995 [206]. The main novelty of this work was to explicitly establish the link between the statistical Clarke's model for fading channels [207] and the FSMC states. In particular, each FSMC state in their model represented a range of received signal-to-noise ratio, which in turn determined the error probability in that state. Based on this assumption, Wang and Moayeri provided analytical

expressions for states, state transition probabilities, and error probabilities in each state. The original FSMC modeling of fading channels as proposed in [206] or its variations are still widely used in the literature.

Almost concurrently with Wang and Moayeri, Goldsmith and Varaiya proposed a new iterative method for computing the information rates and capacity of data-independent FSMC models with i.i.d inputs. They also introduced a maximum-likelihood decision feedback decoding technique for the receiver that took the inherent channel memory into account [201]. The work by Goldsmith [201] was a generalization of an earlier study by Mushkin and Bar-David in [208] on the capacity and coding for the GEC.

In the design of wireless communication systems FSMCs have been traditionally used to model error bursts in fading channels. This provides an improvement of performance measures in the physical or media access control layers. Since 1997, FSMC models have enabled closed-form or simulation-based analysis of system-level performance measures, such as packet throughput [209,210], PED [211], and PER [212] through bursty wireless channels. The BER in more sophisticated communications systems that include receiver diversity has been studied using FSMC models in [190].

Since the late 1990s, an active area of research has been to develop practical decoding techniques at the receiver using FSMC models for fading channels. FSMC models enable implementation of mathematically tractable channel estimation and data decoding algorithms for time-varying fading channels [213,214]. Since 1995 [206], first-order FSMC models for fading channels have been the models of choice due to their computational simplicity and the ease with which model parameters can be determined. A first-order Markovian assumption in the FSMC model means that given the previous fading channel state, the current state is statistically independent of all other past and future fading channel states. Ever since, the accuracy of first-order FSMC models for fading channels, compared with higher-order FSMC models, has been the subject of research.

2.4.2 Wireless link

This paragraph provides the mathematical description of single-hop wireless communication links modeled by FSMCs.

Specifically, the sequence $\{\nu_k\}_{k \in \mathbb{N}}$ models the packet arrival process on the actuation link. The value of the random variable ν_k is zero whenever the control packet is lost,

and $\nu_k = 1$ if the control packet is correctly delivered, i.e., $\nu_k \in \mathbb{S}_\nu \triangleq \{0, 1\}$, for any $k \in \mathbb{N}$. Analogously, the sequence $\{\gamma_k\}_{k \in \mathbb{N}}$ describes the packet arrival process on the wireless sensing link. Particularly, $\gamma_k = 0$ if the sensing packet is lost and $\gamma_k = 1$ if it is successfully delivered, i.e., for all $k \in \mathbb{N}$, $\gamma_k \in \mathbb{S}_\gamma \triangleq \{0, 1\}$. The processes ν_k and γ_k are collections of binary random variables and the probability of having a packet loss or a correct packet transmission over each link depends on its SINR. The SINR is determined by propagational environment and related physical phenomena [62]. SINR is a stochastic process and can be abstracted by a Markov chain. Each Markov mode is associated with a certain PEP.

Consider the stochastic basis $(\Omega, \mathcal{F}, \{\mathcal{F}_k\}_{k \in \mathbb{N}}, \mathbb{P})$, where Ω is the sample space, \mathcal{F} is the σ -algebra of (Borel) measurable events, $\{\mathcal{F}_k\}_{k \in \mathbb{N}}$ is the related filtration, and \mathbb{P} is the probability measure. Sensing link and actuation link modes are the output of the Markov chains $\eta : \mathbb{N} \times \Omega \rightarrow \mathbb{S}_\eta \subseteq \mathbb{N}$ and $\theta : \mathbb{N} \times \Omega \rightarrow \mathbb{S}_\theta \subseteq \mathbb{N}$, respectively. Indeed, the Markov modes of $\{\eta_k\}_{k \in \mathbb{N}}$ and $\{\theta_k\}_{k \in \mathbb{N}}$ belong to finite sets $\mathbb{S}_\eta = \{1, 2, \dots, I\}$ and $\mathbb{S}_\theta = \{1, 2, \dots, N\}$, respectively.

Remark 2 Previous works such as [48, 49] do not consider the communication channel mode, but actually the receiver has access to this information, by performing a channel state estimation [61]. The novelty of this paper lies within the output-feedback control in the FSMC setting.

Moreover, the described Markov chains are characterized by time-invariant TPMs: the TPM $P = [p_{ij}]_{i,j=1}^N$ is associated with the Markov chain $\{\theta_k\}$ and the TPM $Q = [q_{mn}]_{m,n=1}^I$ is associated with the Markov chain $\{\eta_k\}$.

Each TPM may be obtained by integrating the joint probability density function of the SINR over two consecutive packet transmissions and over the desired regions [1, 62]. The TPM values may also be validated through the empirical data from a measurement campaign for calibrating the theoretical model parameters. The uncertainties in TPM values neglected in this work can then be addressed via a polytopic model [64, 67, 215–220].

Remark 3 The network-induced communication delays due to multiple path routing and time-varying processing delays in relay nodes of multi-hop networks are not an issue for single-hop sensing and actuation links with scheduled medium access considered in this paper and extensively used in delay-sensitive control applications relying, e.g., on the low latency deterministic network mode of IEEE 802.15.4e.

The entries of TPMs P and Q are defined as follows,

$$p_{ij} \triangleq \mathbb{P}(\theta_{k+1} = j \mid \theta_k = i), \quad q_{mn} \triangleq \mathbb{P}(\eta_{k+1} = n \mid \eta_k = m), \quad (2.2)$$

satisfying: $\sum_{j \in \mathbb{S}_\theta} p_{ij} = 1$, $\sum_{n \in \mathbb{S}_\eta} q_{mn} = 1$, $i \in \mathbb{S}_\theta$, $m \in \mathbb{S}_\eta$.

Since the probability of a packet loss depends on the mode of the Markov chain, the values of ν_k and γ_k are either zero or one, with certain probabilities depending on the current Markov mode.

Remark 4 In this network scenario, up-link and down-link models are split up. This separation already exists in literature [48, 221]. However, unlike the previous literature, the research presented in this thesis explicitly considers the channel mode (see Remark 2) by providing two independent FSMCs for sensing link and actuation link, respectively.

Sensing FSMC

Let y_k denote the measurement received by the output-feedback controller at time $k \in \mathbb{N}$. The general model for the sensing link is

$$y_k = \gamma_k y_k^s.$$

The value of the random variable γ_k when the current Markov mode is $\eta_k \in \mathbb{S}_\eta$ is a function of η_k , and, for notational convenience, it is denoted as

$$\gamma_k = \gamma(\eta_k).$$

The probability of having a successful packet delivery on the sensing link depends on the current Markov mode $\eta_k = m$, i.e.,

$$\hat{\gamma}_m \triangleq \mathbb{P}(\gamma_k = 1 \mid \eta_k = m), \quad \mathbb{P}(\gamma_k = 0 \mid \eta_k = m) = 1 - \hat{\gamma}_m, \quad (2.3)$$

are the probability that the packet is successfully delivered at time $k \in \mathbb{N}$, and the likelihood of a packet loss occurrence conditioned to $\eta_k = m$, respectively. Fig. 2.2 provides a graphical representation of the FSMC model on the sensing link.

Let $\pi_m(k)$ denote the probability $\mathbb{P}(\eta_k = m)$, for $m \in \mathbb{S}_\eta$, $k \in \mathbb{N}$. The variable $\pi_m(k)$ can also be written through the indicator function $\mathbf{1}_{\{\eta_k=m\}}$, as $\pi_m(k) = \mathbb{E}[\mathbf{1}_{\{\eta_k=m\}}]$, see [4]. Let us introduce $\boldsymbol{\pi}(k)$, given by $\boldsymbol{\pi}(k) = [\pi_m(k)]_{m=1}^I$.

For what concerns the process $\{\gamma_k\}$, applying Bayes Law, the Markov property, and the independence between $\{\gamma_k\}$ and $\{\eta_k\}$, for $m, n \in \mathbb{S}_\eta$, the following equalities hold [92],

$$\begin{aligned} \mathbb{P}(\gamma_{k+1} = 1, \eta_{k+1} = n \mid \eta_k = m) &= \hat{\gamma}_n q_{mn}, \\ \mathbb{P}(\gamma_{k+1} = 0, \eta_{k+1} = n \mid \eta_k = m) &= (1 - \hat{\gamma}_n) q_{mn}. \end{aligned}$$

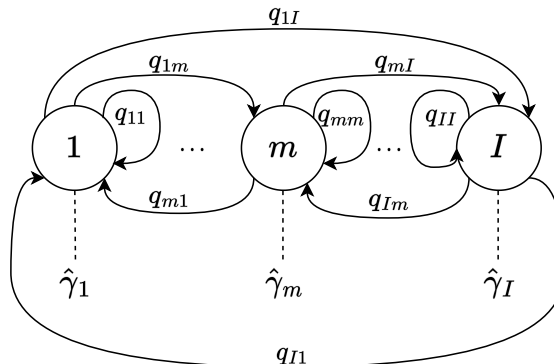


Figure 2.2: FSMC model for sensing link: the Markov chain η_k represents the evolution of the channel, while successful packet delivery and PER come from $\hat{\gamma}_m$, $m \in \mathbb{S}_\eta$.

Actuation FSMC

In the sensing link, the controller is the receiver and has direct access to the channel information (see Remark 2). For the actuation link, the controller is the transmitter and can access the actuation channel information by an acknowledgement message, as the reader may notice in Fig. 2.1. Obviously, the acknowledgement message is received after the transmission, so there is a one time-step delay. Let $u_k \in \mathbb{F}^{n_u}$ denote the control law computed by the controller, and let u_k^c denote the digital control input received by the D/A block at time $k \in \mathbb{N}$. The general model for the actuation link is

$$u_k^c = \nu_k u_k.$$

The value of the random variable ν_k when the current Markov mode is $\theta_k \in \mathbb{S}_\theta$ is a function of θ_k , and, for notational convenience, it is denoted as follows,

$$\nu_k = \nu(\theta_k).$$

The probability of the correct packet delivery on actuation link depends on the current mode of the actuation link, that is, $\theta_k = i$, i.e.,

$$\hat{\nu}_i \triangleq \mathbb{P}(\nu_k = 1 \mid \theta_k = i), \quad \mathbb{P}(\nu_k = 0 \mid \theta_k = i) = 1 - \hat{\nu}_i, \quad (2.4)$$

are the probability that the packet is correctly delivered at time $k \in \mathbb{N}$, and the likelihood that the control packet is lost conditioned to $\theta_k = i$, respectively. Fig. 2.3 provides a graphical representation of the FSMC model on the actuation link.

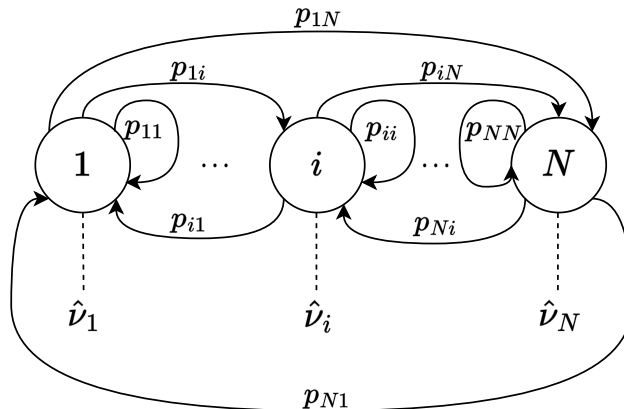


Figure 2.3: FSMC model for actuation link: the Markov chain θ_k represents the evolution of the channel, while successful packet delivery and PER come from \hat{v}_i , $i \in \mathbb{S}_\theta$.

For $i \in \mathbb{S}_\theta$, $k \in \mathbb{N}$, the probability $\mathbb{P}(\theta_k = i)$ is denoted by $\varpi_i(k)$. For $\ell, i \in \mathbb{S}_\theta$, $k \in \mathbb{N}$, the joint probability of being in an augmented Markov state (θ_{k-1}, θ_k) , $\mathbb{P}(\theta_{k-1} = \ell, \theta_k = i)$ is denoted by $\tilde{\varpi}_{\ell i}(k)$. Moreover, the quantity $\tilde{\varpi}_{\ell i}(k)$ may be written using the indicator function $\mathbf{1}_{\{\theta_{k-1}=\ell, \theta_k=i\}}$, as $\tilde{\varpi}_{\ell i}(k) = \mathbb{E}[\mathbf{1}_{\{\theta_{k-1}=\ell, \theta_k=i\}}]$ [4].

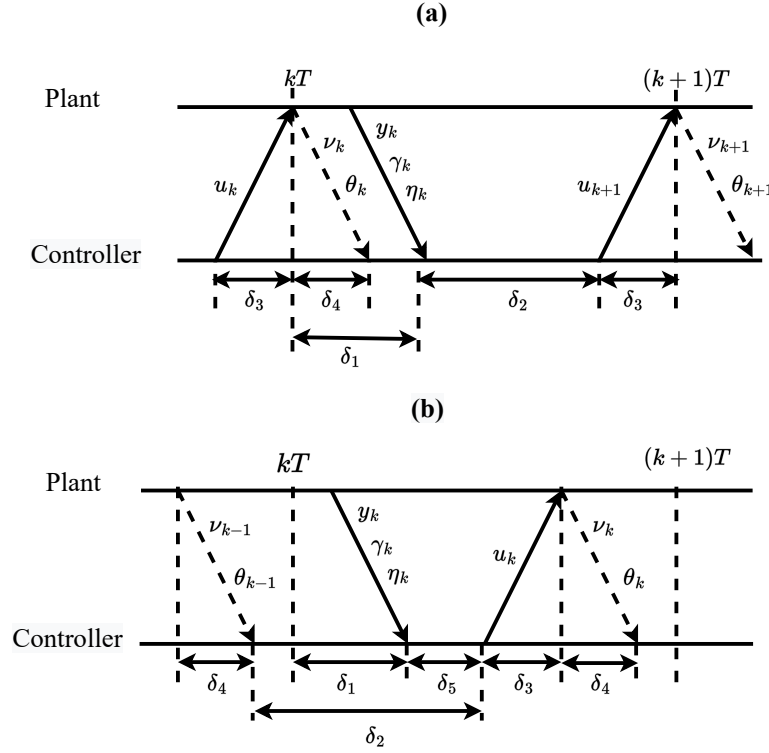
Let us introduce for $k \in \mathbb{N}$, the variable $\tilde{\varpi}(k)$ given by $\tilde{\varpi}(k) = [\tilde{\varpi}_{\ell i}(k)]_{\ell, i=1}^N$. The probability $\tilde{\varpi}_{\ell i}(k)$ evolves according to the following equations, for $\ell, i \in \mathbb{S}_\theta$, $k \in \mathbb{N}$ [79]:

$$\begin{aligned} \mathbb{P}(\theta_{k+1} = j, \theta_k = i \mid \theta_k \neq i, \theta_{k-1} = \ell) &= 0, \\ \mathbb{P}(\theta_{k+1} = j, \theta_k = i \mid \theta_k = i, \theta_{k-1} = \ell) &= p_{ij}. \end{aligned}$$

Recalling that the availability of actuation link mode is affected by one time-step delay, that is, θ_{k-1} (see Fig. 2.1), the aggregated Markov state (θ_k, θ_{k-1}) is considered [79]. This memory introduced by the presented aggregation is fictitious: the aggregated Markov chain satisfies the Markov property of the memoryless chain $\{\theta_k\}$. Moreover, the probabilities of the joint process $(\nu_k, \theta_k, \theta_{k-1})$ can be computed as shown in [79].

2.5 The information set

The scenario depicted in Fig. 2.4 shows the information flow of actuation and sensing data between the plant and the controller, under TCP-like protocols, i.e., in the presence of acknowledgement messages [48]. Transmissions and computations do not happen instantly: as the reader may see in Fig. 2.4, actuation and sensing transmission time (δ_3



- δ_1 Sensing transmission time (from sensors to controller)
- δ_2 Computation time of the controller
- δ_3 Actuation transmission time (from controller to actuators)
- δ_4 Acknowledgment transmission time
- δ_5 Time needed for estimate correction with the current output measurement

Figure 2.4: Information flow timing between the plant and the controller used for the next-step predictor (a) and the current estimator (b).

and δ_1 , respectively) are greater than zero, as well as the control law computation time (denoted by δ_2) and the acknowledgement transmission time δ_4 . Two different scenarios may arise: either the time interval δ_2 needed to the controller for the computations of estimation and control law is comparable to the sampling period T (this may happen when slow computers are used to control high-order systems) or the time needed for the estimation is very small compared to the sampling period [181]. The first case is depicted in Fig. 2.4(a), where the computation time δ_2 is comparable to

the sampling period T . The suitable estimation technique in this case is provided by the next-step predictor, that requires the measurements up through the previous time instant [181, Chapter 8]. By considering the delay δ_1 introduced by the sensing transmission, the controller owns the whole information necessary for the estimation needed in the computation of u_{k+1} exactly at $kT + \delta_1$.

Formally, the information set available to the output-feedback controller for the computation of u_{k+1} , based on the next-step predictor is

$$\mathcal{F}_l^{k+1} = \{(u_t)_{t=0}^k, (y_t)_{t=0}^k, (\nu_t)_{t=0}^k, (\gamma_t)_{t=0}^k\}.$$

The information set \mathcal{F}_l^{k+1} implies that in the next-step predictor-based output-feedback, the control law u_{k+1} does not depend on the most recent observation [181, Chapter 8]. Thus, the estimate vector might not be as accurate as the one obtained with the most recent measurement. For high-order systems controlled by slow computers, or whenever the sampling periods are comparable to the computation time, the time interval between the observation instant and the validity time of the control output allows the computer to complete the calculations [181].

In many systems however, the computation time required to evaluate the estimation is quite short compared to the sampling period (see δ_5 in Fig. 2.4(b)), and the delay of almost a cycle between the measurement and the proper time to apply the resulting control calculation represents an unnecessary waste. Therefore, the controller may exploit the current output measurement to obtain a more accurate state estimation. Fig. 2.4(b) shows the time diagram of a two-step estimation algorithm: the first step predicts the state estimate based on the measurement from the previous time-step, while the following step corrects the predicted estimate by integrating the most recent measurement.

The time needed to perform the last step (concerning the estimate correction and control law computations) denoted by δ_5 , is contained in δ_2 , and its brevity enables the control law transmission within the proper time window, coherently with the scenario described above of a controller with higher performance, [181, Chapter 8]. Notably, the current measurement is used within a different estimation technique (hereafter, current estimator) that provides a more accurate estimated state vector based on the most recent output information.

The information set used for computing the control law u_k during δ_5 , denoted by \mathcal{F}_c^k , collects the information received up through $kT + \delta_1$, as follows,

$$\mathcal{F}_c^k \triangleq \{(u_t)_{t=0}^{k-1}, (y_t)_{t=0}^k, (\nu_t)_{t=0}^{k-1}, (\gamma_t)_{t=0}^k\}.$$

Notice that the current control input based on \mathcal{F}_c^k has access to the most recent observation. Exploiting this additional information considerably increases the performance resulting in lower estimation error cost, as also explained in the following sections.

Remark 5 A natural alternative to the considered estimators is the mode-independent estimator based on Kalman filter described in [48] by Schenato et al., which does not require a channel state estimation, and thus, results in a less complex design.

However, the estimator in [48] may fail to support a stable output-feedback controller over FSMCs, as discussed in the numerical case study.

The necessary condition for a stable mode-independent estimation and control over fading Markov channels is the system should behave well, i.e., it should be Strong-MSD and Strong-MS stabilizable, as detailed in Section 2.11.

2.6 Wireless control network model

Given the system described by (2.1) and actuation and sensing FSMCs, the stochastic system describing the WCN architecture in Fig. 2.1 can be written as follows,

$$\begin{cases} x_{k+1} = Ax_k + \nu_k Bu_k + Gw_k, \\ y_k = \gamma_k Lx_k + \gamma_k Hw_k, \\ z_k = Cx_k + \nu_k Du_k, \end{cases} \quad (2.5)$$

with $z_k \in \mathbb{F}^{n_z}$ (needed to define the performance index of the optimal controller), C and D matrices of appropriate sizes.

Remark 6 Both ν_k and γ_k depend on the corresponding channel mode according to the FSMC model, i.e., $\gamma_k = \gamma(\eta_k)$ and $\nu_k = \nu(\theta_k)$, respectively (see Section 2.4.2). Therefore, let us refer to the system described by (2.5) as MJLS.

2.6.1 Assumptions on wireless control network model

The reader can find the main assumptions on the wireless control network scenario in the following. The noise sequence $\{w_k\}$ is assumed to be independent of the initial state x_0 and the sequences $\{\nu_k\}$ and $\{\gamma_k\}$.

Moreover,

$$\mathbb{E}[w_k] = \mathbf{O}_{n_w}, \quad \mathbb{E}[w_k w_k^*] = \mathbb{I}_{n_w}, \quad \mathbb{E}[w_k w_l^*] = \mathbf{O}_{n_w}, \quad (2.6)$$

For any k, l in \mathbb{N} , $k \neq l$, see also [4].

Without loss of generality, the system matrices are assumed to be constant matrices of appropriate sizes [4, Section 5.2], such that

$$GH^* = 0, \quad HH^* \succ 0, \quad C^*D = 0, \quad D^*D \succ 0. \quad (2.7)$$

Similarly to [4, Section 5.3], the following technical assumptions are provided, for $k \in \mathbb{N}$:

- a.1) initial conditions x_0 , θ_0 , and η_0 are independent random variables,
- a.2) white noise sequence $\{w_k\}$ is independent of initial conditions (x_0, ν_0, γ_0) and of processes $\{\nu(\theta_k)\}$ and $\{\gamma(\eta_k)\}$, for any k ,
- a.3) Markov chains $\{\theta_k\}$, $\{\eta_k\}$ and the noise sequence $\{w_k\}$ are independent,
- a.4) Markov chains $\{\theta_k\}$ and $\{\eta_k\}$ are ergodic, with steady-state probability distributions

$$\begin{aligned} \tilde{\omega}_{\ell i}^{\infty} &\triangleq \lim_{k \rightarrow \infty} \tilde{\omega}_{\ell i}(k), \\ \varpi_i^{\infty} &\triangleq \lim_{k \rightarrow \infty} \varpi_i(k), \\ \pi_m^{\infty} &\triangleq \lim_{k \rightarrow \infty} \pi_m(k), \end{aligned}$$

for $\ell, i \in \mathbb{S}_{\theta}$ and $m \in \mathbb{S}_{\eta}$.

Let us set $\tilde{\omega}^{\infty} = [\tilde{\omega}_{\ell i}^{\infty}]_{\ell, i=1}^N$ and $\pi^{\infty} = [\pi_m^{\infty}]_{m=1}^I$.

This thesis aims to solve, as one of its contributions, the output-feedback control problem over FSMCs with two different estimation techniques guaranteeing the infinite horizon convergence of the state in *MS*. This property is known as *MSS* [4, Definition 3.8, pp. 36–37]. The mean square stability (*MSS*) notion involves the second moment of the state and it is presented in the following.

Definition 1 The MJLS described by (2.5) is MSS if there exist equilibrium points $\hat{\mu}$ and \hat{Q} (independent from initial conditions) such that, for any initial condition (x_0, ν_0, γ_0) , the following equalities are satisfied:

$$\lim_{k \rightarrow \infty} \|\mathbb{E}(x_k) - \hat{\mu}\| = 0, \quad (2.8)$$

$$\lim_{k \rightarrow \infty} \|\mathbb{E}(x_k x_k^*) - \hat{Q}\| = 0. \quad (2.9)$$

2.7 Output-feedback controller

This section shows two alternative output-feedback control systems for the problem formalized in Section 2.2.

Moreover, this section reports the formal definition concerning the structural property of *MS* stabilizability with delay introduced in [79].

2.7.1 Control synthesis based on next-step predictor

Consider the scenario introduced in Fig. 2.4(a) and the related information set \mathcal{F}_l^k , $k \in \mathbb{N}$.

The optimal next-step-predictor-based Markov jump output-feedback control system relying on \mathcal{F}_l^k for the synthesis of u_k is

$$\mathcal{G}_l : \begin{cases} \check{x}_{k+1} = \check{A}(\nu_k, \theta_{k-1}, \gamma_k, \eta_k) \check{x}_k + \check{B}(\eta_k) y_k, \\ u_k = \check{F}(\theta_{k-1}) \check{x}_k, \end{cases} \quad (2.10)$$

with \check{x}_k being the estimated state obtained by the next-step predictor. The controller \mathcal{G}_l (with optimal matrices $\check{A}(\nu_k, \theta_{k-1}, \gamma_k, \eta_k)$, $\check{B}(\eta_k)$, and $\check{F}(\theta_{k-1})$ to be found) should guarantee *MSS* of the closed-loop system (see Definition 1). The sequences of matrices $\check{\mathbf{F}} = [\check{F}(\ell)]_{\ell=1}^N$ and $\check{\mathbf{B}} = [\check{B}(n)]_{n=1}^I$ are the solutions of the optimal control and of the optimal filtering problem, respectively.

2.7.2 Output-feedback controller with current estimator

Consider the scenario in Fig. 2.4(b) and the related information set \mathcal{F}_c^k . The optimal Markov jump output-feedback control system based on the current estimator relies

on \mathcal{F}_c^k for the synthesis of u_k and it is given by

$$\mathcal{G}_c : \begin{cases} \tilde{x}_{k+1} = \hat{A}(\gamma_k, \eta_k) \tilde{x}_k + \hat{B}(\eta_k) y_k + \hat{C}(\nu_k, \theta_{k-1}) \hat{x}_k, \\ \hat{x}_{k+1} = \tilde{x}_{k+1} + \hat{D}(\eta_{k+1}) [y_{k+1} - \gamma_{k+1} L \tilde{x}_{k+1}], \\ u_k = \hat{F}(\theta_{k-1}) \hat{x}_k, \end{cases} \quad (2.11)$$

with \tilde{x}_k and \hat{x}_k , prediction state and correction state at time $k \in \mathbb{N}$, respectively, obtained using the current estimator. The controller \mathcal{G}_c (with optimal matrices $\hat{A}(\gamma_k, \eta_k)$, $\hat{B}(\eta_k)$, $\hat{C}(\nu_k, \theta_{k-1})$, $\hat{D}(\eta_{k+1})$, and $\hat{F}(\theta_{k-1})$ to be found) should guarantee the MSS of the closed-loop system (see Definition 1). The sequences of matrices $\hat{\mathbf{F}} = [\hat{F}(\ell)]_{\ell=1}^N$ and $\hat{\mathbf{D}} = [\hat{D}(n)]_{n=1}^I$ are the solutions of optimal control and filtering problem, respectively.

Remark 7 Both \mathcal{G}_l and \mathcal{G}_c should achieve the MSS of the closed-loop system.

The current estimator provides a valid alternative to the next-step predictor and the proper control strategy should be chosen according to the calculating capacity of the controller. Recall the computation time δ_5 , depicted in Fig. 2.4(b): δ_5 is required for the correction of the predicted estimate. When δ_5 is under a certain threshold, the suitable controller is \mathcal{G}_c , otherwise \mathcal{G}_l should be preferred, as it is also pointed out in Remark 8.

2.7.3 The Linear Quadratic Regulator

The necessary condition for an optimal infinite horizon solution of the wireless control problem is the MS stabilizability with delay. The structural property of MS stabilizability with delay is formally described by the following definition.

Definition 2 (MS stabilizability with delay) The MJLS described by (2.5) is MS stabilizable with one time-step delayed actuation link mode observation if, for any initial condition (x_0, θ_0) , and for each mode $\ell \in \mathbb{S}_\theta$, there exists a mode-dependent gain F_ℓ , such that $u_k = F_{\theta_{k-1}} x_k$ (i.e., the control law with one time-step delay actuation link mode observation) is the MS stabilizing state-feedback for (2.5).

Let $F_\ell \in \mathbb{F}^{n_u \times n_x}$, $\ell \in \mathbb{S}_\theta$, denote the optimal mode-dependent control gain with one time-step delayed operational mode observation of the actuation link (see [79] for the solution of the infinite horizon optimal control problem and [52] for a more general result).

For any $\mathbf{X} = [X_l]_{l=1}^N \in \mathbb{H}^{Nn_x,+}$, $l \in \mathbb{S}_\theta$, let us define $\mathcal{A}_l(\mathbf{X})$ and $\mathcal{C}_l(\mathbf{X})$, as follows:

$$\begin{aligned}\mathcal{A}_l(\mathbf{X}) &\triangleq A^* \left(\sum_{i=1}^N p_{li} X_i \right) A + C^* C, \\ \mathcal{C}_l(\mathbf{X}) &\triangleq A^* \left(\sum_{i=1}^N p_{li} \hat{\nu}_i X_i \right) B,\end{aligned}$$

respectively.

Let us also define $\mathcal{B}_l(\mathbf{X})$ and $\mathcal{X}_l(\mathbf{X})$ as,

$$\begin{aligned}\mathcal{B}_l(\mathbf{X}) &\triangleq \sum_{i=1}^N p_{li} \hat{\nu}_i (B^* X_i B + D^* D), \\ \mathcal{X}_l(\mathbf{X}) &\triangleq \mathcal{A}_l(\mathbf{X}) - \mathcal{C}_l(\mathbf{X}) \mathcal{B}_l^{-1}(\mathbf{X}) \mathcal{C}_l^*(\mathbf{X}),\end{aligned}$$

respectively.

For $l \in \mathbb{S}_\theta$, the set of equations $X_l = \mathcal{X}_l(\mathbf{X})$ is the set of control coupled algebraic Riccati equations (hereafter, control CAREs). The necessary condition for the existence of the *MS* stabilizing solution $\tilde{\mathbf{X}} \in \mathbb{H}^{Nn_x,+}$ of the control CAREs is the *MS* stabilizability with delay of the MJLS described by (2.5) (see Definition 2).

If $\tilde{\mathbf{X}} \in \mathbb{H}^{Nn_x,+}$ is the *MS* stabilizing solution of the control CAREs, then the state-feedback control input $F_{\theta_{k-1}} x_k$ stabilizes the system, with one time-step delay in the observation of the actuation link mode in the *MS* sense (see 79).

The optimal control problem solution is obtained by using the LMI approach 52.

The optimized performance index is given by

$$J_h = \limsup_{t \rightarrow \infty} \frac{1}{t} \mathbb{E} \left[\sum_{k=0}^t (z_k z_k^*) | \mathcal{F}_h^k \right],$$

with z_k in (2.5), $h = L$ for the next-step predictor and $h = C$ for the current estimator. The performance index achieved by the optimal control law is

$$J_h^* = \sum_{i=1}^N \varpi_i^\infty \text{tr} (G^* X_i G).$$

2.8 Estimation techniques

The output-feedback controllers introduced in Section 2.7 rely either on the next-step predictor (\mathcal{G}_l) or on the current estimator (\mathcal{G}_c). The aim of the control law is ensuring

the MSS of the closed-loop system. The aim of each estimator is ensuring MSS of the estimation error dynamical system associated with the chosen estimation technique. The structural property concerning the MSS is formally defined in the following.

Definition 3 The MJLS described by (2.5) is MSD if there exists an estimator such that the corresponding estimation error system is MSS.

Remark 8 For the case in which the information on the output of the system and on the Markov chain are available at each time-step, the best linear estimator of $x(k)$ is the Kalman filter (see [4, Remark 5.2]). In offline computations of the Kalman filter, the solutions of the difference Riccati equations and of the time-varying Kalman gain are sample-path dependent, and the number of sample paths grows exponentially in time. Thus, Kalman filter offline implementation is inadvisable here [180].

On the other hand, an online implementation of the Kalman filter requires online matrix inversions which might have a heavy computational burden. Therefore, this work takes into account a different class of estimators with filtering gains pre-computed offline. This avoids online matrix inversions and reduces the computational burden.

2.8.1 The Markovian next-step predictor

This subsection briefly recalls the Markovian next-step predictor presented in [92], given by

$$\check{\mathcal{G}} : \begin{cases} \check{x}_{k+1} = A\check{x}_k + \nu_k B u_k - \check{M}_{\eta_k} (y_k - \gamma_k L \check{x}_k), \\ u_k = F_{\theta_{k-1}} \check{x}_k, \\ \check{x}(0) = \check{x}_0, \end{cases} \quad (2.12)$$

with \check{M}_m , $m \in \mathbb{S}_\eta$, mode-dependent filtering gain obtained as solution of the next-step predictor filtering problem, which relies on the information set \mathcal{F}_l^k .

Note that when the controller makes the computations for \check{x}_{k+1} , it knows whether the packets containing the control law u_k and the measurement y_k have been received or not. Indeed, this information is contained in \mathcal{F}_l^{k+1} , which is exploited for computing the proper control input to apply at time $k+1$, that is $u_{k+1} = F_{\theta_k} \check{x}_{k+1}$. Let us define the next-step predictor estimation error at time-step $k \in \mathbb{N}$ as $\check{e}_k \triangleq x_k - \check{x}_k$. The error dynamics are derived as follows:

$$\check{e}_{k+1} = (A + \gamma_k \check{M}_{\eta_k} L) \check{e}_k + (G + \gamma_k \check{M}_{\eta_k} H) w_k. \quad (2.13)$$

2.8.2 The Markovian current estimator

The current estimator [181, Chapter 8] over the FSMC results in the following MJLS,

$$\hat{\mathcal{G}} : \begin{cases} \hat{x}_{k+1} = \tilde{x}_{k+1} - \widehat{M}_{\eta_{k+1}} [y_{k+1} - \gamma_{k+1} L \tilde{x}_{k+1}], \\ y_{k+1} = \gamma_{k+1} L x_{k+1} + \gamma_{k+1} H w_{k+1}, \\ u_k = F_{\theta_{k-1}} \hat{x}_k, \end{cases} \quad (2.14)$$

with \widehat{M}_m , $m \in \mathbb{S}_\eta$, mode-dependent filtering gain obtained by solving the current estimator problem that relies on the information set \mathcal{F}_c^k [181]. The variables \tilde{x}_k and \hat{x}_k are the predicted and the estimated state vectors at time-step $k \in \mathbb{N}$, respectively. The current estimator is a two-step estimation algorithm: the first step computes the prediction

$$\tilde{x}_{k+1} = A \hat{x}_k + \nu_k B u_k,$$

based on the measurement from the previous time-step, while the following step corrects the predicted estimate by integrating the most recent measurement. The estimated state vector resulting from this correction with y_{k+1} is \hat{x}_{k+1} .

Define the prediction error at time-step $k \in \mathbb{N}$ as

$$e_k \triangleq x_k - \tilde{x}_k.$$

The resulting estimated state Markov jump system is

$$\hat{x}_{k+1} = \tilde{x}_{k+1} - \gamma_{k+1} \widehat{M}_{\eta_{k+1}} L e_{k+1} - \gamma_{k+1} \widehat{M}_{\eta_{k+1}} H w_{k+1}. \quad (2.15)$$

Remark 9 At time-step $k+1$, the predicted state \tilde{x}_{k+1} is corrected exploiting the prediction error e_{k+1} , through the most recent output measurement.

By substituting \hat{x}_k , obtained from (2.15), in the prediction, the expression of \tilde{x}_{k+1} depends on the prediction error, as follows,

$$\tilde{x}_{k+1} = A \tilde{x}_k + \nu_k B u_k - \gamma_k A \widehat{M}_{\eta_k} L e_k - \gamma_k A \widehat{M}_{\eta_k} H w_k. \quad (2.16)$$

Therefore, the prediction error MJLS is given by

$$e_{k+1} = \left(A + \gamma_k A \widehat{M}_{\eta_k} L \right) e_k + \left(G + \gamma_k A \widehat{M}_{\eta_k} H \right) w_k. \quad (2.17)$$

Define the estimation error for the current estimator as $\hat{e}_k \triangleq x_k - \hat{x}_k$. Consequently, the following equality holds

$$\hat{e}_{k+1} = e_{k+1} + \gamma_{k+1} \widehat{M}_{\eta_{k+1}} L e_{k+1} + \gamma_{k+1} \widehat{M}_{\eta_{k+1}} H w_{k+1}. \quad (2.18)$$

Remark 10 In the next-step predictor, the estimation error coincides with the prediction error. In the current estimator, when the prediction error e_k converges to zero, by (2.18), the estimation error goes to zero. Thus, (2.18) and (2.17) are equivalent at the steady-state.

Remark 11 Neither the control input nor the Markov chain $\{\theta_k\}$ are involved in the MJLSs (2.13) and (2.17). This implies that the optimal mode-dependent next-step predictor gain \check{M}_m and the current estimator gain \widehat{M}_m , $m \in \mathbb{S}_\eta$, can be designed independently from the optimal mode-dependent control gain F_ℓ , $\ell \in \mathbb{S}_\theta$.

2.8.3 Computational complexity

It is well known that the total number of *floating-point operations* or *flops* to carry out the presented estimation algorithms may provide a rough estimate of the computation time [222]. Given the state estimate vector, the number of flops needed for the evaluation of the control law is $O(n_u n_x)$. Moreover, the computational complexity of both the next-step predictor and the current state estimation numerical algorithms is the same: $O(n_x^2 + n_x n_u + n_y + n_x n_y)$.

The physical constraint for estimator implementation is obtained comparing δ_2 (the time needed for all the computations leading to the control law) and the sampling time T . If the condition $\delta_2 < T$ is satisfied, then the next-step predictor represents a viable technique. Under this constraint, if δ_5 (which is shorter than δ_2 as already seen in Section 2.5) is such that the control transmission remains inside the proper time window, the current estimation is feasible and provides a more accurate result.

Remark 12 The physical constraints (concerning the computation time) discussed above provide necessary conditions for implementation. However, taking into account combined packet losses in both communication channels, as well as considering the actuation delay, the infinite horizon output-feedback control is not easy to be modeled and formally solved. Trivially, when all the communication is lost, an unstable plant

cannot be stabilized remotely. The conditions concerning the theoretical existence of the the infinite horizon estimators and controllers operating over FSMCs can be based on the MS detectability and stabilizability notions (discussed in the following sections) guaranteeing a MS stable behavior of estimators and controller with pre-computed gains.

2.9 Observer stability analysis

Let us recall that the *MSD* notion has been introduced by Definition 3 in Section 2.8. This section provides the *MSD* specializations for the next-step predictor and the current estimator, respectively.

2.9.1 The operators

This paragraph introduces the mathematical formalism 4 and the operators, that have been exploited in the WCN investigations leading to the separation principle. Specifically, the operators presented in the following are crucial to formalize the mathematical problem concerning the separation principle over FSMCs. The operators and the mathematical preliminaries introduced in this paragraph are instrumental for the *MSS* analysis 4.

For all $\mathbf{S} = [S_m]_{m=1}^I$, $\mathbf{T} = [T_m]_{m=1}^I$, both in \mathbb{H}^{In_x} , the inner product is given by

$$\langle \mathbf{S}; \mathbf{T} \rangle \triangleq \sum_{m=1}^I \text{tr} (S_m^* T_m).$$

Let us define the operators

$$\begin{aligned} \mathcal{E}(\cdot) &\triangleq [\mathcal{E}_m(\cdot)]_{m=1}^I, \\ \mathcal{D}(\cdot) &\triangleq [\mathcal{D}_m(\cdot)]_{m=1}^I, \\ \mathcal{T}(\cdot) &\triangleq [\mathcal{T}_m(\cdot)]_{m=1}^I, \\ \mathcal{L}(\cdot) &\triangleq [\mathcal{L}_m(\cdot)]_{m=1}^I, \\ \mathcal{V}(\cdot) &\triangleq [\mathcal{V}_m(\cdot)]_{m=1}^I. \end{aligned}$$

all in $\mathbb{B}(\mathbb{H}^{In_x})$, for all $\mathbf{S} = [S_m]_{m=1}^I$ in \mathbb{H}^{In_x} , $m, n \in \mathbb{S}_\eta$, as follows,

$$\mathcal{E}_m(\mathbf{S}) \triangleq \sum_{n=1}^I q_{mn} S_n, \quad \mathcal{D}_n(\mathbf{S}) \triangleq \sum_{m=1}^I q_{mn} S_m, \quad (2.19)$$

$$\mathcal{T}_n(\mathbf{S}) \triangleq \sum_{m=1}^I q_{mn} \left\{ \hat{\gamma}_m \hat{\Gamma}_{m1} S_m \hat{\Gamma}_{m1}^* + (1 - \hat{\gamma}_m) \hat{\Gamma}_{m0} S_m \hat{\Gamma}_{m0}^* \right\}, \quad (2.20)$$

$$\mathcal{L}_m(\mathbf{S}) \triangleq \hat{\gamma}_m \Gamma_{m1}^* \mathcal{E}_m(\mathbf{S}) \Gamma_{m1} + (1 - \hat{\gamma}_m) \Gamma_{m0}^* \mathcal{E}_m(\mathbf{S}) \Gamma_{m0}, \quad (2.21)$$

$$\mathcal{V}_n(\mathbf{S}) \triangleq \hat{\gamma}_n \Gamma_{n1} \mathcal{D}_n(\mathbf{S}) \Gamma_{n1}^* + (1 - \hat{\gamma}_n) \Gamma_{n0} \mathcal{D}_n(\mathbf{S}) \Gamma_{n0}^*, \quad (2.22)$$

where the matrices Γ_{n1} , Γ_{n0} , $\hat{\Gamma}_{n1}$, and $\hat{\Gamma}_{n0}$ are arbitrary matrices in $\mathbb{F}^{n_x \times n_x}$ that will be specialized later in this Chapter, while q_{mn} and $\hat{\gamma}_n$ are those defined by (2.2) and (2.3), respectively.

Let us define the operators \mathcal{O} and $\hat{\mathcal{O}}$, as follows,

- $\mathcal{O}(\cdot, \cdot) : \mathbb{H}^{In_x, n_y} \times \mathbb{R}^I \rightarrow \mathbb{H}^{In_x}$, with $\mathcal{O}(\cdot, \cdot) \triangleq [\mathcal{O}_m(\cdot, \cdot)]_{m=1}^I$,
- $\hat{\mathcal{O}}(\cdot, \cdot) : \mathbb{H}^{In_x, n_y} \times \mathbb{R}^I \rightarrow \mathbb{H}^{In_x}$, with $\hat{\mathcal{O}}(\cdot, \cdot) \triangleq [\hat{\mathcal{O}}_m(\cdot, \cdot)]_{m=1}^I$,

for $\mathbf{M} \triangleq [M_n]_{n=1}^I$ arbitrary matrix in \mathbb{H}^{In_x, n_y} , and $\boldsymbol{\alpha} = [\alpha_n]_{n=1}^I$ arbitrary vector in \mathbb{R}^I , $n \in \mathbb{S}_\eta$, as

$$\mathcal{O}_n(\mathbf{M}, \boldsymbol{\alpha}) \triangleq \alpha_n (GG^* + \hat{\gamma}_n M_n H H^* M_n^*), \quad (2.23)$$

$$\hat{\mathcal{O}}_n(\mathbf{M}, \boldsymbol{\alpha}) \triangleq \sum_{m=1}^I q_{mn} \alpha_m (GG^* + \hat{\gamma}_m A M_m H H^* M_m^* A^*). \quad (2.24)$$

Given $\mathcal{K}_{m\kappa} = \bar{\Gamma}_{m\kappa} \otimes \Gamma_{m\kappa}$, $\kappa = 0, 1$, define the matrices \mathcal{N} and \mathcal{C} , both in $\mathbb{F}^{In_x^2 \times In_x^2}$, as,

$$\mathcal{N} \triangleq \bigoplus_{m=1}^I (\hat{\gamma}_m \mathcal{K}_{m1}) + \bigoplus_{m=1}^I ((1 - \hat{\gamma}_m) \mathcal{K}_{m0}), \quad \mathcal{C} \triangleq Q' \otimes \mathbb{I}_{n_x^2}. \quad (2.25)$$

Remark 13 The matrices \mathcal{N} and \mathcal{C} are designed with the aim of providing a suitable methodology for the test of detectability conditions in Definitions 4 and 5, as will be discussed later. However, even though the aim is the same as in 4, differently from 4, \mathcal{N} and \mathcal{C} account for the general FSMC scenario, i.e., they involve the probability $\hat{\gamma}_m$, $m \in \mathbb{S}_\eta$.

Proposition 1 Consider the operators \mathcal{T} , \mathcal{L} , \mathcal{V} in $\mathbb{B}(\mathbb{H}^{In_x})$, defined in (2.20), (2.21), and (2.22), respectively. Then, the following statements hold.

i) The spectral radius of the operator \mathcal{L} is equal to the spectral radius of the operator \mathcal{V} , i.e., $\rho(\mathcal{L}) = \rho(\mathcal{V})$,

ii) if $\widehat{\Gamma}_{m0} = \Gamma_{m0}$ and $\widehat{\Gamma}_{m1} = \Gamma_{m1}$ for all $m \in \mathbb{S}_\eta$, then $\rho(\mathcal{L}) = \rho(\mathcal{V}) = \rho(\mathcal{T})$.

Proof 1 (Proof of Proposition 1) See Appendix A.

Remark 14 Proposition 1 shows the equivalence of operators \mathcal{V} , \mathcal{T} , and \mathcal{L} , concerning the spectral radius [4, Chapter 3].

2.9.2 Next-step predictor stability analysis

The next-step predictor stability analysis is based on the infinite horizon solution of filtering CAREs, which are derived as on the asymptotic solution of difference Riccati equations and obtained by defining the first and second moments of the error $\check{e}_k, k \in \mathbb{N}$, as follows,

$$\check{m}_n(k) \triangleq \mathbb{E} \left[\check{e}_k \mathbf{1}_{\{\eta_{k-1}=n\}} \right], \quad \check{\mathbf{m}}(k) \triangleq \left[\check{m}_n(k) \right]_{n=1}^I \in \mathbb{F}^{In_x}, \quad (2.26)$$

$$\check{Y}_n(k) \triangleq \mathbb{E} \left[\check{e}_k \check{e}_k^* \mathbf{1}_{\{\eta_{k-1}=n\}} \right], \quad \check{\mathbf{Y}}(k) \triangleq \left[\check{Y}_n(k) \right]_{n=1}^I \in \mathbb{H}^{In_x,+}, \quad (2.27)$$

for $n \in \mathbb{S}_\eta$.

Consequently,

- the expected value of the next-step predictor estimation error \check{e}_k is given by

$$\mathbb{E}[\check{e}_k] = \sum_{n=1}^I \check{m}_n(k),$$

- the mean square of the next-step predictor estimation error is given by

$$\mathbb{E}[\check{e}_k \check{e}_k^*] = \sum_{n=1}^I \check{Y}_n(k).$$

For arbitrary matrices Γ_{n1} and Γ_{n0} in $\mathbb{F}^{n_x \times n_x}$, $n \in \mathbb{S}_\eta$, define $\check{\mathcal{B}} \in \mathbb{F}^{In_x \times In_x}$ as

$$\check{\mathcal{B}} \triangleq \left(\left(\bigoplus_{n=1}^I (\hat{\gamma}_n \Gamma_{n1}) \right) + \left(\bigoplus_{n=1}^I ((1 - \hat{\gamma}_n) \Gamma_{n0}) \right) \right) (Q' \otimes \mathbb{I}_{n_x}). \quad (2.28)$$

Define also the sequence of matrices given by $\check{\mathbf{M}} \triangleq [\check{M}_m]_{m=1}^I$, i.e., the sequence of mode-dependent filtering gains in (2.12) providing the solution of the next-step predictor filtering problem. Hence, the following statement can be proved.

Proposition 2 Consider the error system described by (2.13). Then, for all $k \in \mathbb{N}$, the following equalities hold:

$$\check{\mathbf{m}}(k+1) = \check{\mathbf{B}}\check{\mathbf{m}}(k), \quad \check{\mathbf{Y}}(k+1) = \mathcal{V}(\check{\mathbf{Y}}(k)) + \mathcal{O}(\check{\mathbf{M}}, \boldsymbol{\pi}(k)), \quad (2.29)$$

with $\check{\mathbf{B}}$, \mathcal{V} , and \mathcal{O} defined in (2.28), (2.22) and (2.23), for $\Gamma_{n0} = A$ and $\Gamma_{n1} = A + \check{M}_n L$, $n \in \mathbb{S}_\eta$.

Proof 2 (Proof of Proposition 2) See Appendix A.

The following definition provides a specialization of Definition 3 for the next-step predictor scenario.

Definition 4 (MSD) The MJLS described by (2.5) is MSD if, for each Markov mode $n \in \mathbb{S}_\eta$, there exists a mode-dependent filtering gain $\check{M}_n \in \mathbb{F}^{n_x \times n_y}$, such that $\rho(\mathcal{V}) < 1$, $\mathcal{V} \in \mathbb{B}(\mathbb{H}^{I n_x})$ defined in (2.22), for $\Gamma_{n1} = A + \check{M}_n L$ and $\Gamma_{n0} = A$.

From now on, the expression *MSD* will refer to Definition 4.

Remark 15 By applying the results from [4, Section 3.4.2], the property provided by Definition 4 is equivalent to the MSS of the error system (2.13) obtained for the next-step predictor.

2.9.3 Current estimator stability analysis

Analogous steps for the next-step predictor stability analysis can be applied to the current estimator and they are reported in the following.

Let us define for $n \in \mathbb{S}_\eta$, $k \in \mathbb{N}$, $m_n(k)$ and $Z_n(k)$, as follows,

$$m_n(k) \triangleq \mathbb{E} [e_k \mathbf{1}_{\{\eta_k=n\}}], \quad \mathbf{m}(k) \triangleq [m_n(k)]_{n=1}^I \in \mathbb{F}^{I n_x}, \quad (2.30)$$

$$Z_n(k) \triangleq \mathbb{E} [e_k e_k^* \mathbf{1}_{\{\eta_k=n\}}], \quad \mathbf{Z}(k) \triangleq [Z_n(k)]_{n=1}^I \in \mathbb{H}^{I n_x, +}. \quad (2.31)$$

Consequently,

- the expectation of the prediction error is given by

$$\mathbb{E}[e_k] = \sum_{n=1}^I m_n(k),$$

- the mean square of the prediction error is given by

$$\mathbb{E}[e_k e_k^*] = \sum_{n=1}^I Z_n(k).$$

For arbitrary matrices $\hat{\Gamma}_{n1}$ and $\hat{\Gamma}_{n0} \in \mathbb{F}^{n_x \times n_x}$, $n \in \mathbb{S}_\eta$, define $\hat{\mathcal{B}} \in \mathbb{F}^{In_x \times In_x}$ as

$$\hat{\mathcal{B}} \triangleq (Q' \otimes \mathbb{I}_{n_x}) \left(\bigoplus_{n=1}^I (\hat{\gamma}_n \hat{\Gamma}_{n1}) + \bigoplus_{n=1}^I ((1 - \hat{\gamma}_n) \hat{\Gamma}_{n0}) \right). \quad (2.32)$$

Let us define the sequence of matrices given by $\hat{\mathbf{M}} = [\hat{M}_m]_{m=1}^I$, that is, a sequence of mode-dependent filtering gains in (2.14) providing the solution of the filtering problem in the current estimator setup.

The following proposition formalizes the dynamics of the observation error first and second moments.

Proposition 3 Consider the error system described by (2.17). Then, for all $k \in \mathbb{N}$, the following equalities hold:

$$\mathbf{m}(k+1) = \hat{\mathcal{B}}\mathbf{m}(k), \quad \mathbf{Z}(k+1) = \mathcal{T}(\mathbf{Z}(k)) + \hat{\mathcal{O}}(\hat{\mathbf{M}}, \boldsymbol{\pi}(k)), \quad (2.33)$$

with $\hat{\mathcal{B}}$, \mathcal{T} , and $\hat{\mathcal{O}}$ defined in (2.32), (2.20), and (2.24), respectively, for $\hat{\Gamma}_{n1} = A + A\hat{M}_n L$ and $\hat{\Gamma}_{n0} = A$, $n \in \mathbb{S}_\eta$.

Proof 3 (Proof of Proposition 3) See Appendix A.

The following definition adapts Definition 3 to the current estimator scenario.

Definition 5 (Strict-MSD) The MJLS described by (2.5) is Strict-MSD if, for each Markov mode $n \in \mathbb{S}_\eta$, there exists a mode-dependent filtering gain $\hat{M}_n \in \mathbb{F}^{n_x \times n_y}$, such that $\rho(\mathcal{T}) < 1$, with $\mathcal{T} \in \mathbb{B}(\mathbb{H}^{In_x})$ defined in (2.20), for $\hat{\Gamma}_{n1} = A + A\hat{M}_n L$ and $\hat{\Gamma}_{n0} = A$.

Proposition 4 Assume that the MJLS described by (2.5) is Strict-MSD. Then, (2.5) is MSD according to Definition 4.

Proof 4 (Proof Proposition 4) See Appendix A.

Remark 16 By the results from [4, Section 3.4.2] applied to the operator \mathcal{T} (with \mathcal{T} as in Definition 5), the condition on the spectral radius of the operator \mathcal{T} , i.e., $\rho(\mathcal{T}) < 1$, is equivalent to the property of the MSS of the error system described by (2.17).

2.9.4 The next-step predictor filtering coupled algebraic Riccati equations

In the next-step predictor setup, the optimal mode-dependent filtering gain results from the optimization of the following performance index:

$$J_L^* = \limsup_{t \rightarrow \infty} \frac{1}{t} \mathbb{E} \left[\sum_{k=0}^t (\check{e}_k \check{e}_k^* | \mathcal{F}_l^k) \right].$$

Obtaining the optimal performance index in the next-step predictor scenario necessitates dealing with next-step predictor filtering CAREs, introduced as follows.

Let us define for any $\mathbf{Y} \in \mathbb{H}^{I n_x, *}$ and $\boldsymbol{\alpha} = [\alpha_n]_{n=1}^I \in \mathbb{R}^I$, the following operators,

$$\begin{aligned} \check{\mathcal{A}}_n(\mathbf{Y}, \boldsymbol{\alpha}) &\triangleq AD_n(\mathbf{Y})A^* + \alpha_n GG^*, \\ \check{\mathcal{B}}_n(\mathbf{Y}) &\triangleq AD_n(\mathbf{Y})L^*, \\ \check{\mathcal{R}}_n(\mathbf{Y}, \boldsymbol{\alpha}) &\triangleq \alpha_n HH^* + LD_n(\mathbf{Y})L^*, \\ \check{\mathcal{C}}_n(\mathbf{Y}) &\triangleq \hat{\gamma}_n^{\frac{1}{2}} \check{\mathcal{B}}_n(\mathbf{Y}), \end{aligned}$$

for $n \in \mathbb{S}_\eta$.

Consider the set \mathbb{W} , defined as follows:

$$\mathbb{W} = \{(\mathbf{Y}, \boldsymbol{\alpha}) \in \mathbb{H}^{I n_x, *} \times \mathbb{R}^I, \text{ such that } \check{\mathcal{R}}_n(\mathbf{Y}, \boldsymbol{\alpha}) \text{ is non-singular for any } n \in \mathbb{S}_\eta\}.$$

For $(\mathbf{Y}, \boldsymbol{\alpha}) \in \mathbb{W}$, define the operators

$$\begin{aligned} \mathcal{M}(\cdot, \cdot) &: \mathbb{W} \rightarrow \mathbb{H}^{I n_x, n_y}, \\ \mathcal{Y}(\cdot, \cdot) &: \mathbb{W} \rightarrow \mathbb{H}^{I n_x}, \end{aligned}$$

as

$$\begin{aligned} \mathcal{M}(\mathbf{Y}, \boldsymbol{\alpha}) &= [\mathcal{M}_n(\mathbf{Y}, \boldsymbol{\alpha})]_{n=1}^I, \\ \mathcal{Y}(\mathbf{Y}, \boldsymbol{\alpha}) &= [\mathcal{Y}_n(\mathbf{Y}, \boldsymbol{\alpha})]_{n=1}^I, \end{aligned}$$

with

$$\mathcal{M}_n(\mathbf{Y}, \boldsymbol{\alpha}) \triangleq -\check{\mathcal{B}}_n(\mathbf{Y}) \check{\mathcal{R}}_n^{-1}(\mathbf{Y}, \boldsymbol{\alpha}), \quad (2.34)$$

$$\mathcal{Y}_n(\mathbf{Y}, \boldsymbol{\alpha}) \triangleq \check{\mathcal{A}}_n(\mathbf{Y}, \boldsymbol{\alpha}) - \check{\mathcal{C}}_n(\mathbf{Y}) \check{\mathcal{R}}_n^{-1}(\mathbf{Y}, \boldsymbol{\alpha}) \check{\mathcal{C}}_n^*(\mathbf{Y}), \quad (2.35)$$

for any $n \in \mathbb{S}_\eta$ (see [4] Section A.1)].

For notational convenience, let us set $\mathcal{M}(\mathbf{Y}) = \mathcal{M}(\mathbf{Y}, \boldsymbol{\pi}^\infty)$, $\mathcal{Y}(\mathbf{Y}) = \mathcal{Y}(\mathbf{Y}, \boldsymbol{\pi}^\infty)$, and, for $n \in \mathbb{S}_\eta$, $\check{\mathcal{R}}_n(\mathbf{Y}) = \check{\mathcal{R}}_n(\mathbf{Y}, \boldsymbol{\pi}^\infty)$, $\check{\mathcal{A}}_n(\mathbf{Y}) = \check{\mathcal{A}}_n(\mathbf{Y}, \boldsymbol{\pi}^\infty)$.

In the next-step predictor setting, the filtering CAREs are the set of equations given by

$$Y_n = \mathcal{Y}_n(\mathbf{Y}), \quad n \in \mathbb{S}_\eta. \quad (2.36)$$

The optimal infinite horizon mode-dependent filtering gain is obtained from the solution of the following optimization problem:

$$\max \operatorname{tr} \left(\sum_{n=1}^I Y_n \right) \quad (2.37a)$$

subject to

$$\begin{bmatrix} -Y_n + \check{\mathcal{A}}_n(\mathbf{Y}) & \check{\mathcal{C}}_n(\mathbf{Y}) \\ \check{\mathcal{C}}_n^*(\mathbf{Y}) & \check{\mathcal{R}}_n(\mathbf{Y}) \end{bmatrix} \succeq 0, \quad (2.37b)$$

$$\check{\mathcal{R}}_n(\mathbf{Y}) \succ 0, \quad \mathbf{Y} \in \mathbb{H}^{I n_x, *}, \quad n \in \mathbb{S}_\eta. \quad (2.37c)$$

Define the sets \mathbb{L} and \mathbb{M} as follows,

$$\begin{aligned} \mathbb{L} &\triangleq \{ \mathbf{Y} \in \mathbb{H}^{I n_x, *}; \check{\mathcal{R}}_n(\mathbf{Y}) \text{ non-singular for any } n \in \mathbb{S}_\eta \}, \\ \mathbb{M} &\triangleq \{ \mathbf{Y} \in \mathbb{L}; \check{\mathcal{R}}(\mathbf{Y}) \succ 0 \text{ and } -\mathbf{Y} + \mathcal{Y}(\mathbf{Y}) \succeq 0 \}. \end{aligned}$$

Then, the *MS* stabilizing filtering gain is given by

$$\check{M}_n = \mathcal{M}_n(\mathbf{Y}), \quad n \in \mathbb{S}_\eta, \quad (2.38)$$

where $\mathbf{Y} \in \mathbb{L}$ is the *MS* stabilizing solution of (2.36) [4] Section A.1].

Definition 6 (*MS stabilizing solution of (2.36)*) $\mathbf{Y} \in \mathbb{L}$ is the *MS* stabilizing solution of the filtering CAREs (2.36) if it satisfies (2.36) and $\rho(\mathcal{V}) < 1$, with $\mathcal{V} \in \mathbb{B}(\mathbb{H}^{I n_x})$ defined in (2.22), for $\Gamma_{n1} = A + \mathcal{M}_n(\mathbf{Y})L$ and $\Gamma_{n0} = A$, $n \in \mathbb{S}_\eta$; i.e., $\mathcal{M}_n(\mathbf{Y})$ stabilizes the error system (2.13) in the *MS* sense.

The maximal solution of equations (2.36) and the solution of the optimization problem presented in (2.37) coincide, as stated in the following theorem.

Theorem 1 Assume that the MJLS described by (2.5) is MSD.

Then, the following statements are equivalent:

i) there exists $\mathbf{Y}^+ \in \mathbb{M}$ satisfying the filtering CAREs (2.36), such that $\mathbf{Y}^+ \succeq \mathbf{Y}$, for all $\mathbf{Y} \in \mathbb{M}$,

ii) there exists a solution $\hat{\mathbf{Y}}$ for the convex programming problem described in (2.37).

Moreover, the two solutions coincide, i.e., $\hat{\mathbf{Y}} = \mathbf{Y}^+$.

Proof 5 (Proof of Theorem 1) See Appendix A.

The maximal solution and the *MS* stabilizing solution of the filtering CAREs (2.36) are connected, as stated in the following theorem.

Theorem 2 There exists at most one MS stabilizing solution of the filtering CAREs (2.36), which coincides with the maximal solution in the set \mathbb{M} , that is, the solution of the convex programming problem described in (2.37).

Proof 6 (Proof of Theorem 2) See Appendix A.

The *MS* stabilizing filtering gain (2.38) is computed exploiting the maximal solution of the filtering CAREs (2.36), i.e., the solution of the convex programming problem (2.37), as stated in Theorem 2.

Consequently, the optimal performance index achieved by the next-step predictor is

$$J_L^* = \sum_{m=1}^I \text{tr}(Y_m),$$

with $\mathbf{Y} = [Y_m]_{m=1}^I$ being the maximal solution of the filtering CAREs (2.36). The necessary condition for the existence of the *MS* stabilizing solution of the filtering CAREs is the *MSD* of system (2.5).

2.9.5 The current estimator filtering coupled algebraic Riccati equations

The optimal mode-dependent filtering gain of the current estimator results from the optimization of the following performance index,

$$J_C^* = \limsup_{t \rightarrow \infty} \frac{1}{t} \mathbb{E} \left[\sum_{k=0}^t (e_k e_k^*) \mid \mathcal{F}_c^k \right].$$

Remark 17 The current estimator performance index J_C^* (computed exploiting the prediction error) can be compared to the next-step predictor performance index J_L^* (computed exploiting the estimation error) because the estimation error for the next-step predictor and the prediction error for the current estimator are equivalent at the steady-state, see Remark 10.

For $\mathbf{Z} = [Z_m]_{m=1}^I \in \mathbb{H}^{In_x, *}$ and $\boldsymbol{\alpha} = [\alpha_n]_{n=1}^I \in \mathbb{R}^I$, define $\widehat{\mathcal{A}}_n(\mathbf{Z}, \boldsymbol{\alpha})$, $\widehat{\mathcal{R}}_n(\mathbf{Z}, \boldsymbol{\alpha})$, and $\widehat{\mathcal{C}}_n(\mathbf{Z})$, as

$$\begin{aligned}\widehat{\mathcal{A}}_n(\mathbf{Z}, \boldsymbol{\alpha}) &\triangleq AZ_nA^* + \alpha_n GG^*, \\ \widehat{\mathcal{R}}_n(\mathbf{Z}, \boldsymbol{\alpha}) &\triangleq LZ_nL^* + \alpha_n HH^*, \\ \widehat{\mathcal{C}}_n(\mathbf{Z}) &\triangleq AZ_nL^*,\end{aligned}$$

for $n \in \mathbb{S}_\eta$.

Consider the set \mathbb{W}_c , defined as follows,

$$\mathbb{W}_c = \{(\mathbf{Z}, \boldsymbol{\alpha}) \in \mathbb{H}^{In_x, *} \times \mathbb{R}^I, \text{ such that } \widehat{\mathcal{R}}_n(\mathbf{Z}, \boldsymbol{\alpha}) \text{ is non-singular for any } n \in \mathbb{S}_\eta\}.$$

For $(\mathbf{Z}, \boldsymbol{\alpha}) \in \mathbb{W}_c$, let us define the operators

$$\begin{aligned}\mathcal{Z}(\cdot, \cdot) &: \mathbb{W}_c \rightarrow \mathbb{H}^{In_x}, \\ \widehat{\mathcal{M}}(\cdot, \cdot) &: \mathbb{W}_c \rightarrow \mathbb{H}^{In_x, n_y},\end{aligned}$$

as follows [4, Section A.1],

$$\begin{aligned}\mathcal{Z}(\mathbf{Z}, \boldsymbol{\alpha}) &= [\mathcal{Z}_n(\mathbf{Z}, \boldsymbol{\alpha})]_{n=1}^I, \\ \mathcal{Z}_n(\mathbf{Z}, \boldsymbol{\alpha}) &\triangleq \sum_{m=1}^I q_{mn} \{ \widehat{\mathcal{A}}_m(\mathbf{Z}, \boldsymbol{\alpha}) - \hat{\gamma}_m \widehat{\mathcal{C}}_m(\mathbf{Z}) \widehat{\mathcal{R}}_m^{-1}(\mathbf{Z}, \boldsymbol{\alpha}) \widehat{\mathcal{C}}_m^*(\mathbf{Z}) \}, \\ \widehat{\mathcal{M}}(\mathbf{Z}, \boldsymbol{\alpha}) &= [\widehat{\mathcal{M}}_n(\mathbf{Z}, \boldsymbol{\alpha})]_{n=1}^I, \\ \widehat{\mathcal{M}}_n(\mathbf{Z}, \boldsymbol{\alpha}) &\triangleq -Z_n L^* \widehat{\mathcal{R}}_n^{-1}(\mathbf{Z}, \boldsymbol{\alpha}).\end{aligned}$$

For notational convenience, let us set $\widehat{\mathcal{M}}(\mathbf{Z}) = \widehat{\mathcal{M}}(\mathbf{Z}, \boldsymbol{\pi}^\infty)$ and $\mathcal{Z}(\mathbf{Z}) = \mathcal{Z}(\mathbf{Z}, \boldsymbol{\pi}^\infty)$.

The following equations are the current estimator filtering CAREs:

$$\mathcal{Z}_n(\mathbf{Z}) \triangleq \sum_{m=1}^I q_{mn} \{ \widehat{\mathcal{A}}_m(\mathbf{Z}, \boldsymbol{\pi}^\infty) - \hat{\gamma}_m \widehat{\mathcal{C}}_m(\mathbf{Z}) \widehat{\mathcal{R}}_m^{-1}(\mathbf{Z}, \boldsymbol{\pi}^\infty) \widehat{\mathcal{C}}_m^*(\mathbf{Z}) \}, \quad (2.39)$$

$$\widehat{\mathcal{M}}_n(\mathbf{Z}, \boldsymbol{\pi}^\infty) \triangleq -Z_n L^* \widehat{\mathcal{R}}_n^{-1}(\mathbf{Z}, \boldsymbol{\pi}^\infty). \quad (2.40)$$

The following lemma states the equivalence of the filtering CAREs solutions and the filtering gains, for the next-step predictor and the current estimator.

Lemma 1 The following statements are equivalent:

- i) For any $\mathbf{Y}(0) \in \mathbb{H}^{I n_x, +}$, $\mathbf{Y}(k) \in \mathbb{H}^{I n_x, +}$, $k \in \mathbb{N}$, satisfying $\mathbf{Y}(k+1) = \mathcal{Y}(\mathbf{Y}(k), \boldsymbol{\pi}(k))$, with \mathcal{Y} defined in (2.35), converges to $\mathbf{Y} \in \mathbb{H}^{I n_x, +}$ satisfying $\mathbf{Y} = \mathcal{Y}(\mathbf{Y})$.
- ii) For any $\mathbf{Z}(0) \in \mathbb{H}^{I n_x, +}$, $\mathbf{Z}(k) \in \mathbb{H}^{I n_x, +}$, $k \in \mathbb{N}$, satisfying $\mathbf{Z}(k+1) = \mathcal{Z}(\mathbf{Z}(k), \boldsymbol{\pi}(k))$, converges to $\mathbf{Z} \in \mathbb{H}^{I n_x, +}$ satisfying $\mathbf{Z} = \mathcal{Z}(\mathbf{Z})$.

Moreover, the mode-dependent filtering gain that stabilizes the error system (2.17) in the MS sense is $\widehat{M}_n = \widehat{M}_n(\mathbf{Z})$, and the optimal performance index achieved by the current estimator is $J_C^* = \sum_{n=1}^I \text{tr}(Z_n)$, with $\mathbf{Z} = [Z_n]_{n=1}^I \in \mathbb{H}^{I n_x}$, Z_n given by $Z_n = \mathcal{D}_n(\mathbf{Y})$, $n \in \mathbb{S}_\eta$, and \mathbf{Y} maximal solution of (2.36).

Proof 7 (Proof of Lemma 1) See Appendix A.

Remark 18 The next-step predictor and the current estimator are equivalent from the steady-state point of view, as stated in Lemma 1. However, their difference in performance (indicated by the indexes J_L and J_C) and physical constraints (see Remark 12) allow for choosing the most suitable estimator for a specific scenario, as shown in Sections 2.5 and 2.8.3.

Remark 19 If the matrix A is non-singular, then, from Lemma 1, the next-step predictor filtering gain can be computed as follows, $\check{M}_n = A^{-1} \widehat{M}_n$.

2.10 The separation principle

This paragraph illustrates the statements of the separation principle for the next-step predictor and the current estimator scenarios, respectively.

2.10.1 The next-step predictor separation principle

Consider the optimal matrices in (2.10), that can be written as follows:

$$\begin{aligned} \check{A}(\nu_k, \theta_{k-1}, \gamma_k, \eta_k) &= A + \nu_k B F_{\theta_{k-1}} + \gamma_k \check{M}_{\eta_k} L, \\ \check{B}(\eta_k) &= -\check{M}_{\eta_k}, \quad \check{F}(\theta_{k-1}) = F_{\theta_{k-1}}. \end{aligned}$$

Then, the optimal output-feedback controller (2.10) coincides with (2.12), and the closed-loop system dynamics are

$$x_{k+1} = (A + \nu_k B F_{\theta_{k-1}}) x_k - \nu_k B F_{\theta_{k-1}} \check{e}_k + G w_k. \quad (2.41)$$

Recalling the error dynamics described in (2.13), the closed-loop system is described as follows,

$$\check{\mathcal{G}}_{cl} : \mathcal{E}_{k+1} = \mathbf{\Gamma}(\nu_k, \theta_{k-1}, \gamma_k, \eta_k) \mathcal{E}_k + \mathbf{\Sigma}(\gamma_k, \eta_k) w_k, \quad (2.42)$$

$$\begin{aligned} \mathcal{E}_k &\triangleq \begin{bmatrix} x_k \\ \check{e}_k \end{bmatrix}, & \mathbf{\Sigma}(\gamma_k, \eta_k) &\triangleq \begin{bmatrix} G \\ G + \gamma_k \check{M}_{\eta_k} H \end{bmatrix}, \\ \mathbf{\Gamma}(\nu_k, \theta_{k-1}, \gamma_k, \eta_k) &\triangleq \begin{bmatrix} (A + \nu_k B F_{\theta_{k-1}}) & -\nu_k B F_{\theta_{k-1}} \\ \mathbb{O}_{n_x} & (A + \gamma_k \check{M}_{\eta_k} L) \end{bmatrix}. \end{aligned}$$

Theorem 3 Given the MJLS described by (2.5) and the next-step predictor described by (2.12), the following statements are equivalent:

- i) the closed-loop system dynamics (2.41) can be made MSS;
- ii) the MJLS described by (2.5) is both
 - ii-a) MSD,
 - ii-b) MS stabilizable with one time-step delayed observation of actuation link mode.

Proof 8 (Proof of Theorem 3) See Appendix A.

2.10.2 The current estimator separation principle

Consider the optimal matrices in (2.11), that can be written as follows:

$$\begin{aligned} \hat{A}(\gamma_k, \eta_k) &\triangleq A + \gamma_k A \hat{M}_{\eta_k} L, & \hat{B}(\eta_k) &\triangleq -A \hat{M}_{\eta_k}, \\ \hat{F}(\theta_{k-1}) &\triangleq F_{\theta_{k-1}}, & \hat{C}(\nu_k, \theta_{k-1}) &\triangleq \nu_k B F_{\theta_{k-1}}, & \hat{D}(\eta_k) &\triangleq -\hat{M}_{\eta_k}. \end{aligned}$$

Then, (2.14)-(2.16) coincide with (2.11), and the dynamics of the closed-loop system are the following:

$$\begin{aligned} x_{k+1} &= \left(A + \nu_k B F_{\theta_{k-1}} \right) x_k + \left(G - \gamma_k \nu_k B F_{\theta_{k-1}} \widehat{M}_{\eta_k} H \right) w_k \\ &\quad - \left(\nu_k B F_{\theta_{k-1}} + \gamma_k \nu_k B F_{\theta_{k-1}} \widehat{M}_{\eta_k} L \right) e_k. \end{aligned} \quad (2.43)$$

By recalling the error dynamics described in (2.17), the closed-loop system is written in a compact form, as follows:

$$\begin{aligned} \widehat{\mathcal{G}}_{cl} : \mathcal{X}_{k+1} &= \Psi(\nu_k, \theta_{k-1}, \gamma_k, \eta_k) \mathcal{X}_k + \Omega(\nu_k, \theta_{k-1}, \gamma_k, \eta_k) w_k, \\ \text{with } \Psi(\nu_k, \theta_{k-1}, \gamma_k, \eta_k) &\triangleq \begin{bmatrix} (A + \nu_k B F_{\theta_{k-1}}) & -(\nu_k B F_{\theta_{k-1}} + \gamma_k \nu_k B F_{\theta_{k-1}} \widehat{M}_{\eta_k} L) \\ \mathbb{O}_{n_x} & (A + \gamma_k A \widehat{M}_{\eta_k} L) \end{bmatrix}, \\ \mathcal{X}_k &\triangleq \begin{bmatrix} x_k \\ e_k \end{bmatrix}, \quad \Omega(\nu_k, \theta_{k-1}, \gamma_k, \eta_k) \triangleq \begin{bmatrix} G - \gamma_k \nu_k B F_{\theta_{k-1}} \widehat{M}_{\eta_k} H \\ G + \gamma_k A \widehat{M}_{\eta_k} H \end{bmatrix}. \end{aligned}$$

Remark 20 The matrices $\Psi(\nu_k, \theta_{k-1}, \gamma_k, \eta_k)$ and $\Gamma(\nu_k, \theta_{k-1}, \gamma_k, \eta_k)$ are upper triangular block diagonal matrices as in [4], i.e., the error dynamics (driven by $\{\eta_k\}$) do not depend on the state dynamics (induced by $\{\theta_k\}$). Differently from [4], the closed-loop dynamical matrices Γ and Ψ contain the Markov jumps not only of the Markov chain $\{\eta_k\}$ (sensing link mode observation) but of the Markov chain $\{\theta_k\}$ (actuation link dynamics mode observation) too (see the FSMC model in Section 2.4.2). Moreover, this model accounts for the mode observation delay affecting the Markov chain $\{\theta_k\}_{k \in \mathbb{N}}$.

Theorem 4 Given the MJLS described by (2.5) and the current estimator described by (2.14), the following statements are equivalent:

- i) the closed-loop system dynamics (2.43) can be made MSS;
- ii) the MJLS described by (2.5) is both
 - ii-a) Strict-MSD,
 - ii-b) MS stabilizable with one time-step delayed observation of actuation link mode.

Proof 9 (Proof of Theorem 4) See Appendix A.

2.11 Mode-independent output-feedback

Under the conditions presented in this section, the designer can use mode-independent control and filtering gains. The advantage of mode-independence concerns the reduced computational burden, especially when the number of modes increases. The strong *MS* stabilizability (defined in the following) guarantees the existence of a mode-independent control gain, which is *MS* stabilizing.

On the other hand, the following definitions of *Strong-MSD* and *Strong-Strict-MSD* provide the basis for deriving sufficient conditions guaranteeing the existence of a mode-independent filtering gain, which makes the estimation error system *MSS*.

Definition 7 (Strong-MS stabilizability) The MJLS described by (2.5) is Strong-MS stabilizable with one time-step delayed actuation link mode observation if, for any initial condition (x_0, θ_0) , there exists a mode-independent control gain $F^b \in \mathbb{F}^{n_u \times n_x}$ such that $u_k = F^b x_k$ is the MS stabilizing state-feedback for (2.5).

The following *Strong-MSD* and *Strong-Strict-MSD* notions instead concern the sensing link.

Definition 8 (Strong-MSD) The MJLS described by (2.5) is Strong-MSD if there exists a mode-independent filtering gain $\check{M}^b \in \mathbb{F}^{n_x \times n_y}$, such that $\rho(\mathcal{V}) < 1$, with $\mathcal{V} \in \mathbb{B}(\mathbb{H}^{I^{n_x}})$ defined in (2.22), for $\Gamma_{n1} = A + \check{M}^b L$, $\Gamma_{n0} = A$, and $n \in \mathbb{S}_\eta$.

Definition 9 (Strong-Strict-MSD) The MJLS described by (2.5) is Strong-Strict-MSD if there exists a mode-independent filtering gain $\widehat{M}^b \in \mathbb{F}^{n_x \times n_y}$, such that $\rho(\mathcal{T}) < 1$, with $\mathcal{T} \in \mathbb{B}(\mathbb{H}^{I^{n_x}})$ defined in (2.20), for $\widehat{\Gamma}_{n1} = A + A\widehat{M}^b L$, $\widehat{\Gamma}_{n0} = A$, and $n \in \mathbb{S}_\eta$.

Proposition 5 Consider the MJLS described by (2.5). The following statements hold.

- i) Strong-MSD implies MSD.
- ii) Strong-Strict-MSD implies Strict-MSD and Strong-MSD.

Proof 10 (Proof of Proposition 5) See Appendix A.

Remark 21 Strong-Strict-MSD implies all the detectability notions concerning the FSMC model. Thus, the Strong-Strict-MSD is the strongest detectability notion, while MSD is the weakest one.

Let us introduce the mode-independent output-feedback recalling the filtering and control modified algebraic Riccati equations (MARE) reported in the following [48, 223].

To this end, define

$$\begin{aligned}\mathring{\mathcal{A}}^b(Y^b) &\triangleq AY^bA^* + GG^*, & \mathring{\mathcal{C}}^b(Y^b) &\triangleq AY^bL^*, \\ \mathring{\mathcal{R}}^b(Y^b) &\triangleq LY^bL^* + HH^*, & \mathring{\mathcal{M}}^b(Y^b) &= -Y^bL^*\mathring{\mathcal{R}}^b(Y^b)^{-1}, \\ \mathcal{A}^b(X^b) &\triangleq A^*X^bA + C^*C, & \mathcal{C}^b(X^b) &\triangleq B^*X^bA, \\ \mathcal{R}^b(X^b) &\triangleq B^*X^bB + D^*D, & \mathcal{F}^b(X^b) &= -\mathcal{R}^b(X^b)^{-1}\mathcal{C}^b(X^b).\end{aligned}$$

for $Y^b, X^b \in \mathbb{F}_*^{n_x \times n_x}$. Consider the sets

$$\begin{aligned}\mathbb{L}^b &\triangleq \{Y^b \in \mathbb{F}_*^{n_x \times n_x} \text{ such that } \mathring{\mathcal{R}}^b(Y^b) \text{ is non-singular}\}, \\ \mathbb{L}^b &\triangleq \{X^b \in \mathbb{F}_*^{n_x \times n_x} \text{ such that } \mathcal{R}^b(X^b) \text{ is non-singular}\}.\end{aligned}$$

For $Y_\infty^b \in \mathbb{L}^b, X_\infty^b \in \mathbb{L}^b$, the filtering and control MARE are

$$Y_\infty^b = \mathring{\mathcal{A}}^b(Y_\infty^b) - \mathring{\gamma}\mathring{\mathcal{C}}^b(Y_\infty^b)\mathring{\mathcal{R}}^b(Y_\infty^b)^{-1}\mathring{\mathcal{C}}^{b*}(Y_\infty^b), \quad (2.44)$$

$$X_\infty^b = \mathcal{A}^b(X_\infty^b) - \mathring{\nu}\mathcal{C}^{b*}(X_\infty^b)\mathcal{R}^b(X_\infty^b)^{-1}\mathcal{C}^b(X_\infty^b). \quad (2.45)$$

Under the strong *MS* stabilizability condition, the mode-independent *MS* stabilizing control gain exists, and it is given by $F^b = \mathcal{F}^b(X_\infty^b)$, with $X_\infty^b \in \mathbb{L}^b$ satisfying [2.45] [79]. Moreover, the critical arrival probability on the actuation link is defined as

$$\nu_c \triangleq \inf_\nu \{0 \leq \nu \leq 1 \text{ such that } X_\infty^b \succeq 0 \text{ satisfies [2.45]}\}$$

[48, Lemma 5.4 (a)], and the critical observation arrival probability on the sensing link is denoted by γ_c [48, Theorem 5.5]. By [48, Lemma 5.4, Theorem 5.5], ν_c and γ_c satisfy

$$p_{\min} \leq \nu_c \leq p_{\max}$$

and

$$p_{\min} \leq \gamma_c \leq \gamma_{\max} \leq p_{\max},$$

where

$$p_{\min} \triangleq 1 - \frac{1}{\max_h |\lambda_h^u(A)|^2} \text{ and } p_{\max} \triangleq 1 - \frac{1}{\prod_h |\lambda_h^u(A)|^2} \quad (2.46)$$

with $\lambda_h^u(A)$ being the h -th unstable eigenvalue of A , and

$$\gamma_{\max} \triangleq \inf_\gamma \{0 \leq \gamma \leq 1 \text{ such that } Y_\infty^b \succeq 0 \text{ satisfies [2.44]}\}.$$

Remark 22 Strong-MSD condition guarantees the existence of the mode-independent filtering gain, that can be computed as $\check{M}^b = A\check{M}^b(Y_\infty^b)$, with $Y_\infty^b \in \mathring{\mathbb{L}}^b$ satisfying (2.44). Moreover, if Strong-Strict-MSD is satisfied, the existence of the current estimator mode-independent filtering gain is guaranteed. In this case, the filtering gain can be computed as follows: $\widehat{M}^b = \mathring{M}^b(Y_\infty^b)$, with $Y_\infty^b \in \mathring{\mathbb{L}}^b$.

The results illustrated by the following theorem provide the evidence of the existing connection between the optimal mode-dependent filtering CARE solution and the mode-independent solutions of the filtering MARE. Specifically, the solutions of the filtering problem are equivalent under particular conditions. The same holds for the control problem [79, Theorem 3].

Theorem 5 Assume that $\hat{\nu} = \sum_{i=1}^N \varpi_i \hat{\nu}_i$, $\hat{\gamma} = \sum_{m=1}^I \pi_m^\infty \hat{\gamma}_m$. Then, the following statements hold.

- i) The solution of the filtering MARE provides the mode-independent solution of the filtering CAREs.
- ii) The solution of the control MARE provides the mode-independent solution of the control CAREs.

Proof 11 (Proof of Theorem 5) See Appendix A.

Structural properties such as stabilizability and detectability in the mean square sense can be also studied by exploiting the mathematical instruments of LMIs [4, Section 3.5]. LMIs used for testing MS detectability conditions over FSMCs are introduced in the following.

$$A^* Z_m A + \hat{\gamma}_m A^* W_{m2} L + \hat{\gamma}_m L^* W_{m2}^* A + \hat{\gamma}_m L^* W_{m3} L - W_{m1} \prec 0; \quad (2.47a)$$

$$\begin{bmatrix} Z_m & W_{m2} \\ W_{m2}^* & W_{m3} \end{bmatrix} \succeq 0; \quad (2.47b)$$

$$Z_m \succeq \mathcal{E}_m(\mathbf{W}_1), \quad W_{m1} \succ 0, \quad Z_m \succ 0, \quad m \in \mathbb{S}_\eta, \quad (2.47c)$$

$\mathbf{W}_1 = [W_{m1}]_{m=1}^I$, $\mathbf{Z} = [Z_m]_{m=1}^I$ in $\mathbb{H}^{In_x,+}$, $\mathbf{W}_2 = [W_{m2}]_{m=1}^I$ in \mathbb{H}^{In_x, n_y} , and $\mathbf{W}_3 = [W_{m3}]_{m=1}^I$ in $\mathbb{H}^{In_y,+}$.

Proposition 6 Consider the MJLS described by (2.5) and the following statements.

- i) The MJLS described by (2.5) is MSD.
- ii) The MJLS described by (2.5) is Strict-MSD.
- iii) there exist

$$\begin{aligned}\mathbf{W}_1 &= [W_{m1}]_{m=1}^I, \quad \mathbf{Z} = [Z_m]_{m=1}^I \in \mathbb{H}^{I n_x, +}, \\ \mathbf{W}_2 &= [W_{m2}]_{m=1}^I \in \mathbb{H}^{I n_x, n_y}, \quad \mathbf{W}_3 = [W_{m3}]_{m=1}^I \in \mathbb{H}^{I n_y, +},\end{aligned}$$

satisfying conditions (2.47).

Then, statement (i) holds if and only if statement (iii) holds and statement (ii) implies statement (iii). Furthermore, if the matrix A is non-singular, statement (ii) holds if and only if statement (iii) is satisfied.

Proof 12 (Proof of Proposition 6) See Appendix A.

The following set of LMIs is exploited for testing *Strong-MSD* and *Strong-Strict-MSD*.

$$A^*ZA + \hat{\gamma}_m A^*W_2L + \hat{\gamma}_m L^*W_2^*A + \hat{\gamma}_m L^*W_3L - W_{m1} \prec 0; \quad (2.48a)$$

$$\begin{bmatrix} Z & W_2 \\ W_2^* & W_3 \end{bmatrix} \succeq 0; \quad (2.48b)$$

$$Z \succeq \mathcal{E}_m(\mathbf{W}_1), \quad W_{m1} \succ 0, \quad Z \succ 0, \quad m \in \mathbb{S}_\eta, \quad (2.48c)$$

$\mathbf{W}_1 = [W_{m1}]_{m=1}^I$ in $\mathbb{H}^{I n_x, +}$, Z in $\mathbb{F}_+^{n_x \times n_x}$, W_2 in $\mathbb{F}^{n_x \times n_y}$, W_3 in $\mathbb{F}_+^{n_y \times n_y}$.

Proposition 7 Consider the MJLS described by (2.5) and the following statements.

- i) There exist $\mathbf{W}_1 = [W_{m1}]_{m=1}^I$ in $\mathbb{H}^{I n_x, +}$, $Z \in \mathbb{F}_+^{n_x \times n_x}$, $W_2 \in \mathbb{F}^{n_x \times n_y}$, $W_3 \in \mathbb{F}_+^{n_y \times n_y}$, satisfying conditions (2.48).
- ii) The MJLS described by (2.5) is Strong-MSD.
- iii) The MJLS described by (2.5) is Strong-Strict-MSD.

Then, statement (i) implies statement (ii).

Moreover, if the matrix A is non-singular, statement (i) implies statement (iii).

Proof 13 (Proof of Proposition 7) See Appendix A.

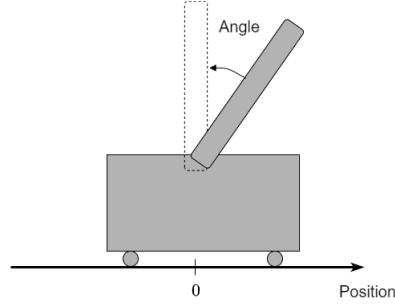


Figure 2.5: Inverted pendulum on a cart

2.12 Numerical case study

2.12.1 The inverted pendulum on a cart

This section presents the wireless output-feedback control of an inverted pendulum on a cart [224], controlled remotely over TCP-like lossy sensing and actuation links. The considered cart and pendulum masses are 0.5kg and 0.2kg, inertia about the pendulum mass center is 0.006 kg·m², distance from the pivot to the pendulum mass center is 0.3m, coefficient of friction for the cart is 0.1. The system state is defined by $x = [\delta x, \delta \dot{x}, \delta \phi, \delta \dot{\phi}]'$, with $\delta x(t) = x(t) - x^*$, $\delta \phi(t) = \phi(t) - \phi^*$, where x is the cart position, ϕ is the pendulum angle from vertical, x^* and ϕ^* are the equilibrium point position and angle. The designed control law aims to stabilize the pendulum in the upright position corresponding to unstable equilibrium point $x^* = 0$ m, $\phi^* = 0$ rad. The optimal Markov jump output-feedback controllers (2.10) and (2.11) have been applied to the discrete-time linear model derived from the continuous-time nonlinear model by linearization. The state-space model of the system is linearized around the unstable equilibrium point and discretized with sampling period $T_s = 0.01$ s. The obtained system matrices [92] are the following:

$$A = \begin{bmatrix} 1.000 & 0.010 & 0.000 & 0.000 \\ 0.000 & 0.998 & 0.027 & 0.000 \\ 0.000 & 0.000 & 1.002 & 0.010 \\ 0.000 & -0.005 & 0.312 & 1.002 \end{bmatrix},$$

$$B = 10^{-1} \times \begin{bmatrix} 0.00091 \\ 0.182 \\ 0.0023 \\ 0.474 \end{bmatrix}.$$

Remark 23 With the matrix A defined above the probabilities p_{\min} and p_{\max} computed according to equation (2.46) are given by

$$p_{\min} = p_{\max} = 0.10538.$$

The weighting matrices in z_k are

$$C^*C = \bigoplus(1000, 0.1, 10000, 0.1),$$

$$D = 1,$$

while matrices H and G are such that

$$HH^* = \mathbb{I}_{n_x} \succ 0, \quad GG^* = \begin{bmatrix} \mathbb{I}_2 & \mathbb{I}_2 \\ \mathbb{I}_2 & \mathbb{I}_2 \end{bmatrix}.$$

The process noise is characterized by the covariance matrix $\mathbb{E}[w_k w_k^*] = \Sigma_w$, with $\Sigma_w = 2 \cdot 10^{-6} \mathbb{I}_4$.

The state matrix A is unstable since it has an eigenvalue in 1.057, but it is easy to verify that $D^*D \succ 0$, the pair (A, B) is controllable, while (A, L) is observable, so the closed-loop system is asymptotically stable if $\nu_k = 1$ and $\gamma_k = 1$ for any k .

Moreover, the necessary conditions for the existence of the MS stabilizing solution for the control and filtering CAREs are satisfied. FSMC models with TPMs in $\mathbb{R}^{4 \times 4}$ describe the double-sided packet loss. These channels are obtained by following the systematic procedure in [62] that accounts for path loss, shadow fading, transmission power control, and interference. The partitioning of the SINR range is based on the values of PEP so that each SINR threshold corresponds to a specific PEP value.

The following paragraphs show the simulation results obtained by applying output-feedback control theory over FSMCs.

2.12.2 Detectability analysis

In this paragraph, the proposed methodology is applied to the study of the MSD conditions.

Let us introduce the two main parameters for the FSMC configuration:

- the distance between the transmitter-receiver couple of interest denoted by d_0 ,
- the distance between the interfering transmitter and receiver of interest denoted by d_i .

Consider the following two configurations:

(i) $d_0 = 18$ m and $d_i = 15$ m,

(ii) $d_0 = 16$ m and $d_i = 8$ m.

Configuration (i)

The resulting sensing link TPM under configuration (i) is given by

$$Q = \begin{bmatrix} 0.6164 & 0.0381 & 0.1606 & 0.1849 \\ 0.6126 & 0.0382 & 0.1616 & 0.1876 \\ 0.6115 & 0.0382 & 0.1619 & 0.1884 \\ 0.6083 & 0.0384 & 0.1627 & 0.1906 \end{bmatrix}.$$

The probability of receiving the packet in each mode of the FSMC is

$$\hat{\gamma} = [0.014 \quad 0.5026469 \quad 0.9337680 \quad 1].$$

Conditions (2.47) and conditions (2.48) are both satisfied.

Consequently,

- from Proposition 6, the system is *MSD* and *Strict-MSD*,
- from Proposition 7, the system is *Strong-MSD* and *Strong-Strict-MSD*.

From the spectral radius analysis, it follows that

$$\rho(\mathcal{V}) = \rho(\mathcal{T}) = 0.979735651,$$

with *Markovian filtering*, i.e., with

- \mathcal{V} defined in (2.22) for $\Gamma_{n1} = A + \check{M}_n L$ and $\Gamma_{n0} = A, \check{M}_n$ Markovian mode-dependent next-step predictor filtering gain,
- \mathcal{T} defined in (2.20) for $\hat{\Gamma}_{n1} = A + A\hat{M}_n L$ and $\hat{\Gamma}_{n0} = A, \hat{M}_n$ Markovian mode-dependent current estimator filtering gain.

The spectral radius obtained with the Bernoullian filtering is given by

$$\rho(\mathcal{V}) = \rho(\mathcal{T}) = 0.979741917.$$

The mean square state trajectories in Fig. 2.6 highlight that the closed-loop system is *MSS*.

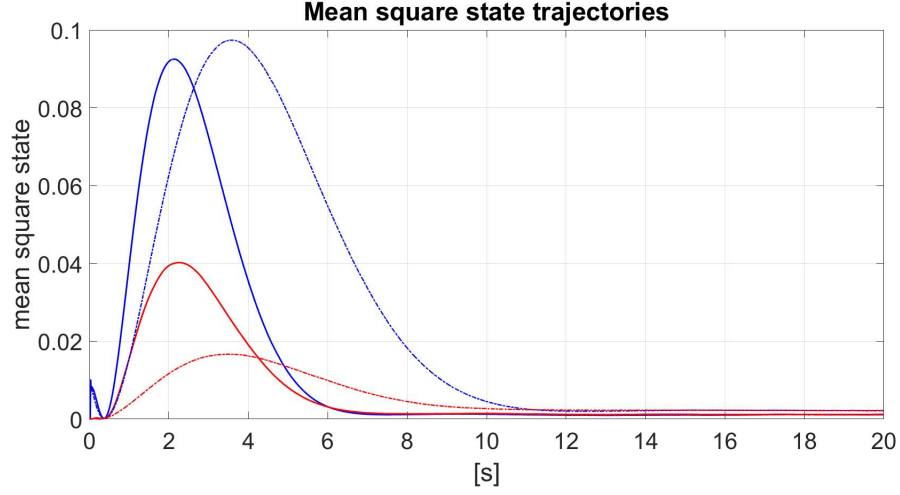


Figure 2.6: Closed-loop mean square state trajectories in configuration (i)

- blue obtained with the Markovian next-step predictor;
- red obtained with the Markovian current estimator;
- dashed blue obtained with the Bernoullian next-step predictor;
- dashed red obtained with the Bernoullian current estimator.

Configuration (ii)

The resulting sensing link TPM under configuration (ii) is given by

$$Q = \begin{bmatrix} 0.9265 & 0.0131 & 0.0403 & 0.0201 \\ 0.9241 & 0.0135 & 0.0415 & 0.0210 \\ 0.9237 & 0.0135 & 0.0417 & 0.0211 \\ 0.9227 & 0.0137 & 0.0422 & 0.0215 \end{bmatrix}.$$

The probability of receiving the packet in each mode of the FSMC is

$$\hat{\gamma} = [0.004 \quad 0.4993460 \quad 0.9209712 \quad 1.0000000]$$

Conditions (2.47) and conditions (2.48) are not satisfied.

Consequently,

- from Proposition 6, the system is neither *MSD* nor *Strict-MSD*,
- as long as properties *Strong-MSD* and *Strong-Strict-MSD*, since conditions (2.48) are only sufficient, the spectral radius analysis is needed to obtain appropriate conclusions.

Table 2.1: Performance indexes obtained by next-step predictor (J_L^*), current estimator (J_C^*), Bernoullian filter (J_B^*) in configuration (i) and in configuration (ii).

	J_L^*	J_C^*	J_B^*
Configuration (i)	$\approx 4 \times 10^{-4}$	$\approx 3 \times 10^{-4}$	$\approx 2 \times 10^2$
Configuration (ii)	$\approx 10^9$	$\approx 10^8$	$\approx 10^9$

From the spectral radius analysis, it follows that

$$\rho(\mathcal{V}) = \rho(\mathcal{T}) = 1.042641679,$$

with *Markovian filtering*, i.e., with

- \mathcal{V} defined in (2.22) for $\Gamma_{n1} = A + \check{M}_n L$ and $\Gamma_{n0} = A, \check{M}_n$ Markovian mode-dependent next-step predictor filtering gain,
- \mathcal{T} defined in (2.20) for $\hat{\Gamma}_{n1} = A + A\hat{M}_n L$ and $\hat{\Gamma}_{n0} = A, \hat{M}_n$ Markovian mode-dependent current estimator filtering gain.

As the reader may notice both LMIs conditions (2.47) and spectral radius analysis highlight that the system is neither *MSD* nor *Strict-MSD*.

The spectral radius obtained with the Bernoullian filtering is given by

$$\rho(\mathcal{V}) = \rho(\mathcal{T}) = 1.042641295.$$

From the spectral radius analysis for the Bernoullian observer provided above, it follows that the system is not *Strong-MSD* nor *Strong-Strict-MSD*.

Finally, the mean square state trajectories in Fig. 2.7 and the average state trajectories in Fig. 2.8 highlight that the closed-loop system is not *MSS*. Indeed, as the reader may note both the mean square trajectories, in Fig. 2.7, as well as the average trajectories, in Fig. 2.8, show a divergent behavior.

As the reader may note by observing Table 2.1, the values of the performance indexes J_L^* , J_C^* and J_B^* in configuration (ii) are larger with respect to the corresponding values in configuration (i).

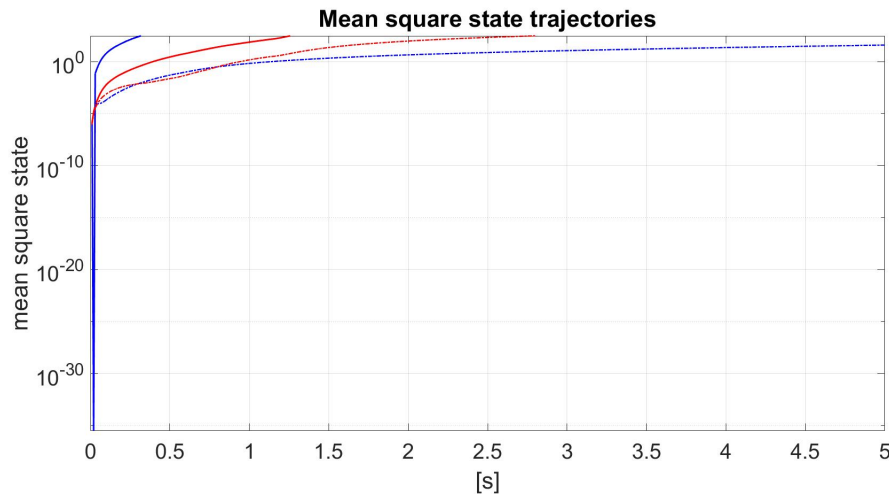


Figure 2.7: Closed-loop mean square state trajectories in configuration (ii)

- blue obtained with the Markovian next-step predictor;
- red obtained with the Markovian current estimator;
- dashed blue obtained with the Bernoullian next-step predictor;
- dashed red obtained with the Bernoullian current estimator.

This is because configuration (i) satisfies the properties of *MSD*, *Strict-MSD*, *Strong-MSD*, *Strong-Strict-MSD*.

Moreover, comparing the performance indexes in configuration (i), it follows that $J_L^* > J_C^*$ showing that the cost achieved by the next-step predictor is higher with respect to the cost achieved by the current estimator. However, the highest cost is achieved by the Bernoullian observer with $J_B^* \approx 2 \times 10^2$.

The two configurations presented (configuration (i) and configuration (ii)) highlight two opposite scenarios in terms of *MSD properties*.

The following paragraph investigates the existence of a limit case, where *MSD* and *Strict-MSD* are satisfied, while the *Strong-MSD* and *Strong-Strict-MSD* are not satisfied.

Limit case for detectability analysis

Simulation results highlight the existence of a limit case for detectability conditions. When considering the distance between the transmitter-receiver couple of interest $d_0 = 17.348$ m and distance between the interfering transmitter and receiver of interest

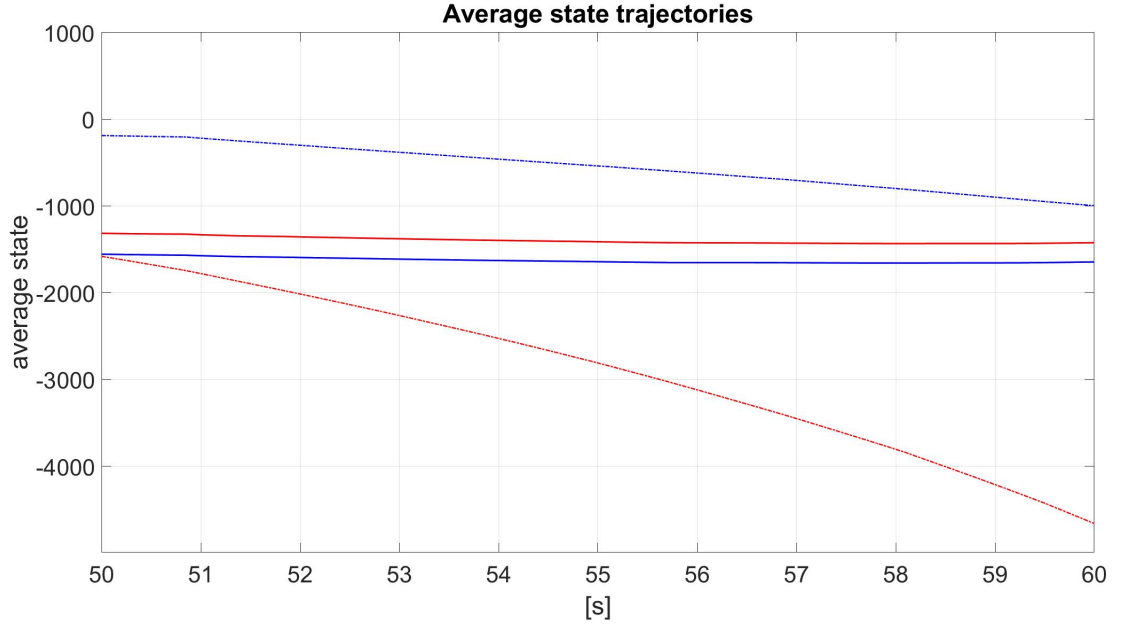


Figure 2.8: Closed-loop average state trajectories in configuration (ii)

- blue obtained with the Markovian next-step predictor;
- red obtained with the Markovian current estimator;
- dashed blue obtained with the Bernoullian next-step predictor;
- dashed red obtained with the Bernoullian current estimator.

$d_{i,1} = 9.548$ m, the resulting sensing link TPM is given by

$$Q_1 = \begin{bmatrix} 0.8855395 & 0.0184352 & 0.0603969 & 0.0356284 \\ 0.8825920 & 0.0187857 & 0.0617956 & 0.0368267 \\ 0.8820434 & 0.0188504 & 0.0620549 & 0.0370513 \\ 0.8806549 & 0.0190134 & 0.0627101 & 0.0376216 \end{bmatrix}.$$

The probabilities of receiving the packet in each mode of the sensing link are denoted by

$$\hat{\gamma}_1 = [0.005 \quad 0.5000509 \quad 0.9237605 \quad 1].$$

Conditions (2.47) are satisfied. From Proposition 6, the system is *MSD* and *Strict-MSD*. As far as strong conditions (2.48) go, they are not satisfied. Since conditions (2.48) are only sufficient, the spectral radius analysis is needed to obtain appropriate conclusions. From the spectral radius analysis, it follows that

$$\rho(\mathcal{V}) = \rho(\mathcal{T}) = 0.999999983,$$

with *Markovian filtering*, i.e., with

- \mathcal{V} defined in (2.22) for $\Gamma_{n1} = A + \check{M}_n L$ and $\Gamma_{n0} = A$, \check{M}_n Markovian mode-dependent next-step predictor filtering gain,
- \mathcal{T} defined in (2.20) for $\hat{\Gamma}_{n1} = A + A\hat{M}_n L$ and $\hat{\Gamma}_{n0} = A$, \hat{M}_n Markovian mode-dependent current estimator filtering gain.

The spectral radius obtained with the Bernoullian filtering is given by

$$\rho(\mathcal{V}) = \rho(\mathcal{T}) = 1.000000074,$$

- \mathcal{V} defined in (2.22) for $\Gamma_{n1} = A + \check{M}^b L$ and $\Gamma_{n0} = A$, \check{M}^b Bernoullian mode-independent next-step predictor filtering gain,
- \mathcal{T} defined in (2.20) for $\hat{\Gamma}_{n1} = A + A\hat{M}^b L$ and $\hat{\Gamma}_{n0} = A$, \hat{M}^b Bernoullian mode-independent current estimator filtering gain.

In this case, the condition $\hat{\gamma} > \gamma_{\max}$ from [48, Theorem 5.6] is satisfied.

However, the system is unstable with the Bernoullian filtering because the system is neither *Strong-MSD* nor *Strong-Strict-MSD*.

This limit case reveals that the Bernoullian output-feedback controller may fail in making the closed-loop system *MSS* when strong detectability conditions are not satisfied, while the Markovian output-feedback controller achieves this aim over the FSMCs.

2.12.3 Stabilizability analysis

The *MS* stabilizability analysis is presented through the limit case obtained under the following configuration.

Consider $d_0 = 17.348$ m and $d_{i,2} = 10$ m.

Then, the actuation link TPM is

$$P_2 = \begin{bmatrix} 0.8647302 & 0.0208232 & 0.0701174 & 0.0443292 \\ 0.8615749 & 0.0211698 & 0.0715631 & 0.0456922 \\ 0.8609554 & 0.0212373 & 0.0718457 & 0.0459616 \\ 0.8593737 & 0.0214086 & 0.0725659 & 0.0466518 \end{bmatrix}.$$

The probabilities of receiving the packet in each mode of the actuation link are given by

$$\hat{v}_2 = [0.006 \quad 0.5003405 \quad 0.9248986 \quad 1].$$

Let us introduce the operator the operator $\widehat{\mathcal{L}}$ [79] that will be exploited in the spectral radius analysis.

For $\mathbf{V} = [V_{ij}]_{i,j=1}^N \in \mathbb{F}^{Nn_x \times Nn_x}$, define $\widehat{\mathcal{L}}(\cdot) = [\widehat{\mathcal{L}}_{ij}(\cdot)]_{i,j=1}^N \in \mathbb{B}(\mathbb{F}^{Nn_x \times Nn_x})$, with

$$\begin{aligned} \widehat{\mathcal{L}}_{ij}(\mathbf{V}) \triangleq & \left\{ A \sum_{l=1}^N V_{li} A^* + \hat{\nu}_i B \sum_{l=1}^N F_l V_{li} F_l^* B^* \right. \\ & \left. + \hat{\nu}_i B \sum_{l=1}^N F_l V_{li} A^* + \hat{\nu}_i A \sum_{l=1}^N V_{li} F_l^* B^* \right\} p_{ij}. \end{aligned} \quad (2.49)$$

From the spectral radius analysis it follows that

- $\rho(\widehat{\mathcal{L}}) = 1.000388084$ using the Bernoullian control gain, i.e., F^b ,
- $\rho(\widehat{\mathcal{L}}) = 0.996248733$ with the Markovian mode-dependent control gain, i.e., F_ℓ , $\ell \in \mathbb{S}_\eta$.

This case highlights that even though the condition $\hat{\nu} > \nu_c$ from [48, Theorem 5.6] is satisfied, the system is unstable with the Bernoullian controller because the system is not Strong-MS stabilizable (recall Definition [7]), see also Remark [24]

The Bernoullian control law is not able to make the closed-loop system MSS, while the Markovian control achieves this aim.

Varying distances d_i between the interfering transmitter and receiver of interest positioned at $d_0 = 17.348$ m from its transmitter, we distinguish four cases:

(a) $d_i \leq 9.547$ m,

(b) $d_i = 9.548$ m,

(c) $d_i \in [9.549 \text{ m}, 12.100 \text{ m}]$,

(d) $d_i \geq 12.101$ m.

Table [2.2] provides insights on the detectability and stabilizability for each of these cases: the check mark indicates that the notion holds, while the cross mark reveals that its required conditions are not satisfied.

Remark 24 The results presented in this Chapter are more general with respect to the ones by Schenato et al. [48]. As also pointed out in the detectability and stabilizability analysis, even though in this example the conditions by Schenato et al. are satisfied, the system is not MSS with the Bernoullian mode-independent controller. This is because Strong-MS stabilizability and Strong-MSD are not satisfied.

Table 2.2: Detectability and stabilizability analysis summary

	(a)	(b)	(c)	(d)
<i>MSD</i>	✗	✓	✓	✓
<i>Strict-MSD</i>	✗	✓	✓	✓
<i>Strong-MSD</i>	✗	✗	✓	✓
<i>Strong-Strict-MSD</i>	✗	✗	✓	✓
<i>MS stabilizability</i>	✗	✗	✓	✓
<i>Strong-MS stabilizability</i>	✗	✗	✗	✓

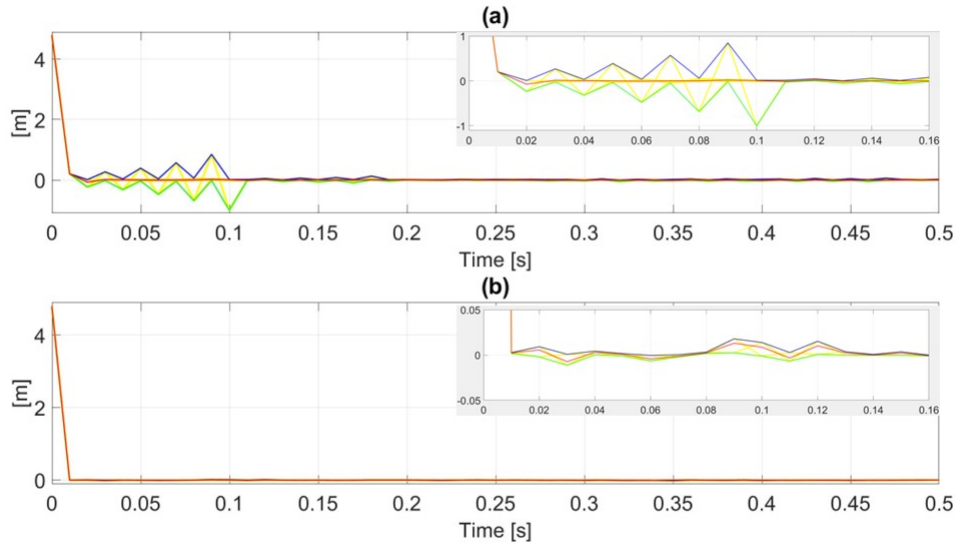


Figure 2.9: The charts report:

- estimation error on cart position obtained by Monte Carlo simulations in yellow;
 - the average error trajectory in red;
 - the maximum error trajectory in blue;
 - the minimum error trajectory in green,
- concerning the next-step predictor (a) and the current estimator (b). The top right of each panel reports a zoom in for each plot.

2.12.4 Performance analysis and comparison

Consider the distances $d_0 = 17.348$ m, $d_{i,3} = 14$ m (corresponding to the case (d) in Table 2.2) and covariance matrix Σ_w provided above. The performance indexes obtained in case (d) are:

- $J_L^* = 0.0001109$, that is, the performance index achieved by the Markovian next-step predictor,
- $J_C^* = 0.0000746$, that is, the performance index achieved by the Markovian current estimator,
- $J_B^* = 209.8934328$, that is, the performance index achieved by the Bernoullian observer.

The reported performance indexes highlight the fact that the presented mode-independent estimation techniques are easier to implement, but their average cost is larger than the one obtained by the Markovian filtering.

Moreover, the spectral radius of \mathcal{T} and \mathcal{V} are the same for both mode-dependent Markovian filters because these estimators are equivalent at the steady-state, see Remark 10.

However, the advantage of the current estimator compared to the next-step predictor is that it involves the most recent measurement in the estimation, yielding a smaller performance index. Fig. 2.10 provides the evidence of the comparison described above: the closed-loop mean square state trajectories depicted in Fig. 2.10 are obtained with 1000 independent Monte Carlo simulations. As the reader may notice, the current estimator leads to the closed-loop mean square state trajectory that remains far below the closed-loop mean square state trajectory provided by next-step predictor.

Consider now the scenario with distances $d_0 = 17.348$ m, $d_{i,3} = 14$ m, where $\Sigma_w = qq'$, with $q = [0.003, 1, -0.005, -2.150]'$ 48.

This case is reported in Fig. 2.9 to emphasize the performance differences existing between the next-step predictor and the current estimator.

The first difference can be individuated in the resulting performance indexes $J_L^* = 65$ for the next-step predictor, and $J_C^* = 43$ for the current estimator.

The performance index analysis shows that the cost achieved by the next-step predictor is higher with respect to the one achieved by the current estimator, see also Remark 17. Moreover, Fig. 2.9 highlights the behavior of the error trajectories for each observer.

After the transient, the error trajectories obtained by the current estimator become smooth faster with respect to the error trajectories obtained by the next-step predictor, which takes 20 samples to become smooth.

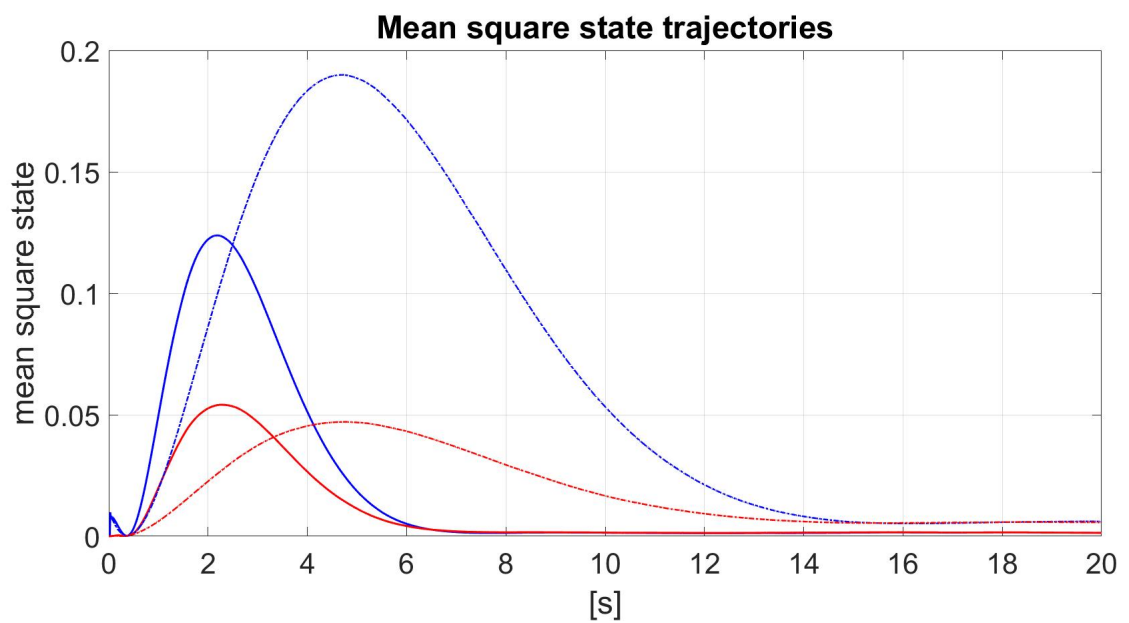


Figure 2.10: Mean square state trajectories in closed-loop in

- blue obtained with the Markovian next-step predictor;
- red obtained with the Markovian current estimator;
- dashed blue obtained with the Bernoullian next-step predictor;
- dashed red obtained with the Bernoullian current estimator.

3

Privacy guarantees

Contents

3.1 Chapter outline	77
3.2 Problem formulation	77
3.2.1 Secrecy mechanism	79
3.2.2 Wireless link	79
3.2.3 Probabilistic framework	82
3.3 Optimal mean square expected secrecy	83
3.4 Main result	86
3.5 Eavesdropper characterization	87
3.6 Example	88
3.6.1 Finite-state Markov channel scenario	89

This chapter is based on the paper by *Impicciatore et al.*, titled “Secure state estimation over Markov wireless communication channels” [87], that presents results obtained during the visiting period at the University of Pennsylvania, under the supervision of Professor George J. Pappas and through the collaboration with Dr. Anastasios Tsiamis.

This Chapter addresses the problem of remote state estimation with secrecy against eavesdropping: this work moves from the secrecy notion proposed in [38, Definition 1 (perfect expected secrecy)] for a Bernoulli packet-dropping wireless link and provides the definition of optimal mean square expected secrecy over FSMCs.

The original notion of perfect expected secrecy [38, Definition 1] requires implementations of the Kalman filter over Bernoulli packet dropping links [49, 88].

However, under FSMCs, any offline computation of the Kalman filter gains would require a combinatorially increasing, with the time-horizon, amount of memory.

For this reason, an alternative practical notion of expected secrecy is considered: optimal mean square expected secrecy over FSMCs. This alternative definition accounts for the minimum MSE, over minimum mean square Markov jump filters, with a finite number of offline-computed gains.

In particular, the definition provided in this chapter requires the eavesdropper MSE to grow unbounded, while the user MSE remains bounded. This new definition requires the adoption of a different approach and utilize tools for the stability analysis of MJLSs [4, 79]. The employed secrecy mechanism randomly withholds information with some probability, similarly to [38]. The aim of this chapter is providing bounds for tuning the secrecy mechanism design.

3.1 Chapter outline

The Chapter is organized as follows.

- Section 3.2 provides the problem formulation.
- Section 3.3 introduces the optimal mean square expected secrecy notion over FSMCs.
- Section 3.4 illustrates the main achievements in this research line.
- Section 3.5 presents an eavesdropper characterization.
- Section 3.6 shows the effectiveness of the proposed approach through an example.
- proofs and technical results are reported in Appendix B.

3.2 Problem formulation

This section presents a detailed description of the scenario investigated in this chapter.

Consider the remote architecture depicted in Fig. 3.1. A sensor transmits a system state information to the estimator over a legitimate user link (in lightblue). The

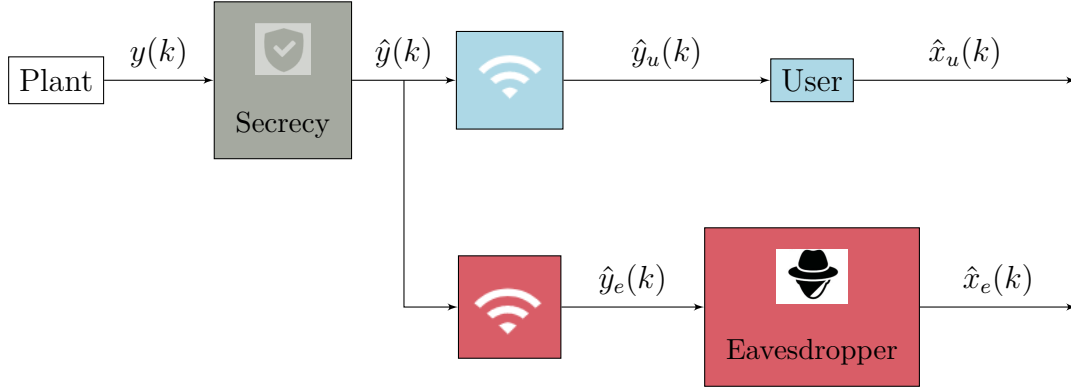


Figure 3.1: Remote estimation architecture.

communication from the plant to the legitimate user occurs over a wireless connection as the reader may see in Fig. 3.1. The shared nature of the wireless medium causes an eavesdropping risk [34, 37, 38, 86]. Indeed, a malicious agent, called eavesdropper, may overhear the information on the wireless link. In Fig. 3.1, the presence of the eavesdropper (in lightred) is modeled through the wireless eavesdropper link in lightred.

Each connection, either the user link or the eavesdropper link, may be affected by packet losses [74] and is modeled by a FSMC. The FSMC [1] is an abstraction widely used to design wireless communication systems, see Chapter 2 for more details. The following discrete-time linear system describes the plant

$$\begin{cases} x(k+1) = Ax(k) + w(k), \\ y(k) = Lx(k) + v(k), \end{cases} \quad (3.1)$$

where $x(k) \in \mathbb{R}^{n_x}$ is the state and $y(k) \in \mathbb{R}^{n_y}$ is the system's output, while $k \in \mathbb{N}$ is the (discrete) time. The signals $w(k) \in \mathbb{R}^{n_x}$ and $v(k) \in \mathbb{R}^{n_y}$ are the process and measurement noise respectively: $w(k)$ and $v(k)$ are i.i.d. independent Gaussian random variables with zero mean and covariance matrices $Q, R \succ 0$ respectively. The initial state x_0 is Gaussian with zero mean and covariance matrix $\Sigma_0 \succ 0$.

Let us introduce the first assumption concerning the considered discrete-time linear system.

Assumption 1 The system described by (3.1) is unstable, i.e., $\rho(A) > 1$.

Even without eavesdroppers, estimation of unstable open-loop systems has been a problem of independent interest in control systems (see [49] for instance). The

ultimate goal is to close the loop and apply control, but first, estimation of the open-loop system should be studied. Besides, if the system is stable, the eavesdropper can predict the state with more accuracy, even without eavesdropping, since the state remains close to the origin.

3.2.1 Secrecy mechanism

The secrecy mechanism adopted is introduced in [38]: the sensor transmits the output of the plant $y(k)$ with probability $\lambda \in [0, 1]$ and it transmits no information (denoted by the symbol ϵ) with probability $1 - \lambda$. Formally,

$$\hat{y}(k) = \begin{cases} y(k) & \text{if } \nu(k) = 1 \\ \epsilon & \text{if } \nu(k) = 0 \end{cases} \quad \forall k \geq 0. \quad (3.2)$$

As the reader may see in (3.2), the secrecy mechanism works by randomly withholding the output of the plant $y(k)$, according to the value of the binary variable $\nu(k)$, that is the outcome of the secrecy mechanism.

Particularly, $\nu(k)$ is a binary random variable characterized by the secrecy parameter λ , as follows,

$$\begin{aligned} \mathbb{P}(\nu(k) = 1) &= \lambda, \\ \mathbb{P}(\nu(k) = 0) &= 1 - \lambda. \end{aligned}$$

For the sake of simplicity in the notation, in the rest of this chapter, the subscript i will be used to indicate an agent operating at the receiver's end.

Formally, $i \in \{u, e\}$, where

- u refers to the user,
- e marks the eavesdropper.

Finally, the i -th link denotes the wireless link between the plant and the agent i .

3.2.2 Wireless link

This section describes the mathematical model of the wireless link.

Let us introduce the variable $\hat{y}_i(k)$, that denotes the measurement received by the

agent i at time $k \in \mathbb{N}$. The general model for the agent's link is

$$\hat{y}_i(k) = \begin{cases} \hat{y}(k) & \text{if } \xi_i(k) = 1 \\ \epsilon & \text{if } \xi_i(k) = 0 \end{cases} \quad \forall k \geq 0, \quad (3.3)$$

where ϵ means no information. As the reader may notice observing equation (3.3), $\hat{y}_i(k)$ is equal to the variable $\hat{y}(k)$, i.e., the output of the secrecy mechanism, or ϵ according to the value assumed by $\xi_i(k)$.

The value of $\xi_i(k)$, $k \in \mathbb{N}$, describes the packet arrival process on the i -th link:

- $\xi_i(k) = 0$ if the packet is lost,
- $\xi_i(k) = 1$ if the packet is correctly delivered.

The process $\xi_i(k)$ is a binary random variable and the probability of having a packet loss or a correct packet transmission over the link i depends on the SINR. The SINR is determined by physical phenomena and model parameters (see [62]) such as path loss, shadow fading, interference and also the nature of the environment (domestic or industrial).

The SINR is a stochastic process and it is typically approximated by a finite state Markov chain [1], denoted as $\eta_i(k)$.

The i -th wireless link is mathematically described by a wireless channel model [74], that is, the FSMC [1], composed by two stochastic processes:

- the process $\xi_i(k)$, that describes packet arrival or packet loss occurrences on the i -th link,
- the process $\eta_i(k)$, that describes the current Markov mode of the i -th link in terms of SINR.

In the FSMC model, the probability of having a zero or a one for the variable $\xi_i(k)$ depends on the current mode of the Markov chain $\eta_i(k)$.

Let us introduce the set of Markov modes for the finite-state Markov chains $\eta_i(k)$, with $i \in \{u, e\}$, $k \in \mathbb{N}$. Recall that each Markov chain $\eta_i(k)$ approximates the SINR on the link i .

Let the index set \mathbb{S} of the Markov chains η_i be defined as follows, $\mathbb{S} \triangleq \{1, \dots, N\}$. Then, $\eta_i(k) \in \{s_{i,m}\}_{m \in \mathbb{S}}$ (see [62]).

Each agent i estimates the SINR process during a learning phase and thus, it knows the number of modes, the transition probabilities, and the probability distribution of the Markov chain η_i . For each mode of $\eta_i(k)$, the value of $\xi_i(k)$ can be either zero or one with certain probabilities. For $m \in \mathbb{S}$, let the variable $\hat{\gamma}_{i,m}$ denote the probability that $\xi_i(k) = 1$, given the mode of the Markov chain $\eta_i(k)$ for $k \in \mathbb{N}$,

$$\begin{aligned}\mathbb{P}(\xi_i(k) = 1 \mid \eta_i(k) = s_{i,m}) &= \hat{\gamma}_{i,m}, \\ \mathbb{P}(\xi_i(k) = 0 \mid \eta_i(k) = s_{i,m}) &= 1 - \hat{\gamma}_{i,m}.\end{aligned}$$

When a packet loss on the i -th link has occurred or the secrecy mechanism has withheld the output information, the agent i interprets the system state message as lost. Specifically, based on error detection and correction mechanisms the receiver decides whether the packet is ϵ and should be dropped. For most communication protocols receiver also performs SINR estimation for each received packet and thus the agent i always knows the mode of the i -th link $\eta_i(k)$.

From (3.2)-(3.3) the received measurement $\hat{y}_i(k)$ is different from ϵ if and only if the product between the secrecy mechanism outcome $\nu(k)$ and the process $\xi_i(k)$ is equal to one, i.e., $\nu(k)\xi_i(k) = 1$.

Let us introduce a binary variable depending on the link i , for the product between $\nu(k)$ and $\xi_i(k)$. Let us define the variable $\varphi_i(k)$, as follows,

$$\varphi_i(k) \triangleq \nu(k)\xi_i(k).$$

For $i \in \{u, e\}$, $m \in \mathbb{S}$,

$$\begin{aligned}\mathbb{P}(\varphi_i(k) = 1 \mid \eta_i(k) = s_{i,m}) &= \lambda\hat{\gamma}_{i,m}, \\ \mathbb{P}(\varphi_i(k) = 0 \mid \eta_i(k) = s_{i,m}) &= 1 - \lambda\hat{\gamma}_{i,m}.\end{aligned}$$

Each agent i owns an information set, that includes:

- the value of \hat{y}_i from the time instant zero to the current time instant,
- the value of the product between the value of ν and the value of ξ_i from the time instant zero to the current time instant,
- the Markov mode of the wireless link η_i from the time instant zero to the current time instant.

Formally, the information set available to the agent i at time $k \in \mathbb{N}$ is given by

$$\mathcal{F}_i(k) = \{(\hat{y}_i(t))_{t=0}^k, (\varphi_i(t))_{t=0}^k, (\eta_i(t))_{t=0}^k\}. \quad (3.4)$$

Remark 25 Consider the information set $\mathcal{F}_i(k)$ in (3.4). Recall the definition of $\hat{y}_i(k)$ in (3.3) and the secrecy mechanism (3.2). It is straightforward to see that with the knowledge of $\hat{y}_i(k)$ and $\varphi_i(k)$, the agent i is aware of $y(k)$.

3.2.3 Probabilistic framework

This paragraph introduces more details on the probabilistic framework that is used to describe the wireless link.

Let us introduce the probability $\pi_{i,m}(k)$, defined as follows,

$$\pi_{i,m}(k) \triangleq \mathbb{P}(\eta_i(k) = s_{i,m}),$$

with $0 < \pi_{i,m}(k) < 1$, for any k , for $m \in \mathbb{S}$, $i \in \{u, e\}$.

A TPM associated with the Markov chain $\eta_i(k)$ is denoted by $P_i \triangleq [p_{i,mn}]_{m,n=1}^N$,

$$p_{i,mn} = \mathbb{P}(\eta_i(k+1) = s_{i,n} \mid \eta_i(k) = s_{i,m}), \quad \sum_{n=1}^N p_{i,mn} = 1.$$

The main technical assumptions (that are similar to [4, Section 5.3]) are presented in the following (with $i \in \{u, e\}$ and $k \in \mathbb{N}$):

- i) the initial conditions $x_0, \eta_{i,0}$ are independent random variables,
- ii) the white noise sequences $\{w(k)\}$ and $\{v(k)\}$ are independent of the initial conditions $(x_0, \nu(0))$ and of the processes $\xi_i(k)$, for any discrete-time $k \in \mathbb{N}$,
- iii) the Markov chains $\{\eta_i(k)\}$ and the noise sequences $\{w(k)\}$ and $\{v(k)\}$ are independent,
- iv) the Markov chains $\{\eta_i(k)\}$ are ergodic, with steady state probability distributions

$$\pi_{i,m}^\infty = \lim_{k \rightarrow \infty} \pi_{i,m}(k),$$

$m \in \mathbb{S}$.

This work aims to design an estimator of the class of mean square Markov jump filters (see [4, Chapter 5.3]) together with a secrecy mechanism, such that the user MSE remains bounded, while the eavesdropper MSE is unbounded. The formal guarantees of this secrecy notion can be found in Section 3.3 (see Definition 10).

The variables ψ_i and ζ_i introduced in the following will be exploited in the statement and in the proof of the main result.

For $i \in \{u, e\}$,

- ψ_i denotes the average probability of intercepting a measurement on the i -th link, when $\lambda = 1$,
- ζ_i is the average probability of intercepting a measurement for $\lambda \in [0, 1)$.

Formally, for $i \in \{u, e\}$, ψ_i and ζ_i are defined as follows,

$$\begin{aligned}\psi_i &\triangleq \sum_{m=1}^N \pi_{i,m}^\infty \hat{\gamma}_{i,m}, \\ \zeta_i &\triangleq \psi_i \lambda.\end{aligned}$$

3.3 Optimal mean square expected secrecy

This section presents the infinite horizon minimum mean square Markov jump filter [4, Chapter 5.3] with the estimation technique provided by an estimator called current estimator [181, Chapter 8.2.4].

Specifically, the estimator provides at each step a model prediction obtained from the estimated state at the previous step. This prediction is corrected by the current measurement received $\hat{y}_i(k)$.

Remark 26 It is well known that for the case in which the information on the output of the system and on the Markov chain are available at each time step $k \in \mathbb{N}$, the best linear estimator of $x(k)$ is the Kalman filter [4, Remark 5.2]. An offline computation of the Kalman filter is inadvisable here as pointed out in [180]. The reason is that the solution of the difference Riccati equation and the time varying Kalman gain are sample path dependent and the number of sample paths grows exponentially in time. On the other hand, an online computation of the Kalman filter requires online matrix inversions which might require a lot of computation. For this reason, a different class of estimators is taken into account: for this class of estimators filtering gains are

pre-computed offline. This allows us to avoid online matrix inversions, thus, reducing the computational burden.

Recall that the agent i receives a quantity that is different from ϵ if and only if the following equality is satisfied,

$$\varphi_i(k) = 1,$$

(see Remark [25](#)).

Consequently, the current estimated state dynamics can be written as follows (see also [181](#), eq. (8.33)-(8.34)), for $i \in \{u, e\}$:

$$\hat{x}_i(k) = \bar{x}_i(k) - \varphi_i(k) \widehat{M}_{i, \eta_i(k)} [y(k) - L\bar{x}_i(k)], \quad (3.5)$$

$$\bar{x}_i(k+1) = A\hat{x}_i(k), \quad (3.6)$$

where $\widehat{M}_{i, \eta_i(k)}$ is the mode-dependent filtering gain, whose explicit expression can be found later in [3.11](#).

Since the filtering gain depends on the mode of the Markov chain at time k , and the Markov chain has a given finite set of modes, it can be computed offline (see Remark [28](#)).

From [3.5](#)-[3.6](#), by defining the error as follows,

$$\tilde{e}_i(k) = x(k) - \bar{x}_i(k), \quad i \in \{u, e\},$$

the error system is given by

$$\tilde{e}_i(k+1) = \left(A + \varphi_i(k) A \widehat{M}_{i, \eta_i(k)} L \right) \tilde{e}_i(k) + w(k) + \varphi_i(k) A \widehat{M}_{i, \eta_i(k)} v(k), \quad (3.7)$$

see also [181](#), eq. (8.36)].

Remark 27 The error system described by [3.7](#) is a discrete-time MJLS (see for instance [4](#)).

The notation presented in [4](#) is adopted here: for $i \in \{u, e\}$, $m \in \mathbb{S}$, let us define $\mathbf{Z}_i(k) \triangleq [Z_{i,m}(k)]_{m=1}^N \in \mathbb{H}^{Nn_x, +}$,

$$Z_{i,m}(k) \triangleq \mathbb{E} \left[\tilde{e}_i(k) \tilde{e}_i^*(k) \mathbf{1}_{\{\eta_i(k)=s_{i,m}\}} \right],$$

with $\mathbf{1}_{\{\eta_i(k)=s_{i,m}\}}$ denoting the indicator function defined in the usual way.

The MSE can be written as follows (see for instance [4](#), [92](#)),

$$\mathbb{E} [\tilde{e}_i(k) \tilde{e}_i^*(k)] = \sum_{m=1}^N Z_{i,m}(k). \quad (3.8)$$

Given the MSE expression, the following definition introduces the notion of optimal mean square expected secrecy over FSMCs, with the estimation error obtained applying the minimum mean square Markov jump filter [4, Chapter 5.3], instead of the Kalman filter [38].

Definition 10 (Secrecy over FSMCs) Given the system described by (3.1) and the FSMCs (3.3), a secrecy mechanism (3.2) achieves optimal mean square expected secrecy over FSMCs if and only if, for any initial condition $\mathbf{Z}_i(0) \in \mathbb{H}^{Nn_x,+}$, $i \in \{u, e\}$, both of the following conditions hold:

$$\begin{aligned} \lim_{k \rightarrow \infty} \mathbf{tr} \{ \mathbb{E} [\tilde{e}_u(k) \tilde{e}_u^*(k)] \} &< \infty, \\ \lim_{k \rightarrow \infty} \mathbf{tr} \{ \mathbb{E} [\tilde{e}_e(k) \tilde{e}_e^*(k)] \} &= \infty. \end{aligned}$$

Let us introduce an important assumption concerning the secrecy mechanism and the user MSE (see also [38]).

Assumption 2 Let us assume that when the secrecy mechanism

$$\hat{y}(k) = y(k),$$

is employed for all $k \geq 0$, i.e., when $\lambda = \frac{\zeta_u}{\psi_u} = 1$, the user MSE is bounded, i.e.,

$$\lim_{k \rightarrow \infty} \mathbf{tr} \{ \mathbb{E} [\tilde{e}_u(k) \tilde{e}_u^*(k)] \} < \infty,$$

for any initial condition $\mathbf{Z}_u(0) \in \mathbb{H}^{Nn_x,+}$.

The following operator is instrumental for the presentation of the Algebraic Riccati equation and for the technical results exploited in the proof of the main theorem.

Let us define the operator

$$\mathcal{X}_\lambda : \mathbb{F}_+^{n_x \times n_x} \times \mathbb{R}^+ \times \mathbb{R}^+ \rightarrow \mathbb{F}_+^{n_x \times n_x},$$

with $\lambda \in [0, 1]$.

For $X \in \mathbb{F}_+^{n_x \times n_x}$, $\alpha > 0$, $\phi \in \mathbb{R}^+$, let $\mathcal{X}_\lambda(X, \alpha, \phi)$ be defined as follows,

$$\begin{aligned} \mathcal{X}_\lambda(X, \alpha, \phi) &\triangleq (1 - \lambda\phi) \{AXA^* + \alpha Q\} \\ &\quad + \lambda\phi \left(AXA^* + \alpha Q - AXL^* (LXL^* + \alpha R)^{-1} LXA^* \right). \end{aligned} \quad (3.9)$$

Proposition 8 Consider the error system described by the MJLS (3.7).

Under Assumption 2, for $m, n \in \mathbb{S}$, $i \in \{u, e\}$, the filtering coupled algebraic Riccati equations (CAREs) are given by

$$Z_{i,n} = \sum_{m=1}^N p_{i,mn} \mathcal{X}_\lambda \left(Z_{i,m}, \pi_{i,m}^\infty, \hat{\gamma}_{i,m} \right), \quad (3.10)$$

$$\widehat{M}_{i,m} = -Z_{i,m} L^* \left(LZ_{i,m} L^* + \pi_{i,m}^\infty R \right)^{-1}. \quad (3.11)$$

Proof 14 (Proof of Proposition 8) See Appendix B.

Remark 28 The filtering gain can be computed offline from the minimization of the MSE, according to the procedure shown in [92] and reported in Appendix A of this thesis. Particularly, each agent i knows the matrices of the system, as well as the mode of the Markov chain η_i . Formally, for $m \in \mathbb{S}$, the filtering gain $\widehat{M}_{i,m}$ is given by (3.11), where $Z_{i,m}$ is the solution of (3.10).

3.4 Main result

This section presents necessary and sufficient conditions concerning the FSMC probabilities such that optimal mean square expected secrecy over FSMCs is guaranteed.

Theorem 6 Consider the system described by (3.1), the secrecy mechanism given by (3.2), and FSMCs described by (3.3).

Under Assumption 1 and Assumption 2, the secrecy mechanism achieves optimal mean square expected secrecy over FSMCs if and only if

$$\psi_u > \psi_e. \quad (3.12)$$

In particular, there exists a probability $\zeta_c \in [0, 1)$ such that optimal mean square expected secrecy is guaranteed if and only if the probability λ in the secrecy mechanism satisfies the following inequalities

$$\frac{\zeta_c}{\psi_u} < \lambda \leq \min \left\{ \frac{\zeta_c}{\psi_e}, 1 \right\}. \quad (3.13)$$

Remark 29 The inequality $\psi_u > \psi_e$ is a reasonable condition for secrecy in many cases of interest. Indeed, it is plausible that the propagation environment leads to an average probability of intercepting the measurement over the eavesdropper link, ψ_e , which is

strictly less than ψ_u , for instance because the eavesdropper might be further away from the source.

The result in (3.12) shows that optimal mean square expected secrecy over FSMCs can be achieved if and only if there is channel disparity between the user and the eavesdropper, i.e., the user has a higher probability of packet reception on average.

Specifically, under the condition on channel disparity, optimal mean square expected secrecy over FSMCs can be achieved by properly tuning the withholding probability of the secrecy mechanism. This fact implies that a criterion on the withholding probability λ is needed for the secrecy mechanism designer. This criterion is shown in (3.13).

Proof 15 (Proof of Theorem 6) See Appendix B.

3.5 Eavesdropper characterization

Given the propagation environment, a designer can deduce possible positions of eavesdroppers, decide which are of the most concern, and derive an eavesdropper's TPM.

This section provides link quality constraints used to design the secrecy mechanism attempting to increase the eavesdropper MSE to infinity. More specifically, if the eavesdropper TPM P_e is known, the designer is able to construct the matrix \mathcal{A}_e , defined as follows,

$$\mathcal{A}_e \triangleq \left[P'_e \otimes \mathbb{I}_{n_x^2} \right] \left[\bigoplus_{m=1}^N (1 - \lambda \hat{\gamma}_{e,m}) (\bar{A} \otimes A) \right].$$

For $\mathbf{V} = [V_m]_{m=1}^N \in \mathbb{H}^{Nn_x,*}$ define for $n \in \mathbb{S}$,

$$\mathcal{S}_{e,n}(\mathbf{V}) \triangleq \sum_{m=1}^N p_{e,mn} (1 - \lambda \hat{\gamma}_{e,m}) AV_m A^* + \pi_{e,n}^\infty Q.$$

The following proposition proves that the operator $\mathcal{S}_{e,n}$ defined above provides a lower bound to the eavesdropper MSE, under the estimator defined in (3.5). Hence, the above recursion can be exploited to test whether the eavesdropper has MSE that increases to infinity.

Proposition 9 Consider the system described by (3.1) and the secrecy mechanism (3.2). The following statements hold, for $n \in \mathbb{S}$,

- If the spectral radius of the matrix \mathcal{A}_e is strictly less than one, i.e., $\rho(\mathcal{A}_e) < 1$, then

$$\lim_{k \rightarrow \infty} \mathbf{tr} \{Z_{e,n}(k)\} \geq \mathbf{tr} \{S_{e,n}\},$$

with $S_{e,n} = \mathcal{S}_{e,n}(\mathbf{S}_e)$ and $\mathbf{S}_e = [S_{e,n}]_{n=1}^N \in \mathbb{H}^{Nn_x,+}$.

- If the spectral radius of the matrix \mathcal{A}_e is greater than or equal to one, i.e., $\rho(\mathcal{A}_e) \geq 1$, then

$$\lim_{k \rightarrow \infty} \mathbf{tr} \{Z_{e,n}(k)\} = +\infty.$$

Proof 16 (Proof of Proposition 9) See appendix B.

Remark 30 Proposition 9 provides novel covariance lower bounds for the eavesdropper MSE. Such a lower bound could be used as a guide to tune the withholding probability of the secrecy mechanism.

3.6 Example

This section examines an inverted pendulum on a cart [224] whose parameters are estimated remotely over a wireless link exposed to an eavesdropper. The considered cart's and pendulum's masses are 0.5 kg and 0.2 kg, inertia about the pendulum's mass center is $0.006 \text{ kg} \cdot \text{m}^2$, distance from the pivot to the pendulum's mass center is 0.3 m, coefficient of friction for the cart is 0.1. The discrete-time system has been obtained from discretization with sampling $T_s = 0.01 \text{ s}$ and linearization of the dynamical continuous time nonlinear model around the unstable equilibrium points $\mathbf{x}^* = 0 \text{ m}$, $\phi^* = 0 \text{ rad}$. The resulting matrix A of the discrete-time system is such that $\rho(A) \approx 1.1 > 1$, and thus, Assumption 1 is satisfied. This unstable plant evolves in open-loop.

Recall that, when the propagation environment is known, a designer can deduce which are the possible eavesdropping configurations allowing to overhear the user's messages. Consider two independent wireless links: one link for the user, the other one for the eavesdropper.

The formal mathematical description of each propagation environment (either the user propagation environment or the eavesdropper propagation environment) accounts for the following couples:

- transmitter/receiver couple,
- transmitter/interferer couple.

For each propagation environment, the transmitter/receiver couple is the couple of interest, while the transmitter/interferer couple models some interference that affects the propagation environment and that characterize both the user and the eavesdropper wireless link.

Consider the following parameters:

- d_u denotes the distance of the couple of interest for the user,
- d_e denotes the distance of the couple of interest for the eavesdropper,
- \tilde{d}_u denotes the distance of the couple transmitter/interferer for the user,
- \tilde{d}_e denotes the distance of the couple transmitter/interferer for the eavesdropper.

3.6.1 Finite-state Markov channel scenario

Consider the following wireless link scenario resulting in the FSMC model [\[1, 79\]](#), with the following parameters:

- $d_u = 17$ m,
- $\tilde{d}_u = 15$ m,
- $d_e = 19$ m,
- $\tilde{d}_e = 13$ m.

Consider the configuration described above for the user and the eavesdropper.

The TPM describing the user FSMC, denoted by P_u , is given by

$$P_u = \begin{bmatrix} 0.5679349 & 0.0394557 & 0.1725174 & 0.220092 \\ 0.5642459 & 0.0395369 & 0.1733422 & 0.222875 \\ 0.56307 & 0.0395617 & 0.1736014 & 0.2237669 \\ 0.5596774 & 0.0396311 & 0.1743412 & 0.2263503 \end{bmatrix}.$$

The probabilities of receiving the packet in each mode of the user FSMC are given by $\hat{\gamma}_{u,m}$, $m = 1, 2, \dots, N$, that are the entries of the vector $\hat{\gamma}_u$, as follows,

$$\hat{\gamma}_u = [0.016 \quad 0.5030050 \quad 0.9351091 \quad 1].$$

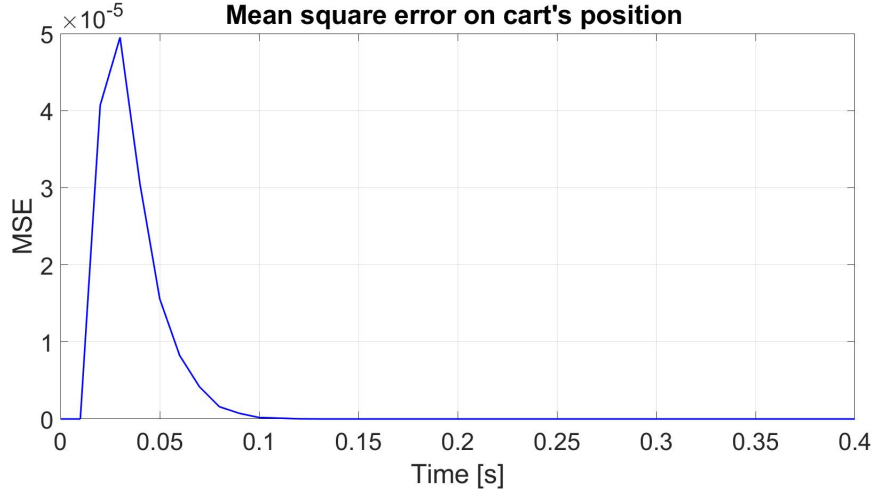


Figure 3.2: User MSE obtained with FSMC model resulting from user parameters $d_u = 17$ m, $\tilde{d}_u = 15$ m, and with secrecy parameter $\lambda = 1$.

The TPM describing the eavesdropper FSMC, denoted by P_e , is

$$P_e = \begin{bmatrix} 0.7663241 & 0.0298952 & 0.1116115 & 0.0921692 \\ 0.7626088 & 0.0301756 & 0.1130374 & 0.0941782 \\ 0.7617196 & 0.0302419 & 0.1133766 & 0.0946619 \\ 0.7593571 & 0.0304166 & 0.1142745 & 0.0959518 \end{bmatrix}$$

The probabilities of receiving the packet in each mode of the eavesdropper FSMC are given by $\hat{\gamma}_{e,m}$, $m = 1, 2, \dots, N$, that are the entries of the vector $\hat{\gamma}_e$, as follows,

$$\hat{\gamma}_e = [0.009 \quad 0.5014132 \quad 0.9290699 \quad 1].$$

When the secrecy mechanism is not applied, i.e., when the parameter $\lambda = 1$, the user MSE is bounded, i.e., Assumption 2 is satisfied, as the reader can see in Fig. 3.2. The limit probability of intercepting the measurement when secrecy is applied is given by $\zeta_c \approx 0.105$.

The secrecy parameter λ guaranteeing the optimal mean square expected secrecy over the FSMC scenario depicted above belongs to the interval $(0.26, 0.48]$.

The results obtained in simulations are shown in Fig. 3.3 and in Fig. 3.4.

Fig. 3.3 shows the error trajectories $\tilde{e}_i(k)$, $i \in \{u, e\}$, obtained from 1000 Monte Carlo simulations for the user (blue lines) and for the eavesdropper (red lines) with $\lambda = 0.3$.

As the reader can see, the user error trajectories have a convergent behavior, while the eavesdropper error trajectories diverge.

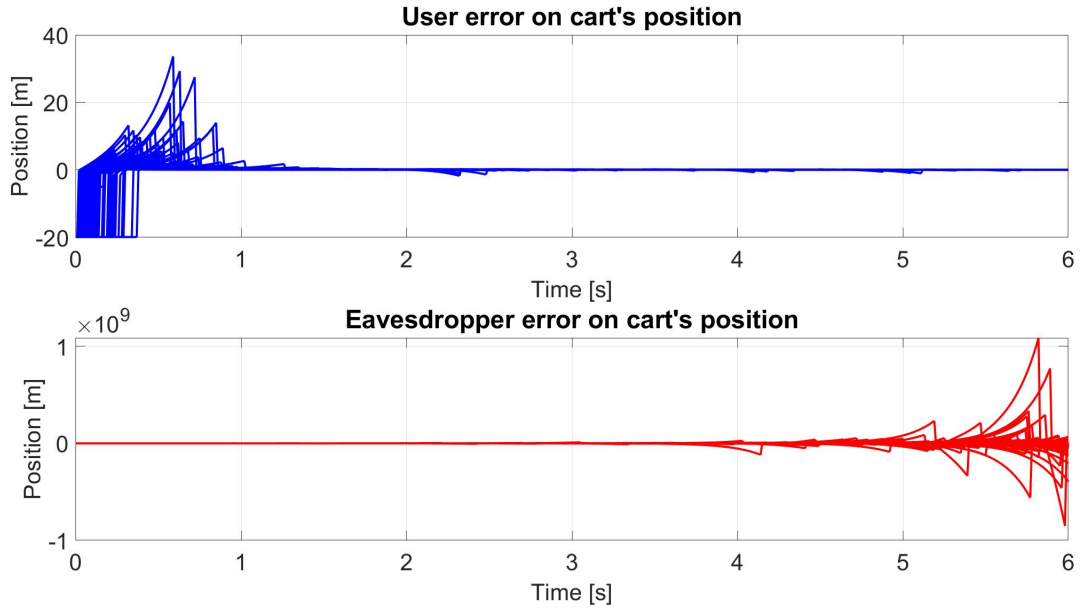


Figure 3.3: Error trajectories on cart's position obtained with $\lambda = 0.3$.

- The figure at the top shows error trajectories on cart's position for the user in blue.
- The figure at the bottom shows error trajectories on cart's position for the eavesdropper in red.

Consider now Fig. 3.4, that reports the eavesdropper MSE (red line) and the user MSE (blue line) on cart's position with $\lambda = 0.3$. The reader may notice that the eavesdropper MSE shows a worse behavior with respect to the user MSE: this is induced by the relation existing between the average probabilities of successfully receiving the system state message, ψ_e and ψ_u , over the eavesdropper and the user link, respectively. Particularly, in the reported example $\psi_e = 0.219$, $\psi_u = 0.413$, and thus $\psi_e < \psi_u$, as required by Theorem 6.

Compare now Fig. 3.5 (obtained without a secrecy mechanism) and Fig. 3.4 (obtained with the proposed secrecy mechanism). The reader may notice that the secrecy mechanism makes the eavesdropper MSE go to infinity, while the user MSE remains bounded (see Fig. 3.4).

The example reported above concludes this chapter, where secure state estimation over Markov wireless communication channels is presented.

The secrecy notion investigated in [38] is brought to the FSMC scenario, which requires re-definition of estimation problem and a novel technical procedure for deriving the secrecy conditions.

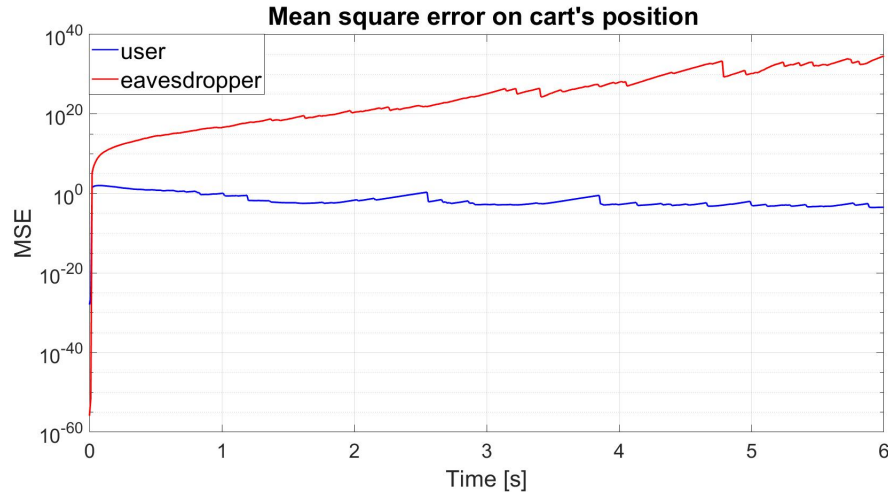


Figure 3.4: The figure reports the MSE on cart's position for the user (blue line) and for the eavesdropper (red line) with $\lambda = 0.3$.

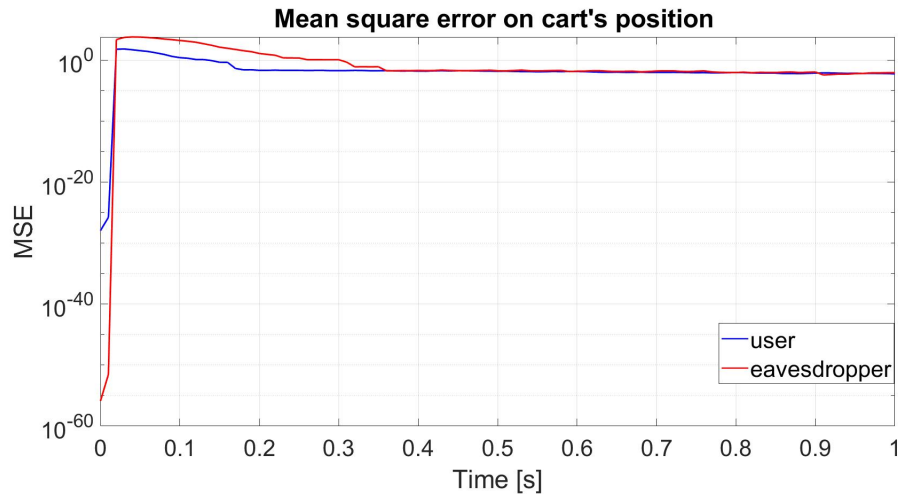


Figure 3.5: The figure reports the MSE on cart's position for the user (blue line) and for the eavesdropper (red line) with $\lambda = 1$.

Moreover, this chapter solves a secrecy design problem satisfying the described formal requirements over FSMCs. Finally, the effectiveness of the proposed approach is shown through the example of an inverted pendulum on a cart whose parameters are estimated remotely over a wireless link exposed to an eavesdropper.

4

On discrete-time Markovian switching nonlinear systems

Contents

4.1 Chapter outline	94
4.2 The probabilistic space	95
4.3 Problem Formulation	97
4.4 Exponential mean square stability characterization	100
4.5 Exponential mean square ISS characterization	101
4.6 The pth moment ISS	103
4.7 Sufficient conditions for pth moment ISS	104
4.8 Illustrative examples	105
4.8.1 Example 2	106
4.8.2 Application to wireless control network scenarios	110
4.8.3 Statistical results	121

Discrete-time Markovian switching systems provide a good approximation of WCNs [62, 66, 67] because Markov chains are able to model bursts of packet losses [1].

There is a wide literature concerning stability investigations for discrete-time Markov jump linear systems [4], while only few works such as [3, 145] investigate the mean square stability notion in the nonlinear framework.

This chapter addresses the problems concerning stability [225] and input-to-state stability [118] analysis of discrete-time Markovian switching nonlinear systems [3].

[100]. The challenges concerning discrete-time Markovian switching nonlinear systems addressed by this PhD work are presented in the works by *Impicciatore et al.* [97, 142]. When the plant has a general mathematical model (that can be for instance nonlinear [94]) the modeling strategies based on discrete-time Markovian switching nonlinear systems [3] play a key role because Markovian switching nonlinear systems provide good approximations of the analyzed system.

Discrete-time Markovian switching systems, also known as *Markov jump systems*, are particularly useful for modeling systems subject to abrupt changes, such as WCNs. As discussed in the previous chapters, a wireless channel may suffer from packet losses [4, 67, 98, 99]. Markovian switching nonlinear systems [3, 100] are good approximations of WCNs when the plant is characterized by nonlinear dynamics [94].

4.1 Chapter outline

This section provides a brief summary of the chapter, as follows.

- Section [4.2] reports the probabilistic space exploited in this chapter.
- Section [4.3] illustrates the formal description of the problem addressed by this chapter.
- Section [4.4] provides the results obtained for *EMSS*.
- Section [4.5] presents the results obtained for *EMS-ISS*.
- Section [4.6] illustrates the notions of p th moment ISS and p th moment exponential ISS.
- Section [4.7] provides the sufficient conditions guaranteeing p th moment ISS and p th moment exponential ISS.
- Section [4.8] provides some examples validating the presented results.
- proofs of Lemmas and Theorems are reported in Appendix C.

4.2 The probabilistic space

Consider the stochastic basis defined by the quadruple $(\Omega, \mathcal{F}, \{\mathcal{F}_k\}_{k \in \mathbb{N}}, \mathbb{P})$, where Ω is the sample space, \mathcal{F} is the corresponding σ -algebra of events, $\{\mathcal{F}_k\}_{k \in \mathbb{N}}$ is the filtration, \mathbb{P} is the probability measure.

Let $\mathbb{E}[\cdot]$ denote the expectation of a random variable with respect to \mathbb{P} , and let $\mathbb{E}[\cdot | \mathcal{F}_k]$ denote the conditional expectation of a random variable on the filtration $\{\mathcal{F}_k\}_{k \in \mathbb{N}}$.

Consider a switching signal given by the Markov chain $\{r(k)\}_{k \in \mathbb{N}}$ defined on the probability space $(\Omega, \mathcal{F}, \{\mathcal{F}_k\}, \mathbb{P})$. For each time $k \in \mathbb{N}$, $r(k)$ takes values in the set $\mathcal{S} \triangleq \{1, \dots, N\}$.

For all operational modes of the Markov chain $i, j \in \mathcal{S}$, and for all $k \in \mathbb{N}$, the transition probabilities are defined by

$$p_{ij} \triangleq \mathbb{P}(r(k+1) = j | r(k) = i) \geq 0, \quad \sum_{j=1}^N p_{ij} = 1. \quad (4.1)$$

Consequently, the TPM of the Markov chain is defined as $P \triangleq [p_{ij}]_{i,j=1}^N$.

The realizations of the Markov chain are called switching paths. Some definitions given in [3, 100] are reported in the following.

Definition 11 The set of all admissible transitions of the Markov chain $\{r(k)\}_{k \in \mathbb{N}}$, is defined as follows,

$$\mathcal{E} \triangleq \{(i, j) \in \mathcal{S} \times \mathcal{S} \mid p_{ij} > 0\}.$$

Definition 12 For any given $i \in \mathcal{S}$, let the set of reachable modes from i be defined as follows,

$$\mathcal{S}_i^{\text{out}} \triangleq \{j \in \mathcal{S} \mid (i, j) \in \mathcal{E}\}.$$

For any $\ell \in \mathbb{N}$, $i \in \mathcal{S}$, let $\mathbf{r}_\ell(i)$ denote an *admissible switching path* of length ℓ , starting from the mode i . Particularly, the path $\mathbf{r}_\ell(i)$ contains ℓ modes of the switching signal, included the initial mode.

Formally, $\mathbf{r}_\ell(i)$ is defined for $\ell \in \mathbb{N}$, and $i \in \mathcal{S}$, as:

$$\mathbf{r}_\ell(i) \triangleq \begin{cases} \{i\}, & \ell = 0, 1, \\ \{i, j_1\}, j_1 \in \mathcal{S}_i^{\text{out}}, & \ell = 2, \\ \{i, j_1, \dots, j_{\ell-1}\}, j_1 \in \mathcal{S}_i^{\text{out}}, j_{h+1} \in \mathcal{S}_{j_h}^{\text{out}}, & \\ h = 1, 2, \dots, \ell - 2, & \ell \geq 3. \end{cases} \quad (4.2)$$

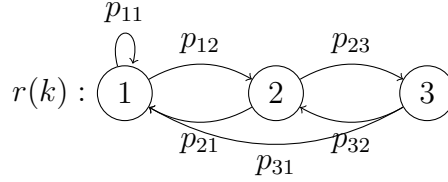


Figure 4.1: State diagram of the Markov chain considered in Example 1.

Definition 13 For any mode of the Markov chain, $i \in \mathcal{S}$, the collection of all admissible switching paths $\mathbf{r}_\ell(i)$, $\ell \in \mathbb{N}$, defined in (4.2), is denoted by $\mathcal{R}_\ell(i)$.

Remark 31 Notice that the collections $\mathcal{R}_0(i)$ and $\mathcal{R}_1(i)$, $i \in \mathcal{S}$, contain only one path $\mathbf{r}_0(i)$, and $\mathbf{r}_1(i)$, respectively. Thus, their cardinality is

$$|\mathcal{R}_0(i)| = |\mathcal{R}_1(i)| = 1,$$

for any $i \in \mathcal{S}$.

Consider the Markov chain depicted in Fig. 4.1; in the following example different sets of admissible switching paths are identified depending on the length of the path and on the initial mode of the given Markov chain.

Example 1 Consider the Markov chain in Fig. 4.1. Let $p_{ij} > 0$ for $(i, j) \notin \{(2, 2), (3, 3), (1, 3)\}$ and let $p_{13} = p_{22} = p_{33} = 0$. The set $\mathcal{S} = \{1, 2, 3\}$ contains all modes of the Markov chain, while the set of admissible transitions is

$$\mathcal{E} = \{(1, 1), (1, 2), (2, 1), (2, 3), (3, 1), (3, 2)\}.$$

Notice that the self-loops $(2, 2)$, $(3, 3)$ are not admissible. We have, for instance, the following collections of admissible switching paths.

- The collection of all admissible switching paths of length 2, emanating from the mode $i = 1 \in \mathcal{S}$ is given by

$$\mathcal{R}_2(1) = \left\{ \{1, 1\}, \{1, 2\} \right\}.$$

- The collection of all admissible switching paths of length 3, emanating from the mode $i = 2 \in \mathcal{S}$ is given by

$$\mathcal{R}_3(2) = \left\{ \{2, 1, 1\}, \{2, 1, 2\}, \{2, 3, 2\}, \{2, 3, 1\} \right\}.$$

Let the set $\mathcal{Q}_\ell(i)$ be defined for any $\ell \in \mathbb{N}$, $i \in \mathcal{S}$, as follows,

$$\mathcal{Q}_\ell(i) \triangleq \mathbb{N}_{[1, |\mathcal{R}_\ell(i)|]}.$$

Then, each index $q \in \mathcal{Q}_\ell(i)$ can be associated with an *admissible switching path* belonging to the set $\mathcal{R}_\ell(i)$, $\ell \in \mathbb{N}$ (see [3], Section 4.2).

Let the symbol $\mathbf{r}_\ell^q(i)$, $q \in \mathcal{Q}_\ell(i)$, denote the q th *admissible switching path* belonging to the set $\mathcal{R}_\ell(i)$.

Clearly,

$$\mathcal{Q}_0(i) = \mathcal{Q}_1(i) = \{1\}.$$

Indeed, from Remark [31], $\mathcal{R}_0(i)$ and $\mathcal{R}_1(i)$ contain only one *admissible switching path*.

Thus, their cardinalities are given by

$$|\mathcal{R}_1(i)| = |\mathcal{R}_0(i)| = 1.$$

Since the switching signal $r(k)$, $k \in \mathbb{N}$, is a Markov chain with a certain TPM, each *admissible switching path* $\mathbf{r}_\ell^q(i) \in \mathcal{R}_\ell(i)$ is associated with a certain probability of occurrence, denoted by $\mathbf{p}_\ell^q(i)$, $q \in \mathcal{Q}_\ell(i)$, for any $\ell \in \mathbb{N}$, $i \in \mathcal{S}$.

Clearly,

$$\mathbf{p}_0^1(i) = \mathbf{p}_1^1(i) = 1.$$

4.3 Problem Formulation

Consider the following discrete-time Markovian switching nonlinear system, defined on the aforementioned stochastic basis $(\Omega, \mathcal{F}, \{\mathcal{F}_k\}, \mathbb{P})$:

$$\begin{cases} x(k+1) = f_{r(k)}(x(k), u(k)), & k \in \mathbb{N}, \\ x(0) = \xi \in \mathbb{R}^n, & r(0) = i \in \mathcal{S}, \end{cases} \quad (4.3)$$

where $x(k) \in \mathbb{R}^n$ is the state of the system and $u(k) \in \mathbb{R}^m$ is the input signal. The set of input sequences is defined by

$$\mathcal{U} \triangleq \{u : \mathbb{N} \rightarrow \mathbb{R}^m\}.$$

For any $i \in \mathcal{S}$,

$$f_i : \mathbb{R}^n \times \mathbb{R}^m \rightarrow \mathbb{R}^n$$

is a locally bounded function satisfying $f_i(0,0) = 0$, continuous at zero.

The solution of (4.3) is denoted by $\Phi(k, \xi, i, \mathbf{r}_k^q(i), u)$, $k \in \mathbb{N}$, and corresponds to initial conditions $\xi \in \mathbb{R}^n$, $i \in \mathcal{S}$, switching path $\mathbf{r}_k^q(i) \in \mathcal{R}_k(i)$, $q \in \mathcal{Q}_k(i)$, and input signal $u \in \mathcal{U}$.

Remark 32 The system is clearly forward complete, since for any $k \in \mathbb{N}$, any given initial condition $\xi \in \mathbb{R}^n$, any given Markovian initial mode $i \in \mathcal{S}$, any given input signal $u \in \mathcal{U}$, and any given admissible switching path of length $k \in \mathbb{N}$, $\mathbf{r}_k^q(i) \in \mathcal{R}_k(i)$, $q \in \mathcal{Q}_k(i)$, the solution of (4.3) exists at k , see [4].

Let

$$x(k) \triangleq x(k, \xi, i, u)$$

denote a trajectory, that evolves according to (4.3), with initial conditions $\xi \in \mathbb{R}^n$, $i \in \mathcal{S}$, and input signal $u \in \mathcal{U}$.

Remark 33 The value of $x(k, \xi, i, u)$ is determined not only by the time instant $k \in \mathbb{N}$, by the initial conditions $\xi \in \mathbb{R}^n$ and $i \in \mathcal{S}$, and by the input signal $u \in \mathcal{U}$, but by the admissible switching path in the set $\mathcal{R}_k(i)$ too. Without any priori knowledge (except the initial mode $i \in \mathcal{S}$) of the switching path, there are different possible values that the variable $x(k, \xi, i, u)$, $k \in \mathbb{N}$, can assume, according to the TPM P . Indeed, $x(k, \xi, i, u)$ is a random variable on the stochastic basis $(\Omega, \mathcal{F}, \{\mathcal{F}_k\}, \mathbb{P})$.

Let us consider the second moment of $x(k, \xi, i, u)$, i.e., $\mathbb{E}[\|x(k, \xi, i, u)\|^2]$, that is given by

$$\mathbb{E}[\|x(k, \xi, i, u)\|^2] = \sum_{q \in \mathcal{Q}_k(i)} \mathbf{p}_k^q(i) \|\Phi(k, \xi, i, \mathbf{r}_k^q(i), u)\|^2, \quad (4.4)$$

$k \in \mathbb{N}$, $\xi \in \mathbb{R}^n$, $i \in \mathcal{S}$, $u \in \mathcal{U}$.

The usual definition of *EMSS* (see [3, 4, 67]) and the definition of *EMS-ISS* (see [142]) are reported in the following.

Definition 14 (EMSS) The system described by (4.3), with $u(\cdot) \equiv 0$, is said to be *EMSS* if there exist positive constants $\theta, \zeta \in \mathbb{R}^+$ with $\theta \geq 1$, $0 < \zeta < 1$, such that for any initial condition $\xi \in \mathbb{R}^n$, for any $i \in \mathcal{S}$, $\mathbb{E}[\|x(k, \xi, i, 0)\|^2]$ satisfies the following inequality, for any $k \in \mathbb{N}$:

$$\mathbb{E}[\|x(k, \xi, i, 0)\|^2] \leq \theta \zeta^k \|\xi\|^2. \quad (4.5)$$

Definition 15 (EMS-ISS) The system described by (4.3) is said to be EMS-ISS if there exist positive constants $\theta, \zeta \in \mathbb{R}^+$ with $\theta \geq 1$, $0 < \zeta < 1$, and a \mathcal{K} -function η , such that for any initial condition $\xi \in \mathbb{R}^n$, for any $i \in \mathcal{S}$, and for any input signal $u \in \mathcal{U}$, $\mathbb{E}[\|x(k, \xi, i, u)\|^2]$ satisfies the following inequality, for any $k \in \mathbb{N}$:

$$\mathbb{E}[\|x(k, \xi, i, u)\|^2] \leq \theta \zeta^k \|\xi\|^2 + \eta \left(\sup_{s=0, \dots, k-1} (\|u(s)\|) \right), \quad (4.6)$$

where the second term of the sum in the right-hand side of (4.6) is taken equal to zero for $k = 0$.

Remark 34 Definitions 14 and 15 concern EMSS and EMS-ISS, where expected values of the state and other stochastic notions such as the transition probability matrix are involved, which clearly are not involved in the deterministic case (see for instance [134, 136]). Lyapunov characterization of the global asymptotic stability and input-to-state stability for deterministic non switching and switching discrete-time systems clearly do not apply to the stochastic framework here considered (see [225, 226] and [136]).

Lyapunov characterizations of EMSS and of EMS-ISS are provided in this chapter. Here, it is proved that the sufficient conditions guaranteeing EMSS (introduced in [3]) are also necessary, complementing the results in [3]. The main result presented in [97] concerns the Lyapunov characterization of EMS-ISS: sufficient conditions guaranteeing p th moment exponential ISS [142, Corollary 1] with $p = 2$ (i.e., EMS-ISS) are proved to be also necessary. This chapter involves both the results introduced in the conference contribution [142], as well as the results in [97].

Remark 35 Previous works such as [136, 137] do not consider the stochastic character of the switching rule. But, in many cases such as wireless control network scenarios, Markov jump systems are a viable mathematical model to lay some groundwork for the development of suitable theoretical conditions for analysis and design of wireless control networks.

Remark 36 A widely used mathematical setting for control, state estimation and secrecy over wireless communication networks is based on Markov jump linear systems [62, 79, 87, 92]. Indeed, the process to control is typically linearized around an equilibrium point [92, Section VI]. This work provides Lyapunov characterizations of EMSS and EMS-ISS of discrete-time Markovian switching nonlinear systems, with focus on the general nonlinear case.

4.4 Exponential mean square stability characterization

Let us consider a scalar function

$$V : \mathbb{R}^n \times \mathcal{S} \rightarrow \mathbb{R}^+, \quad (4.7)$$

with $V(0, i) = 0$, for all $i \in \mathcal{S}$, and let us introduce the operator $\mathcal{L}V$ as follows,

$$\mathcal{L}V : \mathbb{R}^n \times \mathbb{R}^m \times \mathcal{S} \rightarrow \mathbb{R},$$

associated with the scalar function V introduced above.

The operator $\mathcal{L}V$ is defined for $\xi \in \mathbb{R}^n$, $u \in \mathbb{R}^m$, and $i \in \mathcal{S}$ as:

$$\mathcal{L}V(\xi, u, i) \triangleq \left(\sum_{j \in \mathcal{S}} p_{ij} V(f_i(\xi, u), j) \right) - V(\xi, i). \quad (4.8)$$

The following theorem provides necessary and sufficient conditions for *EMSS* of system (4.3), with $u(\cdot) \equiv 0$. The sufficiency part in the next theorem is already stated in [3, Theorem 20 (b)]: the result concerning the necessity part is provided here.

Theorem 7 The following statements are equivalent:

- a) the system described by (4.3), with $u(\cdot) \equiv 0$, is *EMSS*;
- b) there exist a function $V : \mathbb{R}^n \times \mathcal{S} \rightarrow \mathbb{R}^+$, positive real numbers α_l , $l = 1, 2, 3$, such that the following inequalities hold for all $i \in \mathcal{S}$, $\xi \in \mathbb{R}^n$,

$$b_1) \quad \alpha_1 \|\xi\|^2 \leq V(\xi, i) \leq \alpha_2 \|\xi\|^2;$$

$$b_2) \quad \mathcal{L}V(\xi, 0, i) \leq -\alpha_3 \|\xi\|^2.$$

Proof 17 (Proof of Theorem 7) All the details of the proof are reported in Appendix C. Anyway, the reader can find here the main line of reasoning. The sufficiency part (i.e., (b) \implies (a)) has been already proved in [3, Theorem 20 (b)], as discussed above.

*As far as the proof of the converse implication (i.e., (a) \implies (b)), the main idea consists in the construction of the Lyapunov function V satisfying (b₁) and (b₂). The point is to show that V satisfies conditions (b₁) and (b₂) exploiting the *EMSS* assumption (in statement (a)) and applying the Markov property.*

4.5 Exponential mean square ISS characterization

The following theorem provides necessary and sufficient conditions for *EMS-ISS* of system (4.3).

Theorem 8 The following statements are equivalent:

- a) the system described by (4.3) is *EMS-ISS*;
- a) there exist a function $V : \mathbb{R}^n \times \mathcal{S} \rightarrow \mathbb{R}^+$, positive real numbers α_l , $l = 1, 2, 3$, and a function α_4 of class \mathcal{K} , such that the following inequalities hold for all $i \in \mathcal{S}$, $\xi \in \mathbb{R}^n$, $u \in \mathbb{R}^m$,

$$b_1) \quad \alpha_1 \|\xi\|^2 \leq V(\xi, i) \leq \alpha_2 \|\xi\|^2;$$

$$b_2) \quad \mathcal{L}V(\xi, u, i) \leq -\alpha_3 \|\xi\|^2 + \alpha_4(\|u\|).$$

Remark 37 The results on Lyapunov characterizations of *EMSS* and *EMS-ISS* here provided are the first necessary and sufficient Lyapunov conditions in literature for stability of discrete-time Markovian switching nonlinear systems. Extension of these necessary and sufficient conditions for instance to the case of mean square (not necessarily exponential) input-to-state stability seems extremely challenging. There is indeed a serious obstacle to the use of nonlinear functions in the stochastic framework, due to the well known fact that in general, for a nonlinear function α of class \mathcal{K} , the equality

$$\alpha \left(\mathbb{E} \left[\|x\|^2 \right] \right) = \mathbb{E} \left[\alpha \left(\|x\|^2 \right) \right]$$

does not hold.

For the sufficiency part, in Theorem 8, one could replace positive reals α_i , $i = 1, 2, 3$, with suitable functions α_i , $i = 1, 2, 3$ of class \mathcal{K}_∞ . But then the following inequalities are needed to be satisfied:

$$\begin{aligned} \alpha_1 \left(\mathbb{E} \left[\|x(k)\|^2 \right] \right) &\leq \mathbb{E} \left[\alpha_1 \left(\|x(k)\|^2 \right) \right], \\ \mathbb{E} \left[\alpha_2 \left(\|x(k)\|^2 \right) \right] &\leq \alpha_2 \left(\mathbb{E} \left[\|x(k)\|^2 \right] \right), \\ \mathbb{E} \left[\alpha_3 \left(\|x(k)\|^2 \right) \right] &\geq \alpha_3 \left(\mathbb{E} \left[\|x(k)\|^2 \right] \right), \end{aligned}$$

which, by [141, Jensen's inequality], require the functions α_1 , α_3 to be convex and α_2 to be concave. Furthermore, clearly we also need the standard inequality

$$\alpha_1(s) \leq \alpha_2(s),$$

for any $s \in \mathbb{R}^+$, which is in this case an interesting constraint (as α_1 is needed convex and α_2 is needed concave). Sufficient Lyapunov conditions for the mean square input-to-state stability are given by conditions (b₁), (b₂) in Theorem 8, where the positive reals α_i , $i = 1, 2, 3$, there used, are replaced by functions α_1 , α_2 , α_3 satisfying the above properties. Whether or not these conditions could be also necessary for the mean square input-to-state stability, is a challenging question. We conjecture here that, due to the particular properties required for the comparison functions, these conditions are not necessary. Proving, or disproving, this conjecture, is a not easy task, beyond the aims of this work. We highlight that, for instance, if one would try the disproof, [114, Proposition 7], a key result for the Lyapunov characterization of ISS in the deterministic case (see [136, Lemmas 2,3,4]), would be inconclusive for a general function β of class \mathcal{KL} , involved in the mean square ISS inequality, because of the required above properties of related comparison functions.

Proof 18 (Proof of Theorem 8) All the details of the proof are reported in the Appendix C. Anyway, the reader can find here the main line of reasoning.

The first part of the proof shows that the statement (a) implies robust exponential mean square stability of system (4.3) (see Definition 19). The last part shows that robust exponential mean square stability of system (4.3) implies statement (b). Finally, the proof of the implication (b) \implies (a) is provided.

Remark 38 The proof of Theorem 8 makes use of a standard procedure (see [113, 114, 225–227]) for deterministic nonlinear systems, here deeply re-elaborated in a stochastic discrete-time setting. The proof provided in this article involves expected values of the state and other stochastic notions, such as the transition probability matrix (see references [3, 4]), which clearly are not involved in the deterministic case (see for instance [113, 134, 226]). The standard procedure in the deterministic case makes use of the Lyapunov characterization of robust asymptotic stability (see [113, Section 2.2], [226, Lemma 3.8, Lemma 3.11] for deterministic non switching systems and [136, Lemma 1] for deterministic switching systems). The approach adopted in this proof

exploits the Lyapunov characterization of the robust exponential mean square stability (see Appendix C, Definition [19](#)).

Remark 39 The presented Lyapunov characterization makes use of multiple Lyapunov functions. The common Lyapunov function approach is a particular case. Moreover, the proposed methodology accounts for the stochastic insight of the switching rule. Indeed, the operator $\mathcal{L}V$ contains the transition probabilities of the Markovian switching rule in its expression.

4.6 The p th moment ISS

This section introduces input-to-state stability notions concerning the p th moment of the state of system [\(4.3\)](#), i.e., $\mathbb{E}[\|x(k)\|^p]$, with $p > 0$.

Specifically, p th moment ISS generalizes the input-to-state stability notions in the mean square sense.

Let us consider the p th moment of the state of system [\(4.3\)](#) $x(k, \xi, i, u)$, i.e., $\mathbb{E}[\|x(k, \xi, i, u)\|^p]$, that is given by

$$\mathbb{E}[\|x(k, \xi, i, u)\|^p] = \sum_{q \in \mathcal{Q}_k(i)} \mathbf{p}_k^q(i) \|\Phi(k, \xi, i, \mathbf{r}_k^q(i), u)\|^p, \quad (4.9)$$

with $p > 0$.

Definition 16 (p th moment ISS) The system described by [\(4.3\)](#) is said to be p th moment ISS if there exist $p > 0$, a function β of class \mathcal{KL} and a \mathcal{K} -function η , such that for all initial conditions $(x_0, i) \in \mathbb{R}^n \times \mathcal{S}$, for all input signals $u \in \mathcal{U}$, the p th moment of $x(k)$, denoted by $\mathbb{E}[\|x(k)\|^p]$, satisfies the following inequality, for any $k \in \mathbb{N}$:

$$\mathbb{E}[\|x(k)\|^p] \leq \beta(\|x_0\|^p, k) + \eta\left(\sup_{s=0, \dots, k-1} (\|u(s)\|)\right), \quad (4.10)$$

where the second term of the sum in the right-hand side of [\(4.10\)](#) is taken equal to zero for $k = 0$.

The following definition introduces the p th moment exponential ISS, that is concerned the classical ISS notion, with the \mathcal{KL} function β , which is exponential in the time argument [\[3, 94\]](#).

Definition 17 (pth moment exponential ISS) The system described by (4.3) is said to be pth moment exponentially ISS if there exist $p > 0$, $\theta, \zeta \in \mathbb{R}^+$, with $\theta \geq 1$, $0 < \zeta < 1$, and a \mathcal{K} -function η , such that for all initial conditions $(x_0, i) \in \mathbb{R}^n \times \mathcal{S}$, for all input signals $u \in \mathcal{U}$, the pth moment of $x(k)$, denoted by $\mathbb{E}[\|x(k)\|^p]$, satisfies the following inequality, for any $k \in \mathbb{N}$:

$$\mathbb{E}[\|x(k)\|^p] \leq \theta \zeta^k \|x_0\|^p + \eta \left(\sup_{s=0, \dots, k-1} (\|u(s)\|) \right), \quad (4.11)$$

where the second term of the sum in the right-hand side of (4.11) is taken equal to zero for $k = 0$.

4.7 Sufficient conditions for pth moment ISS

Consider the scalar function $V : \mathbb{R}^n \times \mathcal{S} \rightarrow \mathbb{R}^+$, defined in (4.7). The following theorem provides sufficient conditions for the pth moment ISS property.

Theorem 9 (Sufficient conditions for pth moment ISS) Let there exist a function

$$V : \mathbb{R}^n \times \mathcal{S} \rightarrow \mathbb{R}^+,$$

positive real numbers $\alpha_1, \alpha_2 > 0$, a \mathcal{K}_∞ convex function γ and a function δ of class \mathcal{K} , such that the following conditions hold for all $i \in \mathcal{S}$, $\xi \in \mathbb{R}^n$, $u \in \mathbb{R}^m$:

- a) $\alpha_1 \|\xi\|^p \leq V(\xi, i) \leq \alpha_2 \|\xi\|^p$;
- b) $\mathcal{L}V(\xi, u, i) \leq -\gamma(\|\xi\|^p) + \delta(\|u\|)$.

Then, the system described by (4.3) is pth moment ISS.

Proof 19 (Proof of Theorem 9) See Appendix C.

Remark 40 If $p = 2$, then the system described by (4.3) is second moment ISS, i.e., mean square ISS (see Definition 16 with $p = 2$). Note that second moment ISS implies the stability of the second moment, i.e., the mean-square stability (see [3, Definition 18]).

Corollary 1 (Sufficient conditions for p th moment exponential ISS) Let there exist a function

$$V : \mathbb{R}^n \times \mathcal{S} \rightarrow \mathbb{R}^+,$$

positive real numbers $\alpha_1, \alpha_2 > 0$, a \mathcal{K} -function δ and a \mathcal{K}_∞ linear function $\gamma(s) = \tilde{\gamma}s$, $s \in \mathbb{R}^+$, with $\tilde{\gamma}$ positive real, such that the following conditions hold, for all $i \in \mathcal{S}$, $\xi \in \mathbb{R}^n$, $u \in \mathbb{R}^m$:

- a) $\alpha_1 \|\xi\|^p \leq V(\xi, i) \leq \alpha_2 \|\xi\|^p$;
- b) $\mathcal{L}V(\xi, u, i) \leq -\tilde{\gamma} \|\xi\|^p + \delta(\|u\|)$.

Then, the system described by (4.3) is p th moment exponentially ISS.

Proof 20 (Proof of Corollary 1) See Appendix C.

4.8 Illustrative examples

This section illustrates some examples [97, 142] showing the effectiveness of the methodology presented in this chapter.

The aforementioned examples are summarized in the following.

- Paragraph 4.8.1 provides the first example of this section, that is here called *Example 2*, see also [97, Example 1]. Specifically, the example illustrated in Paragraph 4.8.1 moves from an example provided in literature on a discrete-time switching nonlinear system, that is, [228, Example 4.1], where the setting is deterministic. In *Example 2* a Markov chain governing the switching rule is introduced and the *EMS-ISS* analysis is applied.
- Paragraph 4.8.2 provides (with *Example 3* and *Example 4*) an application of the proposed methodology to stability analysis of WCNs.

4.8.1 Example 2

Consider the discrete-time switching model analysed in [228, Example 4.1], where for any $i \in \{1, 2, 3\}$ the function $f_i : \mathbb{R}^2 \times \mathbb{R} \rightarrow \mathbb{R}^2$ is defined, for $x = [x_1 \ x_2]^T \in \mathbb{R}^2$, $u \in \mathbb{R}$, as

$$\begin{aligned} f_1(x, u) &= \begin{bmatrix} 0.5x_2 + 0.4x_2 \exp(-|x_2|) + \exp(-|x_1|)u \\ 0.6x_1 + \exp(-|x_2|)u \end{bmatrix}, \\ f_2(x, u) &= \begin{bmatrix} 1.4x_1 \sin(x_1) + \exp(-|x_1|)u \\ \sqrt{2}x_2 + \exp(-|x_2|)u \end{bmatrix}, \\ f_3(x, u) &= \begin{bmatrix} 1.3x_1 + \exp(-|x_1|)u \\ 1.2x_2 \cos(x_2) + \exp(-|x_2|)u \end{bmatrix}. \end{aligned} \tag{4.12}$$

The subsystem 1 is ISS, while the subsystems 2 and 3 are not ISS (see [228]). Consider a switching signal given by the Markov chain $r(k) \in \{1, 2, 3\}$ depicted in Fig. 4.2 and characterized by the TPM

$$P = \begin{bmatrix} p & 1-p & 0 \\ 1-q_1-q_2 & q_1 & q_2 \\ 1 & 0 & 0 \end{bmatrix}, \tag{4.13}$$

with

$$\begin{aligned} 0 &< p < 1, \\ 0 &< q_1 < 1, \\ 0 &< q_2 < 1, \\ q_1 + q_2 &< 1. \end{aligned}$$

Notice that system (4.12), with switching signal given by the Markov chain $\{r(k)\}_{k \in \mathbb{N}}$ is in the class of systems considered in (4.3).

The ISS analysis presented in [228] refers to a switching system with both ISS and not ISS modes and with deterministic switching signals characterized by edge dependent dwell-time constraints. Thus, the approach proposed in [228] cannot be applied to the scenario presented in this work, where the switching rule obeys to a Markov chain with a given TPM. This is the reason why the example provided in this paragraph focuses on the relevant study of *EMS-ISS* of system (4.12) with respect to the input u .

In particular, notice that the probability of the self-loop on the unstable subsystem 2 is not zero. Therefore, the switching signal may rest in the unstable subsystem 2 for a finite arbitrary number K of steps with non-zero probability $(1 - q_1)q_1^K$ [138].

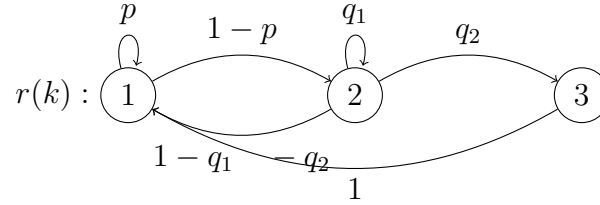


Figure 4.2: State diagram of the Markov chain $r(k)$ in *Example 2*.

Remark 41 The model considered in this chapter, i.e., discrete-time nonlinear systems with Markovian switching rule, allows for both arbitrary and non arbitrary switching.

For instance, if for some $i, j \in \mathcal{S}$, $p_{ij} = 0$, then the switching from mode i to mode j is not allowed.

Consider *Example 2*. The transition probabilities p_{13} , p_{32} , p_{33} are zero: the transitions $(1, 3)$, $(3, 2)$ and $(3, 3)$ are not admissible. *Example 2* shows how the proposed Lyapunov approach can be applied also in this case.

Consider the following candidate Lyapunov function

$$V : \mathbb{R}^2 \times \{1, 2, 3\} \rightarrow \mathbb{R}^+,$$

defined for $\xi = [\xi_1 \ \xi_2]^T$ in \mathbb{R}^2 and for $i \in \{1, 2, 3\}$ as

$$V(\xi, i) = \lambda_i \xi_1^2 + \sigma_i \xi_2^2, \quad (4.14)$$

with

$$\lambda_i, \sigma_i > 0.$$

By choosing

$$\alpha_1 = \min_{i=1,2,3} \{\lambda_i, \sigma_i\},$$

$$\alpha_2 = \max_{i=1,2,3} \{\lambda_i, \sigma_i\},$$

it follows that, for any $\xi \in \mathbb{R}^2$, any $i \in \{1, 2, 3\}$, the following inequalities hold,

$$\alpha_1 \|\xi\|^2 \leq V(\xi, i) \leq \alpha_2 \|\xi\|^2,$$

and consequently, condition (b_1) of Theorem 8 is satisfied by the candidate Lyapunov function V introduced in (4.14).

Consider $\mathcal{L}V$ defined in (4.8).

The following inequalities hold, for any $\xi \in \mathbb{R}^2$, any $u \in \mathbb{R}$, any $i \in \{1, 2, 3\}$.

$$\begin{aligned}
\mathcal{L}V(\xi, u, 1) &= pV(f_1(\xi, u), 1) + (1-p)V(f_1(\xi, u), 2) - V(\xi, 1) \\
&\leq p\lambda_1\xi_2^2 + (1-p)\lambda_2\xi_2^2 + (p\sigma_1 + (1-p)\sigma_2)0.72\xi_1^2 - \lambda_1\xi_1^2 - \sigma_1\xi_2^2 + \tilde{S}u^2 \\
&\leq -\lambda_1 \left[1 - \left(p\frac{\sigma_1}{\lambda_1} + (1-p)\frac{\sigma_2}{\lambda_1} \right) 0.72 \right] \xi_1^2 \\
&\quad - \sigma_1 \left[1 - \left(p\frac{\lambda_1}{\sigma_1} + (1-p)\frac{\lambda_2}{\sigma_1} \right) \right] \xi_2^2 + \tilde{S}u^2, \\
\mathcal{L}V(\xi, u, 2) &= (1-q_1-q_2)V(f_2(\xi, u), 1) + q_1V(f_2(\xi, u), 2) + q_2V(f_2(\xi, u), 3) - V(\xi, 2) \\
&= 3.4[(1-q_1-q_2)\lambda_1 + q_1\lambda_2 + q_2\lambda_3]\xi_1^2 + 3.4[(1-q_1-q_2)\sigma_1 + q_1\sigma_2 + q_2\sigma_3]\xi_2^2 \\
&\quad - \lambda_2\xi_1^2 - \sigma_2\xi_2^2 + \tilde{S}u^2 \\
&\leq -\lambda_2 \left[1 - 3.4 \left(q_1 + q_2\frac{\lambda_3}{\lambda_2} + (1-q_1-q_2)\frac{\lambda_1}{\lambda_2} \right) \right] \xi_1^2 \\
&\quad - \sigma_2 \left[1 - 3.4 \left(q_1 + q_2\frac{\sigma_3}{\sigma_2} + (1-q_1-q_2)\frac{\sigma_1}{\sigma_2} \right) \right] \xi_2^2 + \tilde{S}u^2, \\
\mathcal{L}V(\xi, u, 3) &= 1 \times V(f_3(\xi, u), 2) - V(\xi, 3) \\
&\leq 3\lambda_2\xi_1^2 + 2.64\sigma_2\xi_2^2 - \lambda_3\xi_1^2 - \sigma_3\xi_2^2 + \tilde{S}u^2 \\
&\leq -\lambda_3 \left[1 - 3\frac{\lambda_2}{\lambda_3} \right] \xi_1^2 - \sigma_3 \left[1 - 2.64\frac{\sigma_2}{\sigma_3} \right] \xi_2^2 + \tilde{S}u^2,
\end{aligned}$$

with \tilde{S} positive real number.

Consequently, the following inequalities are satisfied, for any $\xi \in \mathbb{R}^2$, any $u \in \mathbb{R}$, any $i \in \{1, 2, 3\}$,

$$\begin{aligned}
\mathcal{L}V(\xi, u, i) &\leq -\min \left\{ \lambda_1 \left[1 - \left(p\frac{\sigma_1}{\lambda_1} + (1-p)\frac{\sigma_2}{\lambda_1} \right) 0.72 \right], \lambda_3 \left(1 - \frac{3\lambda_1}{\lambda_3} \right), \right. \\
&\quad \left. \sigma_1 \left[1 - \left(p\frac{\lambda_1}{\sigma_1} + (1-p)\frac{\lambda_2}{\sigma_1} \right) 1.2 \right], \sigma_3 \left(1 - \frac{2.64\sigma_1}{\sigma_3} \right), \right. \\
&\quad \left. \lambda_2 \left[1 - 3.4 \left(q_1 + q_2\frac{\lambda_3}{\lambda_2} + (1-q_1-q_2)\frac{\lambda_1}{\lambda_2} \right) \right], \right. \\
&\quad \left. \sigma_2 \left[1 - 3.4 \left(q_1 + q_2\frac{\sigma_3}{\sigma_2} + (1-q_1-q_2)\frac{\sigma_1}{\sigma_2} \right) \right] \right\} \|\xi\|^2 + \tilde{S}u^2,
\end{aligned}$$

with \tilde{S} positive real number.

Define the function $\alpha_3 : \mathbb{R}^+ \rightarrow \mathbb{R}^+$, for $s \in \mathbb{R}^+$, as $\alpha_3 \triangleq \tilde{\alpha}_3 s$, with $\tilde{\alpha}_3$ defined as follows,

$$\begin{aligned} \tilde{\alpha}_3 \triangleq \min & \left\{ \lambda_1 \left[1 - \left(p \frac{\sigma_1}{\lambda_1} + (1-p) \frac{\sigma_2}{\lambda_1} \right) 0.72 \right], \lambda_3 \left(1 - \frac{3\lambda_1}{\lambda_3} \right), \right. \\ & \sigma_1 \left[1 - \left(p \frac{\lambda_1}{\sigma_1} + (1-p) \frac{\lambda_2}{\sigma_1} \right) 1.2 \right], \sigma_3 \left(1 - \frac{2.64\sigma_1}{\sigma_3} \right), \\ & \lambda_2 \left[1 - 3.4 \left(q_1 + q_2 \frac{\lambda_3}{\lambda_2} + (1-q_1-q_2) \frac{\lambda_1}{\lambda_2} \right) \right], \\ & \left. \sigma_2 \left[1 - 3.4 \left(q_1 + q_2 \frac{\sigma_3}{\sigma_2} + (1-q_1-q_2) \frac{\sigma_1}{\sigma_2} \right) \right] \right\}. \end{aligned}$$

Consequently, the following inequality holds for any $\xi \in \mathbb{R}^2$, any $u \in \mathbb{R}$, any $i \in \{1, 2, 3\}$,

$$\mathcal{L}V(\xi, u, i) \leq -\tilde{\alpha}_3 \|\xi\|^2 + \alpha_4(\|u\|),$$

where α_4 is a function of class \mathcal{K} .

Condition (b₂) of Theorem 8 is satisfied if $\tilde{\alpha}_3 > 0$, i.e., under the following constraints for $\lambda_i, \sigma_i > 0$, $i = 1, 2, 3$:

$$0.72 \left(p \frac{\sigma_1}{\lambda_1} + (1-p) \frac{\sigma_2}{\lambda_1} \right) < 1, \quad (4.15a)$$

$$1.2 \left(p \frac{\lambda_1}{\sigma_1} + (1-p) \frac{\lambda_2}{\sigma_1} \right) < 1, \quad (4.15b)$$

$$3.4 \left(q_1 + q_2 \frac{\lambda_3}{\lambda_2} + (1-q_1-q_2) \frac{\lambda_1}{\lambda_2} \right) < 1, \quad (4.15c)$$

$$3.4 \left(q_1 + q_2 \frac{\sigma_3}{\sigma_2} + (1-q_1-q_2) \frac{\sigma_1}{\sigma_2} \right) < 1, \quad (4.15d)$$

$$\frac{\lambda_1}{\lambda_3} < \frac{1}{3}, \quad \frac{\sigma_1}{\sigma_3} < 0.38, \quad (4.15e)$$

$$0 < p < 1, \quad 0 < q_1 < 1, \quad 0 < q_2 < 1, \quad q_1 + q_2 < 1. \quad (4.15f)$$

Thus, by Theorem 8, system (4.12) is *EMS-ISS* for all probabilities p, q_1, q_2 such that the constraints (4.15) are satisfied.

For an analysis of allowed probability sets and related statistics and simulations, see Paragraph 4.8.3.

Remark 42 The Lyapunov functions are chosen as quadratic ones, with coefficients λ_i, σ_i , $i = 1, 2, 3$ (see (4.14)). The presented methodology finds the coefficients λ_i, σ_i , $i = 1, 2, 3$, and the transition probabilities p, q_1, q_2 , such that the parametric constraints (4.15) are satisfied. The choice does not distinguish a-priori among *ISS* ($i = 1$) and not *ISS* ($i = 2, 3$) modes.

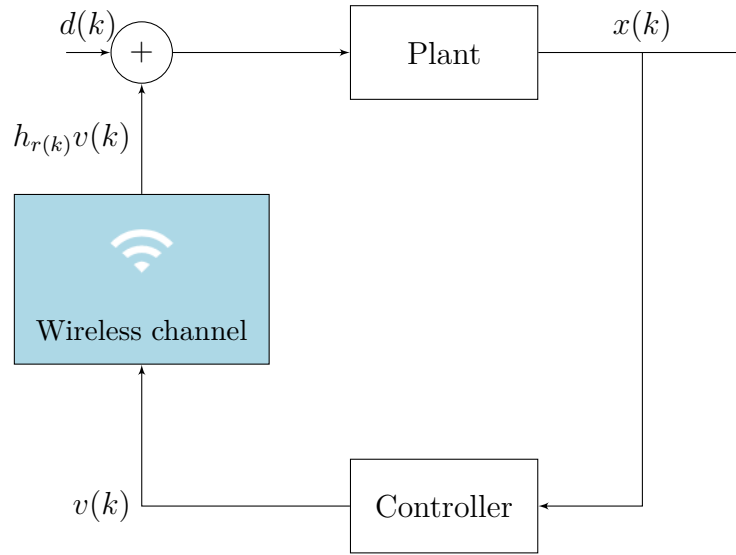


Figure 4.3: Block diagram showing a wireless control network architecture.

4.8.2 Application to wireless control network scenarios

Consider the WCN scenario in Fig. 4.3; the following example highlights the impact of the wireless channel on the control loop concerning the property of *EMS-ISS*.

Consider a nonlinear discrete-time plant controlled through a nonlinear state feedback (see Fig. 4.3). In Fig. 4.3 the control law $v(k)$, $k \in \mathbb{N}$, is sent to the actuators through a wireless communication channel that may suffer from packet losses. If the packet is successfully delivered, the actuators execute the control law, otherwise the system evolves in open-loop until a successful delivery of the control input occurs. Indeed, when a packet loss occurs the input is zero. The discrete-time Markov chain $r(k)$, $k \in \mathbb{N}$, in Fig. 4.4 provides the mathematical model of the wireless channel (see [1, 62] and the references therein). The mode $r(k)$ corresponds to the mode of the wireless communication channel at time $k \in \mathbb{N}$, and $r(k)$ takes values in the finite set $\{1, 2\}$: the channel mode is $r(k) = 1$ when the packet containing the control input is successfully delivered, while it is $r(k) = 2$ otherwise.

The TPM containing the transition probabilities of the Markov chain in Fig. 4.4 is provided by

$$P = \begin{bmatrix} p & 1-p \\ 1-q & q \end{bmatrix}, \quad p, q \in (0, 1).$$

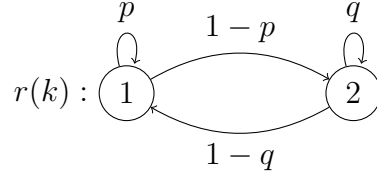


Figure 4.4: State diagram of the Markov chain $r(k)$ modeling the wireless channel in *Example 3*: p is the probability of having two consecutive correct packet deliveries, while q is the probability of having two consecutive packet losses.

For $k \in \mathbb{N}$, let $h_{r(k)}$ be equal to 1 if the channel mode is $r(k) = 1$, and let $h_{r(k)}$ be equal to 0 if the channel mode is $r(k) = 2$.

Formally,

$$h_{r(k)} = \begin{cases} 1, & \text{if } r(k) = 1, \\ 0, & \text{if } r(k) = 2. \end{cases} \quad (4.16)$$

The term $h_{r(k)}$ multiplies the control input $v(k)$ and if the mode of $r(k)$ is 1, then the control input is correctly delivered, otherwise the packet containing the control input is lost and the input is zero.

Consequently, we have $h_1 = 1$ and $h_2 = 0$.

Assume that the system is affected by an additive time-varying disturbance on the actuators $d(k)$ (see Fig. [4.3](#)) independent from the control input and uniformly bounded for $k \in \mathbb{N}$.

The following example provides the Lyapunov analysis of *EMS-ISS* with respect to disturbance d .

4.8.2.1 Example 3

Consider the setting presented above for WCNs, where for any $i \in \{1, 2\}$ the plant is described by the function

$$g_i : \mathbb{R}^2 \times \mathbb{R}^2 \times \mathbb{R}^2 \rightarrow \mathbb{R}^2,$$

defined, for $k \in \mathbb{N}$,

$$\begin{aligned} x(k) &= \begin{bmatrix} x_1(k) \\ x_2(k) \end{bmatrix} \in \mathbb{R}^2, & v(k) &= \begin{bmatrix} v_1(k) \\ v_2(k) \end{bmatrix} \in \mathbb{R}^2, \\ d(k) &= \begin{bmatrix} d_1(k) \\ d_2(k) \end{bmatrix} \in \mathbb{R}^2, \end{aligned}$$

as follows,

$$g_{r(k)}(x(k), v(k), d(k)) = \begin{bmatrix} \frac{6}{5}x_1(k) \tanh(x_2(k)) + h_{r(k)}v_1(k) + d_1(k) \\ \frac{3}{2}x_2(k) (\sin(x_1(k)) + \cos(x_1(k))) + h_{r(k)}v_2(k) + d_2(k) \end{bmatrix},$$

where $x(k)$, $v(k)$ are the state and the control input, respectively.

The additive time-varying disturbance $d(k)$, $k \in \mathbb{N}$, is independent from the control input $v(k)$ and uniformly bounded.

The nonlinear control law $v(k)$ is given by:

$$v(k) = \begin{bmatrix} -\frac{6}{5}x_1(k) \tanh(x_2(k)) + \frac{1}{4}x_1(k) \\ -\frac{3}{2}x_2(k) (\sin(x_1(k)) + \cos(x_1(k))) + \frac{1}{4}x_2(k) \end{bmatrix}.$$

When the mode of the communication channel is $r(k) = 1$, $k \in \mathbb{N}$, the control input $v(k)$ is correctly delivered and applied.

The closed-loop system is thus described by the function

$$f_1 : \mathbb{R}^2 \times \mathbb{R}^2 \rightarrow \mathbb{R}^2,$$

defined, for

$$x = \begin{bmatrix} x_1 \\ x_2 \end{bmatrix} \in \mathbb{R}^2 \quad d = \begin{bmatrix} d_1 & d_2 \end{bmatrix} \in \mathbb{R}^2,$$

as follows,

$$f_1(x, d) = \begin{bmatrix} \frac{1}{4}x_1 + d_1 \\ \frac{1}{4}x_2 + d_2 \end{bmatrix}. \quad (4.17)$$

When the mode of the communication channel is $r(k) = 2$, $k \in \mathbb{N}$, i.e., the input is zero, the open-loop subsystem is described by the function

$$f_2 : \mathbb{R}^2 \times \mathbb{R}^2 \rightarrow \mathbb{R}^2,$$

defined, for

$$x = \begin{bmatrix} x_1 \\ x_2 \end{bmatrix} \in \mathbb{R}^2 \quad d = \begin{bmatrix} d_1 & d_2 \end{bmatrix} \in \mathbb{R}^2,$$

as follows,

$$f_2(x, d) = \begin{bmatrix} \frac{6}{5}x_1 \tanh(x_2) + d_1 \\ \frac{3}{2}x_2(\sin(x_1) + \cos(x_1)) + d_2 \end{bmatrix}. \quad (4.18)$$

Notice that system $f_i(x, d)$, with $i = 1, 2$, is exactly the one considered in (4.3), where the switching signal is $r(k) \in \{1, 2\}$, $k \in \mathbb{N}$, and the input signal is the disturbance $d(k)$, $k \in \mathbb{N}$.

Moreover, the subsystem obtained for $r(k) = 1$ in (4.17) is ISS, while the subsystem obtained for $r(k) = 2$ in (4.18) is not ISS.

This example provides the *EMS-ISS* analysis of system $f_i(x, d)$, $i = 1, 2$, with respect to the disturbance d .

Consider the candidate Lyapunov function

$$V : \mathbb{R}^2 \times \{1, 2\} \rightarrow \mathbb{R}^+,$$

defined for $\xi = [\xi_1 \ \xi_2]^T \in \mathbb{R}^2$ and for $i \in \{1, 2\}$ as

$$V(\xi, i) = \lambda_i \xi_1^2 + \sigma_i \xi_2^2, \quad (4.19)$$

with $\lambda_i, \sigma_i > 0$. By choosing

$$\begin{aligned} \alpha_1 &= \min_{i \in \{1, 2\}} \{\lambda_i, \sigma_i\}, \\ \alpha_2 &= \max_{i \in \{1, 2\}} \{\lambda_i, \sigma_i\}, \end{aligned}$$

it follows that, for any $\xi \in \mathbb{R}^2$, any $i \in \{1, 2\}$, the following inequalities hold,

$$\alpha_1 \|\xi\|^2 \leq V(\xi, i) \leq \alpha_2 \|\xi\|^2,$$

and consequently, condition (b₁) of Theorem 8 is satisfied by the candidate Lyapunov function V introduced in (4.19).

The next step consists in verifying condition (b₂) of Theorem 8.

Consider $\mathcal{L}V$ defined in (4.8).

From equations (4.17) and (4.18), by applying the expression of $\mathcal{L}V$ in (4.8), from Young's inequality [229], the following inequalities hold, for any $\xi \in \mathbb{R}^2$, any

$d \in \mathbb{R}^2$, any $i \in \{1, 2\}$,

$$\begin{aligned}
\mathcal{L}V(\xi, d, 1) &= \sum_{j=1}^2 p_{1j} V(f_1(\xi, d), j) - V(\xi, 1) = \\
&= pV(f_1(\xi, d), 1) + (1-p)V(f_1(\xi, d), 2) - \lambda_1 \xi_1^2 - \sigma_1 \xi_2^2 = \\
&= p\lambda_1 \left(\frac{1}{4}\xi_1 + d_1\right)^2 + p\sigma_1 \left(\frac{1}{4}\xi_2 + d_2\right)^2 + \\
&+ (1-p)\lambda_2 \left(\frac{1}{4}\xi_1 + d_1\right)^2 + (1-p)\sigma_2 \left(\frac{1}{4}\xi_2 + d_2\right)^2 - \lambda_1 \xi_1^2 - \sigma_1 \xi_2^2 \\
&\leq -\lambda_1 \left[1 - \left(p + (1-p)\frac{\lambda_2}{\lambda_1}\right) \frac{1}{8}\right] \xi_1^2 + \\
&- \sigma_1 \left[1 - \left(p + (1-p)\frac{\sigma_2}{\sigma_1}\right) \frac{1}{8}\right] \xi_2^2 + \tilde{S}\|d\|^2, \\
\mathcal{L}V(\xi, d, 2) &= \sum_{j=1}^2 p_{2j} V(f_2(\xi, d), j) - V(\xi, 2) = \\
&\leq [(1-q)\lambda_1 + q\lambda_2] \left(\frac{36}{25}\xi_1^2 + d_1^2 + \frac{6}{5}\xi_1^2 + \frac{6}{5}d_1^2\right) + \\
&+ [(1-q)\sigma_1 + q\sigma_2] \left(\frac{9}{2}\xi_2^2 + d_2^2 + \frac{3}{2} \times 2\xi_2(\sin(\xi_1) + \cos(\xi_1))^*d\right) + \\
&- \lambda_2 \xi_1^2 - \sigma_2 \xi_2^2 \leq \\
&\leq [(1-q)\lambda_1 + q\lambda_2] \left(\frac{36}{25}\xi_1^2 + d^2 + \frac{6}{5}\xi_1^2 + \frac{6}{5}d^2\right) + \\
&+ [(1-q)\sigma_1 + q\sigma_2] \left(\frac{9}{2}\xi_2^2 + d^2 + \frac{3}{2}\xi_2^2 + 3d^2\right) - \lambda_2 \xi_1^2 - \sigma_2 \xi_2^2 \\
&\leq -\lambda_2 \left[1 - \left(q + (1-q)\frac{\lambda_1}{\lambda_2}\right) \frac{66}{25}\right] \xi_1^2 + \\
&- \sigma_2 \left[1 - \left(q + (1-q)\frac{\sigma_1}{\sigma_2}\right) 6\right] \xi_2^2 + \tilde{S}\|d\|^2,
\end{aligned}$$

with \tilde{S} positive real number.

Consequently, the following inequality holds, for any $\xi \in \mathbb{R}^2$, any $d \in \mathbb{R}^2$, any $i \in \{1, 2\}$,

$$\mathcal{L}V(\xi, d, i) \leq -\alpha_3 \|\xi\|^2 + \alpha_4 (\|d\|),$$

with α_4 function of class \mathcal{K} , and α_3 defined as follows,

$$\alpha_3 \triangleq \min \left\{ \lambda_1 \left(1 - \left(p + (1-p) \frac{\lambda_2}{\lambda_1} \right) \frac{1}{8} \right), \right. \\ \sigma_1 \left(1 - \left(p + (1-p) \frac{\sigma_2}{\sigma_1} \right) \frac{1}{8} \right), \\ \lambda_2 \left(1 - \left(q + (1-q) \frac{\lambda_1}{\lambda_2} \right) \frac{66}{25} \right), \\ \left. \sigma_2 \left(1 - \left(q + (1-q) \frac{\sigma_1}{\sigma_2} \right) 6 \right) \right\}.$$

Recall that condition (b_2) of Theorem [8](#) is satisfied if $\alpha_3 > 0$.

The real number α_3 is strictly positive if the following conditions hold for $\lambda_i, \sigma_i > 0$, $i = 1, 2$:

$$L_{1,B} < \frac{\lambda_2}{\lambda_1} < U_{1,B}, \quad (4.20a)$$

$$L_{2,B} < \frac{\sigma_2}{\sigma_1} < U_{2,B}, \quad (4.20b)$$

$$0 < p < 1, \quad 0 < q < 1, \quad (4.20c)$$

where the quantities $L_{1,B}$, $L_{2,B}$, and $U_{1,B}$, $U_{2,B}$ are given by

$$L_{1,B} = \frac{66(1-q)}{(25-66q)}, \\ L_{2,B} = \frac{6(1-q)}{(1-6q)}, \\ U_{1,B} = U_{2,B} = \frac{(8-p)}{(1-p)}.$$

Thus, the considered Markovian switching system $f_i(x, d)$, $i = 1, 2$ is *EMS-ISS* by Theorem [8](#), for all the pairs of probabilities $(p, q) \in (0, 1) \times (0, 1)$ such that the constraints [\(4.20\)](#) are satisfied.

For an analysis of allowed probability sets and related statistics and simulations, see Paragraph [4.8.3](#).

4.8.2.2 Example 4

Consider a WCN scenario where a nonlinear system is controlled through a nonlinear state feedback, and the control law is sent to the actuators through a communication channel that may suffer from packet-losses, see Fig. [4.3](#).

If the packet is successfully delivered, the actuators are able to execute the control law, otherwise the system evolves in open-loop until a successful delivery of the control input occurs.

Let us also assume that the system is affected by an additive bounded disturbance on the actuators, independent from the control input.

Let us model the closed-loop system, using a discrete-time nonlinear Markovian switching system, as follows,

$$x(k+1) = \sqrt[2]{a^2 x^2(k) + h_{r(k)} v(k) + c d^2(k)}, \quad (4.21)$$

where $x(k), v(k) \in \mathbb{R}$ are the state and the control input, respectively.

The additive time-varying disturbance $d(k) \in \mathbb{R}$ is a bounded quantity for any $k \in \mathbb{N}$.

The quantities $a \in \mathbb{R}$, $c \in \mathbb{R}^+$ are constant values: let us choose $a = 2$, $c = 1$. The discrete-time time-homogeneous Markov chain $r(k)$ depicted in Fig. 4.4, $k \in \mathbb{N}$, accounts for the mode of the communication channel and takes values in the finite set $S = \{1, 2\}$. The value of $h_{r(k)}$ defined in (4.16) depends on the mode $r(k) = i \in S$ of the Markov chain.

The mode $i = 1$ corresponds to the situation in which the control input is successfully delivered, then $h_1 = 1$, while the mode $i = 2$ corresponds to the situation in which a packet-loss occurs and the system evolves in open-loop, i.e. $h_2 = 0$.

Consider the nonlinear control law given by equation (4.22):

$$v(k) = -R x^2(k). \quad (4.22)$$

Thus, the closed-loop system is:

$$x(k+1) = f_{r(k)}(x(k), d(k)), \quad (4.23)$$

with

$$f_{r(k)}(x(k), d(k)) = \sqrt[2]{(a^2 - h_{r(k)} R) x^2(k) + c d^2(k)}$$

In order to have the root well defined, the feedback gain R should be such that:

$$a^2 - h_i R \geq 0,$$

for any $i \in S$.

Therefore, the feedback gain R is chosen such that

$$a^2 - R = \frac{1}{5}, \quad \implies \quad R = \frac{19}{5}.$$

The aforementioned control stabilizes the closed-loop system in case of absence of packet losses and disturbances.

Indeed, under the following conditions,

- $h_r(k) = 1$, for any $k \in \mathbb{N}$, i.e., absence of packet losses,
- $d(k) = 0$, for any $k \in \mathbb{N}$, i.e., absence of disturbances,

the closed-loop system is given by:

$$x(k+1) = \sqrt[2]{\frac{1}{5}x^2} = \sqrt[2]{\frac{1}{5}}|x|. \quad (4.24)$$

The system (4.24) is clearly globally asymptotically stable, since $\sqrt[2]{\frac{1}{5}} < 1$.

Taking into account the occurrence of packet losses and the presence of the disturbances, the closed-loop system can be formally written as follows,

$$\mathcal{G} : \begin{cases} f_1(x, d) = \sqrt[2]{\frac{1}{5}x^2 + d^2}, \\ f_2(x, d) = \sqrt[2]{4x^2 + d^2}, \end{cases} \quad (4.25)$$

which is a discrete-time nonlinear Markovian switching system, as the one introduced in (4.3), with the bounded disturbance d , as input.

The aim of this example is studying the second moment of the state, i.e., what happens when the exponent p equals 2, that is, the mean square input-to-state stability of the system described by (4.25), with respect to the disturbance d .

Let us apply the conditions provided by *Theorem 9*, considering three different cases, corresponding to three different TPMs.

Specifically, each case shows what happens considering a given TPM (with given transition probabilities from one mode of the communication channel to the other one).

- Case 1.

$$P_1 = \begin{bmatrix} \frac{3}{4} & \frac{1}{4} \\ 1 & 0 \end{bmatrix},$$

- Case 2.

$$P_2 = \begin{bmatrix} \frac{3}{4} & \frac{1}{4} \\ \frac{4}{5} & \frac{1}{5} \end{bmatrix},$$

- Case 3.

$$P_3 = \begin{bmatrix} \frac{3}{4} & \frac{1}{4} \\ \frac{3}{5} & \frac{2}{5} \end{bmatrix}.$$

The probabilities of transitions starting from the mode $i = 1$ are always the same in the three cases, while the probability of a transition from the mode $i = 2$ to the mode $i = 2$ (corresponding to the occurrence of bursts of packet losses) increases.

Consequently, the probability of a transition from the mode $i = 2$ to the mode $i = 1$ (corresponding to control recover after packet loss occurrence) decreases in the three cases.

Multiple Lyapunov functions can be chosen in the three cases, such as, $V(\xi, i)$, defined for $\xi \in \mathbb{R}$, $i \in S$, as follows,

$$V(\xi, i) = \lambda_i \xi^2, \quad (4.26)$$

with the coefficients $\lambda_i > 0$, for all $i \in S$.

Particularly, by choosing α_1 and α_2 as,

$$\alpha_1 = \min_{i \in S} \{\lambda_i\},$$

$$\alpha_2 = \max_{i \in S} \{\lambda_i\},$$

the candidate Lyapunov function introduced in (4.26) satisfies condition (a) in Theorem 9.

Case 1

Consider the TPM P_1 .

Then, $\mathcal{L}V(\xi, d, 1)$ and $\mathcal{L}V(\xi, d, 2)$ can be computed applying the expression introduced in (4.8), as follows,

$$\mathcal{L}V(\xi, d, 1) = -\lambda_1 \left[1 - \left(\frac{3}{4} + \frac{1}{4} \frac{\lambda_2}{\lambda_1} \right) \frac{1}{5} \right] \xi^2 + \left(\frac{3}{4} \lambda_1 + \frac{1}{4} \lambda_2 \right) d^2, \quad (4.27)$$

$$\mathcal{L}V(\xi, d, 2) = -\lambda_2 \left(1 - \frac{\lambda_1}{\lambda_2} \frac{1}{4} \right) \xi^2 + \lambda_1 d^2. \quad (4.28)$$

From the expressions of $\mathcal{L}V(\xi, d, 1)$ in (4.27) and $\mathcal{L}V(\xi, d, 2)$ in (4.28), the candidate Lyapunov function introduced in (4.26) satisfies condition (b) in Theorem 9 if the following inequalities are satisfied, i.e.,

$$1 - \left(\frac{3}{4} + \frac{1}{4} \frac{\lambda_2}{\lambda_1} \right) \frac{1}{5} > 0, \quad (4.29)$$

$$1 - \frac{\lambda_1}{\lambda_2} 4 > 0. \quad (4.30)$$

Inequality (4.29) and inequality (4.30) are satisfied if and only if

$$4 < \frac{\lambda_2}{\lambda_1} < 17.$$

Then, let us define the function $\gamma_1 \in \mathcal{K}_\infty$, as follows,

$$\gamma_1(s) \triangleq \min \left\{ \lambda_1 \left[1 - \left(\frac{3}{4} + \frac{1}{4} \frac{\lambda_2}{\lambda_1} \right) \frac{1}{5} \right], \lambda_2 \left(1 - \frac{\lambda_1}{\lambda_2} 4 \right) \right\} s,$$

with $s \in \mathbb{R}^+$.

Let us also introduce the \mathcal{K} -function δ_1 as follows,

$$\delta_1(s) \triangleq \max \left\{ \frac{3}{4} \lambda_1 + \frac{1}{4} \lambda_2, \lambda_1 \right\} s^2,$$

with $s \in \mathbb{R}^+$.

Then, the following inequality is satisfied for any ξ, d in \mathbb{R} , any $i \in S$,

$$\mathcal{L}V(\xi, d, i) \leq -\gamma_1(|\xi|^2) + \delta_1(|d|). \quad (4.31)$$

From (4.31), it follows that the system described by (4.25) is second moment exponentially ISS by Corollary 1, i.e., the system described by (4.25) is *EMS-ISS*.

Case 2

Consider now the TPM P_2 .

Then, $\mathcal{L}V(\xi, d, 1)$ and $\mathcal{L}V(\xi, d, 2)$ can be computed applying the expression introduced in (4.8), as follows,

$$\mathcal{L}V(\xi, d, 1) = -\lambda_1 \left[1 - \left(\frac{3}{4} + \frac{1}{4} \frac{\lambda_2}{\lambda_1} \right) \frac{1}{5} \right] \xi^2 + \left(\frac{3}{4} \lambda_1 + \frac{1}{4} \lambda_2 \right) d^2, \quad (4.32)$$

$$\mathcal{L}V(\xi, d, 2) = -\lambda_2 \left[1 - \left(\frac{1}{5} + \frac{4}{5} \frac{\lambda_1}{\lambda_2} \right) 4 \right] \xi^2 + \left(\frac{4}{5} \lambda_1 + \frac{1}{5} \lambda_2 \right) d^2. \quad (4.33)$$

Applying the same reasoning presented in **Case 1**, from the expressions of $\mathcal{L}V(\xi, d, 1)$ in (4.32) and $\mathcal{L}V(\xi, d, 2)$ in (4.33), the candidate Lyapunov function introduced in (4.26) satisfies condition (b) in Theorem 9 if the following inequalities are satisfied, i.e.,

$$1 - \left(\frac{3}{4} + \frac{1}{4} \frac{\lambda_2}{\lambda_1} \right) \frac{1}{5} > 0, \quad (4.34)$$

$$1 - \left(\frac{1}{5} + \frac{4}{5} \frac{\lambda_1}{\lambda_2} \right) 4 > 0. \quad (4.35)$$

Inequality (4.34) and inequality (4.35) are satisfied if and only if

$$16 < \frac{\lambda_2}{\lambda_1} < 17.$$

Then, let us define the function $\gamma_2 \in \mathcal{K}_\infty$, as follows,

$$\gamma_2(s) \triangleq \min \left\{ \lambda_1 \left[1 - \left(\frac{3}{4} + \frac{1}{4} \frac{\lambda_2}{\lambda_1} \right) \frac{1}{5} \right], \lambda_2 \left[1 - \left(\frac{1}{5} + \frac{4}{5} \frac{\lambda_1}{\lambda_2} \right) 4 \right] \right\} s,$$

with $s \in \mathbb{R}^+$.

Let us also introduce the \mathcal{K} -function δ_2 as follows,

$$\delta_2(s) \triangleq \max \left\{ \left(\frac{3}{4} \lambda_1 + \frac{1}{4} \lambda_2 \right), \left(\frac{4}{5} \lambda_1 + \frac{1}{5} \lambda_2 \right) \right\} s^2,$$

with $s \in \mathbb{R}^+$.

Then, the following inequality is satisfied for any ξ, d in \mathbb{R} , any i in S ,

$$\mathcal{L}V(\xi, d, i) \leq -\gamma_2(|\xi|^2) + \delta_2(|d|). \quad (4.36)$$

From (4.36), it follows that the system described by (4.25) is second moment exponentially ISS by Corollary 9, i.e., the system described by (4.25) is *EMS-ISS*.

Remark 43 Note that the condition concerning λ_2/λ_1 is more restrictive with respect to the previous case.

Case 3

Consider now the TPM P_3 .

Then, $\mathcal{L}V(\xi, d, 1)$ and $\mathcal{L}V(\xi, d, 2)$ can be computed applying the expression introduced in (4.8), as follows,

$$\mathcal{L}V(\xi, d, 1) = -\lambda_1 \left[1 - \left(\frac{3}{4} + \frac{1}{4} \frac{\lambda_2}{\lambda_1} \right) \frac{1}{5} \right] \xi^2 + \left(\frac{3}{4} \lambda_1 + \frac{1}{4} \lambda_2 \right) d^2, \quad (4.37)$$

$$\mathcal{L}V(\xi, d, 2) = -\lambda_2 \left[1 - \left(\frac{2}{5} + \frac{3}{5} \frac{\lambda_1}{\lambda_2} \right) 4 \right] \xi^2 + \left(\frac{3}{5} \lambda_1 + \frac{2}{5} \lambda_2 \right) d^2. \quad (4.38)$$

Applying the same reasoning presented in **Case 1** and in **Case 2**, from the expression of $\mathcal{LV}(\xi, d, 1)$ in (4.37) and $\mathcal{LV}(\xi, d, 2)$ in (4.37), the candidate Lyapunov function introduced in (4.26) satisfies condition (b) in Theorem 9 if the following inequalities are satisfied, i.e.,

$$1 - \left(\frac{3}{4} + \frac{1}{4} \frac{\lambda_2}{\lambda_1} \right) \frac{1}{5} > 0, \quad (4.39)$$

$$1 - \left(\frac{2}{5} + \frac{3}{5} \frac{\lambda_1}{\lambda_2} \right) 4 > 0. \quad (4.40)$$

Inequality (4.39) and inequality (4.40) are satisfied if and only if

$$\frac{\lambda_2}{\lambda_1} < 17,$$

which follows from inequality (4.39), and

$$\frac{\lambda_1}{\lambda_2} < -\frac{1}{4},$$

which follows from inequality (4.40).

Since $\lambda_1, \lambda_2 > 0$, the sufficient conditions given by Theorem 9 are not satisfied and, in this case, the use of this candidate Lyapunov function does not provide any conclusion concerning the second moment ISS of the system described by (4.25).

4.8.3 Statistical results

Fig. 4.5 illustrates Monte Carlo simulations of trajectories generated by the system described by (4.12) in *Example 2*: the input signal is a bounded disturbance generated as a random process with uniform distribution between ± 0.02 .

Moreover, the transition probabilities of the Markov chain in simulations are chosen such that conditions (b₁) and (b₂) of Theorem 8 are satisfied, see (4.15) $a - f$.

Fig. 4.6 depicts Monte Carlo simulations of trajectories generated by the system $f_i(x, d)$, $i = 1, 2$ in *Example 3*: the process disturbances are assumed to be random processes with uniform distribution between ± 0.02 .

Also in this case, the transition probabilities of the Markov chain in simulations are chosen such that conditions (b₁) and (b₂) of Theorem 8 are satisfied.

Consider Fig. 4.5 and Fig. 4.6:

- the state trajectories associated with switching paths generated by Monte Carlo simulations are denoted by $(x_{1,aggr.}, x_{2,aggr.})$ and are plotted in yellow,
- the maximum trajectories are denoted by $(x_{1,max}, x_{2,max})$ and are plotted in blue,
- the minimum trajectories are denoted by $(x_{1,min}, x_{2,min})$ and are plotted in green,
- the average evolution of state trajectories are denoted by $(x_{1,avg}, x_{2,avg})$ and are plotted in red.

As the reader can see from Fig. 4.5 and from Fig. 4.6, the state trajectories have an exponential decrease and finally remain bounded. Thus, the results reflect the analysis presented in this section. Fig. 4.7 shows the region determined by the values

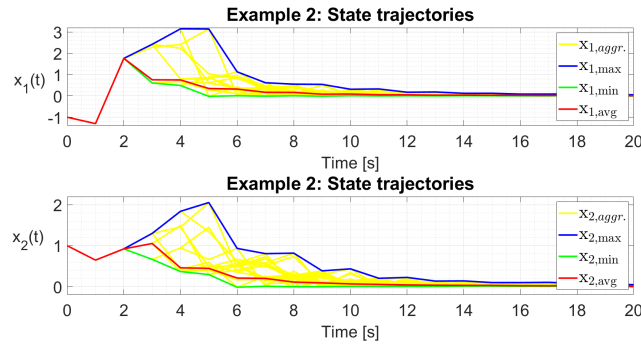


Figure 4.5: Traces obtained in *Example 2* with $p = 0.98$, $q_1 = q_2 = 0.039$.

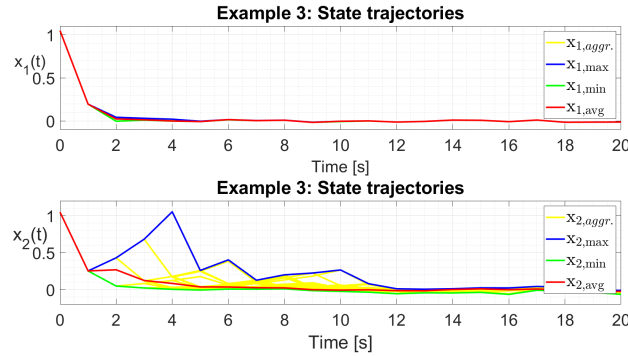


Figure 4.6: Traces obtained in *Example 3* with $p = 0.43$, $q = 0.099$.

of transition probabilities p and $q_1 = q_2 = q$, such that condition (b) of Theorem 8 is satisfied for *Example 2*.

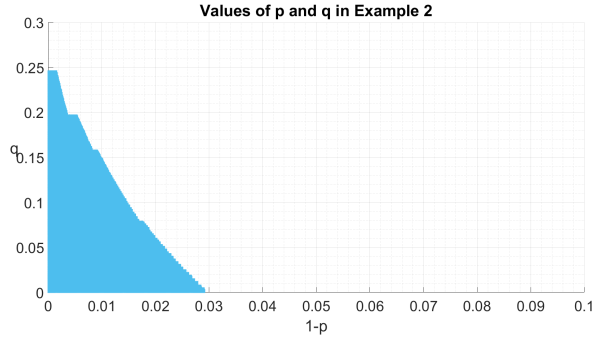


Figure 4.7: Pairs $(1 - p, q)$: EMS-ISS holds in *Example 2*, with $q_1 = q_2 = q$.

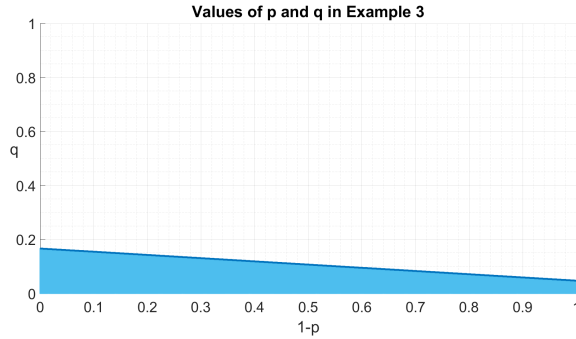


Figure 4.8: Pairs $(1 - p, q)$: EMS-ISS holds in *Example 3*.

Fig. 4.8 shows the region of pairs $(1 - p, q)$ (in *Example 3*) such that condition (b) of Theorem 8 is satisfied (lightblue region) and the evolution of the maximum probability q (the probability of a burst of packet losses) with respect to $1 - p$ (with p probability of a burst of successful packet delivery) such that condition (b) of Theorem 8 is satisfied (darkblue line).

Remark 44 An interesting insight of the presented methodology is the key role played by the transition probabilities, that can be interpreted in terms of average time spent in each subsystem (ISS and not ISS). Indeed, from Markov chain theory (see [138]), once entered in subsystem i , the exit-time from i follows a geometric distribution with parameter $1 - p_{ii}$ (p_{ii} is the self-loop probability of the mode i). The time spent in i is characterized by the average value $1/(1 - p_{ii})$, and also by the variance $p_{ii}/(1 - p_{ii})^2$.

Fig. 4.9 depicts statistical results for Monte Carlo simulations of the trajectories generated by the system described by (4.25) for **Case 1** and **Case 2** of Example 4, respectively. The aforementioned trajectories have been obtained using the MATLAB environment and considering 1000 simulations.

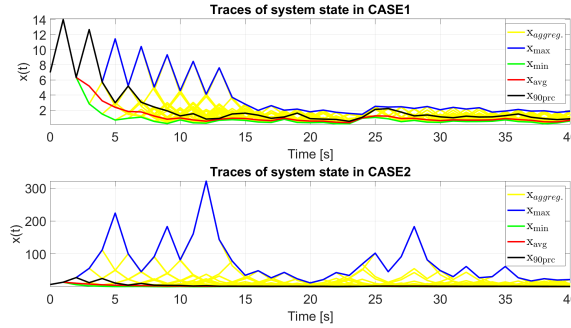


Figure 4.9: Traces of system state obtained in **Case 1** and in **Case 2**, respectively.

The initial condition is $x_0 = 7$ and the additive time-varying disturbance is given by $d(t)$, with $|d(t)| \leq 1$ for any $t \in \mathbb{N}$, in both the cases.

Consider Fig. [4.9](#) and Fig. [4.10](#):

- the yellow trajectories denoted by $x_{1,aggr.}$, $x_{2,aggr.}$ are state trajectories associated to different switching paths, that are admissible according to the TPMs P_1 (for **Case 1**) and P_2 (for **Case 2**),
- the maximal trajectories are denoted by $(x_{1,max}, x_{2,max})$ and are illustrated by the blue trace,
- the minimum trajectories are denoted by $(x_{1,min}, x_{2,min})$ and are plotted by the green trace,
- the average evolution of state trajectories are denoted by $(x_{1,avg}, x_{2,avg})$ and are plotted in red,
- the black line shows the 90th percentile of the state, this means that the 90% of trajectories can be found below the black line.

Moreover, Fig. [4.10](#) shows the traces of the 90th percentile of the state, considered without other trajectories, in order to focus on the decrease characterizing the largest number of trajectories. Indeed, in these two cases, after a transient, the trajectories have an exponential decrease, as we expected.

Furthermore, they finally remain bounded, since the disturbance is bounded. The transient has not the same duration in the two cases, as highlighted by Fig. [4.10](#). In **Case 1**, the transient is approximately 10s, while in **Case 2** it is approximately

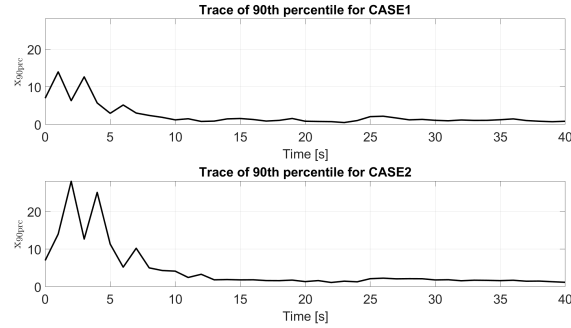


Figure 4.10: Traces of 90th percentile obtained in **CASE 1** and in **CASE 2**, respectively.

15 s (see Fig. [4.10](#)). In **Case 1**, the probability of control recover after failure is equal to 1, while the probability of consecutive packet-losses is 0. In **Case 2**, the probability of recover after failure (given by $4/5$) decreases and, consequently, the probability of consecutive failures (given by $1/5$) increases with respect to the previous case. This is the reason why the transient duration is larger in **Case 2** with respect to the transient duration in **Case 1**.

This chapter illustrates a complete Lyapunov characterization for *EMSS* and *EMSS-ISS* of discrete-time Markovian switching nonlinear systems. Some examples of the proposed approach are provided.

Particularly, the examples reveal the effectiveness of the presented methodology especially in the stability analysis of WCNs. Indeed, the proposed methodology allows to carry out the stability analysis of a discrete-time nonlinear system involved in a wireless control loop taking into account the probability of bursts of packet losses on the wireless channel.

5

Discrete-time systems with Markovian delays

Contents

5.1 Chapter outline	127
5.2 Notation and basic definitions	128
5.3 Problem formulation	128
5.4 Main result	132
5.5 Example	133
5.5.1 Statistical results	137

Among the challenges addressed by WCN literature the reader may find the problems caused by delays, that may affect transmissions [74, 148] and lead to stability degradation.

Discrete-time systems subject to Markovian delays are able to provide the mathematical description of WCNs with delays modeled by Markov chains.

This chapter addresses the problems concerning exponential mean square stability analysis of discrete-time nonlinear systems [94] subject to Markovian delays.

Exponential mean square stability notion has been already investigated for discrete-time Markovian switching linear systems without delays [4]. Only few works such as [3, 145] investigate this stability notion in the nonlinear framework.

However, when considering discrete-time nonlinear systems with Markovian delays, the mean square stability notion results to be particularly useful for investigating the behavior of the system, given the stochastic property provided by the Markovian delays.

The research line presented in this chapter is based on the paper by *Impicciatore et al.* [173] and provides two main contributions.

- Firstly, this chapter shows that when considering discrete-time delay systems with delay signals constrained to follow a delay digraph [160,169,170], the discrete-time delay system can be rewritten as a discrete-time Markov jump system [3,4] if the delay switching rule satisfies the Markov property.
- Secondly, this part of the thesis extends sufficient Lyapunov conditions existing for the global asymptotic stability property of discrete-time delay systems with delays digraphs [169,170] to the study of mean square stability.

Particularly, this research moves from the work by *Pepe* [169] that focuses on delay-dependent Lyapunov functions for discrete-time systems with constrained time delays.

In this chapter, the stability analysis is carried out via multiple Lyapunov functions [136,142] depending on the mode of the Markov chain, that governs the switching delay.

An important feature of the involved Lyapunov inequalities, shared with the cases of delay-dependent and delay-independent Lyapunov functions [160,169], is that lower and upper bounds of Lyapunov functions, as well as the related difference operators, are given in the weakest form, as far as norms and seminorms of the (memory) state are concerned.

5.1 Chapter outline

The chapter is organized as follows.

- Section [5.2] provides some useful notation concerning time-delay systems that is exploited only in this chapter.
- Section [5.3] introduces discrete-time delay systems with Markovian delay signals.
- Section [5.4] illustrates the main result concerning sufficient Lyapunov conditions guaranteeing exponential mean square stability.

- Section 5.5 provides an example that illustrates the effectiveness of the presented result.
- Proofs of Lemmas and theorems are reported in Appendix D.

5.2 Notation and basic definitions

This section provides the notation concerning time-delay systems that is used only in this chapter. For positive real Δ and positive integer n , the symbol \mathcal{C} denotes the space of functions mapping the set $\{-\Delta, -\Delta + 1, \dots, 0\}$ into \mathbb{R}^n .

For $\phi \in \mathcal{C}$,

$$\|\phi\|_\infty = \max\{\|\phi(-j)\| : j = 0, 1, \dots, \Delta\}.$$

For any non-negative integer c (or for $c = +\infty$), for any function

$$x : \{-\Delta, -\Delta + 1, \dots, c\} \rightarrow \mathbb{R}^n,$$

for any integer $k \in [0, c]$, x_k is the function in \mathcal{C} defined, for

$$\tau \in \{-\Delta, -\Delta + 1, \dots, 0\},$$

as

$$x_k(\tau) = x(k + \tau).$$

Consider in this chapter the stochastic basis defined by the quadruple $(\Omega, \mathcal{G}, \{\mathcal{G}_k\}, \mathbb{P})$, where Ω is the sample space, \mathcal{G} is the corresponding σ -algebra of events, $\{\mathcal{G}_k\}_{k \in \mathbb{N}}$ is the filtration, \mathbb{P} is the probability measure.

5.3 Problem formulation

This chapter focuses on the discrete-time delay system [160] introduced in the following as,

$$\begin{aligned} x(k+1) &= f(x(k), x(k-d_1(k)), \dots, x(k-d_r(k))), \\ x(\theta) &= \xi_0(\theta), \theta \in \{-\Delta, -\Delta+1, \dots, 0\}, \end{aligned} \quad (5.1)$$

where:

- $k \in \mathbb{N}$,
- the maximum involved time delay denoted by Δ is a known positive integer,
- $x(j) \in \mathbb{R}^n$, $j \geq -\Delta$,
- for $1 \leq i \leq r$, r known positive integer, $d_i(k) \in \{0, 1, \dots, \Delta\}$, $k \in \mathbb{N}$, is a time-varying time delay,
- the function $f : \mathbb{R}^{n(r+1)} \rightarrow \mathbb{R}^n$ satisfies the equality $f(0, 0, \dots, 0) = 0$,
- $\xi_0 \in \mathcal{C}$.

Let the vector $d(k)$, $k \in \mathbb{N}$,

$$d(k) = [d_1(k) \quad d_2(k) \quad \dots \quad d_r(k)]^T,$$

denote the vector collecting all time delays at time k .

For r known positive integer, let

$$D \subset \{0, 1, \dots, \Delta\}^r,$$

be the set of allowed values for the time-delays vector $d(k)$, that is, for any $k \in \mathbb{N}$, $d(k) \in D$.

The system (5.1) can be rewritten by using the following equation, (see 160 and references therein):

$$\begin{aligned} x_{k+1} &= F(x_k, d(k)), \\ x_0 &= \xi_0, \quad \xi_0 \in \mathcal{C}, \end{aligned} \tag{5.2}$$

with

- $x_k \in \mathcal{C}$,
- $x_k(\theta) = x(k + \theta)$, $k \in \mathbb{N}$.

The map

$$F : \mathcal{C} \times D \rightarrow \mathcal{C}$$

is defined, for $\phi \in \mathcal{C}$, $d \in D$, as follows,

$$F(\phi, d)(\theta) = \begin{cases} f(\phi(0), \phi(-d_1), \dots, \phi(-d_r)), & \theta = 0, \\ \phi(\theta + 1), & \theta = -\Delta, -\Delta + 1, \dots, -1. \end{cases} \quad (5.3)$$

Let us define the Markov chain as follows,

$$\eta : \mathbb{N} \rightarrow \mathcal{S},$$

with $\mathcal{S} \triangleq \{1, \dots, s\}$, where s is the cardinality of D , $s = |D|$.

The TPM of the Markov chain η is defined as $P \triangleq [p_{ij}]_{i,j \in \mathcal{S}}$, with the transition probabilities p_{ij} defined for $i, j \in \mathcal{S}$, as follows,

$$p_{ij} \triangleq \mathbb{P}(\eta(k+1) = j | \eta(k) = i), \quad (5.4)$$

$$\sum_{j \in \mathcal{S}} p_{ij} = 1, \quad 0 \leq p_{ij} \leq 1. \quad (5.5)$$

Let us make the following assumptions.

Assumption 3 The delay $d(k+1)$ depends only on the delay at the previous step $d(k)$, $k \in \mathbb{N}$.

Assumption 4 The prior knowledge on the transition from $d(k)$ to $d(k+1)$ is given by a transition probability.

Let the function $H : D \rightarrow \mathcal{S}$ be a bijective function defined for all $\delta_i \in D$, and for all $i \in \mathcal{S}$, as follows,

$$H(\delta_i) \triangleq i. \quad (5.6)$$

The inverse function of H is

$$H^{-1} : \mathcal{S} \rightarrow D,$$

defined for all $i \in \mathcal{S}$ and for all $\delta_i \in D$, as follows,

$$H^{-1}(i) \triangleq \delta_i. \quad (5.7)$$

Consider for $i, j \in \mathcal{S}$, the transition probability p_{ij} defined in (5.4).

By applying the definition of p_{ij} in (5.4) and the definition of the functions H and H^{-1} , the following equalities hold:

$$\begin{aligned} p_{ij} &= \mathbb{P}(\eta(k+1) = j | \eta(k) = i) \\ &= \mathbb{P}\left(H(d(k+1)) = H(\delta_j) | H(d(k)) = H(\delta_i)\right) \\ &= \mathbb{P}(d(k+1) = \delta_j | d(k) = \delta_i), \end{aligned} \quad (5.8)$$

for all $\delta_i, \delta_j \in D$, for all $i, j \in \mathcal{S}$.

Consequently, the modes of the Markov chain $\{\eta(k)\}_{k \in \mathbb{N}}$, with TPM $P = [p_{ij}]_{i,j \in \mathcal{S}}$, p_{ij} transition probabilities defined by (5.4), are associated to the delays in the set D , through the function H^{-1} .

Let $\mathcal{E}(D)$ denote the finite set of all pairs $(\delta_i, \delta_j) \in D \times D$, $i, j \in \mathcal{S}$ such that, for any $k \in \mathbb{N}$, if $d(k) = \delta_i$, then $d(k+1) = \delta_j$ is allowed.

The set $\mathcal{E}(D)$ is formally defined as follows,

$$\mathcal{E}(D) \triangleq \{(\delta_i, \delta_j) \in D \times D, \quad \delta_i, \delta_j \in D, i, j \in \mathcal{S} \mid p_{ij} > 0\}. \quad (5.9)$$

Thus, the system described by (5.2) can be written as a Markov jump system (see [4, 67] and the references therein) defined on the stochastic basis $(\Omega, \mathcal{G}, \mathcal{G}_k, \mathbb{P})$, as follows,

$$\begin{aligned} x_{k+1} &= F(x_k, H^{-1}(\eta(k))), \\ x_0 &= \xi_0, \quad \xi_0 \in \mathcal{C}, \end{aligned} \quad (5.10)$$

with

- $x_k \in \mathcal{C}$,
- $x_k(\theta) = x(k + \theta)$,
- $k \in \mathbb{N}$.

Thus, the map F defined by (5.3), can be rewritten for all $\phi \in \mathcal{C}$, for all $H^{-1}(i) \in D$, for all $i \in \mathcal{S}$, as follows:

$$F(\phi, H^{-1}(i))(\theta) = \begin{cases} f(\phi(0), \phi(-H_1^{-1}(i)), \dots, \phi(-H_r^{-1}(i))), & \text{if } \theta = 0, \\ \phi(\theta + 1), & \text{if } \theta = -\Delta, -\Delta + 1, \dots, -1, \end{cases} \quad (5.11)$$

with

$$H^{-1}(i) = \left[H_1^{-1}(i) \quad \dots \quad H_r^{-1}(i) \right]^T \in D, \quad (5.12)$$

for all $i \in \mathcal{S}$.

Let $x_k(\xi_0)$, $k \in \mathbb{N}$, denote the trajectory that evolves according to (5.10), corresponding to initial state $\xi_0 \in \mathcal{C}$.

Recall that the following equality holds,

$$x_k(\xi_0)(0) = x(k, \xi_0),$$

$k \in \mathbb{N}$.

Remark 45 Notice that the variable $x(k, \xi_0) \in \mathbb{R}^n$, $\xi_0 \in \mathcal{C}$, $k \in \mathbb{N}$, is a random variable on the stochastic basis $(\Omega, \mathcal{G}, \mathcal{G}_k, \mathbb{P})$, since the delay evolves according to a discrete-time Markov chain, with given transition probabilities.

Thus, the investigation illustrated in this chapter focuses on the behaviour of the second moment of $x(k, \xi_0)$, $k \in \mathbb{N}$, $\xi_0 \in \mathcal{C}$.

The following definition introduces the notion of *EMSS* for the system described by (5.1).

Definition 18 The system described by (5.1) is *EMSS* if there exist $M, \zeta \in \mathbb{R}^+$ with $M \geq 1$ and $0 < \zeta < 1$ such that for any $\xi_0 \in \mathcal{C}$, the following inequality holds,

$$\mathbb{E}[\|x(k, \xi_0)\|^2] \leq M\zeta^k \left(\|\xi_0\|_\infty \right)^2. \quad (5.13)$$

5.4 Main result

In this section, we provide the main result of the chapter.

The following theorem illustrates sufficient Lyapunov conditions guaranteeing the *EMSS* of the system described by (5.1).

Theorem 10 Let there exist a function

$$V : \mathcal{C} \times D \rightarrow \mathbb{R}^+,$$

real positive numbers α_i , $i = 1, 2, 3$, such that, for all $\phi \in \mathcal{C}$, for all $H^{-1}(i) \in D$, for all $i \in \mathcal{S}$, the following inequalities hold:

$$i) \alpha_1 \|\phi(0)\|^2 \leq V(\phi, H^{-1}(i)) \leq \alpha_2 \|\phi\|_\infty^2$$

$$ii) \mathcal{L}V(\phi, H^{-1}(i)) \triangleq \sum_{j \in \mathcal{S}} p_{ij} V(F(\phi, H^{-1}(i)), H^{-1}(j)) - V(\phi, H^{-1}(i)) \leq -\alpha_3 \|\phi(0)\|^2.$$

Then, the system described by (5.1) is EMSS.

Proof 21 (Proof of Theorem 10) See Appendix D.

5.5 Example

This section presents a numerical example with the aim of providing an application of the methodology illustrated by Theorem 10.

Consider the following scalar nonlinear system (see [169], Example 2) described by the equation, for $k \in \mathbb{N}$,

$$\begin{cases} x(k+1) = \text{sat}(x(k)) - \gamma \text{sat}(x(k-d(k))), \\ x(\tau) = \xi_0(\tau), \tau \in \{-2, -1, 0\}, \end{cases} \quad (5.14)$$

with

- $\xi_0 \in \mathcal{C}$, $x(k) \in \mathbb{R}$, $\gamma \in [1, 1.2]$,

The system described by (5.14) is unstable if $d(k) = 2$ for all $k \in \mathbb{N}$.

Consider the set of delays $D = \{0, 2\}$, and consider the Markov chain $\{\eta_k\}_{k \in \mathbb{N}}$ in Fig. 5.1, with the set of Markov modes given by $\mathcal{S} = \{1, 2\}$.

Let the bijective function $H : D \rightarrow \mathcal{S}$, be defined as follows,

$$H(d) = \begin{cases} 1, & \text{if } d = 0, \\ 2, & \text{if } d = 2, \end{cases} \quad (5.15)$$

for all $d \in D$. Let the function $H^{-1} : \mathcal{S} \rightarrow D$ be defined as follows,

$$H^{-1}(i) = \begin{cases} 0 & \text{if } i = 1, \\ 2 & \text{if } i = 2, \end{cases} \quad (5.16)$$

for all $i \in \mathcal{S}$.

The TPM associated with the Markov chain $\{\eta_k\}_{k \in \mathbb{N}}$ is given by

$$P = \begin{bmatrix} p & 1-p \\ 1-q & q \end{bmatrix}, \quad (5.17)$$

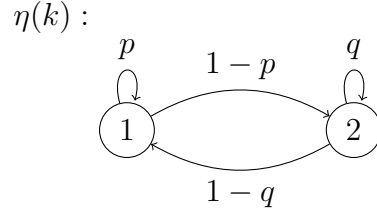


Figure 5.1: The Figure depicts the state diagram of the Markov chain $\eta(k)$ modeling the switching delay: p stands for the probability of having a delay $d(k+1) = 0$, provided that the previous delay is $d(k) = 0$, while q stands for the probability of having a delay $d(k+1) = 2$, provided that the previous delay is $d(k) = 2$.

with $p, q \in (0, 1)$.

The set $\mathcal{E}(D)$ is given by

$$\mathcal{E}(D) = \{(0, 0), (0, 2), (2, 0), (2, 2)\}. \quad (5.18)$$

The aim of this example is studying the *EMSS* property of the system described by (5.14) by applying Theorem 10.

Consider a candidate Lyapunov function

$$V : \mathcal{C} \times D \rightarrow \mathbb{R}^+,$$

defined by

$$V(\phi, H^{-1}(i)) = \lambda_i \sup_{j=0,1,2} 2^{j-1} \gamma^j e^{-j} \|\phi(-j)\|^2, \quad (5.19)$$

for all $\phi \in \mathcal{C}$, all $H^{-1}(i) \in D$, all $i \in \mathcal{S}$, with $\lambda_i \in \mathbb{R}^+$, $i \in \mathcal{S}$, $\gamma \in [1, 1.2]$.

Pick $\alpha_1, \alpha_2 \in \mathbb{R}^+$ as follows,

$$\alpha_1 = \min_{i \in \mathcal{S}} \lambda_i, \quad \alpha_2 = 2\gamma^2 \max_{i \in \mathcal{S}} \lambda_i, \quad (5.20)$$

with $\gamma \in [1, 1.2]$.

Thus, condition (i) of Theorem 10 is satisfied.

In order to verify condition (ii), we consider the expression of $\mathcal{L}V(\phi, H^{-1}(i))$, for all

$\phi \in \mathcal{C}$, for all $H^{-1}(i) \in D$, for all $i \in \mathcal{S}$. We obtain the following equalities/inequalities

$$\begin{aligned}
\mathcal{L}V(\phi, H^{-1}(1)) &= pV(F(\phi, H^{-1}(1)), H^{-1}(1)) + (1-p)V(F(\phi, H^{-1}(1)), H^{-1}(2)) \\
&\quad - V(\phi, H^{-1}(1)) \\
&= (p\lambda_1 + (1-p)\lambda_2) \sup_{j=0,1,2} 2^{j-1}\gamma^j e^{-j} \|F(\phi, H^{-1}(1))(-j)\|^2 \\
&\quad - \lambda_1 \sup_{j=0,1,2} 2^{j-1}\gamma^j e^{-j} \|\phi(-j)\|^2 \\
&\leq (p\lambda_1 + (1-p)\lambda_2) 2^{-1} \|(1-\gamma)\text{sat}(\phi(0))\|^2 \\
&\quad + (p\lambda_1 + (1-p)\lambda_2) \sup_{j=1,2} 2^{j-1}\gamma^j e^{-j} \|\phi(-j+1)\|^2 \\
&\quad - \lambda_1 \sup_{j=0,1,2} 2^{j-1}\gamma^j e^{-j} \|\phi(-j)\|^2 \\
&\leq (p\lambda_1 + (1-p)\lambda_2) \left(2^{-1}(1-\gamma)^2 \|\phi(0)\|^2 + \right. \\
&\quad \left. + 2\gamma e^{-1} \sup_{\theta=0,1,2} 2^{\theta-1}\gamma^\theta e^{-\theta} \|\phi(-\theta)\|^2 \right) + \\
&\quad - \lambda_1 \sup_{\theta=0,1,2} 2^{\theta-1}\gamma^\theta e^{-\theta} \|\phi(-\theta)\|^2 \\
&\leq (p\lambda_1 + (1-p)\lambda_2) \left((1-\gamma)^2 + 2\gamma e^{-1} \right) \sup_{\theta=0,1,2} 2^{\theta-1}\gamma^\theta e^{-\theta} \|\phi(-\theta)\|^2 \\
&\quad - \lambda_1 \sup_{\theta=0,1,2} 2^{\theta-1}\gamma^\theta e^{-\theta} \|\phi(-\theta)\|^2 \\
&\leq -\omega_1 \sup_{\theta=0,1,2} 2^{\theta-1}\gamma^\theta e^{-\theta} \|\phi(-\theta)\|^2, \tag{5.21a}
\end{aligned}$$

$$\omega_1 \triangleq \lambda_1 \left[1 - \left(p + (1-p)\frac{\lambda_2}{\lambda_1} \right) \left((1-\gamma)^2 + 2\gamma e^{-1} \right) \right], \tag{5.21b}$$

$$\begin{aligned}
\mathcal{L}V(\phi, H^{-1}(2)) &= (1-q)V(F(\phi, H^{-1}(2)), H^{-1}(1)) \\
&\quad + qV(F(\phi, H^{-1}(2)), H^{-1}(2)) - V(\phi, H^{-1}(2)) \\
&= ((1-q)\lambda_1 + q\lambda_2) \sup_{j=0,1,2} 2^{j-1}\gamma^j e^{-j} \|F(\phi, H^{-1}(2))(-j)\|^2 \\
&\quad - \lambda_2 \sup_{j=0,1,2} 2^{j-1}\gamma^j e^{-j} \|\phi(-j)\|^2 \\
&\leq ((1-q)\lambda_1 + q\lambda_2) \left(2^{-1} \|F(\phi, H^{-1}(2))(0)\|^2 \right. \\
&\quad \left. + \sup_{j=1,2} 2^{j-1}\gamma^j e^{-j} \|\phi(-j+1)\|^2 \right) \\
&\quad - \lambda_2 \sup_{j=0,1,2} 2^{j-1}\gamma^j e^{-j} \|\phi(-j)\|^2 \\
&\leq ((1-q)\lambda_1 + q\lambda_2) \left(2^{-1} \|F(\phi, H^{-1}(2))(0)\|^2 \right. \\
&\quad \left. + \sup_{j=1,2} 2^{j-1}\gamma^j e^{-j} \|\phi(-j+1)\|^2 \right) \\
&\quad - \lambda_2 \sup_{j=0,1,2} 2^{j-1}\gamma^j e^{-j} \|\phi(-j)\|^2 \\
&\leq ((1-q)\lambda_1 + q\lambda_2) \left(2^{-1} \|\text{sat}(\phi(0)) - \gamma \text{sat}(\phi(-2))\|^2 + \right. \\
&\quad \left. + 2\gamma e^{-1} \sup_{j=1,2} 2^{(j-1)-1}\gamma^{j-1} e^{-j+1} \|\phi(-j+1)\|^2 \right) \\
&\quad - \lambda_2 \sup_{\theta=0,1,2} 2^{\theta-1}\gamma^\theta e^{-\theta} \|\phi(-\theta)\|^2 \\
&\leq ((1-q)\lambda_1 + q\lambda_2) \left(\|\phi(0)\|^2 + \gamma^2 \|\phi(-2)\|^2 \right. \\
&\quad \left. + 2\gamma e^{-1} \sup_{\theta=0,1,2} 2^{\theta-1}\gamma^\theta e^{-\theta} \|\phi(-\theta)\|^2 \right) \\
&\quad - \lambda_2 \sup_{\theta=0,1,2} 2^{\theta-1}\gamma^\theta e^{-\theta} \|\phi(-\theta)\|^2 \\
&\leq ((1-q)\lambda_1 + q\lambda_2) \left((2 + 2^{-1}e^2 + 2\gamma e^{-1}) \right. \\
&\quad \left. \times \sup_{\theta=0,1,2} 2^{\theta-1}\gamma^\theta e^{-\theta} \|\phi(-\theta)\|^2 \right) \\
&\quad - \lambda_2 \sup_{\theta=0,1,2} 2^{\theta-1}\gamma^\theta e^{-\theta} \|\phi(-\theta)\|^2 \\
&\leq -\omega_2 \sup_{\theta=0,1,2} 2^{\theta-1}\gamma^\theta e^{-\theta} \|\phi(-\theta)\|^2, \tag{5.21c}
\end{aligned}$$

$$\omega_2 \triangleq \lambda_2 \left[1 - \left(q + (1-q)\frac{\lambda_1}{\lambda_2} \right) \left(2 + \frac{1}{2}e^2 + 2\gamma e^{-1} \right) \right]. \tag{5.21d}$$

Under the following constraints

$$L_B < \frac{\lambda_2}{\lambda_1} < U_B, \quad (5.22a)$$

with

$$U_B = \frac{1 - ((1 - \gamma)^2 + 2\gamma e^{-1})p}{((1 - \gamma)^2 + 2\gamma e^{-1})(1 - p)}, \quad (5.22b)$$

$$L_B = \frac{(4 + e^2 + 4\gamma e^{-1})(1 - q)}{2 - (4 + e^2 + 4\gamma e^{-1})q}, \quad (5.22c)$$

$$(p, q) \in (0, 1) \times (0, 1), q < \frac{2}{4 + e^2 + 4\gamma e^{-1}}, \gamma \in [1, 1.2]; \quad (5.22d)$$

the coefficients ω_1 and ω_2 belong to \mathbb{R}^+ .

Consequently, the following inequality holds for all $\phi \in \mathcal{C}$, all $H^{-1}(i) \in D$, all $i \in \mathcal{S}$,

$$\mathcal{L}V(\phi, H^{-1}(i)) \leq -\alpha_3 \|\phi(0)\|^2, \quad (5.23)$$

with $\alpha_3 \in \mathbb{R}^+$, defined as follows,

$$\alpha_3 \triangleq \frac{1}{2} \min\{\omega_1, \omega_2\}. \quad (5.24)$$

Thus, condition (ii) of Theorem 10 is satisfied and the system described by (5.14) is EMSS.

5.5.1 Statistical results

In Fig. 5.2 the reader can see the Monte Carlo simulations of the trajectories generated by the system (5.14), considering values of the pairs (p, q) such that conditions (i) and (ii) of Theorem 10 are satisfied. Fig. 5.2 reports five different colors.

- The yellow trajectories, denoted as x_{aggr} , correspond to the state trajectories associated with different switching paths (that are admissible according to the TPM P),
- the maximum trajectory is denoted as x_{max} and it is plotted in blue,
- the minimum trajectory is denoted as x_{min} and it is plotted in green,
- the average evolution of the state trajectories is denoted as x_{avg} ,

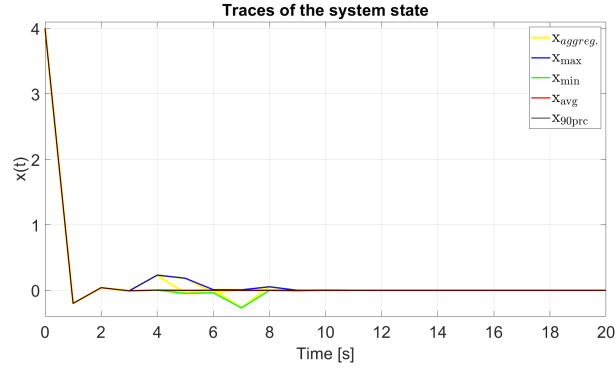


Figure 5.2: Traces of system state obtained with $\gamma = 1.2, p = 0.992$, and $q = 0.007$.

- the evolution of the 90-th percentile of the state trajectories denoted as x_{90perc} , is given by the black line.

Fig. 5.3, Fig. 5.4, and Fig. 5.5 show the regions of pairs (p, q) such that conditions (i) and (ii) of Theorem 10 are satisfied (light blue region) and the evolution of the maximum q with respect to p such that the condition (i) and (ii) of Theorem 10 are satisfied (dark blue line). By comparing Figures 5.3, 5.4, and 5.5, the reader may notice that the aforementioned region becomes smaller and smaller when the parameter γ increases.

This chapter establishes a transformation of nonlinear time-delay systems where delays signals are driven by a Markov chain to nonlinear time-delay Markov jump systems. It also introduces the definition of *EMSS* property for nonlinear time-delay Markov jump systems. Finally, sufficient Lyapunov conditions for the *EMSS* property are here illustrated.

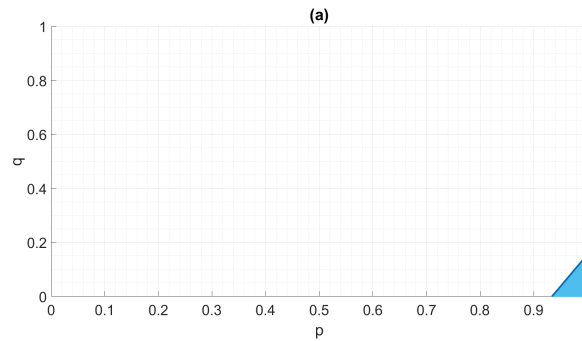


Figure 5.3: The figure shows the region of couples $(p, q) \in (0, 1) \times (0, 1)$ such that conditions of Theorem 10 are satisfied with $\gamma = 1$.

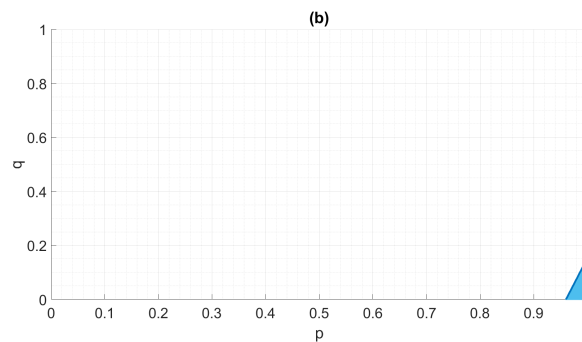


Figure 5.4: The figure shows the region of couples $(p, q) \in (0, 1) \times (0, 1)$ such that conditions of Theorem 10 are satisfied with $\gamma = 1.1$.

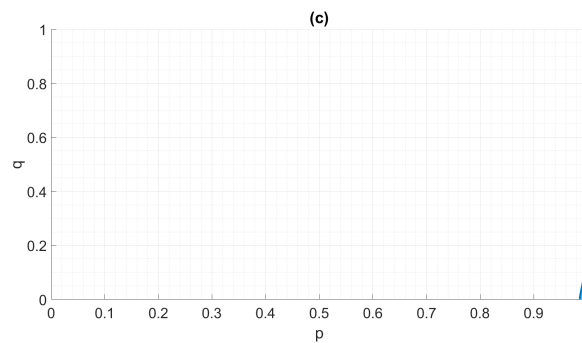


Figure 5.5: The figure shows the regions of couples $(p, q) \in (0, 1) \times (0, 1)$ such that conditions of Theorem 10 are satisfied with $\gamma = 1.2$.

6

Conclusions

This chapter provides some concluding remarks on this research work whose main achievements are summarized in the following.

- The introduction of structural properties specific for the finite-state Markov channel scenario, such as stabilizability with one time step delay and detectability over finite-state Markov channels. The investigations on proper guarantees of the separation principle over finite-state Markov channels [77,92] (topic illustrated in Chapter 2).
- The applications of the modeling approach based on the finite-state Markov channel and Markov jump linear system theory for the development of privacy guarantees [87] (topic illustrated in Chapter 3).
- The extension of the Markov jump model to the nonlinear case (as good approximation of wireless control networks with nonlinear plant dynamics) and the Lyapunov characterizations for discrete-time Markov jump systems of exponential mean square stability and exponential mean square input-to-state stability [97] (topic illustrated in Chapter 4).
- The application of the theory developed for exponential mean square stability and exponential mean square input-to-state stability to the case of discrete-time nonlinear systems subject to Markovian delays [173] (topic illustrated in Chapter 5).

Chapter 2 presents estimation techniques and detectability conditions for WCNs modeled via MJLSs (under TCP-like communication scheme). The results on the separation principle for double-sided packet loss scenarios over finite-state Markov channels generalize the results from [48] by using the Markov modeling of the wireless channel and introducing the stabilizability and detectability conditions accounting for the communication link mode, see also Remark 24. As future developments on this research line, the author aims to investigate the same WCN scenario under a UDP-like communication scheme.

Chapter 3 provides secure state estimation over Markov wireless communication channels.

The secrecy notion in [38] is conveyed to FSMCs, which require re-definition of estimation problem and a novel technical procedure for deriving the secrecy conditions.

Moreover, Chapter 3 illustrates the design of a secrecy mechanism satisfying the described formal requirements over FSMCs, and the effectiveness of the achieved result is shown in the example of an inverted pendulum on a cart whose parameters are estimated remotely over a wireless link exposed to an eavesdropper.

Chapter 4 illustrates a complete Lyapunov characterization for *EMSS* and *EMSS-ISS* of discrete-time Markovian switching nonlinear systems. Some examples of the proposed approach are provided. Particularly, the examples reveal the effectiveness of the presented methodology especially in the stability analysis of WCNs.

Indeed, the proposed methodology allows to carry out the stability analysis of a discrete-time nonlinear system involved in a wireless control loop taking into account the probability of bursts of packet losses on the wireless channel.

Control design strategies for packet-loss effect mitigation can be object of future investigations. Further very challenging research topic is the proof of the existence, or of the non-existence, of Lyapunov functions satisfying conditions (b) in Theorem 8 with suitable convex-concave \mathcal{K}_∞ comparison functions, for the (general, not exponential) mean square ISS.

Chapter 5 establishes a transformation of nonlinear time-delay systems where delays signals are driven by a Markov chain to nonlinear time-delay Markov jump systems. The presented work also provides related sufficient Lyapunov conditions for the *EMSS* property.

Appendix A

Appendix outline

This appendix reports the proofs of theorems and lemmas concerning the results presented in Chapter 2.

Technical preliminaries

Since, for finite-dimensional linear spaces, all norms are equivalent, [230, Theorem 4.27] from a topological viewpoint, as vector norms we use variants of vector p -norms. For what concerns the matrix norms, we use ℓ_1 and ℓ_2 norms [231, p. 341], which treat $n_r \times n_c$ matrices as vectors of size $n_r n_c$, and use one of the related p -norms. The definition of ℓ_1 and ℓ_2 norms is based on the operation of vectorization of a matrix, $\text{vec}(\cdot)$, which is further used in the definition of the operator $\hat{\varphi}(\cdot)$, to be applied to any block matrix, e.g., $\Phi = [\Phi_m]_{m=1}^C$: $\hat{\varphi}(\Phi) \triangleq [\text{vec}(\Phi_1), \dots, \text{vec}(\Phi_C)]'$. The linear operator $\hat{\varphi}(\cdot)$ is a uniform homeomorphism, its inverse operator $\hat{\varphi}^{-1}(\cdot)$ is uniformly continuous [232], and any bounded linear operator in $\mathbb{B}(\mathbb{F}^{C n_r \times n_c})$ can be represented in $\mathbb{B}(\mathbb{F}^{C n_r n_c})$ through $\hat{\varphi}(\cdot)$.

Mode-dependent estimation techniques

Proof 22 (Proof of Proposition 1) Let us prove that condition (i) is satisfied. Define matrices Λ_1 and Λ_2 , as follows,

$$\Lambda_1 \triangleq \mathcal{N}\mathcal{C}, \quad \Lambda_2 \triangleq \mathcal{N}^*\mathcal{C}^*$$

with \mathcal{C} and \mathcal{N} in (2.25).

By linear algebra arguments (see also [4, Remark 3.3]), it follows that

$$\rho(\Lambda_1) = \rho(\Lambda_2).$$

For all $\mathbf{S} = [S_m]_{m=1}^I$ in \mathbb{H}^{In_x} , the following equalities hold,

$$\hat{\varphi}(\mathcal{V}(\mathbf{S})) = \mathbf{\Lambda}_1 \hat{\varphi}(\mathbf{S}), \quad \hat{\varphi}(\mathcal{L}(\mathbf{S})) = \mathbf{\Lambda}_2 \hat{\varphi}(\mathbf{S}),$$

see, e.g., [4, Proposition 3.2, Remark 3.5], and thus, $\rho(\mathcal{L}) = \rho(\mathcal{V})$, i.e., condition (i) is satisfied.

Let us prove now that condition (ii) is satisfied.

For all $m \in \mathbb{S}_\eta$, consider the matrices $\hat{\Gamma}_{m0}$ and $\hat{\Gamma}_{m1}$, such as,

$$\hat{\Gamma}_{m0} = \Gamma_{m0}, \quad \hat{\Gamma}_{m1} = \Gamma_{m1}.$$

Moreover, define the matrix $\mathbf{\Lambda}_3$, as follows,

$$\mathbf{\Lambda}_3 \triangleq \mathcal{CN}.$$

Then, by linear algebra arguments, the following equalities hold:

$$\rho(\mathbf{\Lambda}_1) = \rho(\mathbf{\Lambda}_2) = \rho(\mathbf{\Lambda}_3).$$

Recalling that $\hat{\varphi}(\mathcal{T}(\mathbf{S})) = \mathbf{\Lambda}_3 \hat{\varphi}(\mathbf{S})$, for all $\mathbf{S} \in \mathbb{H}^{In_x}$, condition (ii) follows.

Proof 23 (Proof of Proposition 2) The first part of the proof shows the validity of equation

$$\check{\mathbf{m}}(k+1) = \check{\mathbf{B}}\check{\mathbf{m}}(k),$$

in (2.29). From equations (2.26) and (2.13), applying the assumption on the noise sequence $\mathbb{E}[w_k] = \mathbf{O}_{n_w}$, the following equality holds,

$$\check{m}_n(k+1) = \sum_{m=1}^I \mathbb{E} \left[\left(A + \gamma_k \check{M}_{\eta_k} L \right) \check{e}_k \mathbf{1}_{\{\eta_k=n\}} \mathbf{1}_{\{\eta_{k-1}=m\}} \right]. \quad (1)$$

From (1), applying the definition of indicator function, the definition of the probability $\hat{\gamma}_m$, $m \in \mathbb{S}_\eta$ in (2.3), and the definition of transition probabilities q_{mn} , $m, n \in \mathbb{S}_\eta$ in (2.2), it follows that:

$$\check{m}_n(k+1) = \sum_{m=1}^I q_{mn} \left(A + \hat{\gamma}_n \check{M}_n L \right) \mathbb{E} \left[\check{e}_k \mathbf{1}_{\{\eta_{k-1}=m\}} \right]. \quad (2)$$

From (2), by applying the definition of $\check{m}_m(k)$, $m \in \mathbb{S}_\eta$ in (2.26), it follows that

$$\check{m}_n(k+1) = \sum_{m=1}^I q_{mn} \left(A + \hat{\gamma}_n \check{M}_n L \right) \check{m}_m(k). \quad (3)$$

From (3), applying the definition of $\check{\mathbf{m}}(k)$ in (2.26) and the definition of $\check{\mathbf{B}}$ in (2.28) for $\Gamma_{n0} = A$ and $\Gamma_{n1} = A + \check{M}_n L$, $n \in \mathbb{S}_\eta$,

$$\check{\mathbf{m}}(k+1) = \check{\mathbf{B}}\check{\mathbf{m}}(k).$$

The second part of the proof shows the validity of equation

$$\check{\mathbf{Y}}(k+1) = \mathcal{V}(\check{\mathbf{Y}}(k)) + \mathcal{O}(\check{\mathbf{M}}, \boldsymbol{\pi}(k)),$$

in (2.29).

From equations (2.27) and (2.13), applying the following properties,

- the independence between the noise sequence w_k , $k \in \mathbb{N}$, and the estimation error \check{e}_k ,
- the independence of w_k , $k \in \mathbb{N}$, and $\{\eta_k\}_{k \in \mathbb{N}}$ (see assumption a.3 in Chapter 2),
- the property $\mathbb{E}[w_k] = \mathbf{O}_{n_w}$,

the following equality is obtained.

$$\begin{aligned} \check{Y}_n(k+1) &= \sum_{m=1}^I \mathbb{E} \left[\left(A + \gamma_k \check{M}_{\eta_k} L \right) \check{e}_k \check{e}_k^* \left(A + \gamma_k \check{M}_{\eta_k} L \right)^* \mathbf{1}_{\{\eta_k=n\}} \mathbf{1}_{\{\eta_{k-1}=m\}} \right] \\ &\quad + \sum_{m=1}^I \mathbb{E} \left[\left(G + \gamma_k \check{M}_{\eta_k} H \right) w_k w_k^* \left(G + \gamma_k \check{M}_{\eta_k} H \right)^* \mathbf{1}_{\{\eta_k=n\}} \mathbf{1}_{\{\eta_{k-1}=m\}} \right]. \end{aligned} \quad (4)$$

From (4), applying the following properties,

- the definition of indicator function,
- the definition of the probability $\hat{\gamma}_m$, $m \in \mathbb{S}_\eta$ in (2.3),
- the definition of transition probabilities q_{mn} , $m, n \in \mathbb{S}_\eta$ in (2.2),
- the assumption $GH^* = 0$ in (2.7),
- the definition of $\check{Y}_m(k)$ in (2.27),

it follows that:

$$\begin{aligned} \check{Y}_n(k+1) &= \sum_{m=1}^I q_{mn} \{ A\check{Y}_m(k)A^* + \hat{\gamma}_n \check{M}_n L\check{Y}_m(k)A^* + \hat{\gamma}_n A\check{Y}_m(k)L^* \check{M}_n^* + \\ &\quad \hat{\gamma}_n \check{M}_n L\check{Y}_m(k)L^* \check{M}_n^* \} + \\ &\quad + \sum_{m=1}^I q_{mn} \{ \pi_m(k-1) G\mathbb{E}[w_k w_k^*] G^* + \pi_m(k-1) \hat{\gamma}_n \check{M}_n H\mathbb{E}[w_k w_k^*] H^* \check{M}_n^* \}. \end{aligned} \quad (5)$$

Let us recall that $\sum_{m=1}^I q_{mn} \pi_m(k-1) = \pi_n(k)$ and that $\mathbb{E}[w_k w_k^*] = \mathbb{I}_{n_w}$ in (2.6). It follows that:

$$\begin{aligned} \check{Y}_n(k+1) &= \sum_{m=1}^I q_{mn} \{ A\check{Y}_m(k)A^* + \hat{\gamma}_n \check{M}_n L\check{Y}_m(k)A^* + \hat{\gamma}_n A\check{Y}_m(k)L^* \check{M}_n^* + \\ &\quad \hat{\gamma}_n \check{M}_n L\check{Y}_m(k)L^* \check{M}_n^* \} + \\ &\quad + \pi_n(k) G G^* + \pi_n(k) \hat{\gamma}_n \check{M}_n H H^* \check{M}_n^*. \end{aligned} \quad (6)$$

Define now for $n \in \mathbb{S}_\eta$, $\Gamma_{n0} = A$ and $\Gamma_{n1} = A + \check{M}_n L$.

From (6), applying the definition of $\check{Y}(k)$ in (2.27), the definition of \mathcal{V} in (2.22) for Γ_{n0} and Γ_{n1} defined above, the definition of \mathcal{O} in (2.23), the following equality holds:

$$\check{Y}(k+1) = \mathcal{V}(\check{Y}(k)) + \mathcal{O}(\check{\mathbf{M}}, \boldsymbol{\pi}(k)), \quad (7)$$

with $\check{\mathbf{M}} = [\check{M}_m]_{m=1}^I$, $\boldsymbol{\pi}(k) = [\pi_m(k)]_{m=1}^I$.

Proof 24 (Proof of Proposition 3) The first part of the proof shows the validity of equation

$$\mathbf{m}(k+1) = \widehat{\mathbf{B}}\mathbf{m}(k),$$

in (2.33).

From equations (2.30) and (2.17), applying the assumption on the noise sequence $\mathbb{E}[w_k] = \mathbf{O}_{n_w}$ in (2.6), the following equality holds,

$$m_n(k+1) = \sum_{m=1}^I \mathbb{E} \left[\left(A + \gamma_k A \widehat{M}_{\eta_k} L \right) e_k \mathbf{1}_{\{\eta_{k+1}=n\}}, \mathbf{1}_{\{\eta_k=m\}} \right]. \quad (8)$$

From (8), applying the definition of indicator function, the definition of the probability $\hat{\gamma}_m$, $m \in \mathbb{S}_\eta$ in (2.3), and the definition of transition probabilities q_{mn} , $m, n \in \mathbb{S}_\eta$ in (2.2),

it follows that:

$$m_n(k+1) = \sum_{m=1}^I q_{mn} \left(A + \hat{\gamma}_m A \widehat{M}_m L \right) \mathbb{E} \left[e_k \mathbf{1}_{\{\eta_k=m\}} \right]. \quad (9)$$

From (9), by applying the definition of $m_m(k)$, $m \in \mathbb{S}_\eta$ in (2.30), it follows that

$$m_n(k+1) = \sum_{m=1}^I q_{mn} \left(A + \hat{\gamma}_m A \widehat{M}_m L \right) m_m(k). \quad (10)$$

From (10), applying the definition of $\mathbf{m}(k)$ in (2.30) and the definition of $\widehat{\mathcal{B}}$ in (2.32) for $\widehat{\Gamma}_{n0} = A$ and $\widehat{\Gamma}_{n1} = A + A \widehat{M}_n L$, $n \in \mathbb{S}_\eta$,

$$\mathbf{m}(k+1) = \widehat{\mathcal{B}} \mathbf{m}(k).$$

The second part of the proof shows the validity of equation

$$\mathbf{Z}(k+1) = \mathcal{T}(\mathbf{Z}(k)) + \widehat{\mathcal{O}}(\widehat{\mathbf{M}}, \boldsymbol{\pi}(k)),$$

in (2.33).

From equations (2.31) and (2.17), applying the following properties,

- the independence between the noise sequence w_k , $k \in \mathbb{N}$, and the prediction error e_k ,
- the independence of w_k , $k \in \mathbb{N}$, and $\{\eta_k\}_{k \in \mathbb{N}}$ (see assumption a.3 in Chapter 2),
- the property $\mathbb{E}[w_k] = \mathbf{0}_{n_w}$ in (2.6),

the following equality is obtained,

$$\begin{aligned} Z_n(k+1) &= \sum_{m=1}^I \mathbb{E} \left[\left(A + \gamma_k A \widehat{M}_{\eta_k} L \right) e_k e_k^* \left(A + \gamma_k A \widehat{M}_{\eta_k} L \right)^* \mathbf{1}_{\{\eta_{k+1}=n\}}, \mathbf{1}_{\{\eta_k=m\}} \right] + \\ &\quad + \sum_{m=1}^I \mathbb{E} \left[\left(G + \gamma_k A \widehat{M}_{\eta_k} H \right) w_k w_k^* \left(G + \gamma_k A \widehat{M}_{\eta_k} H \right)^* \mathbf{1}_{\{\eta_{k+1}=n\}}, \mathbf{1}_{\{\eta_k=m\}} \right]. \end{aligned} \quad (11)$$

From (11), applying the following properties,

- the definition of indicator function,
- the definition of the probability $\hat{\gamma}_m$, $m \in \mathbb{S}_\eta$, in (2.3),

- the definition of transition probabilities q_{mn} , $m, n \in \mathbb{S}_\eta$ in (2.2),
- the assumption $GH^* = 0$ in (2.7),
- the definition of $Z_m(k)$ in (2.31),

it follows that:

$$\begin{aligned}
Z_n(k+1) &= \sum_{m=1}^I q_{mn} \hat{\gamma}_m \left(A + A\widehat{M}_m L \right) Z_m(k) \left(A + \gamma_{\eta_{k-1}} A\widehat{M}_m L \right)^* \\
&\quad + \sum_{m=1}^I q_{mn} (1 - \hat{\gamma}_m) (AZ_m(k)A^*) \\
&\quad + \sum_{m=1}^I q_{mn} \pi_m(k) \left(G\mathbb{E}[w_k w_k^*] G^* + \hat{\gamma}_m A\widehat{M}_m H \mathbb{E}[w_k w_k^*] H^* \widehat{M}_m^* A^* \right). \quad (12)
\end{aligned}$$

Let us recall that $\mathbb{E}[w_k w_k^*] = \mathbb{I}_{n_w}$ in (2.6). It follows that:

$$\begin{aligned}
Z_n(k+1) &= \sum_{m=1}^I q_{mn} \hat{\gamma}_m \left(A + A\widehat{M}_m L \right) Z_m(k) \left(A + \gamma_{\eta_{k-1}} A\widehat{M}_m L \right)^* \\
&\quad + \sum_{m=1}^I q_{mn} (1 - \hat{\gamma}_m) (AZ_m(k)A^*) \\
&\quad + \sum_{m=1}^I q_{mn} \pi_m(k) \left(GG^* + \hat{\gamma}_m A\widehat{M}_m H H^* \widehat{M}_m^* A^* \right) \quad (13)
\end{aligned}$$

Define now for $n \in \mathbb{S}_\eta$, $\widehat{\Gamma}_{n0} = A$ and $\widehat{\Gamma}_{n1} = A + A\widehat{M}_n L$.

From (13), applying the definition of $\mathbf{Z}(k)$ in (2.27), the definition of \mathcal{T} in (2.20) for $\widehat{\Gamma}_{n0}$ and $\widehat{\Gamma}_{n1}$ defined above, the definition of $\widehat{\mathcal{O}}$ in (2.23), the following equality holds:

$$\mathbf{Z}(k+1) = \mathcal{T}(\mathbf{Z}(k)) + \widehat{\mathcal{O}}(\widehat{\mathbf{M}}, \boldsymbol{\pi}(k)), \quad (14)$$

with $\widehat{\mathbf{M}} = [\widehat{M}_m]_{m=1}^I$, $\boldsymbol{\pi}(k) = [\pi_m(k)]_{m=1}^I$.

Proof 25 (Proof of Proposition 4) Assume that the MJLS described by (2.5) is Strict-MSD.

Then, by Definition 5 there exists a mode-dependent filtering gain $\widehat{M}_n \in \mathbb{F}^{n_x \times n_y}$ such that

$$\rho(\mathcal{T}) < 1,$$

with $\mathcal{T} \in \mathbb{B}(\mathbb{H}^{I n_x})$ in (2.20), for $\hat{\Gamma}_{n1} = A + A\hat{M}_nL$, $\hat{\Gamma}_{n0} = A$, $n \in \mathbb{S}_\eta$.
Pick the next-step predictor filtering gain as follows:

$$\check{M}_n = A\hat{M}_n \in \mathbb{F}^{n_x \times n_y}.$$

By setting

- $\Gamma_{n1} = A + \check{M}_nL$,
- $\Gamma_{n0} = A$,

the following equalities hold,

$$\hat{\Gamma}_{n1} = \Gamma_{n1}, \quad \hat{\Gamma}_{n0} = \Gamma_{n0}.$$

Consider now the operator \mathcal{V} from (2.22), for Γ_{n1} and Γ_{n0} defined above.

By Proposition 1,

$$\rho(\mathcal{V}) = \rho(\mathcal{T}),$$

which implies

$$\rho(\mathcal{V}) < 1.$$

Thus, (2.5) is MSD.

Lemma 2 Suppose that $\mathbf{Y} \in \mathbb{L}$ and for some $\mathbf{M} = [M_n]_{n=1}^I \in \mathbb{F}^{I n_x \times n_y}$, $\hat{\mathbf{Y}} \in \mathbb{H}^{n_x, *}$ satisfies for $n \in \mathbb{S}_\eta$,

$$\begin{aligned} \hat{Y}_n - \hat{\gamma}_n (A + M_nL) \mathcal{D}_n(\hat{\mathbf{Y}}) (A + M_nL)^* - (1 - \hat{\gamma}_n) A \mathcal{D}_n(\hat{\mathbf{Y}}) A^* &= \mathcal{O}_n(M), \\ \mathcal{O}_n(M) &\triangleq \pi_n^\infty (GG^* + \hat{\gamma}_n M_n H H^* M_n^*), \end{aligned} \quad (15)$$

then, for $n \in \mathbb{S}_\eta$,

$$\begin{aligned} &(\hat{Y}_n - Y_n) - \hat{\gamma}_n (A + M_nL) \mathcal{D}_n(\hat{\mathbf{Y}} - \mathbf{Y}) (A + M_nL)^* \\ &- (1 - \hat{\gamma}_n) A \mathcal{D}_n(\hat{\mathbf{Y}} - \mathbf{Y}) A^* \\ &= \mathcal{Y}_n(\mathbf{Y}) - Y_n + \hat{\gamma}_n (M_n - \mathcal{M}_n(\mathbf{Y})) \tilde{\mathcal{R}}_n(\mathbf{Y}) (M_n - \mathcal{M}_n(\mathbf{Y}))^*. \end{aligned} \quad (16)$$

Moreover, if $\widehat{\mathbf{Y}} \in \mathbb{L}$, for $n \in \mathbb{S}_\eta$,

$$\begin{aligned} & (\widehat{Y}_n - Y_n) - \hat{\gamma}_n (A + \mathcal{M}_n(\widehat{\mathbf{Y}})L) \mathcal{D}_n(\widehat{\mathbf{Y}} - \mathbf{Y}) (A + \mathcal{M}_n(\widehat{\mathbf{Y}})L)^* - (1 - \hat{\gamma}_n) A \mathcal{D}_n(\widehat{\mathbf{Y}} - \mathbf{Y}) A^* \\ &= \hat{\gamma}_n (\mathcal{M}_n(\widehat{\mathbf{Y}}) - \mathcal{M}_n(\mathbf{Y})) \tilde{\mathcal{R}}_n(\mathbf{Y}) (\mathcal{M}_n(\widehat{\mathbf{Y}}) - \mathcal{M}_n(\mathbf{Y}))^* \\ &+ \hat{\gamma}_n (M_n - \mathcal{M}_n(\widehat{\mathbf{Y}})) \tilde{\mathcal{R}}_n(\widehat{\mathbf{Y}}) (M_n - \mathcal{M}_n(\widehat{\mathbf{Y}}))^* + \mathcal{Y}_n(\mathbf{Y}) - Y_n. \end{aligned} \quad (17)$$

Furthermore, if $\widehat{\mathbf{X}} \in \mathbb{H}^{I n_x, *}$ and satisfies, for $n \in \mathbb{S}_\eta$, the following equality,

$$\widehat{X}_n - \hat{\gamma}_n (A + \mathcal{M}_n(\widehat{\mathbf{Y}})L) \mathcal{D}_n(\widehat{\mathbf{X}}) (A + \mathcal{M}_n(\widehat{\mathbf{Y}})L)^* - (1 - \hat{\gamma}_n) A \mathcal{D}_n(\widehat{\mathbf{X}}) A^* = \mathcal{O}_n(\mathcal{M}(\widehat{\mathbf{Y}})), \quad (18)$$

for $n \in \mathbb{S}_\eta$ then,

$$\begin{aligned} & (\widehat{Y}_n - \widehat{X}_n) - \hat{\gamma}_n (A + \mathcal{M}_n(\widehat{\mathbf{Y}})L) \mathcal{D}_n(\widehat{\mathbf{Y}} - \widehat{\mathbf{X}}) (A + \mathcal{M}_n(\widehat{\mathbf{Y}})L)^* - \\ & (1 - \hat{\gamma}_n) A \mathcal{D}_n(\widehat{\mathbf{Y}} - \widehat{\mathbf{X}}) A^* \\ &= \hat{\gamma}_n (M_n - \mathcal{M}_n(\widehat{\mathbf{Y}})) \tilde{\mathcal{R}}_n(\widehat{\mathbf{Y}}) (M_n - \mathcal{M}_n(\widehat{\mathbf{Y}}))^*. \end{aligned} \quad (19)$$

Proof 26 (Proof of Lemma 2) Let us show that (16) holds. Consider the left-hand side of (16) for $n \in \mathbb{S}_\eta$, applying (15) and the definitions of $\mathcal{M}_n(\mathbf{Y})$, the right-hand side of (16) is easily obtained.

To show that (17) holds for $n \in \mathbb{S}_\eta$, consider the left-hand side of equality (17), applying the definitions of $\tilde{\mathcal{R}}_n(\widehat{\mathbf{Y}})$, $\tilde{\mathcal{R}}_n(\mathbf{Y})$, $\mathcal{M}_n(\mathbf{Y})$, and (15), equality (17) holds.

Let us show that equality (19) holds. Consider the left-hand side of equality (19), applying the definition of $\mathcal{M}_n(\widehat{\mathbf{Y}})$ and $\tilde{\mathcal{R}}_n(\widehat{\mathbf{Y}})$, and (18), the reader can easily obtain equality (19).

Lemma 3 Consider \mathcal{V} defined in (2.22).

Define the operator $\tilde{\mathcal{V}}$ as follows,

$$\tilde{\mathcal{V}}_n(\mathbf{S}) = \hat{\gamma}_n \Lambda_{n1} \mathcal{D}_n(\mathbf{S}) \Lambda_{n1}^* + (1 - \hat{\gamma}_n) \Lambda_{n0} \mathcal{D}_n(\mathbf{S}) \Lambda_{n0}^*,$$

with matrices Λ_{n1} , Λ_{n0} , matrices in $\mathbb{F}^{n_x \times n_x}$.

Assume now that $\rho(\mathcal{V}) < 1$, and for some $\mathbf{Y} \in \mathbb{H}^{I n_x, +}$ and $\delta > 0$,

$$Y_n - \tilde{\mathcal{V}}_n(\mathbf{Y}) \succeq \delta \hat{\gamma}_n (K_n - M_n) (K_n - M_n)^*, \quad n \in \mathbb{S}_\eta, \quad (20)$$

with $\Lambda_{n1} = A + K_n L$, $\Lambda_{n0} = A$.

Then, $\rho(\tilde{\mathcal{V}}) < 1$.

Proof 27 Set $\tilde{\mathcal{J}} = \tilde{\mathcal{V}}^*$.

Note that for arbitrary $\epsilon > 0$ and $V \in \mathbb{H}^{\mathbf{In}_x,+}$,

$$0 \preceq \hat{\gamma}_n \left[\epsilon (A + M_n L) - \frac{1}{\epsilon} (K_n - M_n) L \right]^* V_n \left[\epsilon (A + M_n L) - \frac{1}{\epsilon} (K_n - M_n) L \right] + (1 - \hat{\gamma}_n) \epsilon^2 A^* V_n A. \quad (21)$$

By applying the previous inequality (21), the following inequality holds,

$$0 \preceq (1 + \epsilon^2) \mathcal{J}_m(\mathbf{V}) + \left(1 + \frac{1}{\epsilon^2}\right) \mathcal{Q}_m(\mathbf{V}),$$

where

$$\begin{aligned} \mathcal{Q}(\cdot) &\triangleq [\mathcal{Q}_m(\cdot)]_{m=1}^I, \\ \mathcal{Q}_m(\mathbf{V}) &\triangleq \sum_{n=1}^I q_{mn} \hat{\gamma}_n L^* (K_n - M_n)^* V_n (K_n - M_n) L, \\ \hat{\mathcal{Q}}(\mathbf{V}) &\triangleq \left(1 + \frac{1}{\epsilon^2}\right) \mathcal{Q}(\mathbf{V}). \end{aligned}$$

Moreover, let us define

$$\hat{\mathcal{J}}(\cdot) \triangleq (1 + \epsilon^2) \mathcal{J}(\cdot).$$

Since $\mathcal{J} = \mathcal{V}^*$, and $\rho(\mathcal{V}) < 1$ by hypothesis, it follows that

$$\rho(\hat{\mathcal{J}}) = \rho(\mathcal{V}) < 1.$$

Let us choose $\epsilon > 0$, such that $\rho(\hat{\mathcal{J}}) < 1$.

Let us define for $t = 0, \dots$, the sequences

$$\begin{aligned} \mathbf{U}(t+1) &\triangleq \tilde{\mathcal{J}}(\mathbf{U}(t)), \quad \mathbf{U}(0) \succeq 0, \\ \mathbf{Z}(t+1) &\triangleq \hat{\mathcal{J}}(\mathbf{Z}(t)) + \hat{\mathcal{Q}}(\mathbf{U}(t)), \quad \mathbf{Z}(0) = \mathbf{U}(0). \end{aligned}$$

At this point, the following inequality should be proved

$$\sum_{s=0}^{\infty} \|\hat{\mathcal{Q}}(\mathbf{U}(s))\|_1 < \infty. \quad (22)$$

Recalling the definition of the norm, the properties of the trace operator, inequality (20) and the definition of inner product, the following equality is satisfied

$$\|\hat{\mathcal{Q}}(\mathbf{U}(s))\|_1 = \sum_{m=1}^I \|\hat{\mathcal{Q}}_m(\mathbf{U}(s))\| \leq c_0 \langle \mathbf{Y} - \tilde{\mathcal{V}}(\mathbf{Y}); \mathbf{U}(s) \rangle.$$

with

$$c_0 \triangleq \frac{1}{\delta} \left(1 + \frac{1}{\epsilon^2}\right) \|L\|^2 I$$

By the properties of the inner product, taking the sum from $s = 0$ to τ , the following inequality is satisfied

$$\sum_{s=0}^{\tau} \|\hat{\mathcal{Q}}(\mathbf{U}(s))\|_1 \leq c_0 \langle \mathbf{Y}; \mathbf{U}(0) \rangle.$$

Taking the limit for $\tau \rightarrow \infty$, (22) holds. Following the same steps provided by [4, Lemma A.8], the following inequality can be proved

$$0 \leq \sum_{t=0}^{\infty} \|\tilde{\mathcal{J}}^t(\mathbf{U}(0))\|_1 = \sum_{t=0}^{\infty} \|\mathbf{U}(t)\|_1 \leq \sum_{t=0}^{\infty} \|\mathbf{Z}(t)\|_1 < \infty.$$

By [4, Proposition 2.5], $\rho(\tilde{\mathcal{J}}) < 1$. Therefore, $\rho(\tilde{\mathcal{V}}) = \rho(\tilde{\mathcal{J}}) < 1$. This completes the proof.

Lemma 4 Assume that the MJLS described by (2.5) is MSD.

Then, there exists $\mathbf{Y}^+ \in \mathbb{M}$, $\mathbf{Y}^+ \succeq \mathbf{Y}$ for any $\mathbf{Y} \in \mathbb{M}$, satisfying (2.36).

Proof 28 (Proof of Lemma 4) Consider an arbitrary $\mathbf{Y} \in \mathbb{M}$.

Let us show that there exists a decreasing sequence $\{\mathbf{Y}^l\}_{l=0}^{\infty}$, $\mathbf{Y}^l \in \mathbb{H}^{I n_x, +}$, satisfying equations (23), for $l = 0, 1, \dots$, with $\mathbf{M}^l \triangleq [M_n^l]_{n=1}^I$

$$\begin{aligned} \mathbf{Y}_n^l - \mathcal{V}_n^l(\mathbf{Y}^l) &= \mathcal{O}_n(\mathbf{M}^l), \quad \text{with } \mathcal{V}^l(\cdot) \triangleq [\mathcal{V}_n^l(\cdot)]_{n=1}^I, \\ \mathcal{V}_n^l(\cdot) &\triangleq \hat{\gamma}_n A_{n1}^l \mathcal{D}_n(\mathbf{Y}^l) A_{n1}^{l*} \\ &\quad + (1 - \hat{\gamma}_n) A_{n0}^l \mathcal{D}_n(\mathbf{Y}^l) A_{n0}^{l*} \\ M_n^l &\triangleq \mathcal{M}_n(\mathbf{Y}^{l-1}), \quad A_{n1}^l \triangleq A + M_n^l L, \quad A_{n0}^l \triangleq A, \quad n \in \mathbb{S}_\eta; \end{aligned} \tag{23}$$

with \mathbf{Y}^l such that

$$\mathbf{Y}^l \succeq \mathbf{Y},$$

and

$$\rho(\mathcal{V}^l) < 1,$$

for all l .

Let us use inductive arguments starting from $l = 0$.

Since the MJLS described by (2.5) is mean square detectable, there exists a mode-dependent filtering gain

$$\mathbf{M}^0 = [M_n^0]_{n=1}^l,$$

such that $\rho(\mathcal{V}^0) < 1$ and from [4, Proposition 3.20], there exists a unique $\mathbf{Y}^0 \in \mathbb{H}^{I_{n_x,+}}$, solution of (2.3), for $l = 0$.

From Lemma 2-(16), recalling that $\rho(\mathcal{V}^0) < 1$ applying again [4, Proposition 3.20], it follows that $\mathbf{Y}^0 \succeq \mathbf{Y}$.

Assume now that there exists a decreasing sequence sequence $\{\mathbf{Y}^l\}_{l=0}^{k-1}$, with $\mathbf{Y}^l \in \mathbb{H}^{I_{n_x,+}}$, unique solution of (2.3) and such that

$$\mathbf{Y}^0 \succeq \mathbf{Y}^1 \succeq \dots \succeq \mathbf{Y}^{k-1} \succeq \mathbf{Y},$$

for any $\mathbf{Y} \in \mathbb{M}$, with $\rho(\mathcal{V}^l) < 1$.

Let us set

$$\begin{aligned} \tilde{R}_n^{k-1} &\triangleq \tilde{\mathcal{R}}_n(\mathbf{Y}^{k-1}), \\ M_n^k &\triangleq \mathcal{M}_n(\mathbf{Y}^{k-1}), \\ A_{n1}^k &\triangleq A + M_n^k L. \end{aligned}$$

Apply now Lemma 2-(17), the following inequality is satisfied:

$$Y_n^{k-1} - Y_n - \mathcal{V}_n^k(\mathbf{Y}^{k-1} - \mathbf{Y}) \succeq \hat{\gamma}_n (M_n^k - M_n^{k-1}) \tilde{R}_n^{k-1} (M_n^k - M_n^{k-1})^*.$$

Recall that \tilde{R}_n^{k-1} has been defined as $\tilde{R}_n^{k-1} \triangleq \tilde{\mathcal{R}}_n(\mathbf{Y}^{k-1})$. Thus, it follows that $\tilde{R}_n^{k-1} \succ \tilde{\mathcal{R}}_n(\mathbf{Y}) \succ 0$, for any $n \in \mathbb{S}_\eta$.

Therefore, it is possible to find a $\delta^{k-1} > 0$, such that

$$\tilde{R}_n^{k-1} \succ \delta^{k-1} \mathbb{I}_{n_x}.$$

Thus, the following inequality is satisfied.

$$Y_n^{k-1} - Y_n - \mathcal{V}_n^k(\mathbf{Y}^{k-1} - \mathbf{Y}) \succeq \delta^{k-1} \hat{\gamma}_n (M_n^k - M_n^{k-1}) (M_n^k - M_n^{k-1})^*.$$

Applying Lemma [3], it follows that $\rho(\mathcal{V}^k) < 1$, and from [4, Proposition 3.20], there exists a unique solution $\mathbf{Y}^k \in \mathbb{H}^{In_x,+}$ of equation (23) for $l = k$. Thus, from Lemma 2-(19), it follows that

$$\begin{aligned} & (\mathbf{Y}_n^{k-1} - \mathbf{Y}_n^k) - \hat{\gamma}_n (A + M_n^k L) \mathcal{D}_n(\mathbf{Y}^{k-1} - \mathbf{Y}^k) (A + M_n^k L)^* \\ & \quad - (1 - \hat{\gamma}_n) A \mathcal{D}_n(\mathbf{Y}^{k-1} - \mathbf{Y}^k) A^* \\ & = \hat{\gamma}_n (M_n^k - M_n^{k-1})^* \tilde{R}_n^{k-1} (M_n^k - M_n^{k-1})^* \succeq 0. \end{aligned}$$

Recall now that $\rho(\mathcal{V}^k) < 1$. From [4, Proposition 3.20], it follows that

$$\mathbf{Y}^{k-1} - \mathbf{Y}^k \succeq 0,$$

i.e.,

$$\mathbf{Y}^{k-1} \succeq \mathbf{Y}^k \succeq \mathbf{Y}.$$

This completes the induction argument. Since $\{\mathbf{Y}^l\}_{l=0}^\infty$ is a decreasing sequence, i.e., $\mathbf{Y}^l \succeq \mathbf{Y}$, for all $l = 0, 1, \dots$, it follows that there exists \mathbf{Y}^+ , such that (see [233], p.79) $\mathbf{Y}^l \rightarrow \mathbf{Y}^+$, as $l \rightarrow \infty$. Clearly, $\mathbf{Y}^+ \succeq \mathbf{Y}$, for all $\mathbf{Y} \in \mathbb{M}$, because \mathbf{Y} is arbitrary.

Furthermore, \mathbf{Y}_n^l satisfies (23), and taking the limit for $l \rightarrow \infty$, it follows that $\mathbf{Y}^+ = \mathcal{Y}(\mathbf{Y}^+)$.

Moreover, $\tilde{R}_n(\mathbf{Y}^+) \succeq \tilde{R}_n(\mathbf{Y}) \succ 0$, i.e. $\mathbf{Y}^+ \in \mathbb{M}$, this completes the Proof.

Proof 29 (Proof of Theorem 1) The implication (i) \implies (ii) follows from the Schur complement [4, Lemma 2.23]. Specifically, from the Schur complement (see [4, Lemma 2.23]) it follows that $\mathbf{Y} \in \mathbb{H}^{In_x,*}$, satisfies (2.37) if and only if

$$-\mathbf{Y} + \mathcal{Y}(\mathbf{Y}) \succeq 0,$$

and

$$\tilde{\mathcal{R}}_n(\mathbf{Y}) \succ 0,$$

for any $n \in \mathbb{S}_\eta$, that is, $\mathbf{Y} \in \mathbb{M}$.

Thus, if $\mathbf{Y}^+ \in \mathbb{M}$ is such that $\mathbf{Y}^+ \succeq \mathbf{Y}$, for any $\mathbf{Y} \in \mathbb{M}$, then

$$\text{tr}(\mathbf{Y}_1^+ + \dots + \mathbf{Y}_I^+) \geq \text{tr}(\mathbf{Y}_1 + \dots + \mathbf{Y}_I),$$

and it follows that \mathbf{Y}^+ is a solution of the convex programming problem described in (2.37).

On the other hand, assume that (ii) holds, i.e., there exists a solution $\widehat{\mathbf{Y}}$ for the convex programming problem described in (2.37).

From the optimality of $\widehat{\mathbf{Y}}$, it follows that

$$\mathrm{tr}(\mathbf{Y}_1^+ - \widehat{\mathbf{Y}}_1) + \mathrm{tr}(\mathbf{Y}_I^+ - \widehat{\mathbf{Y}}_I) \leq 0,$$

for all $\mathbf{Y}^+ \in \mathbb{M}$. Since the MJLS described by (2.5) is mean square detectable, from Lemma 4, there exists $\mathbf{Y}^+ \succeq \widehat{\mathbf{Y}}$ satisfying (2.36). Therefore,

$$\mathbf{Y}_1^+ - \widehat{\mathbf{Y}}_1 \succeq 0, \dots, \mathbf{Y}_I^+ - \widehat{\mathbf{Y}}_I \succeq 0.$$

The two inequalities above hold if and only if

$$\widehat{\mathbf{Y}} = \mathbf{Y}^+.$$

This completes the proof.

Proof 30 (Proof of Theorem 2) Assume that $\widehat{\mathbf{Y}} = [\widehat{\mathbf{Y}}_n]_{n=1}^I$ is a MS stabilizing solution for filtering CAREs (2.36), so that system (2.5) is MSD, with $\check{M}_n = \mathcal{M}_n(\widehat{\mathbf{Y}})$, $n \in \mathbb{S}_\eta$.

From Lemma 4, there exists a maximal solution $\mathbf{Y}^+ \in \mathbb{M}$, satisfying

$$\mathbf{Y}^+ = \mathcal{Y}(\mathbf{Y}^+)$$

By applying Lemma 2-(17), the following equality holds:

$$\begin{aligned} & \widehat{\mathbf{Y}}_n - \mathbf{Y}_n^+ - \hat{\gamma}_n \left(A + \mathcal{M}_n(\widehat{\mathbf{Y}})L \right) \mathcal{D}_n(\widehat{\mathbf{Y}} - \mathbf{Y}^+) \left(A + \mathcal{M}_n(\widehat{\mathbf{Y}})L \right)^* \\ & - (1 - \hat{\gamma}_n) A \mathcal{D}_n(\widehat{\mathbf{Y}} - \mathbf{Y}^+) A^* \\ & = \hat{\gamma}_n \left(\mathcal{M}_n(\widehat{\mathbf{Y}}) - \mathcal{M}_n(\mathbf{Y}^+) \right) \tilde{\mathcal{R}}_n(\mathbf{Y}^+) \left(\mathcal{M}_n(\widehat{\mathbf{Y}}) - \mathcal{M}_n(\mathbf{Y}^+) \right)^*, \end{aligned}$$

for any $n \in \mathbb{S}_\eta$. Since $\tilde{\mathcal{R}}(\mathbf{Y}^+) \succ 0$,

$$\hat{\gamma}_n \left(\mathcal{M}_n(\widehat{\mathbf{Y}}) - \mathcal{M}_n(\mathbf{Y}^+) \right) \tilde{\mathcal{R}}_n(\mathbf{Y}^+) \left(\mathcal{M}_n(\widehat{\mathbf{Y}}) - \mathcal{M}_n(\mathbf{Y}^+) \right)^* \succeq 0.$$

Recall that $\widehat{\mathbf{Y}}$ is a MS stabilizing solution.

From [4, Proposition 3.20] it follows that $\widehat{\mathbf{Y}} - \mathbf{Y}^+ \succeq 0$.

But this also implies $\tilde{\mathcal{R}}(\widehat{\mathbf{Y}}) \succeq \tilde{\mathcal{R}}(\mathbf{Y}^+) \succ 0$.

Therefore $\widehat{\mathbf{Y}} \in \mathbb{M}$.

From Lemma [4](#), $\widehat{\mathbf{Y}} - \mathbf{Y}^+ \preceq 0$. The two inequalities above, given by

$$\begin{aligned}\widehat{\mathbf{Y}} - \mathbf{Y}^+ &\succeq 0, \\ \widehat{\mathbf{Y}} - \mathbf{Y}^+ &\preceq 0,\end{aligned}$$

hold if and only if $\widehat{\mathbf{Y}} = \mathbf{Y}^+$.

This completes the proof.

The following result proves the equivalence of the two estimation techniques (next-step predictor and current estimator) for the *MSS*.

Proof 31 (Proof of Lemma [1](#)) Assume the statement (i) holds, i.e., for any $\mathbf{Y}(0) \in \mathbb{H}^{I n_x, +}$, $\mathbf{Y}(k) \in \mathbb{H}^{I n_x, +}$, $k \in \mathbb{N}$, satisfying $\mathbf{Y}(k+1) = \mathcal{Y}(\mathbf{Y}(k), \boldsymbol{\pi}(k))$, with \mathcal{Y} defined in [\(2.35\)](#), converges to $\mathbf{Y} \in \mathbb{H}^{I n_x, +}$ satisfying $\mathbf{Y} = \mathcal{Y}(\mathbf{Y})$.

Let us set $\mathbf{Y}(0) = [Y_n(0)]_{n=1}^I \in \mathbb{H}^{I n_x, +}$, for any $\mathbf{Z}(0) = [Z_n(0)]_{n=1}^I \in \mathbb{H}^{I n_x, +}$, as follows,

$$Y_n(0) = \widehat{\mathcal{A}}_n(\mathbf{Z}(0), \boldsymbol{\pi}(0)) - \widetilde{\mathcal{B}}_n(\mathbf{Z}(0), \boldsymbol{\pi}(0)),$$

with $\widetilde{\mathcal{B}}_n(\mathbf{Z}(0), \boldsymbol{\pi}(0))$ defined for $n \in \mathbb{S}_\eta$, as follows,

$$\widetilde{\mathcal{B}}_n(\mathbf{Z}(0), \boldsymbol{\pi}(0)) \triangleq \hat{\gamma}_n \widehat{\mathcal{C}}_n(\mathbf{Z}(0)) \widehat{\mathcal{R}}_n^{-1}(\mathbf{Z}(0), \boldsymbol{\pi}(0)) \widehat{\mathcal{C}}_n^*(\mathbf{Z}(0)).$$

By (i), the limit for $k \rightarrow \infty$ of $\mathbf{Y}(k)$ converges to \mathbf{Y} in $\mathbb{H}^{I n_x, +}$ satisfying $\mathbf{Y} = \mathcal{Y}(\mathbf{Y})$.

Then, for $n \in \mathbb{S}_\eta$ and $k \in \mathbb{N}$, the following equalities hold:

$$\begin{aligned}Y_n(k) &= \widehat{\mathcal{A}}_n(\mathbf{Z}(k), \boldsymbol{\pi}(k)) - \widetilde{\mathcal{B}}_n(\mathbf{Z}(k), \boldsymbol{\pi}(k)), \\ Z_n(k+1) &= \mathcal{D}_n(\mathbf{Y}(k)).\end{aligned}$$

with $\widetilde{\mathcal{B}}_n(\mathbf{Z}(k), \boldsymbol{\pi}(k))$ defined for $n \in \mathbb{S}_\eta$, as follows,

$$\widetilde{\mathcal{B}}_n(\mathbf{Z}(k), \boldsymbol{\pi}(k)) \triangleq \hat{\gamma}_n \widehat{\mathcal{C}}_n(\mathbf{Z}(k)) \widehat{\mathcal{R}}_n^{-1}(\mathbf{Z}(k), \boldsymbol{\pi}(k)) \widehat{\mathcal{C}}_n^*(\mathbf{Z}(k)).$$

This implies that the limit for $k \rightarrow \infty$ of $\mathbf{Z}(k)$ converges to $\mathcal{D}(\mathbf{Y}) = \mathcal{Z}(\mathbf{Z})$.

Assume that (ii) holds, i.e., for any $\mathbf{Z}(0) \in \mathbb{H}^{I n_x, +}$, $\mathbf{Z}(k) \in \mathbb{H}^{I n_x, +}$, $k \in \mathbb{N}$, satisfying $\mathbf{Z}(k+1) = \mathcal{Z}(\mathbf{Z}(k), \boldsymbol{\pi}(k))$, converges to $\mathbf{Z} \in \mathbb{H}^{I n_x, +}$ satisfying $\mathbf{Z} = \mathcal{Z}(\mathbf{Z})$.

Let us set $\mathbf{Z}(0) = [Z_m(0)]_{m=1}^I \in \mathbb{H}^{I n_x, +}$, for any $\mathbf{Y}(0) = [Y_m(0)]_{m=1}^I \in \mathbb{H}^{I n_x, +}$, as $\mathbf{Z}(0) = \mathcal{D}(\mathbf{Y}(0))$.

From (ii), it follows that $\lim_{k \rightarrow \infty} \mathbf{Z}(k) = \mathbf{Z}$, with $\mathbf{Z} = \mathcal{Z}(\mathbf{Z})$.

Then, for $m \in \mathbb{S}_\eta$,

$$Y_m(k+1) = \hat{\mathcal{A}}_m(\mathbf{Z}(k), \boldsymbol{\pi}(k)) - \tilde{\mathcal{B}}_m(\mathbf{Z}(k), \boldsymbol{\pi}(k)),$$

and $Z_n(k) = \mathcal{D}_n(\mathbf{Y}(k))$, implying $\lim_{k \rightarrow \infty} \mathbf{Y}(k) = \mathbf{Y}$, $\mathbf{Y} = \mathcal{Y}(\mathbf{Y})$.

Assume that $\mathbf{Y} \in \mathbb{M}$ is the MS stabilizing solution of the filtering CAREs, i.e., $\mathbf{Y} = \mathcal{Y}(\mathbf{Y})$.

Then, $\mathcal{M}_n(\mathbf{Y})$ defined by (2.34) is such that the spectral radius $\rho(\mathcal{V}) < 1$, with $\mathcal{V} \in \mathbb{B}(\mathbb{H}^{In_x})$, defined in (2.22) for $\Gamma_{n1} = A + \mathcal{M}_n(\mathbf{Y})L$, $\Gamma_{n0} = A$, and $n \in \mathbb{S}_\eta$.

By setting $Z_n = \mathcal{D}_n(\mathbf{Y})$, the following equality holds for any $n \in \mathbb{S}_\eta$:

$$\mathcal{M}_n(\mathbf{Y}) = A\hat{\mathcal{M}}_n(\mathbf{Z}).$$

Considering $\hat{\Gamma}_{n1} = A + A\hat{\mathcal{M}}_n(\mathbf{Z})L$ and $\hat{\Gamma}_{n0} = A$, we obtain $\hat{\Gamma}_{n1} = \Gamma_{n1}$ and $\hat{\Gamma}_{n0} = \Gamma_{n0}$.

By Proposition 1, $\rho(\mathcal{V}) = \rho(\mathcal{T})$, and, consequently, $\rho(\mathcal{T}) < 1$.

Moreover, the optimal performance index achieved by the current estimator is

$$J_C^* = \sum_{n=1}^I \text{tr}(Z_n).$$

This completes the proof.

In the following, all mathematical preliminaries and motivations leading to the separation principle are illustrated concerning the output-feedback controller designed with the Markovian next-step predictor. A reduced version of the proof is reported in [92].

Define, for $k \in \mathbb{N}$, $\ell, i, j \in \mathbb{S}_\theta$,

$$\begin{aligned} w_{\ell i}(k) &\triangleq \mathbb{E} \left[x_k \mathbf{1}_{\{\theta_{k-1}=\ell, \theta_k=i\}} \right], \\ W_{\ell i}(k) &\triangleq \mathbb{E} \left[x_k x_k^* \mathbf{1}_{\{\theta_{k-1}=\ell, \theta_k=i\}} \right], \\ \mathbf{w}(k) &\triangleq [w_{\ell i}(k)]_{\ell, i=1}^N, \\ \mathbf{W}(k) &\triangleq [W_{\ell i}(k)]_{\ell, i=1}^N. \end{aligned}$$

For $\mathbf{V} = [V_{ij}]_{i, j=1}^N$ in $\mathbb{F}^{Nn_x \times Nn_x}$, recall the operator $\hat{\mathcal{L}}(\cdot) = [\hat{\mathcal{L}}_{ij}(\cdot)]_{i, j=1}^N$ in $\mathbb{B}(\mathbb{F}^{Nn_x \times Nn_x})$, defined in (2.49), given by

$$\begin{aligned} \hat{\mathcal{L}}_{ij}(\mathbf{V}) &\triangleq \left\{ A \sum_{l=1}^N V_{li} A^* + \hat{v}_i B \sum_{l=1}^N F_l V_{li} F_l^* B^* + \right. \\ &\quad \left. \hat{v}_i B \sum_{l=1}^N F_l V_{li} A^* + \hat{v}_i A \sum_{l=1}^N V_{li} F_l^* B^* \right\} p_{ij}. \end{aligned}$$

For $\mathbf{Y} = [Y_m]_{m=1}^I \in \mathbb{H}^{In_x}$, $\beta = [\beta_{\ell i}]_{\ell, i=1}^N \in \mathbb{R}^{N \times N}$, $i, j \in \mathbb{S}_\theta$, define the operator

$$\mathcal{H}(\cdot, \cdot) : \mathbb{H}^{In_x} \times \mathbb{R}^{N \times N} \rightarrow \mathbb{F}^{Nn_x \times Nn_x},$$

as

$$\mathcal{H}(\mathbf{Y}, \beta) \triangleq [\mathcal{H}_{ij}(\mathbf{Y}, \beta)]_{i, j=1}^N,$$

with

$$\mathcal{H}_{ij}(\mathbf{Y}, \beta) \triangleq \hat{\nu}_i B \sum_{\ell=1}^N \beta_{\ell i} F_\ell \left(\sum_{m=1}^I Y_m \right) F_\ell^* B^* p_{ij} + GG^* \beta_{ij}.$$

Proposition 10 Consider the MJLS described by (2.5) and the closed-loop system dynamics given by equation (2.41).

Then, the following equality holds for any $k \in \mathbb{N}$, $i, j \in \mathbb{S}_\theta$,

$$\begin{aligned} W_{ij}(k+1) &= \hat{\mathcal{L}}_{ij}(\mathbf{W}(k)) + \mathcal{H}_{ij}(\check{\mathbf{Y}}(k), \check{\boldsymbol{\omega}}(k)) - \\ &2\Re \left\{ \hat{\nu}_i B \sum_{\ell=1}^N F_\ell \left(\sum_{m=1}^I \check{m}_m(k) \right) w_{\ell i}^*(k) A^* + \right. \\ &\left. \hat{\nu}_i B \sum_{\ell=1}^N F_\ell \left(\sum_{m=1}^I \check{m}_m(k) \right) w_{\ell i}^*(k) F_\ell^* B^* \right\} p_{ij}. \end{aligned} \quad (24)$$

Proof 32 (Proof of Proposition 10) From (2.41) and (2.13), recalling the definition of $\hat{\mathcal{L}}$ in (2.49), by assumptions (a.2) – (a.3), applying (2.6) and the independence of sequences θ_k and \check{e}_k ,

$$\begin{aligned} W_{ij}(k+1) &= \hat{\mathcal{L}}_{ij}(\mathbf{W}(k)) + \left(\hat{\nu}_i B \sum_{\ell=1}^N \check{\omega}_{\ell i}(k) F_\ell \mathbb{E}[\check{e}_k \check{e}_k^*] F_\ell^* B^* + GG^* \sum_{\ell=1}^N \check{\omega}_{\ell i}(k) \right. \\ &\left. - \hat{\nu}_i 2\Re \left(B \sum_{\ell=1}^N F_\ell \mathbb{E}[\check{e}_k] w_{\ell i}^*(k) A^* + B \sum_{\ell=1}^N F_\ell \mathbb{E}[\check{e}_k] w_{\ell i}^*(k) F_\ell^* B^* \right) \right) p_{ij}, \end{aligned}$$

and thus, equation (24) follows. The proof of the proposition is complete.

Proof 33 (Proof of Theorem 3) Assume that (ii) holds, i.e., the MJLS described by (2.5) is both

ii-a) MSD,

ii-b) MS stabilizable with one time-step delayed observation of actuation link mode.

Then, by Definition 2, there exists a mode-dependent control gain F_ℓ , $\ell \in \mathbb{S}_\theta$, that makes the dynamics of x_k MSS.

Consequently, by [79, Proposition 3], $\rho(\hat{\mathcal{L}}) < 1$, with $\hat{\mathcal{L}}$ in (2.49).

By Definition 4, there exists a mode-dependent filtering gain \check{M}_n , $n \in \mathbb{S}_\eta$, such that $\rho(\mathcal{V}) < 1$, with $\mathcal{V} \in \mathbb{B}(\mathbb{H}^{I^{n_x}})$ in (2.22), for $\Gamma_{n1} = A + \check{M}_n L$ and $\Gamma_{n0} = A$.

By Proposition 2, it follows that

$$\check{Y}(k+1) = \mathcal{V}(\check{Y}(k)) + \mathcal{O}(\check{\mathbf{M}}, \pi(k)). \quad (25)$$

Since $\rho(\mathcal{V}) < 1$, by (a.4), from (25), $\lim_{k \rightarrow \infty} \check{Y}(k) = \check{Y}$,

$$\check{Y} = \mathcal{V}(\check{Y}) + \mathcal{O}(\check{\mathbf{M}}, \pi^\infty), \quad (26)$$

and thus, for $i, j \in \mathbb{S}_\theta$, $\lim_{k \rightarrow \infty} \mathcal{H}_{ij}(\check{Y}(k), \check{\omega}(k)) = \mathcal{H}_{ij}(\check{Y}, \check{\omega}^\infty)$.

From (2.29) and (26), by [4, Propositions 3.6 and 3.36], the following equality is satisfied $\lim_{k \rightarrow \infty} \check{\mathbf{m}}(k) = \mathbf{O}_{I^{n_x}}$. By Proposition 10, for $i, j \in \mathbb{S}_\theta$,

$$\lim_{k \rightarrow \infty} W_{ij}(k+1) = \hat{\mathcal{L}}_{ij}(\mathbf{W}) + \mathcal{H}_{ij}(\check{Y}, \check{\omega}^\infty),$$

and thus, there exists $\mathbf{W} = [W_{ij}]_{i,j=1}^N$, with $W_{ij} \in \mathbb{F}_+^{n_x \times n_x}$ satisfying $W_{ij} = \lim_{k \rightarrow \infty} W_{ij}(k)$.

Moreover, by [79, Proposition 2], $\lim_{k \rightarrow \infty} w_{\ell i}(k) = w_{\ell i} \in \mathbb{F}^{n_x}$, $\ell, i \in \mathbb{S}_\theta$.

Therefore, the closed-loop system is MSS by Definition 1, implying (i). To prove the converse of the theorem, assume now that (i) holds, i.e., the closed-loop system dynamics (2.41) can be made MSS.

Then, there exists $\mathbf{W} = [W_{ij}]_{i,j=1}^N$, with $W_{ij} = \lim_{k \rightarrow \infty} W_{ij}(k)$.

By Proposition 10, W_{ij} , $i, j \in \mathbb{S}_\theta$, can be written as follows. $W_{ij} = \lim_{k \rightarrow \infty} W_{ij}(k+1)$, with $W_{ij}(k+1)$ in (24). Thus, there exists \check{Y} in $\mathbb{H}^{I^{n_x, +}}$, such that $\lim_{k \rightarrow \infty} \check{Y}(k) = \check{Y}$, with \check{Y} satisfying (26).

Therefore, the error system (2.13) is MSS. By [4, Theorem 3.33, Theorem 3.9], it follows that condition (ii-a) holds. Moreover, by [4, Propositions 3.6 and 3.36], $\lim_{k \rightarrow \infty} \check{\mathbf{m}}(k) = \mathbf{O}_{I^{n_x}}$, and thus, the following equality holds for $i, j \in \mathbb{S}_\theta$,

$$W_{ij} = \hat{\mathcal{L}}_{ij}(\mathbf{W}) + \mathcal{H}_{ij}(\check{Y}, \check{\omega}^\infty),$$

implying that the mode-dependent control gain F_ℓ , $\ell \in \mathbb{S}_\theta$, stabilizes the dynamics (2.41) in the MS sense, i.e., condition (ii-b) holds.

The detailed proof of the separation principle concerning the output-feedback control based on the current estimator is presented in the following.

Define the operator $\widehat{\mathcal{H}}(\cdot, \cdot, \cdot)$, as follows,

$$\widehat{\mathcal{H}}(\cdot, \cdot, \cdot) : \mathbb{H}^{I n_x} \times \mathbb{R}^{N \times N} \times \mathbb{R}^I \rightarrow \mathbb{F}^{N n_x \times N n_x},$$

for $\mathbf{Z} = [Z_m]_{m=1}^I$, in $\mathbb{H}^{I n_x}$, $\boldsymbol{\beta} = [\beta_{\ell i}]_{\ell, i=1}^N$ in $\mathbb{R}^{N \times N}$, $\boldsymbol{\sigma} = [\sigma_m]_{m=1}^I \in \mathbb{R}^I$, $i, j \in \mathbb{S}_\theta$, as

$$\widehat{\mathcal{H}}(\mathbf{Z}, \boldsymbol{\beta}, \boldsymbol{\sigma}) \triangleq \left[\widehat{\mathcal{H}}_{ij}(\mathbf{Z}, \boldsymbol{\beta}, \boldsymbol{\sigma}) \right]_{i, j=1}^N,$$

with

$$\begin{aligned} \widehat{\mathcal{H}}_{ij}(\mathbf{Z}, \boldsymbol{\beta}, \boldsymbol{\sigma}) \triangleq & \sum_{\ell=1}^N \sum_{m=1}^I \left\{ \beta_{\ell i} \hat{\nu}_i B F_\ell Z_m F_\ell^* B^* + \beta_{\ell i} \hat{\nu}_i \hat{\gamma}_m B F_\ell \widehat{M}_m L Z_m L^* \widehat{M}_m^* F_\ell^* B^* \right. \\ & + \beta_{\ell i} \hat{\nu}_i \hat{\gamma}_m B F_\ell Z_m L^* \widehat{M}_m^* F_\ell^* B^* + \beta_{\ell i} \hat{\nu}_i \hat{\gamma}_m B F_\ell \widehat{M}_m L Z_m F_\ell^* B^* \\ & \left. + \beta_{\ell i} \sigma_m G G^* + \beta_{\ell i} \sigma_m \hat{\nu}_i \hat{\gamma}_m B F_\ell \widehat{M}_m H H^* \widehat{M}_m^* F_\ell^* B^* \right\} p_{ij}. \end{aligned} \quad (27)$$

Proposition 11 Consider the MJLS described by (2.5) and the closed-loop system dynamics given by equation (2.41).

Then, the following equality holds for any $k \in \mathbb{N}$, $i, j \in \mathbb{S}_\theta$,

$$\begin{aligned} W_{ij}(k+1) = & \widehat{\mathcal{L}}_{ij}(\mathbf{W}(k)) + \widehat{\mathcal{H}}_{ij}(\mathbf{Z}(k), \boldsymbol{\omega}(k), \boldsymbol{\pi}(k)) \\ & + 2\Re \left(\sum_{\ell=1}^N \sum_{m=1}^I \left\{ \hat{\nu}_i B F_\ell m_m(k) w_{\ell i}^*(k) A^* + \hat{\nu}_i \hat{\gamma}_m B F_\ell \widehat{M}_m L m_m(k) w_{\ell i}^*(k) A^* \right. \right. \\ & \left. \left. + \hat{\nu}_i B F_\ell m_m(k) w_{\ell i}^*(k) F_\ell^* B^* + \hat{\nu}_i \hat{\gamma}_m B F_\ell \widehat{M}_m L m_m(k) w_{\ell i}^*(k) F_\ell^* B^* \right\} \right) p_{ij}, \end{aligned} \quad (28)$$

where $\widehat{\mathcal{L}}_{ij}$ and $\widehat{\mathcal{H}}_{ij}$ are defined in (2.49) and (27), respectively.

Proof 34 (Proof of Proposition 11) Recall the closed-loop system dynamics in (2.43) and the error dynamics in (2.17).

Consider the expression of the operator $\widehat{\mathcal{L}}$ in (2.49). By assumptions (a.2) – (a.3), applying the properties $\mathbb{E}[w_k] = \mathbf{0}_{n_w}$ in (2.6), the definition of transition probabilities

in (2.2), the independence of sequences $\{e_k\}$ and $\{\theta_k\}$, $k \in \mathbb{N}$,

$$\begin{aligned}
W_{ij}(k+1) &= \widehat{\mathcal{L}}_{ij}(\mathbf{W}(k)) + \sum_{\ell=1}^N \sum_{m=1}^I \left\{ \widetilde{\omega}_{\ell i}(k) \hat{\nu}_i B F_{\ell} \mathbb{E} \left[e_k e_k^* \mathbf{1}_{\{\eta_k=m\}} \right] F_{\ell}^* B^* \right. \\
&\quad + \widetilde{\omega}_{\ell i}(k) \hat{\nu}_i \hat{\gamma}_m B F_{\ell} \widehat{M}_m L \mathbb{E} \left[e_k e_k^* \mathbf{1}_{\{\eta_k=m\}} \right] L^* \widehat{M}_m^* F_{\ell}^* B^* \\
&\quad + \widetilde{\omega}_{\ell i}(k) \hat{\nu}_i \hat{\gamma}_m B F_{\ell} \mathbb{E} \left[e_k e_k^* \mathbf{1}_{\{\eta_k=m\}} \right] L^* \widehat{M}_m^* F_{\ell}^* B^* \\
&\quad + \left. \widetilde{\omega}_{\ell i}(k) \hat{\nu}_i \hat{\gamma}_m B F_{\ell} \widehat{M}_m L \mathbb{E} \left[e_k e_k^* \mathbf{1}_{\{\eta_k=m\}} \right] F_{\ell}^* B^* \right\} p_{ij} \\
&\quad + \sum_{\ell=1}^N \sum_{m=1}^I \left\{ \widetilde{\omega}_{\ell i}(k) \pi_m(k) G \mathbb{E} \left[w_k w_k^* \right] G^* \right. \\
&\quad + \left. \widetilde{\omega}_{\ell i}(k) \pi_m(k) \hat{\nu}_i \hat{\gamma}_m B F_{\ell} \widehat{M}_m H \mathbb{E} \left[w_k w_k^* \right] H^* \widehat{M}_m^* F_{\ell}^* B^* \right\} p_{ij} \\
&\quad - 2\Re \left\{ \sum_{\ell=1}^N \sum_{m=1}^I \left\{ \hat{\nu}_i B F_{\ell} \mathbb{E} \left[e_k \mathbf{1}_{\{\eta_k=m\}} \right] \mathbb{E} \left[x_k^* \mathbf{1}_{\{\theta_{k-1}=\ell\}} \mathbf{1}_{\{\theta_k=i\}} \right] \right\} A^* \right. \\
&\quad + \hat{\nu}_i \hat{\gamma}_m B F_{\ell} \widehat{M}_m L \mathbb{E} \left[e_k \mathbf{1}_{\{\eta_k=m\}} \right] \mathbb{E} \left[x_k^* \mathbf{1}_{\{\theta_{k-1}=\ell\}} \mathbf{1}_{\{\theta_k=i\}} \right] A^* \\
&\quad + \hat{\nu}_i B F_{\ell} \mathbb{E} \left[e_k \mathbf{1}_{\{\eta_k=m\}} \right] \mathbb{E} \left[x_k^* \mathbf{1}_{\{\theta_{k-1}=\ell\}} \mathbf{1}_{\{\theta_k=i\}} \right] F_{\ell}^* B^* \\
&\quad + \left. \hat{\nu}_i \hat{\gamma}_m B F_{\ell} \widehat{M}_m L \mathbb{E} \left[e_k \mathbf{1}_{\{\eta_k=m\}} \right] \mathbb{E} \left[x_k^* \mathbf{1}_{\{\theta_{k-1}=\ell\}} \mathbf{1}_{\{\theta_k=i\}} \right] F_{\ell}^* B^* \right\} \right\} p_{ij}. \quad (29)
\end{aligned}$$

From (29), by applying the property $\mathbb{E}[w_k w_k^*] = \mathbb{I}_{n_w}$ in (2.6) (see Remark 11), it follows that,

$$\begin{aligned}
W_{ij}(k+1) &= \widehat{\mathcal{L}}_{ij}(\mathbf{W}(k)) + \sum_{\ell=1}^N \sum_{m=1}^I \left\{ \widetilde{\omega}_{\ell i}(k) \hat{\nu}_i B F_{\ell} Z_m(k) F_{\ell}^* B^* \right. \\
&\quad + \widetilde{\omega}_{\ell i}(k) \hat{\nu}_i \hat{\gamma}_m B F_{\ell} \widehat{M}_m L Z_m(k) L^* \widehat{M}_m^* F_{\ell}^* B^* \\
&\quad + \widetilde{\omega}_{\ell i}(k) \hat{\nu}_i \hat{\gamma}_m B F_{\ell} Z_m(k) L^* \widehat{M}_m^* F_{\ell}^* B^* \\
&\quad + \widetilde{\omega}_{\ell i}(k) \hat{\nu}_i \hat{\gamma}_m B F_{\ell} \widehat{M}_m L Z_m(k) F_{\ell}^* B^* \\
&\quad + \widetilde{\omega}_{\ell i}(k) \pi_m(k) G G^* \\
&\quad + \left. \widetilde{\omega}_{\ell i}(k) \pi_m(k) \hat{\nu}_i \hat{\gamma}_m B F_{\ell} \widehat{M}_m H H^* \widehat{M}_m^* F_{\ell}^* B^* \right\} p_{ij} \\
&\quad - 2\Re \left\{ \sum_{\ell=1}^N \sum_{m=1}^I \left\{ \hat{\nu}_i B F_{\ell} m_m(k) w_{\ell i}^*(k) A^* \right. \right. \\
&\quad + \hat{\nu}_i \hat{\gamma}_m B F_{\ell} \widehat{M}_m L m_m(k) w_{\ell i}^*(k) A^* \\
&\quad + \hat{\nu}_i B F_{\ell} m_m(k) w_{\ell i}^*(k) F_{\ell}^* B^* \\
&\quad + \left. \hat{\nu}_i \hat{\gamma}_m B F_{\ell} \widehat{M}_m L m_m(k) w_{\ell i}^*(k) F_{\ell}^* B^* \right\} \right\} p_{ij}. \quad (30)
\end{aligned}$$

Thus, from (30), it follows that equation (28) holds.

The proof of the proposition is complete.

Proof 35 (Proof of Theorem 4) Assume that (ii) holds, i.e., the MJLS described by (2.5) is both

ii-a) Strict-MSD,

ii-b) MS stabilizable with one time-step delayed observation of actuation link mode.

Then, there exists a mode-dependent control gain F_ℓ , $\ell \in \mathbb{S}_\theta$, that makes the dynamics of x_k MSS.

Consequently, by [79, Proposition 3], $\rho(\hat{\mathcal{L}}) < 1$, with $\hat{\mathcal{L}}$ in (2.49).

By Definition 5, there exists a mode-dependent filtering gain \widehat{M}_n , $n \in \mathbb{S}_\eta$, such that $\rho(\mathcal{T}) < 1$, with \mathcal{T} in $\mathbb{B}(\mathbb{H}^{I^{n_x}})$ in (2.20), $\widehat{\Gamma}_{n1} = A + A\widehat{M}_nL$ and $\widehat{\Gamma}_{n0} = A$.

By Proposition 3,

$$\mathbf{Z}(k+1) = \mathcal{T}(\mathbf{Z}(k)) + \widehat{\mathcal{O}}(\widehat{\mathbf{M}}, \boldsymbol{\pi}(k)).$$

Thus, from $\rho(\mathcal{T}) < 1$ and the assumption (a.4),

$$\lim_{k \rightarrow \infty} \mathbf{Z}(k) = \mathbf{Z} \in \mathbb{H}^{I^{n_x,+}},$$

with

$$\mathbf{Z} = \mathcal{T}(\mathbf{Z}) + \widehat{\mathcal{O}}(\widehat{\mathbf{M}}, \boldsymbol{\pi}^\infty). \quad (31)$$

Therefore,

$$\lim_{k \rightarrow \infty} \widehat{\mathcal{H}}_{ij}(\mathbf{Z}(k), \widetilde{\boldsymbol{\omega}}(k), \boldsymbol{\pi}(k)) = \widehat{\mathcal{H}}_{ij}(\mathbf{Z}, \widetilde{\boldsymbol{\omega}}^\infty, \boldsymbol{\pi}^\infty),$$

$i, j \in \mathbb{S}_\theta$. From (2.33) and (31), by [4, Propositions 3.6 and 3.36], $\lim_{k \rightarrow \infty} \mathbf{m}(k) = \mathbf{O}_{I^{n_x}}$.

By Proposition 11,

$$\lim_{k \rightarrow \infty} W_{ij}(k+1) = \widehat{\mathcal{L}}_{ij}(\mathbf{W}) + \widehat{\mathcal{H}}_{ij}(\mathbf{Z}, \widetilde{\boldsymbol{\omega}}^\infty, \boldsymbol{\pi}^\infty),$$

$i, j \in \mathbb{S}_\theta$.

Thus, there exists $\mathbf{W} = [W_{ij}]_{i,j=1}^N$, with W_{ij} in $\mathbb{F}_+^{n_x \times n_x}$, satisfying, for $i, j \in \mathbb{S}_\theta$,

$$W_{ij} = \lim_{k \rightarrow \infty} W_{ij}(k+1).$$

Moreover, by [79, Proposition 2], the following equality is satisfied,

$$\lim_{k \rightarrow \infty} w_{\ell i}(k) = w_{\ell i},$$

with $w_{\ell i} \in \mathbb{F}^{n_x}$, $\ell, i \in \mathbb{S}_\theta$. Therefore, the closed-loop system is MSS, i.e., (i) holds.

To prove the converse statement, assume (i) holds, i.e., the closed-loop system dynamics (2.43) can be made MSS.

Then, there exists $\mathbf{W} = [W_{ij}]_{i,j=1}^N$, with

$$W_{ij} = \lim_{k \rightarrow \infty} W_{ij}(k).$$

By Proposition 11, W_{ij} , $i, j \in \mathbb{S}_\theta$, satisfies (28), with $\mathbf{Z}(k)$ satisfying (2.33).

This implies that there exists \mathbf{Z} in $\mathbb{H}^{I^{n_x, +}}$ such that

$$\lim_{k \rightarrow \infty} \mathbf{Z}(k) = \mathbf{Z}$$

with \mathbf{Z} satisfying (31).

Therefore, the error system (2.17) is MSS, and, by [4, Theorem 3.33, Theorem 3.9], condition (ii-a) holds.

Moreover, by [4, Proposition 3.6, Proposition 3.36], it follows that

$$\lim_{k \rightarrow \infty} \mathbf{m}(k) = \mathbf{O}_{I^{n_x}}.$$

Thus, the following equality holds for $i, j \in \mathbb{S}_\theta$:

$$W_{ij} = \widehat{\mathcal{L}}_{ij}(\mathbf{W}) + \widehat{\mathcal{H}}_{ij}(\mathbf{Z}, \tilde{\boldsymbol{\omega}}^\infty, \boldsymbol{\pi}^\infty),$$

implying that the mode-dependent control gain F_ℓ , $\ell \in \mathbb{S}_\theta$, makes the dynamics (2.43) MSS, i.e., condition (ii-b) holds.

Proofs for the mode-independent output-feedback

This section reports the results on the mode-independent output-feedback controller.

Proof 36 (Proof of Proposition 5) Consider the MJLS described by (2.5).

Assume that (2.5) is Strong-MSD.

Then, there exists a mode-independent filtering gain \check{M}^b in $\mathbb{F}^{n_x \times n_y}$, such that $\rho(\mathcal{V}) < 1$, with $\mathcal{V} \in \mathbb{B}(\mathbb{H}^{I^{n_x}})$ in (2.22), for $\Gamma_{n1} = A + \check{M}^b L$, $\Gamma_{n0} = A$ and $n \in \mathbb{S}_\eta$. Pick the mode-dependent filtering gain

$$\check{M}_n = \check{M}^b, \tag{32}$$

for any $n \in \mathbb{S}_\eta$.

Consider the operator \mathcal{V} defined in (2.22), with

$$\Gamma_{n1} = A + \check{M}_n L, \quad \Gamma_{n0} = A,$$

with \check{M}_n in (32). Then condition $\rho(\mathcal{V}) < 1$ is again satisfied, and the statement (i) holds.

Assume now that (2.5) is Strong-Strict-MSD.

Then, there exists a mode-independent filtering gain \widehat{M}^b in $\mathbb{F}^{n_x \times n_y}$, such that $\rho(\mathcal{T}) < 1$, with $\mathcal{T} \in \mathbb{B}(\mathbb{H}^{I n_x})$ in (2.20), for $\widehat{\Gamma}_{n1} = A + A\widehat{M}^b L$, $\widehat{\Gamma}_{n0} = A$ and $n \in \mathbb{S}_\eta$.

Pick the mode-dependent filtering gain, as follows,

$$\widehat{M}_m = \widehat{M}^b, \tag{33}$$

for any $m \in \mathbb{S}_\eta$, and consider \mathcal{T} defined in (2.20), with

$$\widehat{\Gamma}_{m1} = A + A\widehat{M}_m L, \quad \widehat{\Gamma}_{m0} = A,$$

with \widehat{M}_m in (33), for $m \in \mathbb{S}_\eta$.

The condition $\rho(\mathcal{T}) < 1$ is again satisfied, and the implication Strong-Strict-MSD \implies Strict-MSD holds.

Moreover, if (2.5) is Strong-Strict-MSD, then, there exists a mode-independent filtering gain $\check{M}^b = A\widehat{M}^b$, such that, setting $\Gamma_{n1} = A + \check{M}^b L$ and $\Gamma_{n0} = A$, the following equalities are satisfied:

$$\widehat{\Gamma}_{n0} = \Gamma_{n0}, \quad \widehat{\Gamma}_{n1} = \Gamma_{n1}$$

for any $n \in \mathbb{S}_\eta$.

Consider now \mathcal{V} , with Γ_{n1} , Γ_{n0} defined above.

By Proposition 1, $\rho(\mathcal{V}) = \rho(\mathcal{T})$, which implies $\rho(\mathcal{V}) < 1$, and thus,

$$\text{Strong-Strict-MSD} \implies \text{Strong-MSD}.$$

Proof 37 (Proof of Theorem 5) Condition (ii) follows from [79, Theorem 3], and thus, it remains to prove condition (i).

Recall that $\hat{\gamma} = \sum_{m=1}^I \pi_m^\infty \hat{\gamma}_m$ by assumption.

Moreover, by assumption, $\boldsymbol{\pi}^\infty = [\pi_m^\infty]_{m=1}^I$ is the stationary distribution of the sensing link modes, and thus,

$$\pi_n^\infty = \sum_{m=1}^I q_{mn} \pi_m^\infty.$$

The probability $\hat{\gamma}$, given by

$$\hat{\gamma} = \sum_{n=1}^I \pi_n^\infty \hat{\gamma}_n,$$

can be written as follows,

$$\hat{\gamma} = \sum_{m=1}^I \pi_m^\infty \sum_{n=1}^I q_{mn} \hat{\gamma}_n$$

By applying the property $\sum_{m=1}^I \pi_m^\infty = 1$, the filtering MARE (2.44) can be rewritten as follows,

$$\sum_{m=1}^I \pi_m^\infty \{Y_\infty^b - \mathring{A}^b(Y_\infty^b) + \sum_{n=1}^I q_{mn} \hat{\gamma}_n (\mathring{C}^b(Y_\infty^b) \mathring{R}^b(Y_\infty^b)^{-1} \mathring{C}^{b*}(Y_\infty^b))\} = 0, \quad (34)$$

holding for all $\boldsymbol{\pi}^\infty = [\pi_m]_{m=1}^I$, if and only if, for all $m \leq I$, the following equality is satisfied

$$Y_\infty^b = \mathring{A}^b(Y_\infty^b) - \zeta_m \mathring{C}^b(Y_\infty^b) \mathring{R}^b(Y_\infty^b)^{-1} \mathring{C}^{b*}(Y_\infty^b), \quad (35)$$

with

$$\zeta_m = \sum_{n=1}^I q_{mn} \hat{\gamma}_n.$$

Equation (35) is exactly equation (2.44), where, as required by the mode-independence,

$$Y_m = Y_\infty^b,$$

for any $m \in \mathbb{S}_\eta$.

The proof of the theorem is complete.

Technical results concerning MSD are proved in the following.

Proof 38 (Proof of Proposition 6) Let us prove the equivalence of statement (i) and statement (iii). Assume that statement (i) holds, i.e., the MJLS described by (2.5) is MSD.

Then, there exists a mode-dependent filtering gain $\check{M}_n \in \mathbb{F}^{n_x \times n_y}$, $n \in \mathbb{S}_\eta$, such that $\rho(\mathcal{V}) < 1$, with $\mathcal{V} \in \mathbb{B}(\mathbb{H}^{I^{n_x}})$ in (2.22), for $\Gamma_{n1} = A + \check{M}_n L$ and $\Gamma_{n0} = A$.

Consider the operator $\mathcal{L} \in \mathbb{B}(\mathbb{H}^{I^{n_x}})$ in (2.21), with the same Γ_{n1} and Γ_{n0} given for \mathcal{V} . By Proposition 1, $\rho(\mathcal{V}) = \rho(\mathcal{L})$, and, therefore, $\rho(\mathcal{L}) < 1$. By applying [4, Theorem 3.9], for $\mathbf{V} = [V_m]_{m=1}^I \in \mathbb{H}^{I^{n_x, +}}$, $V_m \succ 0$, $m \in \mathbb{S}_\eta$, the difference $\mathcal{L}_m(\mathbf{V}) - V_m$ results to be $\mathcal{L}_m(\mathbf{V}) - V_m \prec 0$, since the following computations hold, for $m \in \mathbb{S}_\eta$

$$\begin{aligned} \mathcal{L}_m(\mathbf{V}) - V_m &= \\ \hat{\gamma}_m (A + \check{M}_m L)^* \mathcal{E}_m(\mathbf{V}) (A + \check{M}_m L) + (1 - \hat{\gamma}_m) A^* \mathcal{E}_m(\mathbf{V}) A - V_m &= \\ A^* \mathcal{E}_m(\mathbf{V}) A + \hat{\gamma}_m A^* \mathcal{E}_m(\mathbf{V}) \check{M}_m L + \hat{\gamma}_m L^* \check{M}_m^* \mathcal{E}_m(\mathbf{V}) A + \hat{\gamma}_m L^* \check{M}_m^* \mathcal{E}_m(\mathbf{V}) \check{M}_m L - V_m &\prec 0. \end{aligned} \quad (36)$$

Taking $\mathbf{W}_1 = \mathbf{V}$ and $Z_m = \mathcal{E}_m(\mathbf{W}_1)$, condition (2.47c) is satisfied.

Let us choose

$$W_{m2} = Z_m \check{M}_m, \quad W_{m3} = W_{m2}^* Z_m^{-1} W_{m2},$$

Substituting the expressions above in $\mathcal{L}_m(\mathbf{V}) - V_m$, condition (2.47a) follows.

Let us recall that

$$W_{m3} \succeq W_{m2}^* Z_m^{-1} W_{m2},$$

by the Schur complement [4, Lemma 2.23], condition (2.47b) follows.

Thus, statement (i) \implies (iii). Let us prove now that (iii) \implies (i). Assume that (iii) holds, i.e., there exist

$$\begin{aligned} \mathbf{W}_1 &= [W_{m1}]_{m=1}^I, \quad \mathbf{Z} = [Z_m]_{m=1}^I \in \mathbb{H}^{I^{n_x, +}}, \\ \mathbf{W}_2 &= [W_{m2}]_{m=1}^I \in \mathbb{H}^{I^{n_x, n_y}}, \quad \mathbf{W}_3 = [W_{m3}]_{m=1}^I \in \mathbb{H}^{I^{n_y, +}}, \end{aligned}$$

satisfying conditions (2.47).

Let us choose the filtering gain as $\check{M}_m = Z_m^{-1} W_{m2}$. Consider again the operator \mathcal{L} defined above. For $\mathbf{W}_1 \in \mathbb{H}^{I^{n_x, +}}$, as in conditions (2.47), the following equalities are

satisfied, for $m \in \mathbb{S}_\eta$,

$$\begin{aligned}
& \mathcal{L}_m(\mathbf{W}_1) - W_{m1} \\
&= \hat{\gamma}_m \left(A + \check{M}_m L \right)^* \mathcal{E}_m(\mathbf{W}_1) \left(A + \check{M}_m L \right) \\
&+ (1 - \hat{\gamma}_m) A^* \mathcal{E}_m(\mathbf{W}_1) A - W_{m1} \\
&= A^* \mathcal{E}_m(\mathbf{W}_1) A + \hat{\gamma}_m A^* \mathcal{E}_m(\mathbf{W}_1) \check{M}_m L + \hat{\gamma}_m L^* \check{M}_m^* \mathcal{E}_m(\mathbf{W}_1) A \\
&+ \hat{\gamma}_m L^* \check{M}_m^* \mathcal{E}_m(\mathbf{W}_1) \check{M}_m L - W_{m1} \\
&= A^* \mathcal{E}_m(\mathbf{W}_1) A + \hat{\gamma}_m A^* \mathcal{E}_m(\mathbf{W}_1) Z_m^{-1} W_{m2} L \\
&+ \hat{\gamma}_m L^* W_{m2}^* Z_m^{-1} \mathcal{E}_m(\mathbf{W}_1) A + \hat{\gamma}_m L^* W_{m2}^* Z_m^{-1} \mathcal{E}_m(\mathbf{W}_1) Z_m^{-1} W_{m2} L - W_{m1}. \tag{37}
\end{aligned}$$

From (2.47b), by the Schur complement, it follows that

$$W_{m3} \succeq W_{m2}^* Z_m^{-1} W_{m2}, \tag{38}$$

and, from (2.47c),

$$Z_m \succeq \mathcal{E}_m(\mathbf{W}_1),$$

and thus, from (37),

$$\mathcal{L}_m(\mathbf{W}_1) - W_{m1} \preceq A^* Z_m A + \hat{\gamma}_m A^* W_{m2} L + \hat{\gamma}_m L^* W_{m2}^* A + \hat{\gamma}_m L^* W_{m2}^* Z_m^{-1} W_{m2} L - W_{m1}. \tag{39}$$

By recalling (38) and condition (2.47a), from (39), it follows that,

$$\mathcal{L}_m(\mathbf{W}) - W_{m1} \preceq A^* Z_m A + \hat{\gamma}_m A^* W_{m2} L + \hat{\gamma}_m L^* W_{m2}^* A + \hat{\gamma}_m L^* W_{m3} L - W_{m1} \prec 0, \tag{40}$$

for any $n \in \mathbb{S}_\eta$.

Thus, $\mathcal{L}_m(\mathbf{W}_1) - W_{m1} \prec 0$, for any $n \in \mathbb{S}_\eta$. By [4, Theorem 3.9], $\rho(\mathcal{L}) < 1$. Consider the operator \mathcal{V} in (2.22), for $\Gamma_{m1} = A + \check{M}_m L$, $\Gamma_{m0} = A$, and $m \in \mathbb{S}_\eta$.

By Proposition 1: $\rho(\mathcal{V}) = \rho(\mathcal{L})$, and, consequently, $\rho(\mathcal{V}) < 1$. Thus, the MJLS described by (2.5) is MSD, and statement (i) holds.

Assume that statement (ii) holds, i.e., the MJLS described by (2.5) is Strict-MSD.

Then, there exists a mode-dependent filtering gain $\widehat{M}_n \in \mathbb{F}^{n_x \times n_y}$, $n \in \mathbb{S}_\eta$, such that $\rho(\mathcal{T}) < 1$, with $\mathcal{T} \in \mathbb{B}(\mathbb{H}^{I^{n_x}})$ in (2.20), for $\widehat{\Gamma}_{n1} = A + A\widehat{M}_n L$ and $\widehat{\Gamma}_{n0} = A$, $n \in \mathbb{S}_\eta$. Consider the operator $\mathcal{L} \in \mathbb{B}(\mathbb{H}^{I^{n_x}})$ in (2.21), with $\Gamma_{n1} = \widehat{\Gamma}_{n1}$ and $\Gamma_{n0} = \widehat{\Gamma}_{n0}$, for all $n \in \mathbb{S}_\eta$.

By Proposition [1](#), $\rho(\mathcal{T}) = \rho(\mathcal{L})$, and, therefore, $\rho(\mathcal{L}) < 1$. By applying [4](#), [Theorem 3.9], we have that, for $\mathbf{V} = [V_m]_{m=1}^I \in \mathbb{H}^{In_x,+}$, $V_m \succ 0$, $m \in \mathbb{S}_\eta$, $\mathcal{L}_m(\mathbf{V}) - V_m \prec 0$.

By taking $\mathbf{W}_1 = \mathbf{V}$, $Z_m = \mathcal{E}_m(\mathbf{W}_1)$, condition [\(2.47c\)](#) is satisfied. By choosing $W_{m2} = Z_m A \widehat{M}_m$, $W_{m3} = W_{m2}^* Z_m^{-1} W_{m2}$, and substituting these expressions in $\mathcal{L}_m(\mathbf{V}) - V_m$, condition [\(2.47a\)](#) follows.

Recalling that $W_{m3} \succeq W_{m2}^* Z_m^{-1} W_{m2}$, by the Schur complement condition [\(2.47b\)](#) is satisfied, and (iii) holds.

Let us prove that if the matrix A is non-singular, the converse implication, i.e., (iii) \implies (ii), is true.

Assume (iii) holds, i.e.,

Moreover, assume that the matrix A is non-singular. Then, the filtering gain can be chosen as $\widehat{M}_m = A^{-1} Z_m^{-1} W_{m2}$. Consider again the operator \mathcal{L} defined above. From [\(2.47b\)](#), by the Schur complement (see [4](#), Lemma 2.23]), we have $W_{m3} \succeq W_{m2}^* Z_m^{-1} W_{m2}$ and, from [\(2.47c\)](#), $Z_m \succeq \mathcal{E}_m(\mathbf{W}_1)$. Thus, by condition [\(2.47a\)](#), we get $\mathcal{L}_m(\mathbf{W}_1) - W_{m1} \prec 0$ and, by [4](#), [Theorem 3.9], $\rho(\mathcal{L}) < 1$. Consider the operator \mathcal{T} in [\(2.20\)](#), with $\widehat{\Gamma}_{n1} = A + A \widehat{M}_n L$, $\widehat{\Gamma}_{n0} = A$, and $n \in \mathbb{S}_\eta$. This implies that $\widehat{\Gamma}_{n0} = \Gamma_{n0}$, $\widehat{\Gamma}_{n1} = \Gamma_{n1}$, for all $n \in \mathbb{S}_\eta$, and, by Proposition [1](#), $\rho(\mathcal{T}) = \rho(\mathcal{L})$. Therefore, $\rho(\mathcal{T}) < 1$, and condition (ii) holds.

Proof 39 (Proof of Proposition [7](#)) Assume that [\(2.48\)](#) holds for some $\mathbf{W}_1 = [W_{m1}]_{m=1}^I$ in $\mathbb{H}^{In_x,+}$, Z in $\mathbb{F}_+^{n_x \times n_x}$, W_2 in $\mathbb{F}^{n_x \times n_y}$, W_3 in $\mathbb{F}_+^{n_y \times n_y}$, for any $m \in \mathbb{S}_\eta$. From [\(2.48b\)](#), by the Schur complement (see [4](#), Lemma 2.23]), the inequalities below follow,

$$W_3 - W_2^* Z^{-1} W_2 \succeq 0,$$

and thus,

$$W_3 \succeq W_2^* Z^{-1} W_2. \tag{41}$$

Let us choose the mode-independent next-step predictor filtering gain as follows,

$$\check{M}^b = Z^{-1} W_2,$$

and consider the operator \mathcal{L} in $\mathbb{B}(\mathbb{H}^{In_x})$ in [\(2.21\)](#), for

$$\Gamma_{m1} = A + \check{M}^b L, \quad \Gamma_{m0} = A,$$

for any $m \in \mathbb{S}_\eta$. From [\(2.48c\)](#), $\mathcal{E}_m(\mathbf{W}_1) \preceq Z$, for all $m \in \mathbb{S}_\eta$.

By applying the definition of operator \mathcal{L} and by substituting the expression of the filtering gain \check{M}^b , the following equalities/inequalities hold,

$$\begin{aligned}
\mathcal{L}_m(\mathbf{W}_1) - W_{m1} &= \\
&= \hat{\gamma}_m (A + \check{M}^b L)^* \mathcal{E}_m(\mathbf{W}_1) (A + \check{M}^b L) \\
&+ (1 - \hat{\gamma}_m) A^* \mathcal{E}_m(\mathbf{W}_1) A - W_{m1} \\
&= A^* \mathcal{E}_m(\mathbf{W}_1) A + \hat{\gamma}_m A^* \mathcal{E}_m(\mathbf{W}_1) M^b L \\
&+ \hat{\gamma}_m L^* \check{M}^{b*} \mathcal{E}_m(\mathbf{W}_1) A + \hat{\gamma}_m L^* \check{M}^{b*} \mathcal{E}_m(\mathbf{W}_1) \check{M}^b L - W_{m1} \\
&= A^* \mathcal{E}_m(\mathbf{W}_1) A + \hat{\gamma}_m A^* \mathcal{E}_m(\mathbf{W}_1) Z^{-1} W_2 L \\
&+ \hat{\gamma}_m L^* W_2^* Z^{-1} \mathcal{E}_m(\mathbf{W}_1) A \\
&+ \hat{\gamma}_m L^* W_2^* Z^{-1} \mathcal{E}_m(\mathbf{W}_1) Z^{-1} W_2 L - W_{m1} \\
&\preceq A^* Z A + \hat{\gamma}_m A^* W_2 L + \hat{\gamma}_m L^* W_2^* A \\
&+ \hat{\gamma}_m L^* W_2^* Z^{-1} W_2 L - W_{m1}. \tag{42}
\end{aligned}$$

Thus, by recalling (41) and condition (2.48a), from (42), it follows that

$$\mathcal{L}_m(\mathbf{W}_1) - W_{m1} \prec 0.$$

By [4, Theorem 3.9], it follows that $\rho(\mathcal{L}) < 1$.

Consider now the operator \mathcal{V} in $\mathbb{B}(\mathbb{H}^{In_x})$, defined in (2.22), with $\Gamma_{m1} = A + \check{M}^b L$, $\Gamma_{m0} = A$, and $m \in \mathbb{S}_\eta$.

By Proposition 1, $\rho(\mathcal{V}) = \rho(\mathcal{L})$, and, consequently, $\rho(\mathcal{V}) < 1$.

Therefore, the MJLS described by (2.5) is Strong-MSD, and, thus, the proof of the implication (i) \implies (ii) is complete.

Now, assume that conditions (2.48) hold for some Z in $\mathbb{F}_+^{n_x \times n_x}$, $\mathbf{W}_1 = [W_{m1}]_{m=1}^I$ in $\mathbb{H}^{In_x, +}$, W_2 in $\mathbb{F}^{n_x \times n_y}$, and W_3 in $\mathbb{F}_+^{n_y \times n_y}$.

From (2.48b), by the Schur complement (see [4, Lemma 2.23]), we have that

$$W_3 - W_2^* Z^{-1} W_2 \succeq 0,$$

and thus,

$$W_3 \succeq W_2^* Z^{-1} W_2. \tag{43}$$

Let us recall that the matrix A is non-singular by assumption and let us choose the mode-independent current estimator filtering gain as follows,

$$\widehat{M}^b = A^{-1} Z^{-1} W_2.$$

Consider the operator \mathcal{L} in $\mathbb{B}(\mathbb{H}^{I^{n_x}})$ defined in (2.21) with

$$\Gamma_{m1} = A + A\widehat{M}^bL, \quad \Gamma_{m0} = A,$$

for any $m \in \mathbb{S}_\eta$.

From (2.48c) it follows that, $\mathcal{E}_m(\mathbf{W}_1) \preceq Z$, for any $m \in \mathbb{S}_\eta$.

$$\begin{aligned} \mathcal{L}_m(\mathbf{W}_1) - W_{m1} &= \\ &= \hat{\gamma}_m (A + A\widehat{M}^bL)^* \mathcal{E}_m(\mathbf{W}_1) (A + A\widehat{M}^bL) \\ &\quad + (1 - \hat{\gamma}_m) A^* \mathcal{E}_m(\mathbf{W}_1) A - W_{m1} \\ &= A^* \mathcal{E}_m(\mathbf{W}_1) A + \hat{\gamma}_m A^* \mathcal{E}_m(\mathbf{W}_1) A\widehat{M}^bL \\ &\quad + \hat{\gamma}_m L^* \widehat{M}^{b*} A^* \mathcal{E}_m(\mathbf{W}_1) A + \hat{\gamma}_m L^* \widehat{M}^{b*} A^* \mathcal{E}_m(\mathbf{W}_1) A\widehat{M}^bL - W_{m1} \\ &= A^* \mathcal{E}_m(\mathbf{W}_1) A + \hat{\gamma}_m A^* \mathcal{E}_m(\mathbf{W}_1) Z^{-1} W_2 L \\ &\quad + \hat{\gamma}_m L^* W_2^* Z^{-1} \mathcal{E}_m(\mathbf{W}_1) A + \hat{\gamma}_m L^* W_2^* Z^{-1} \mathcal{E}_m(\mathbf{W}_1) Z^{-1} W_2 L - W_{m1}. \\ &\preceq A^* Z A + \hat{\gamma}_m A^* W_2 L + \hat{\gamma}_m L^* W_2^* A \\ &\quad + \hat{\gamma}_m L^* W_2^* Z^{-1} W_2 L - W_{m1}. \end{aligned} \tag{44}$$

Thus, by recalling (43) and condition (2.48a), from (44) it follows that,

$$\mathcal{L}_m(\mathbf{W}_1) - W_{m1} \prec 0.$$

By [4, Theorem 3.9], $\rho(\mathcal{L}) < 1$.

Consider \mathcal{T} in $\mathbb{B}(\mathbb{H}^{I^{n_x}})$ defined in (2.20), for $\widehat{\Gamma}_{m1} = A + A\widehat{M}^bL$, $\widehat{\Gamma}_{m0} = A$, $m \in \mathbb{S}_\eta$.

This implies $\widehat{\Gamma}_{m0} = \Gamma_{m0}$ and $\widehat{\Gamma}_{m1} = \Gamma_{m1}$. By Proposition 1, $\rho(\mathcal{L}) = \rho(\mathcal{T})$, and, consequently, $\rho(\mathcal{T}) < 1$. Thus, the system (2.5) is Strong-Strict-MSD.

Appendix B

Proof of Theorem 6

Proof 40 (Proof of Proposition 8) Consider the MJLS described by equation (3.7) that describes the dynamics of the error \tilde{e}_i , with $i \in \{u, e\}$ denoting the agent (either the user or the eavesdropper).

Consider the MSE expression in (3.8). If there exists a mode-dependent filtering gain such that the MSE is bounded, from Assumption 2, the difference Riccati equation is equivalent to the algebraic Riccati equation (3.10), and the mode-dependent filtering gain is given by (3.11). By applying the reasoning illustrated in the proof of Proposition 3 in Chapter 2 (see Appendix A) and in the proof of [4, Proposition A.23], equations (3.10)-(3.11) follow.

The proof of the proposition is complete.

The following lemmas extend the result presented in [49, Theorem 2] and they are instrumental for the proof of Theorem 6.

Lemma 5 Consider for $\lambda \in [0, 1]$, the operator

$$\mathcal{X}_\lambda : \mathbb{F}_+^{n_x \times n_x} \times \mathbb{R}^+ \times \mathbb{R}^+ \rightarrow \mathbb{F}_+^{n_x \times n_x},$$

defined for $X \in \mathbb{F}_+^{n_x \times n_x}$, $\alpha > 0$, $\phi \in \mathbb{R}^+$ in (3.9).

Let us recall the expression of \mathcal{X}_λ , as follows,

$$\begin{aligned} \mathcal{X}_\lambda(X, \alpha, \phi) &\triangleq (1 - \lambda\phi) \{AXA^* + \alpha Q\} \\ &+ \lambda\phi \left(AXA^* + \alpha Q - AXL^* (LXL^* + \alpha R)^{-1} LXA^* \right). \end{aligned} \quad (45)$$

Then, the following conditions hold.

(a) *Consider $X, Y \in \mathbb{F}_+^{n_x \times n_x}$. If*

$$X \preceq Y,$$

then,

$$\mathcal{X}_\lambda(X, \alpha, \phi) \preceq \mathcal{X}_\lambda(Y, \alpha, \phi)$$

(b) Consider $\hat{\lambda}, \tilde{\lambda} \in [0, 1]$. If

$$\hat{\lambda} \geq \tilde{\lambda},$$

then

$$\mathcal{X}_{\hat{\lambda}}(X, \alpha, \phi) \preceq \mathcal{X}_{\tilde{\lambda}}(X, \alpha, \phi).$$

(c) Consider the positive constant $\beta > 1$.

Then,

$$\mathcal{X}_\lambda(\beta X, \alpha, \phi) \preceq \beta \mathcal{X}_\lambda(X, \alpha, \phi).$$

Proof 41 (Proof of Lemma 5) Let us show that condition (a) is satisfied. Let us define the gain K_X as follows,

$$K_X \triangleq -XL^*(LXL^* + \alpha R)^{-1}.$$

Then, the reader can easily verify that

$$\begin{aligned} \mathcal{X}_\lambda(X, \alpha, \phi) = & (1 - \lambda\phi) \{AXA^* + \alpha Q\} \\ & + \lambda\phi \left\{ (A + AK_X L) X (A + AK_X L)^* + \alpha Q \right. \\ & \left. + \alpha AK_X R K_X^* A^* \right\}. \end{aligned}$$

By applying an approach based on matrix derivatives, it can be shown that K_X minimizes the function $\mathcal{X}_\lambda(X, \alpha, \phi)$ (see [49, Lemma 1]), and thus, recalling that $X \preceq Y$, the following inequality is obtained

$$\mathcal{X}_\lambda(X, \alpha, \phi) \preceq \mathcal{X}_\lambda(Y, \alpha, \phi)$$

Let us show that condition (b) is satisfied, i.e., if

$$\hat{\lambda} \geq \tilde{\lambda},$$

then

$$\mathcal{X}_{\hat{\lambda}}(X, \alpha, \phi) \preceq \mathcal{X}_{\tilde{\lambda}}(X, \alpha, \phi).$$

with $\hat{\lambda}, \tilde{\lambda} \in [0, 1]$.

Assume that $\hat{\lambda} \geq \tilde{\lambda}$.

Then,

$$\begin{aligned} \mathcal{X}_{\hat{\lambda}}(X, \alpha, \phi) &\preceq AXA^* + \alpha Q \\ &\quad - \tilde{\lambda} \phi AXL^* (LXL^* + \alpha R)^{-1} LXA^* \\ &= \mathcal{X}_{\tilde{\lambda}}(X, \alpha, \phi). \end{aligned}$$

Let us show that condition (c) is satisfied.

Assume that $\beta > 1$.

Then,

$$\begin{aligned} \mathcal{X}_{\lambda}(\beta X, \alpha, \phi) &\preceq (1 - \lambda \phi) (\beta AXA^* + \beta \alpha Q) \\ &\quad + \lambda \phi \left(\beta AXA^* + \beta \alpha Q \right. \\ &\quad \left. - \beta AXL^* (L\beta XL^* + \beta \alpha R)^{-1} L\beta XA^* \right) \\ &= \beta \mathcal{X}_{\lambda}(X, \alpha, \phi), \end{aligned}$$

and thus, condition (c) is satisfied.

The proof of the lemma is complete.

The results presented in Lemma 6 and Lemma 7 are exploited in order to study the interval of probabilities in which

$$\lim_{k \rightarrow \infty} \mathbf{tr} \{Z_{i,n}(k)\} = +\infty,$$

and

$$\lim_{k \rightarrow \infty} \mathbf{tr} \{Z_{i,n}(k)\} < \infty,$$

for any initial condition \mathbf{Z}_0 in $\mathbb{H}^{Nn_x, +}$, for $n \in \mathbb{S}$, $i \in \{u, e\}$.

For $\tilde{\mathbf{Y}} = [\tilde{Y}_m]_{m=1}^N$ in $\mathbb{H}^{Nn_x, +}$, a TPM given by $\tilde{P} = [\tilde{p}_{mn}]_{m,n=1}^N$, and probabilities $\alpha_m > 0$, $m \in \mathbb{S}$, consider the following expression for $k \in \mathbb{N}$, $n \in \mathbb{S}$,

$$\tilde{Y}_n(k+1) = \sum_{m=1}^N \tilde{p}_{mn} \mathcal{X}_{\lambda}(\tilde{Y}_m(k), \alpha_m(k), \tilde{\gamma}_m), \quad (46)$$

with $\lambda \in [0, 1]$, given by $\lambda = \frac{\delta}{\sigma}$, $\sigma \in (0, 1]$ and $\delta \in [0, 1]$.

Assumption 5 Assume that for $\lambda = 1$, for any initial condition $\tilde{\mathbf{Y}}_0$ in $\mathbb{H}^{Nn_x,+}$, there exists a positive constant $U_{\tilde{\mathbf{Y}}_0}$ depending on the initial condition $\tilde{\mathbf{Y}}_0$, satisfying the following inequality,

$$U_{\tilde{\mathbf{Y}}_0} < \infty,$$

such that

$$\lim_{k \rightarrow \infty} \mathbf{tr} \left\{ \mathcal{X}_1 \left(\tilde{Y}_m(k), \alpha_m(k), \tilde{\gamma}_m \right) \right\} \leq U_{\tilde{\mathbf{Y}}_0},$$

for any $m \in \mathbb{S}$.

Lemma 6 Consider for $k \in \mathbb{N}$, $n \in \mathbb{S}$, the expression of $\tilde{Y}_n(k)$ in (46).

Under Assumption 1 and Assumption 5, there exists a limit probability $\delta_c \in [0, 1)$ such that

(i) there exists $\tilde{\mathbf{Y}}_0$ in $\mathbb{H}^{Nn_x,+}$, for

$$0 \leq \lambda \leq \frac{\delta_c}{\sigma},$$

such that

$$\lim_{k \rightarrow \infty} \mathbf{tr} \left\{ \tilde{Y}_n(k) \right\} = +\infty,$$

(ii) For any $\tilde{\mathbf{Y}}_0$ in $\mathbb{H}^{Nn_x,+}$, for

$$\frac{\delta_c}{\sigma} < \lambda \leq 1,$$

there exists $W_{\tilde{\mathbf{Y}}_0, \lambda}$, satisfying

$$0 < W_{\tilde{\mathbf{Y}}_0, \lambda} < \infty,$$

such that

$$\lim_{k \rightarrow \infty} \mathbf{tr} \left\{ \tilde{Y}_n(k) \right\} \leq W_{\tilde{\mathbf{Y}}_0, \lambda},$$

with $W_{\tilde{\mathbf{Y}}_0, \lambda}$ positive constant depending on $\tilde{\mathbf{Y}}_0$ and on λ .

Proof 42 (Proof of Lemma 6) Consider (46) for $\lambda = 0$, i.e., (46) becomes

$$\tilde{Y}_n(k+1) = \sum_{m=1}^I \tilde{p}_{mn} \mathcal{X}_0(\tilde{Y}_m(k), \alpha_m(k), \tilde{\gamma}_m), \quad (47)$$

with

$$\mathcal{X}_0(\tilde{Y}_m(k), \alpha_m(k), \tilde{\gamma}_m) = A\tilde{Y}_m(k)A^* + \alpha_m(k)Q$$

By Assumption 1, the matrix A is unstable, i.e., $\rho(A) > 1$.

Then, from (47), it follows that for some initial condition $\tilde{\mathbf{Y}}_0$ in $\mathbb{H}^{Nn_x,+}$,

$$\lim_{k \rightarrow \infty} \mathbf{tr} \{ \tilde{Y}_n(k) \} = +\infty,$$

for $n \in \mathbb{S}$, and condition (i) is satisfied.

When $\lambda = 1$, the expression of $\mathcal{X}_1(\tilde{Y}_m(k), \alpha_m(k), \tilde{\gamma}_m)$ becomes

$$\begin{aligned} \mathcal{X}_1(\tilde{Y}_m(k), \alpha_m(k), \tilde{\gamma}_m) &= A\tilde{Y}_m(k)A^* + \alpha_m(k)Q \\ &\quad - \tilde{\gamma}_m A\tilde{Y}_m(k)L^* \left(L\tilde{Y}_m(k)L^* + \alpha_m(k)R \right)^{-1} L\tilde{Y}_m(k)A^*. \end{aligned}$$

By Assumption 5, for any initial condition $\tilde{\mathbf{Y}}_0$ in $\mathbb{H}^{Nn_x,+}$, there exists a positive constant $U_{\tilde{\mathbf{Y}}_0}$ satisfying the inequalities,

$$0 < U_{\tilde{\mathbf{Y}}_0} < \infty,$$

such that

$$\lim_{k \rightarrow \infty} \mathbf{tr} \{ \mathcal{X}_1(\tilde{Y}_m(k), \alpha_m(k), \tilde{\gamma}_m) \} \leq U_{\tilde{\mathbf{Y}}_0},$$

for any $m \in \mathbb{S}$.

Consequently, for $\lambda = 1$ there exists a positive constant $W_{\tilde{\mathbf{Y}}_0}$ depending on the initial condition $\tilde{\mathbf{Y}}_0$, satisfying

$$U_{\tilde{\mathbf{Y}}_0} \leq W_{\tilde{\mathbf{Y}}_0} < \infty,$$

such that

$$\lim_{k \rightarrow \infty} \sum_{m=1}^N \tilde{p}_{mn} \mathbf{tr} \{ \mathcal{X}_1(\tilde{Y}_m(k), \alpha_m(k), \tilde{\gamma}_m) \} \leq W_{\tilde{\mathbf{Y}}_0},$$

and thus, from (46), condition (ii) is satisfied for $\lambda = 1$.

Fix a $0 < \tilde{\lambda} \leq 1$, such that for any initial condition $\tilde{\mathbf{Y}}_0 \in \mathbb{H}^{Nn_x,+}$ there exists $0 < U_{\tilde{\mathbf{Y}}_0, \tilde{\lambda}} < \infty$, for which

$$\lim_{k \rightarrow \infty} \mathbf{tr} \left\{ \mathcal{X}_{\tilde{\lambda}} \left(\tilde{Y}_m(k), \alpha_m(k), \tilde{\gamma}_m \right) \right\} \leq U_{\tilde{\mathbf{Y}}_0, \tilde{\lambda}} \quad (48)$$

(see [49, Theorem 2]), $m \in \mathbb{S}$.

Consequently, from (48), by applying (46), there exists a positive constant $W_{\tilde{\mathbf{Y}}_0, \tilde{\lambda}}$ depending on the initial condition $\tilde{\mathbf{Y}}_0$ and on $\tilde{\lambda}$, with

$$U_{\tilde{\mathbf{Y}}_0, \tilde{\lambda}} \leq W_{\tilde{\mathbf{Y}}_0, \tilde{\lambda}} < \infty,$$

such that

$$\lim_{k \rightarrow \infty} \sum_{m=1}^N \tilde{p}_{mn} \mathbf{tr} \left\{ \mathcal{X}_{\tilde{\lambda}} \left(\tilde{Y}_m(k), \alpha_m(k), \tilde{\gamma}_m \right) \right\} \leq W_{\tilde{\mathbf{Y}}_0, \tilde{\lambda}}.$$

Pick $\tilde{\delta}$ as follows,

$$\tilde{\delta} = \tilde{\lambda} \sigma.$$

Then, for

$$\hat{\delta} > \tilde{\delta},$$

there exists

$$\hat{\lambda} = \frac{\hat{\delta}}{\sigma} > \frac{\tilde{\delta}}{\sigma} = \tilde{\lambda},$$

and by Lemma 5 (b), for any initial condition $\tilde{\mathbf{Y}}_0$ in $\mathbb{H}^{Nn_x,+}$, there exists $W_{\tilde{\mathbf{Y}}_0, \hat{\delta}/\sigma}$, such that

$$\lim_{k \rightarrow \infty} \sum_{m=1}^N \tilde{p}_{mn} \mathbf{tr} \left\{ \mathcal{X}_{\hat{\delta}/\sigma} \left(\tilde{Y}_m(k), \alpha_m(k), \tilde{\gamma}_m \right) \right\} \leq W_{\tilde{\mathbf{Y}}_0, \hat{\delta}/\sigma},$$

and thus, condition (ii) is satisfied for $\hat{\lambda} = \frac{\hat{\delta}}{\sigma}$.

Define

$$\delta_c \triangleq \inf \left\{ \delta_* : \forall \delta > \delta_*, \forall \tilde{\mathbf{Y}}_0 \in \mathbb{H}^{Nn_x,+}, \exists 0 < W_{\tilde{\mathbf{Y}}_0, \delta/\sigma} < \infty, \right.$$

$$\left. \lim_{k \rightarrow \infty} \sum_{m=1}^N \tilde{p}_{mn} \mathbf{tr} \left\{ \mathcal{X}_{\delta/\sigma} \left(\tilde{Y}_m(k), \alpha_m(k), \tilde{\gamma}_m \right) \right\} \leq W_{\tilde{\mathbf{Y}}_0, \delta/\sigma} \right\}.$$

(see [49, Theorem 2]).

Consequently, condition (ii) is satisfied.

The proof of the lemma is complete.

Lemma 7 Consider for $k \in \mathbb{N}$, $n \in \mathbb{S}$, the expression of $\tilde{Y}_n(k)$ in (46).

Under Assumptions 1 and 5, there exists a limit probability $\delta_c \in [0, 1)$ such that, for any initial condition $\tilde{Y}_0 \in \mathbb{H}^{N_{n_x, +}}$, $n \in \mathbb{S}$,

$$(i) \text{ for } 0 \leq \lambda \leq \frac{\delta_c}{\sigma}: \lim_{k \rightarrow \infty} \mathbf{tr} \left\{ \tilde{Y}_n(k) \right\} = +\infty,$$

(ii) for $\frac{\delta_c}{\sigma} < \lambda \leq 1$, there exists a positive constant $W_{\tilde{Y}_0, \lambda}$ depending on \tilde{Y}_0 , λ , satisfying

$$0 < W_{\tilde{Y}_0, \lambda} < \infty,$$

such that

$$\lim_{k \rightarrow \infty} \mathbf{tr} \left\{ \tilde{Y}_n(k) \right\} \leq W_{\tilde{Y}_0, \lambda}.$$

Proof 43 (Proof of Lemma 7) From Assumption 1 and Assumption 5, by Lemma 6 (ii), condition (ii) in Lemma 7 follows.

Let us prove that Lemma 6 (i) implies condition (i) in Lemma 7.

Let \tilde{Y}'_0 in $\mathbb{H}^{N_{n_x, +}}$ be one initial condition for which the sequence $\tilde{Y}'_m(k)$ is such that

$$\lim_{k \rightarrow \infty} \mathbf{tr} \left\{ \tilde{Y}'_n(k) \right\} = +\infty$$

according to Lemma 6 (i), for $m, n \in \mathbb{S}$.

Also let $\tilde{Y}_m(k)$, $m \in \mathbb{S}$, $k \in \mathbb{N}$, be the sequence with some arbitrary initial condition \tilde{Y}_0 in $\mathbb{H}^{N_{n_x, +}}$.

Notice that if $\tilde{Y}_m(0) = \mathbb{O}_{n_x}$, then $\tilde{Y}_m(1) \succ 0$, $m \in \mathbb{S}$, since $Q \succ 0$.

Thus, it is possible to find a large enough positive constant $\beta > 1$, such that the following inequality holds,

$$\beta \tilde{Y}_m(1) \succeq \tilde{Y}'_m(1), \tag{49}$$

for any $m \in \mathbb{S}$.

Claim 1 There exists a positive constant $\beta > 1$, such that

$$\beta \tilde{Y}_m(k) \succeq \tilde{Y}'_m(k),$$

for any $m \in \mathbb{S}$, for all $k \geq 1$.

Proof 44 (Proof of Claim 1) Assume that at time $\bar{k} \in \mathbb{N}$,

$$\beta \tilde{Y}_m(\bar{k}) \succeq \tilde{Y}'_m(\bar{k}),$$

$m \in \mathbb{S}$.

Let us write the expression of

$$\beta \tilde{Y}_n(\bar{k} + 1),$$

for $n \in \mathbb{S}$.

By the linearity of the sum and by the properties (c) and (a) in Lemma 5, we obtain

$$\begin{aligned} \beta \tilde{Y}_n(\bar{k} + 1) &\succeq \sum_{m=1}^N \tilde{p}_{mn} \mathcal{X}_\lambda(\tilde{Y}'_m(\bar{k}), \alpha_m(\bar{k}), \tilde{\gamma}_m) \\ &= \tilde{Y}'_n(\bar{k} + 1), \end{aligned}$$

and thus, the following inequality is obtained,

$$\beta \tilde{Y}_n(k) \succeq \tilde{Y}'_n(k),$$

for any $k \geq 1$, $n \in \mathbb{S}$.

From (49), by applying Claim 1, it follows that

$$\lim_{k \rightarrow \infty} \mathbf{tr}\{\tilde{Y}_m(k)\} \geq \frac{1}{\beta} \lim_{k \rightarrow \infty} \mathbf{tr}\{\tilde{Y}'_m(k)\},$$

$n \in \mathbb{S}$ implying condition (i).

The proof of the lemma is complete.

Proof 45 (Proof of Theorem 6) Let us show the sufficiency part. Consider for $n \in \mathbb{S}$, $i \in \{u, e\}$, $k \in \mathbb{N}$, the following equality,

$$Z_{i,n}(k+1) = \sum_{m=1}^N p_{i,mn} \mathcal{X}_\lambda(Z_{i,m}(k), \pi_{i,m}(k), \hat{\gamma}_{i,m}).$$

Under Assumption 2, if

$$\lim_{k \rightarrow \infty} \mathbf{tr}\{\mathbb{E}[\tilde{e}_e(k)\tilde{e}_e^*(k)]\} = +\infty,$$

the secrecy mechanism designer can choose

$$\lambda = 1.$$

Otherwise, since Assumptions [1](#)-[2](#) hold, by Lemma [7](#) (in Appendix B) for any $\mathbf{Z}_0 \in \mathbb{H}^{Nn_x,+}$, $m, n \in \mathbb{S}$, $i \in \{u, e\}$,

$$\lim_{k \rightarrow \infty} \text{tr} \{Z_{i,n}(k)\} = +\infty, \quad \text{for } 0 \leq \lambda \leq \frac{\zeta_c}{\psi_i}, \quad (50)$$

$$\lim_{k \rightarrow \infty} \text{tr} \{Z_{i,n}(k)\} < \infty, \quad \text{for } \frac{\zeta_c}{\psi_i} < \lambda \leq 1. \quad (51)$$

This implies that the probability λ in the secrecy mechanism should be designed such that the following inequality holds,

$$\lambda > \frac{\zeta_c}{\psi_u},$$

in order to guarantee [\(51\)](#) for the user MSE.

Since the user MSE is bounded by assumption when $\lambda = 1$, the following inequality is satisfied,

$$\psi_u \times 1 > \zeta_c,$$

and thus, $\psi_u > \zeta_c$, implying $\zeta_c/\psi_u < 1$.

Consider now the eavesdropper MSE. The secrecy parameter λ should be chosen sufficiently small, such that, the inequality

$$\lambda \leq \frac{\zeta_c}{\psi_e},$$

is satisfied.

Therefore, by choosing λ satisfying the following inequalities,

$$\frac{\zeta_c}{\psi_u} < \lambda \leq \min \left\{ \frac{\zeta_c}{\psi_e}, 1 \right\},$$

the secrecy mechanism guarantees optimal mean square expected secrecy over FSMCs by Lemma [7](#).

Notice that the interval $(\zeta_c/\psi_u, \min \{\zeta_c/\psi_e, 1\}]$ is nonempty: $\zeta_c/\psi_u < 1$, and $\psi_u > \psi_e$ implies that $\zeta_c/\psi_u < \zeta_c/\psi_e$.

Let us show the necessity part. If the optimal mean square expected secrecy over FSMCs is achieved by the secrecy mechanism in [\(3.2\)](#), by Lemma [7](#), the following inequalities are satisfied,

$$\begin{aligned} \frac{\zeta_c}{\psi_u} < \lambda \leq 1, \\ \lambda \leq \frac{\zeta_c}{\psi_e}, \end{aligned}$$

implying

$$\frac{\zeta_c}{\psi_u} < \lambda \leq \frac{\zeta_c}{\psi_e}.$$

Consequently, $\lambda\psi_e < \lambda\psi_u$, and finally $\psi_e < \psi_u$.

The proof of the theorem is complete.

Eavesdropper characterization

The following result will be exploited in the proof of Proposition 9, used for the eavesdropper characterization.

Let us recall, for $\mathbf{V} = [V_m]_{m=1}^N$ in $\mathbb{H}^{Nn_x,*}$, for $n \in \mathbb{S}$, the definition of $\mathcal{S}_{e,n}(\mathbf{V})$ (defined in Chapter 3),

$$\mathcal{S}_{e,n}(\mathbf{V}) \triangleq \sum_{m=1}^N p_{e,mn} (1 - \lambda\hat{\gamma}_{e,m}) AV_m A^* + \pi_{e,n}^\infty Q.$$

Let us also recall the definition of \mathcal{A}_e provided in Chapter 3 and defined as follows,

$$\mathcal{A}_e \triangleq [P'_e \otimes \mathbb{I}_{n_x^2}] \left[\bigoplus_{m=1}^N (1 - \lambda\hat{\gamma}_{e,m}) (\bar{A} \otimes A) \right].$$

Proposition 12 There exists $\mathbf{S}_e = [S_{e,n}]_{n=1}^N$ in $\mathbb{H}^{Nn_x,+}$, satisfying

$$S_{e,n} = \mathcal{S}_{e,n}(\mathbf{S}_e),$$

if and only if

$$\rho(\mathcal{A}_e) < 1.$$

Proof 46 (Proof of Proposition 12) By applying the vectorization to the equation $S_{e,n} = \mathcal{S}_{e,n}(\mathbf{S}_e)$, for $\mathbf{S}_e = [S_{e,n}]_{n=1}^N$ in $\mathbb{H}^{Nn_x,+}$, exploiting the properties of the Kronecker product (see for instance 187), the following equality can be easily obtained,

$$\text{vec}^2(\mathbf{S}_e) = \mathcal{A}_e \text{vec}^2(\mathbf{S}_e) + \text{vec}^2(\boldsymbol{\pi}_e^\infty \otimes Q), \quad (52)$$

with $\boldsymbol{\pi}_e^\infty = [\pi_{e,m}^\infty]_{m=1}^N$.

By 4, Proposition 3.36, Proposition 3.38], (52) has a unique solution \mathbf{S}_e in $\mathbb{H}^{Nn_x,+}$, if and only if

$$\rho(\mathcal{A}_e) < 1.$$

The proof of the proposition is complete.

Proof 47 (Proof of Proposition [9](#)) Consider for $k \in \mathbb{N}$, $n \in \mathbb{S}$, the equation

$$S_{e,n}(k+1) = \mathcal{S}_{e,n}(\mathbf{S}_e(k)),$$

$\mathbf{S}_e = [S_{e,n}]_{n=1}^N$ in $\mathbb{H}^{Nn_x,+}$.

Notice that $S_{e,n}(k)$, $k \in \mathbb{N}$, $n \in \mathbb{S}$, is a monotonically increasing sequence, since $Q \succ 0$.

Recall that $Z_{e,n}(0) \succeq 0$ for any $n \in \mathbb{S}$. Clearly,

$$\mathbb{O}_{n_x} = S_{e,n}(0) \preceq Z_{e,n}(0).$$

Moreover,

$$S_{e,n}(k) \preceq Z_{e,n}(k)$$

implies

$$S_{e,n}(k+1) = \mathcal{S}_{e,n}(\mathbf{S}_e(k)) \preceq Z_{e,n}(k+1).$$

By induction arguments,

$$S_{e,n}(k) \preceq Z_{e,n}(k),$$

for any $k \geq 0$.

If

$$\rho(\mathcal{A}_e) < 1,$$

by Proposition [12](#)

$$\lim_{k \rightarrow \infty} \mathbf{tr} \{Z_{e,n}(k)\} \geq \mathbf{tr} \{S_{e,n}\},$$

with

$$S_{e,n} = \mathcal{S}_{e,n}(\mathbf{S}_e),$$

\mathbf{S}_e in $\mathbb{H}^{Nn_x,+}$.

If $\rho(\mathcal{A}_e) \geq 1$, the sequence $S_{e,n}(k)$, $k \in \mathbb{N}$, $n \in \mathbb{S}$, does not converge.

Since $S_{e,n}(k)$, $k \in \mathbb{N}$, $n \in \mathbb{S}$, is a monotonically increasing sequence, the following equality holds,

$$\lim_{k \rightarrow \infty} \mathbf{tr} \{S_{e,n}(k)\} = +\infty,$$

implying that

$$\lim_{k \rightarrow \infty} \mathbf{tr} \{Z_{e,n}(k)\} = +\infty,$$

$n \in \mathbb{S}$.

The proof of the proposition is complete.

Appendix C

Proof of Theorem 7.

Some technical definitions and lemmas, that are useful in the proof of Theorem 7 are reported in the following.

Let us define the function

$$\mathcal{V} : \mathbb{N} \times \mathbb{R}^n \times \mathcal{S} \rightarrow \mathbb{R}^+,$$

for $k \in \mathbb{N}$, $\xi \in \mathbb{R}^n$, $i \in \mathcal{S}$ as

$$\mathcal{V}(k, \xi, i) \triangleq \sum_{q \in \mathcal{Q}_k(i)} \mathbf{p}_k^q(i) \|\Phi(k, \xi, i, \mathbf{r}_k^q(i), 0)\|^2. \quad (53)$$

Remark 46 Notice that, for any $i \in \mathcal{S}$, for $k = 0, 1$, the index q belongs to the singleton set $\mathcal{Q}_k(i) = \{1\}$. Indeed, $\mathbf{r}_0^1(i) = \{i\}$ (recall the definition of admissible switching paths (4.2)), as well as $\mathbf{r}_1^1(i) = \{i\}$.

Consider the time instant $k = 0$, any Markov mode $i \in \mathcal{S}$, any initial condition $\xi \in \mathbb{R}^n$: $\mathbf{r}_0^1(i)$ is the admissible switching path containing only the initial mode of the Markov mode $i \in \mathcal{S}$ and that corresponds to the index q in $\mathcal{Q}_0(i) = \{1\}$. The corresponding solution at time $k = 0$, denoted by $\Phi(0, \xi, i, \mathbf{r}_0^1(i), 0)$, is given by ξ , since the initial condition $\xi \in \mathbb{R}^n$ is given. The initial mode of the Markov chain, denoted by $i \in \mathcal{S}$, is also given. Thus, the probability of occurrence for the switching path $\mathbf{r}_0^1(i)$, denoted by $\mathbf{p}_0^1(i)$, is equal to one.

Consider now the time instant $k = 1$, any Markov mode $i \in \mathcal{S}$, any initial condition $\xi \in \mathbb{R}^n$: $\mathbf{r}_1^1(i)$ is the admissible switching path that contains only the mode $i \in \mathcal{S}$, and that corresponds to the index q in $\mathcal{Q}_1(i) = \{1\}$.

The corresponding solution at time $k = 1$, denoted by

$$\Phi(1, \xi, i, \mathbf{r}_1^1(i), 0),$$

is given by $f_i(\xi, 0)$. Since the initial Markov mode $i \in \mathcal{S}$ is given, the probability of occurrence of the switching path $\mathbf{r}_1^1(i)$, denoted by $\mathbf{p}_1^1(i)$, is equal to one again.

Thus, by evaluating (53) in $k = 0$ and in $k = 1$,

$$\mathcal{V}(0, \xi, i) = \|\xi\|^2, \quad (54a)$$

$$\mathcal{V}(1, \xi, i) = \|f_i(\xi, 0)\|^2, \quad (54b)$$

for any $\xi \in \mathbb{R}^n$, $i \in \mathcal{S}$.

Lemma 8 Assume that (4.3), with $u(\cdot) \equiv 0$, is EMSS.

Let θ, ζ be the positive reals in (4.5).

Then, for any $\xi \in \mathbb{R}^n$, $i \in \mathcal{S}$, the following inequality holds,

$$\mathcal{V}(k, \xi, i) \leq \theta \zeta^k \|\xi\|^2, \quad \forall k \in \mathbb{N}. \quad (55)$$

Proof 48 (Proof of Lemma 8) From Remark 33, by applying (4.4) for $u(\cdot) \equiv 0$, and (53), the following equality holds:

$$\mathcal{V}(k, \xi, i) = \mathbb{E} \left[\|x(k, \xi, i, 0)\|^2 \right]. \quad (56)$$

Since (4.3) is EMSS, by Definition 14, (55) follows from (56).

Lemma 9 Consider the system described by (4.3), with $u(\cdot) \equiv 0$, and consider the function \mathcal{V} , defined by (53).

Then, for any $\xi \in \mathbb{R}^n$, $i \in \mathcal{S}$, the following equality holds

$$\sum_{j \in \mathcal{S}_i^{\text{out}}} p_{ij} \mathcal{V}(k, f_i(\xi, 0), j) = \mathcal{V}(k+1, \xi, i), \quad \forall k \in \mathbb{N}. \quad (57)$$

Proof 49 (Proof of Lemma 9) Let, for $i \in \mathcal{S}$, $\bar{f}_i : \mathbb{R}^n \rightarrow \mathbb{R}^n$ be the function defined for $x \in \mathbb{R}^n$, as $\bar{f}_i(x) = f_i(x, 0)$.

In order to show that equality (57) holds for any $k \in \mathbb{N}$, the proof will treat the following cases separately:

- $k = 0$,
- $k = 1$,
- $k = 2$,

- $k \geq 3$.

From (4.2), for $k = 0$ we have

$$\mathbf{r}_0(i) = \mathbf{r}_1(i) = \{i\}.$$

with $i \in \mathcal{S}$.

For $k = 2$ we have

$$\mathbf{r}_2(i) = \{i, j_1\},$$

with $i \in \mathcal{S}$, $j_1 \in \mathcal{S}_i^{\text{out}}$.

The values of the time index k , given by $k = 0, 1, 2$, are treated as particular cases in order to write equations that are well posed according to the definition of the admissible switching paths (recall (4.2)).

Consider the left-hand side of (57) for $k = 0$.

From (53), by applying (54a), with $\bar{f}_i(\xi) \in \mathbb{R}^n$ as second argument of \mathcal{V} , $j \in \mathcal{S}$ as third argument of \mathcal{V} , recalling (4.1) and (54b), we get the following equalities

$$\sum_{j \in \mathcal{S}_i^{\text{out}}} p_{ij} \mathcal{V}(0, \bar{f}_i(\xi), j) = \sum_{j \in \mathcal{S}_i^{\text{out}}} p_{ij} \|\bar{f}_i(\xi)\|^2 = \mathcal{V}(1, \xi, i),$$

i.e., (57) is satisfied for $k = 0$.

Consider the left-hand side of (57) for $k = 1$.

From (53), by applying (54b), with $\bar{f}_i(\xi) \in \mathbb{R}^n$ as second argument of \mathcal{V} , $j \in \mathcal{S}$ as third argument of \mathcal{V} , we obtain:

$$\sum_{j \in \mathcal{S}_i^{\text{out}}} p_{ij} \mathcal{V}(1, \bar{f}_i(\xi), j) = \sum_{j \in \mathcal{S}_i^{\text{out}}} p_{ij} \|\bar{f}_j(\bar{f}_i(\xi))\|^2.$$

For any $i \in \mathcal{S}$, the switching path $\{i, j\}$, $j \in \mathcal{S}_i^{\text{out}}$, is a switching path of length 2 emanating from the mode $i \in \mathcal{S}$.

Indeed, the probability p_{ij} of the transition $(i, j) \in \mathcal{E}$, corresponds to the probability of a path of length 2, emanating from the mode $i \in \mathcal{S}$, that is $\mathbf{p}_2^q(i)$.

Any mode $j \in \mathcal{S}_i^{\text{out}}$ can be associated with an index $q \in \mathcal{Q}_2(i)$, obtaining the following equalities:

$$\begin{aligned} \sum_{j \in \mathcal{S}_i^{\text{out}}} p_{ij} \|\bar{f}_j(\bar{f}_i(\xi))\|^2 &= \sum_{q \in \mathcal{Q}_2(i)} \mathbf{p}_2^q(i) \|\Phi(2, \xi, i, \mathbf{r}_2^q(i), 0)\|^2 \\ &= \mathcal{V}(2, \xi, i), \end{aligned}$$

so, (57) is satisfied for $k = 1$.

Consider the left-hand side of (57) for $k = 2$.

By applying (53), we obtain

$$\sum_{j \in \mathcal{S}_i^{\text{out}}} p_{ij} \mathcal{V}(2, \bar{f}_i(\xi), j) = \sum_{j \in \mathcal{S}_i^{\text{out}}} p_{ij} \sum_{q \in \mathcal{Q}_2(j)} \mathbf{p}_2^q(j) \left\| \Phi(2, \bar{f}_i(\xi), j, \mathbf{r}_2^q(j), 0) \right\|^2. \quad (58)$$

For any $j \in \mathcal{S}$, $\mathbf{r}_2^q(j)$, $q \in \mathcal{Q}_2(j)$, is a switching path such as $\mathbf{r}_2^q(j) = \{j, j_1\}$, $j_1 \in \mathcal{S}_j^{\text{out}}$, where any mode $j_1 \in \mathcal{S}_j^{\text{out}}$ is associated with an index $q \in \mathcal{Q}_2(j)$. From (58), we get

$$\begin{aligned} \sum_{j \in \mathcal{S}_i^{\text{out}}} p_{ij} \mathcal{V}(2, \bar{f}_i(\xi), j) &= \sum_{j \in \mathcal{S}_i^{\text{out}}} p_{ij} \sum_{j_1 \in \mathcal{S}_j^{\text{out}}} p_{jj_1} \left\| \bar{f}_{j_1} \circ \bar{f}_j \circ \bar{f}_i(\xi) \right\|^2 \\ &= \sum_{j \in \mathcal{S}_i^{\text{out}}} \sum_{j_1 \in \mathcal{S}_j^{\text{out}}} p_{ij} p_{jj_1} \left\| \bar{f}_{j_1} \circ \bar{f}_j \circ \bar{f}_i(\xi) \right\|^2. \end{aligned} \quad (59)$$

By associating with each path of length 3 emanating from the mode $i \in \mathcal{S}$, $\{i, j, j_1\}$, $j \in \mathcal{S}_i^{\text{out}}$, $j_1 \in \mathcal{S}_j^{\text{out}}$, an index $q \in \mathcal{Q}_3(i)$, recalling the definition of $\mathbf{p}_3^q(i)$, from (59), the following equalities hold:

$$\sum_{j \in \mathcal{S}_i^{\text{out}}} p_{ij} \mathcal{V}(2, \bar{f}_i(\xi), j) = \sum_{q \in \mathcal{Q}_3(i)} \mathbf{p}_3^q(i) \left\| \Phi(3, \xi, i, \mathbf{r}_3^q(i), 0) \right\|^2 = \mathcal{V}(3, \xi, i), \quad (60)$$

i.e., (57) is satisfied for $k = 2$.

Consider the left-hand side of (57) for $k \geq 3$.

From (53), we obtain

$$\sum_{j \in \mathcal{S}_i^{\text{out}}} p_{ij} \mathcal{V}(k, \bar{f}_i(\xi), j) = \sum_{j \in \mathcal{S}_i^{\text{out}}} p_{ij} \sum_{q \in \mathcal{Q}_k(j)} \mathbf{p}_k^q(j) \left\| \Phi(k, \bar{f}_i(\xi), j, \mathbf{r}_k^q(j), 0) \right\|^2. \quad (61)$$

From (4.2), it follows that $\mathbf{r}_k^q(j)$, $q \in \mathcal{Q}_k(j)$, $k \geq 3$, is a switching path such as

$$\begin{aligned} \mathbf{r}_k^q(j) &= \{j, j_1, \dots, j_{k-1}\}, \\ j_1 \in \mathcal{S}_j^{\text{out}}, j_{h+1} \in \mathcal{S}_{j_h}^{\text{out}}, h &= 1, \dots, k-2. \end{aligned} \quad (62)$$

For any mode $j \in \mathcal{S}$, each admissible switching path of length k emanating from j , given by $\{j, j_1, \dots, j_{k-1}\}$ (see (62)), is associated with an index $q \in \mathcal{Q}_k(j)$.

Recalling the definition of $\mathbf{p}_k^q(j)$, $q \in \mathcal{Q}_k(j)$, $j \in \mathcal{S}$, applying the Markov property, from (61), the following equalities hold:

$$\begin{aligned}
\sum_{j \in \mathcal{S}_i^{\text{out}}} p_{ij} \mathcal{V}(k, \bar{f}_i(\xi), j) &= \sum_{j \in \mathcal{S}_i^{\text{out}}} p_{ij} \sum_{j_1 \in \mathcal{S}_j^{\text{out}}} \cdots \sum_{j_{k-1} \in \mathcal{S}_{j_{k-2}}^{\text{out}}} p_{jj_1} \cdots p_{j_{k-2}j_{k-1}} \\
&\times \left\| \bar{f}_{j_{k-1}} \circ \cdots \circ \bar{f}_{j_1} \circ \bar{f}_j \circ \bar{f}_i(\xi) \right\|^2 \\
&= \sum_{j \in \mathcal{S}_i^{\text{out}}} \sum_{j_1 \in \mathcal{S}_j^{\text{out}}} \cdots \sum_{j_{k-1} \in \mathcal{S}_{j_{k-2}}^{\text{out}}} p_{ij} p_{jj_1} \cdots p_{j_{k-2}j_{k-1}} \times \\
&\times \left\| \bar{f}_{j_{k-1}} \circ \cdots \circ \bar{f}_{j_1} \circ \bar{f}_j \circ \bar{f}_i(\xi) \right\|^2. \tag{63}
\end{aligned}$$

Notice that for any $j \in \mathcal{S}_i^{\text{out}}$ the path $\{i, j, j_1, \dots, j_{k-1}\}$ is an admissible switching path of length $k + 1$ starting from the mode $i \in \mathcal{S}$.

Thus, we are able to associate with each switching path

$$\{i, j, j_1, \dots, j_{k-1}\},$$

with $j \in \mathcal{S}_i^{\text{out}}$, $j_1 \in \mathcal{S}_j^{\text{out}}$, $j_{h+1} \in \mathcal{S}_{j_h}^{\text{out}}$, $h = 1, \dots, k - 2$, an index \bar{q} belonging to the set $\mathcal{Q}_{k+1}(i)$.

By applying the definition of $\mathbf{p}_{k+1}^{\bar{q}}(i)$, $\bar{q} \in \mathcal{Q}_{k+1}(i)$, from (63), we obtain the following equalities, for all $k \geq 3$:

$$\sum_{j \in \mathcal{S}_i^{\text{out}}} p_{ij} \mathcal{V}(k, \bar{f}_i(\xi), j) = \sum_{\bar{q} \in \mathcal{Q}_{k+1}(i)} \mathbf{p}_{k+1}^{\bar{q}}(i) \times \left\| \Phi(k + 1, \xi, i, \mathbf{r}_{k+1}^{\bar{q}}(i), 0) \right\|^2 = \mathcal{V}(k + 1, \xi, i).$$

The proof of the lemma is complete.

Proof 50 (Proof of Theorem 7) See [3, Theorem 20 (b)] for the proof of the sufficiency part of the theorem.

As far as the proof of the necessity part is concerned, assume that the system described by (4.3), with $u(\cdot) \equiv 0$, is EMSS.

Pick an arbitrary $\xi \in \mathbb{R}^n$, and an arbitrary $i \in \mathcal{S}$.

Consider the function

$$V(\xi, i) = \sum_{k=0}^{\infty} \mathcal{V}(k, \xi, i), \tag{64}$$

with \mathcal{V} defined in (53).

Notice that the sum is convergent by Lemma 8.

Since

$$\mathcal{V}(k, \xi, i) \geq 0,$$

for any $k \in \mathbb{N}$, and

$$\mathcal{V}(0, \xi, i) = \|\xi\|^2,$$

the following inequality holds,

$$\|\xi\|^2 \leq V(\xi, i).$$

Since system (4.3) is EMSS by assumption, by Lemma 8, for all initial conditions $\xi \in \mathbb{R}^n$, and for all $i \in \mathcal{S}$, we obtain:

$$V(\xi, i) \leq \sum_{k=0}^{\infty} \theta \zeta^k \|\xi\|^2 = \frac{\theta}{1-\zeta} \|\xi\|^2,$$

where θ and ζ are the positive reals in (4.5).

Thus, condition (b₁) of the theorem holds, with

$$\alpha_1 = 1, \quad \alpha_2 = \frac{\theta}{1-\zeta}.$$

It follows that, for any $h \in \mathcal{S}$, $V(\cdot, h)$ is locally bounded and continuous at $\xi = 0$.

By recalling that $p_{ij} = 0$ for all $j \notin \mathcal{S}_i^{\text{out}}$, the following equality is satisfied:

$$\sum_{j \in \mathcal{S}} p_{ij} V(f_i(\xi, 0), j) = \sum_{j \in \mathcal{S}_i^{\text{out}}} p_{ij} V(f_i(\xi, 0), j). \quad (65)$$

From (65) and (64), by applying Lemma 9, the following equalities hold

$$\begin{aligned} \sum_{j \in \mathcal{S}} p_{ij} V(f_i(\xi, 0), j) &= \sum_{j \in \mathcal{S}_i^{\text{out}}} p_{ij} \sum_{k=0}^{\infty} \mathcal{V}(k, f_i(\xi, 0), j) \\ &= \sum_{k=0}^{\infty} \sum_{j \in \mathcal{S}_i^{\text{out}}} p_{ij} \mathcal{V}(k, f_i(\xi, 0), j) \\ &= \sum_{k=0}^{\infty} \mathcal{V}(k+1, \xi, i). \end{aligned} \quad (66)$$

From (66), by changing the index in the last sum, we obtain:

$$\sum_{j \in \mathcal{S}} p_{ij} V(f_i(\xi, 0), j) = \sum_{k=1}^{\infty} \mathcal{V}(k, \xi, i). \quad (67)$$

By adding and subtracting the quantity $\mathcal{V}(0, \xi, i)$ to the right-hand side of (67), and by recalling (54a), for any $\xi \in \mathbb{R}^n$, the following equality is satisfied,

$$\sum_{j \in \mathcal{S}} p_{ij} V(f_i(\xi, 0), j) = V(\xi, i) - \|\xi\|^2,$$

and, finally, the inequality

$$\mathcal{L}V(\xi, 0, i) \leq -\|\xi\|^2$$

is obtained.

Thus, condition (b₂) of the theorem is satisfied with $\alpha_3 = 1$.

The proof of the theorem is complete.

Remark 47 Notice that the methodology proposed in the proof of Theorem 7 involves the expected values (see equation (56)) and also the transition probabilities of the switching rule. Indeed, this procedure accounts for admissible transitions (see the definition of $\mathcal{S}_i^{\text{out}}$, for $i \in \mathcal{S}$) and for the probabilities of occurrence of the admissible switching paths, as the reader can easily see from equations (53)-(67). The aforementioned equations are completely different from the ones in the procedure adopted in the proof of global (exponential) asymptotic stability for the deterministic discrete-time switching and non switching case. This work makes use of a deep re-elaboration of the procedures in the deterministic case, where the transition probabilities are not considered at all (see [133], [225], Section 4.3.4. Proof of Theorem 1: the necessity] and [136], Proof of Theorem 1: the necessity]).

Proof of Theorem 8.

In the following, the reader will find some technical definitions and lemmas, that are useful in the proof of Theorem 8.

Let us define as in [136] the set \mathcal{M}_B as follows,

$$\mathcal{M}_B \triangleq \{v : \mathbb{N} \rightarrow B_1^m\}.$$

Consider the following discrete-time Markovian switching system defined on the stochastic basis $(\Omega, \mathcal{F}, \{\mathcal{F}_k\}, \mathbb{P})$ as

$$x^R(k+1) = f_{r(k)}(x^R(k), \rho(\mathbb{E}[\|x^R(k)\|^2]) \delta(k)), k \in \mathbb{N}, \quad (68)$$

where ρ is a globally Lipschitz function of class \mathcal{K}_∞ , $\delta \in \mathcal{M}_B$ is the input signal; $x^R(k) \triangleq x^R(k, \xi, i, \delta)$ is the random variable that evolves according to (68), with initial conditions $\xi \in \mathbb{R}^n$, $i \in \mathcal{S}$, input signal $\delta \in \mathcal{M}_B$. The variable $\Phi^R(k, \xi, i, \mathbf{r}_k^q(i), \delta)$ denotes the solution of (68), at time $k \in \mathbb{N}$, corresponding to initial conditions $\xi \in \mathbb{R}^n$, $i \in \mathcal{S}$, switching path $\mathbf{r}_k^q(i) \in \mathcal{R}_k(i)$, $q \in \mathcal{Q}_k(i)$, input signal $\delta \in \mathcal{M}_B$.

Remark 48 Notice that for any $\xi \in \mathbb{R}^n$, $i \in \mathcal{S}$, $\delta \in \mathcal{M}_B$, the argument of the function ρ , that is $\mathbb{E} \left[\left\| x^R(k) \right\|^2 \right]$, is given by

$$\mathbb{E} \left[\left\| x^R(k, \xi, i, \delta) \right\|^2 \right] = \sum_{q \in \mathcal{Q}_k(i)} \mathbf{p}_k^q(i) \left\| \Phi^R(k, \xi, i, \mathbf{r}_k^q(i), \delta) \right\|^2, \quad (69)$$

for any $k \in \mathbb{N}$.

Indeed, the argument of $\rho(\cdot)$ does not depend on the current value of the Markov mode $r(k)$, but it is computed by considering the probabilities of all admissible switching paths of length k , starting from the mode $i \in \mathcal{S}$ of the Markov chain.

Definition 19 The system described by (4.3) is said to be robustly exponentially mean square stable (REMSS) if there exist a globally Lipschitz function ρ of class \mathcal{K}_∞ , positive real numbers $\mu \geq 1$, and $0 < \omega < 1$, such that for any $\xi \in \mathbb{R}^n$, $i \in \mathcal{S}$, $\delta \in \mathcal{M}_B$, the random variable $x^R(k)$, that evolves according to discrete-time Markovian switching system (68) satisfies the following inequality, for any $k \in \mathbb{N}$:

$$\mathbb{E} \left[\left\| x^R(k, \xi, i, \delta) \right\|^2 \right] \leq \mu \omega^k \|\xi\|^2. \quad (70)$$

Remark 49 The following lemma plays a key role in the proof of the implication EMS-ISS \implies REMSS. This is a difference with respect to the procedure in the deterministic switching framework (see [136]). Specifically, two main challenges arise with respect to [136].

Firstly, in [136] the expected value is not considered.

Secondly, in [136] the robust characterization is not an exponential characterization, and thus, the proof of the implication ISS \implies robust stability does not take into account the exponential decrease rate.

Lemma 10 Let θ, ζ, γ , be positive reals such that:

$$\theta \geq 1, \quad 0 < \zeta < 1, \quad \gamma > 1, \quad \frac{\gamma^\theta}{\gamma^\theta - 1} < \gamma. \quad (71)$$

Let a function $g : \mathbb{N} \rightarrow \mathbb{R}^+$ satisfy the following inequality

$$\Sigma : g(k) \leq \theta \zeta^{k-k_0} g(k_0) + \frac{1}{\gamma \theta} \sup_{t=k_0, k_0+1, \dots, k} g(t), \quad (72)$$

for all $k \geq k_0 \geq 0$.

Then, there exist positive reals μ and ω , with $\mu \geq 1$ and $0 < \omega < 1$, such that the following inequality is satisfied, for all $k \in \mathbb{N}$,

$$g(k) \leq \mu \omega^k g(0). \quad (73)$$

Proof 51 (Proof of Lemma 10) From (72), taking $k_0 = 0$, the following inequality holds,

$$\sup_{t=0,1,\dots,k} g(t) \leq \theta g(0) + \frac{1}{\gamma \theta} \sup_{t=0,1,\dots,k} g(t),$$

which implies the following inequalities

$$\begin{aligned} \left(1 - \frac{1}{\gamma \theta}\right) \sup_{t=0,1,\dots,k} g(t) &\leq \theta g(0), \\ g(k) &\leq \frac{\gamma \theta}{\gamma \theta - 1} \theta g(0), \quad \forall k \geq 0. \end{aligned} \quad (74)$$

Taking (71) into account, let $r > 1$ be a real such that

$$\frac{1}{r} + \frac{1}{\gamma} \frac{\gamma \theta}{\gamma \theta - 1} < 1.$$

We choose a positive integer \bar{k} such that

$$\zeta^{\bar{k}} < \frac{1}{r \theta}. \quad (75)$$

From (72) with $k_0 = 0$ and $k = \bar{k}$, we obtain

$$g(\bar{k}) \leq \theta \zeta^{\bar{k}} g(0) + \frac{1}{\gamma \theta} \sup_{t=0,1,\dots,\bar{k}} g(t). \quad (76)$$

From (76), by applying (75) and (74) it follows that

$$g(\bar{k}) \leq \left(\frac{1}{r} + \frac{1}{\gamma} \frac{\gamma \theta}{\gamma \theta - 1}\right) g(0). \quad (77)$$

Consider (72), choose $k_0 = \bar{k}$, and consider the interval $[\bar{k}, 2\bar{k}]$.

The following inequality holds

$$g(k) \leq \theta \zeta^{k-\bar{k}} g(\bar{k}) + \frac{1}{\gamma \theta} \sup_{t=\bar{k}, \bar{k}+1, \dots, k} g(t), \quad \forall k \in [\bar{k}, 2\bar{k}],$$

which implies:

$$\sup_{t=\bar{k}, \bar{k}+1, \dots, k} g(t) \leq \theta g(\bar{k}) + \frac{1}{\gamma \theta} \sup_{t=\bar{k}, \bar{k}+1, \dots, k} g(t), \quad k \in [\bar{k}, 2\bar{k}]. \quad (78)$$

From (78), we obtain the following inequality:

$$\left(1 - \frac{1}{\gamma \theta}\right) \sup_{t=\bar{k}, \bar{k}+1, \dots, k} g(t) \leq \theta g(\bar{k}), \quad \forall k \in [\bar{k}, 2\bar{k}]. \quad (79)$$

From (79), by applying (77), it follows that:

$$g(k) \leq \frac{\gamma \theta}{\gamma \theta - 1} \theta \left(\frac{1}{r} + \frac{1}{\gamma} \frac{\gamma \theta}{\gamma \theta - 1}\right) g(0), \quad \forall k \in [\bar{k}, 2\bar{k}].$$

Let us prove now that the following inequalities hold for any integer $l \geq 0$,

$$g(l\bar{k}) \leq \left(\frac{1}{r} + \frac{1}{\gamma} \frac{\gamma \theta}{\gamma \theta - 1}\right)^l g(0), \quad (80)$$

and

$$g(k) \leq \frac{\gamma \theta}{\gamma \theta - 1} \theta \left(\frac{1}{r} + \frac{1}{\gamma} \frac{\gamma \theta}{\gamma \theta - 1}\right)^l g(0), \quad \forall k \in [l\bar{k}, (l+1)\bar{k}]. \quad (81)$$

The proof proceeds using inductive arguments.

Assume that there exists $\bar{l} \geq 0$, such that inequalities (80) and (81) hold for all $l \leq \bar{l}$.

Indeed, for $l = 0, 1$, (80) and (81) are satisfied.

Choose $k_0 = \bar{l}\bar{k}$.

By applying (72) for $k = (\bar{l} + 1)\bar{k}$, we obtain

$$\begin{aligned} g((\bar{l} + 1)\bar{k}) &\leq \theta \zeta^{(\bar{l}+1)\bar{k}-\bar{l}\bar{k}} g(\bar{l}\bar{k}) + \frac{1}{\gamma \theta} \sup_{t=\bar{l}\bar{k}, \dots, (\bar{l}+1)\bar{k}} g(t) \\ &\leq \theta \zeta^{\bar{k}} g(\bar{l}\bar{k}) + \frac{1}{\gamma \theta} \frac{\gamma \theta}{\gamma \theta - 1} \theta \left(\frac{1}{r} + \frac{1}{\gamma} \frac{\gamma \theta}{\gamma \theta - 1}\right)^{\bar{l}} g(0) \\ &\leq \theta \frac{1}{r \theta} \left(\frac{1}{r} + \frac{1}{\gamma} \frac{\gamma \theta}{\gamma \theta - 1}\right)^{\bar{l}} g(0) + \\ &\quad + \frac{1}{\gamma} \frac{\gamma \theta}{\gamma \theta - 1} \left(\frac{1}{r} + \frac{1}{\gamma} \frac{\gamma \theta}{\gamma \theta - 1}\right)^{\bar{l}} g(0) \\ &\leq \left(\frac{1}{r} + \frac{1}{\gamma} \frac{\gamma \theta}{\gamma \theta - 1}\right)^{(\bar{l}+1)} g(0). \end{aligned} \quad (82)$$

Thus, (80) holds for $l = \bar{l} + 1$.

Consider now the interval $[(\bar{l} + 1)\bar{k}, (\bar{l} + 2)\bar{k}]$. By applying (72) for $k_0 = (\bar{l} + 1)\bar{k}$, we get the following inequalities

$$\begin{aligned} g(k) &\leq \theta \zeta^{k - (\bar{l} + 1)\bar{k}} g((\bar{l} + 1)\bar{k}) + \frac{1}{\gamma \theta} \sup_{t = (\bar{l} + 1)\bar{k}, \dots, k} g(t), \\ \sup_{t = (\bar{l} + 1)\bar{k}, \dots, k} g(t) &\leq \theta g((\bar{l} + 1)\bar{k}) + \frac{1}{\gamma \theta} \sup_{t = (\bar{l} + 1)\bar{k}, \dots, k} g(t), \end{aligned} \quad (83)$$

for any $k \in [(\bar{l} + 1)\bar{k}, (\bar{l} + 2)\bar{k}]$.

From (83), by applying (82), it follows that for all $k \in [(\bar{l} + 1)\bar{k}, (\bar{l} + 2)\bar{k}]$,

$$g(k) \leq \frac{\gamma \theta}{\gamma \theta - 1} \theta \left(\frac{1}{r} + \frac{1}{\gamma} \frac{\gamma \theta}{\gamma \theta - 1} \right)^{(\bar{l} + 1)} g(0). \quad (84)$$

The previous steps have proved that (81) holds for $l = \bar{l} + 1$.

So (80) and (81) hold for any integer $l \geq 0$.

Let us define

$$\alpha \triangleq \frac{\gamma \theta}{\gamma \theta - 1} \theta, \quad \beta \triangleq \frac{1}{r} + \frac{1}{\gamma} \frac{\gamma \theta}{\gamma \theta - 1}.$$

Notice that by construction $\alpha > 1$ and β satisfies $0 < \beta < 1$.

From (81),

$$g(k) \leq \alpha \beta^l g(0),$$

for any k in $[l\bar{k}, (l + 1)\bar{k}]$, and for any integer $l \geq 0$.

Thus, $g(k)$ satisfies the following inequalities/equalities for any $k \in \mathbb{N}$,

$$g(k) \leq \alpha \beta^{\lceil k/\bar{k} \rceil} g(0) \leq \alpha \beta^{(k/\bar{k} - 1)} g(0) = \frac{\alpha}{\beta} \left(\beta^{1/\bar{k}} \right)^k g(0),$$

and finally,

$$g(k) \leq \mu \omega^k g(0),$$

with

$$\mu \triangleq \frac{\alpha}{\beta}, \quad \omega \triangleq \beta^{1/\bar{k}}$$

Notice that $\mu \geq 1$ and $0 < \omega < 1$.

The proof of the lemma is complete.

The following lemma shows that the property of *EMS-ISS* implies the property of *REMSS*.

Lemma 11 If the system described by (4.3) is *EMS-ISS*, then it is *REMSS*.

Proof 52 (Proof of Lemma 11) Consider the positive real numbers θ and ζ , and the function η of class \mathcal{K} , as in (4.6).

Without any loss of generality, let us assume $\eta(s) \geq s$, $s \in \mathbb{R}^+$ (otherwise, just replace η with $\bar{\eta}$ defined, for $s \in \mathbb{R}^+$, as $\bar{\eta}(s) = \max\{s, \eta(s)\}$).

Let ρ be a globally Lipschitz function of class \mathcal{K}_∞ such that, for $s \in \mathbb{R}^+$, $\rho(s) \leq \eta^{-1}\left(\frac{1}{\theta\gamma}s\right)$, with γ positive real greater than 1 satisfying (71) (see [94, p.130], [234]).

Consider the expected value $\mathbb{E}\left[\|x(k, \xi, i, u)\|^2\right]$, where $x(k, \xi, i, u)$ is the random variable that evolves according to Markovian switching system (4.3).

From (4.6), taking into account that system (4.3) is time invariant, for any $k, k_0 \in \mathbb{N}$ satisfying $0 < k_0 \leq k$, for any $q \in \mathcal{Q}_{k_0}(i)$, $i \in \mathcal{S}$, the following inequality holds,

$$\begin{aligned} \mathbb{E}\left[\|x(k, \Phi(k_0, \xi, i, \mathbf{r}_{k_0}^q(i), u), j_{k_0}, u)\|^2\right] &\leq \theta\zeta^{k-k_0} \|\Phi(k_0, \xi, i, \mathbf{r}_{k_0}^q(i), u)\|^2 \\ &\quad + \eta\left(\sup_{t=k_0, \dots, k-1} \|u(t)\|\right), \end{aligned} \quad (85)$$

where:

$$\mathbf{r}_{k_0}^q(i) = \{j_0, j_1, \dots, j_{k_0-1}\}$$

is an admissible switching path associated with the index $q \in \mathcal{Q}_{k_0}(i)$, given by $j_0 = i$; $j_{k_0} \in \mathcal{S}_{j_{k_0-1}}^{\text{out}}$, i.e., the mode j_{k_0} can be reached in one step from the mode j_{k_0-1} .

Consider the information set

$$\mathcal{F}_{k_0} = \left\{ \Phi(k_0, \xi, i, \mathbf{r}_{k_0}^q(i), u), j_{k_0} \right\}. \quad (86)$$

From (86), the inequality (85) is equivalent to the following inequality

$$\begin{aligned} \mathbb{E}\left[\|x(k, \xi, i, u)\|^2 \mid \mathcal{F}_{k_0}\right] &\leq \theta\zeta^{k-k_0} \mathbb{E}\left[\|x(k_0, \xi, i, u)\|^2 \mid \mathcal{F}_{k_0}\right] \\ &\quad + \eta\left(\sup_{t=k_0, \dots, k-1} \|u(t)\|\right). \end{aligned} \quad (87)$$

From (87), applying the linearity of expectation, the following inequality holds

$$\begin{aligned} \mathbb{E} \left[\mathbb{E} \left[\|x(k, \xi, i, u)\|^2 | \mathcal{F}_{k_0} \right] \right] &\leq \theta \zeta^{k-k_0} \mathbb{E} \left[\mathbb{E} \left[\|x(k_0, \xi, i, u)\|^2 | \mathcal{F}_{k_0} \right] \right] \\ &\quad + \mathbb{E} \left[\eta \left(\sup_{t=k_0, \dots, k-1} \|u(t)\| \right) \right]. \end{aligned}$$

From (144, Theorem 6.5.4] it follows that

$$\begin{aligned} \mathbb{E} \left[\|x(k, \xi, i, u)\|^2 \right] &\leq \theta \zeta^{k-k_0} \mathbb{E} \left[\|x(k_0, \xi, i, u)\|^2 \right] \\ &\quad + \mathbb{E} \left[\eta \left(\sup_{t=k_0, \dots, k-1} \|u(t)\| \right) \right]. \end{aligned} \quad (88)$$

Moreover, $\eta \left(\sup_{t=k_0, \dots, k-1} \|u(t)\| \right)$ is a deterministic non-negative real and its expectation is thus

$$\mathbb{E} \left[\eta \left(\sup_{t=k_0, \dots, k-1} \|u(t)\| \right) \right] = \eta \left(\sup_{t=k_0, \dots, k-1} \|u(t)\| \right). \quad (89)$$

From (88) and (89) the following inequality holds

$$\begin{aligned} \mathbb{E} \left[\|x(k, \xi, i, u)\|^2 \right] &\leq \theta \zeta^{k-k_0} \mathbb{E} \left[\|x(k_0, \xi, i, u)\|^2 \right] \\ &\quad + \eta \left(\sup_{t=k_0, \dots, k-1} \|u(t)\| \right). \end{aligned} \quad (90)$$

From (90) and (4.6) it follows that for any $k_0, k \in \mathbb{N}$, $0 \leq k_0 \leq k$, for any $u \in \mathcal{U}$ satisfying the inequality

$$\|u(s)\| \leq \rho \left(\mathbb{E} \left[\|x(s)\|^2 \right] \right), \quad s \in \mathbb{N}, \quad (91)$$

the expected value $\mathbb{E} \left[\|x(k, \xi, i, u)\|^2 \right]$, satisfies the inequalities

$$\begin{aligned} \mathbb{E} \left[\|x(k, \xi, i, u)\|^2 \right] &\leq \theta \zeta^{k-k_0} \mathbb{E} \left[\|x(k_0, \xi, i, u)\|^2 \right] + \eta \left(\sup_{t=k_0, \dots, k-1} \|u(t)\| \right) \\ &\leq \theta \zeta^{k-k_0} \mathbb{E} \left[\|x(k_0, \xi, i, u)\|^2 \right] + \eta \left(\sup_{t=k_0, \dots, k-1} \rho \left(\mathbb{E} \left[\|x(t, \xi, i, u)\|^2 \right] \right) \right) \\ &\leq \theta \zeta^{k-k_0} \mathbb{E} \left[\|x(k_0, \xi, i, u)\|^2 \right] + \eta \left(\rho \left(\sup_{t=k_0, \dots, k-1} \mathbb{E} \left[\|x(t, \xi, i, u)\|^2 \right] \right) \right) \\ &\leq \theta \zeta^{k-k_0} \mathbb{E} \left[\|x(k_0, \xi, i, u)\|^2 \right] + \frac{1}{\gamma \theta} \sup_{t=k_0, \dots, k-1} \mathbb{E} \left[\|x(t, \xi, i, u)\|^2 \right] \\ &\leq \theta \zeta^{k-k_0} \mathbb{E} \left[\|x(k_0, \xi, i, u)\|^2 \right] + \frac{1}{\gamma \theta} \sup_{t=k_0, \dots, k} \mathbb{E} \left[\|x(t, \xi, i, u)\|^2 \right]. \end{aligned} \quad (92)$$

For any $\delta \in \mathcal{M}_B$, there exists u satisfying (91), such that the expected value $\mathbb{E} [\|x(k, \xi, i, u)\|^2]$ is equal to $\mathbb{E} [\|x^R(k, \xi, i, \delta)\|^2]$.

Thus, from (92), for any $\delta \in \mathcal{M}_B$, for any $k_0, k \in \mathbb{N}$, $0 \leq k_0 \leq k$, the following inequality is satisfied

$$\begin{aligned} \mathbb{E} [\|x^R(k, \xi, i, \delta)\|^2] &\leq \theta \zeta^{k-k_0} \mathbb{E} [\|x^R(k_0, \xi, i, \delta)\|^2] \\ &\quad + \frac{1}{\gamma \theta} \sup_{t=k_0, \dots, k} \mathbb{E} [\|x^R(t, \xi, i, \delta)\|^2]. \end{aligned} \quad (93)$$

Remark 50 The variable $x^R(k, \xi, i, \delta)$ is a random variable, but $\mathbb{E} [\|x^R(k, \xi, i, \delta)\|^2]$ is a function that associates to each $k \in \mathbb{N}$ a value in \mathbb{R}^+ . Thus, setting

$$g(k) = \mathbb{E} [\|x^R(k, \xi, i, \delta)\|^2],$$

the hypothesis of Lemma 10 holds.

Lemma 10 is a technical result that is instrumental for the proof of Lemma 11, which is the key step involved in the necessity part of the proof of Theorem 8: the aim of this strategy is remapping standard procedures for deterministic systems (whose state is $x(k)$) into the stochastic case which involves the expected value $\mathbb{E} [\|x(k, \xi, i, u)\|^2]$ (see equations (4.4)-(4.5)-(4.6)).

From (93), by Lemma 10, it follows that there exist positive reals $\mu \geq 1$ and ω satisfying $0 < \omega < 1$, such that

$$\mathbb{E} [\|x^R(k, \xi, i, \delta)\|^2] \leq \mu \omega^k \|\xi\|^2.$$

The proof of the lemma is complete.

In order to prove Theorem 8, let us introduce the following technical results.

Let us define the function

$$\mathcal{J} : \mathbb{N} \times \mathbb{R}^n \times \mathcal{S} \rightarrow \mathbb{R}^+,$$

for $k \in \mathbb{N}$, $\xi \in \mathbb{R}^n$, $i \in \mathcal{S}$ as

$$\mathcal{J}(k, \xi, i) \triangleq \sup_{\delta \in \mathcal{M}_B} \sum_{q \in \mathcal{Q}_k(i)} \mathbf{p}_k^q(i) \left\| \Phi^R(k, \xi, i, \mathbf{r}_k^q(i), \delta) \right\|^2. \quad (94)$$

From the definition of \mathcal{J} , by following the same reasoning presented above for the operator \mathcal{V} (see (54a)), by evaluating the function \mathcal{J} in $k = 0$, the following equality holds

$$\mathcal{J}(0, \xi, i) = \|\xi\|^2, \quad (95)$$

for any $\xi \in \mathbb{R}^n$, $i \in \mathcal{S}$.

Lemma 12 Assume that the system described by (4.3) is REMSS.

Let μ, ω be the positive reals in (70).

Then, for any $\xi \in \mathbb{R}^n$, $i \in \mathcal{S}$, the following inequality holds

$$\mathcal{J}(k, \xi, i) \leq \mu \omega^k \|\xi\|^2, \quad \forall k \in \mathbb{N}. \quad (96)$$

Proof 53 (Proof of Lemma 12) From (94), by applying (69), the following equality holds for any $\xi \in \mathbb{R}^n$, $i \in \mathcal{S}$, $k \in \mathbb{N}$,

$$\mathcal{J}(k, \xi, i) = \sup_{\delta \in \mathcal{M}_B} \mathbb{E} \left[\left\| x^R(k, \xi, i, \delta) \right\|^2 \right]. \quad (97)$$

By recalling that the system described by (4.3) is REMSS by assumption, from (97) we obtain (96).

The proof of the lemma is complete.

Lemma 13 Consider the system described by (68) and consider the function \mathcal{J} , defined by (94).

Then, for any $\xi \in \mathbb{R}^n$, $i \in \mathcal{S}$, $\delta \in B_1^m$, the following inequality holds for any $k \in \mathbb{N}$,

$$\sum_{j \in \mathcal{S}_i^{\text{out}}} p_{ij} \mathcal{J}(k, f_i(\xi, \rho(\|\xi\|^2)\delta), j) \leq \mathcal{J}(k+1, \xi, i). \quad (98)$$

Proof 54 (Proof of Lemma 13) Consider an arbitrary $\xi \in \mathbb{R}^n$, and an arbitrary $i \in \mathcal{S}$. From (94), the left-hand side of (98) can be written as follows

$$\begin{aligned} \sum_{j \in \mathcal{S}_i^{\text{out}}} p_{ij} \mathcal{J}(k, f_i(\xi, \rho(\|\xi\|^2)\delta), j) &= \sum_{j \in \mathcal{S}_i^{\text{out}}} p_{ij} \sup_{\tilde{\delta} \in \mathcal{M}_B} \sum_{q \in \mathcal{Q}_k(j)} \mathbf{p}_k^q(j) \\ &\quad \times \|\Phi^R(k, f_i(\xi, \rho(\|\xi\|^2)\delta), j, \mathbf{r}_k^q(j), \tilde{\delta})\|^2, \quad k \in \mathbb{N}. \end{aligned} \quad (99)$$

In (99) all $j \in \mathcal{S}_i^{\text{out}}$ are considered. This means that the transition (i, j) is admissible according to the considered Markov mode (i.e., $(i, j) \in \mathcal{E}$). Thus, each admissible switching path of length $k \in \mathbb{N}$, starting in the mode $j \in \mathcal{S}$, can be included in a switching path of length $k+1$, starting in the mode $i \in \mathcal{S}$.

Formally, for any $j \in \mathcal{S}_i^{\text{out}}$, let $\overline{\mathcal{R}}_{k+1}(i, j)$ be defined as follows,

$$\overline{\mathcal{R}}_{k+1}(i, j) \triangleq \left\{ \{i, \mathbf{r}_k^q(j)\}, \quad q \in \mathcal{Q}_k(j) \right\},$$

with $\overline{\mathcal{Q}}_{k+1}(i, j) \triangleq \mathbb{N}_{[1, |\overline{\mathcal{R}}_{k+1}(i, j)|]}$.

Let us define the admissible switching path

$$\mathbf{r}_{k+1}^{\bar{q}}(i) \triangleq \{i, \mathbf{r}_k^q(j)\}, \quad \bar{q} \in \overline{\mathcal{Q}}_{k+1}(i, j), \quad j \in \mathcal{S}_i^{\text{out}}. \quad (100)$$

Remark 51 The sets $\overline{\mathcal{R}}_{k+1}(i, j)$ and $\overline{\mathcal{Q}}_{k+1}(i, j)$ are introduced in the proof of Lemma 6. For $k \in \mathbb{N}$ and Markov modes i, j (j is a Markov mode reachable from the mode i) the set $\overline{\mathcal{R}}_{k+1}(i, j)$ contains all admissible switching paths of length $k + 1$, starting in the Markov mode i , and having the transition (i, j) as first transition. The set $\overline{\mathcal{Q}}_{k+1}(i, j)$ contains all the positive integers from 1 to the cardinality of the set $\overline{\mathcal{R}}_{k+1}(i, j)$, providing the proper indexing for the elements of $\overline{\mathcal{R}}_{k+1}(i, j)$. Finally, notice that $\overline{\mathcal{R}}_{k+1}(i, j) \subseteq \mathcal{R}_{k+1}(i)$.

Let us call

$$\xi^+ \triangleq f_i(\xi, \rho(\|\xi\|^2)\delta)$$

(see [225, Section 4.3.4]).

Recall that for any given initial condition $\xi \in \mathbb{R}^n$, for any $i \in \mathcal{S}$, for any $\tilde{\delta} \in \mathcal{M}_B$,

$$x^R(0, \xi, i, \tilde{\delta}) = \xi.$$

Thus, $x^R(0) = \xi$ is deterministic, and it follows that

$$\rho(\mathbb{E}[\|x^R(0)\|^2]) = \rho(\|\xi\|^2).$$

For any initial mode of the Markov mode $r(0) = i \in \mathcal{S}$, the following equality holds

$$f_{r(0)}(x^R(0), \rho(\mathbb{E}[\|x^R(0)\|^2])\tilde{\delta}(0)) = f_i(\xi, \rho(\|\xi\|^2)\delta), \quad (101)$$

where $\tilde{\delta}(0) = \delta \in B_1^m$.

Since $r(0) = i \in \mathcal{S}$ is known, the left-hand side of (101) is the solution of (68) for $k = 1$, with an admissible switching path that contains only the mode $r(0) = i \in \mathcal{S}$. Indeed, there is only one admissible switching path of length 1, starting in the mode $i \in \mathcal{S}$, and it is given by $\mathbf{r}_1(i) = \{i\}$.

By the reasoning presented above, it follows that

$$f_{r(0)} \left(x^R(0), \rho \left(\mathbb{E} \left[\|x^R(0)\|^2 \right] \right) \tilde{\delta}(0) \right) = \Phi^R \left(1, \xi, i, \mathbf{r}_1(i), \tilde{\delta} \right),$$

which implies

$$\xi^+ = f_i \left(\xi, \rho \left(\|\xi\|^2 \right) \delta \right) = \Phi^R \left(1, \xi, i, \mathbf{r}_1(i), \tilde{\delta} \right),$$

with $\tilde{\delta}(0) = \delta$ in B_1^m .

Then, for any $k \in \mathbb{N}$, $i \in \mathcal{S}$, $j \in \mathcal{S}_i^{out}$, the following equality holds

$$\Phi^R \left(k, \xi^+, j, \mathbf{r}_k^q(j), \tilde{\delta} \right) = \Phi^R \left(k+1, \xi, i, \mathbf{r}_{k+1}^{\bar{q}}(i), \tilde{\delta} \right),$$

where $\mathbf{r}_{k+1}^{\bar{q}}(i)$ is defined in (100), with $q \in \mathcal{Q}_k(j)$, $\bar{q} \in \bar{\mathcal{Q}}_{k+1}(i, j)$, $\tilde{\delta} \in \mathcal{M}_B$, $\tilde{\delta}(0) = \delta$. Thus, the right-hand side of (99) can be written as follows:

$$\begin{aligned} & \sum_{j \in \mathcal{S}_i^{out}} p_{ij} \sup_{\tilde{\delta} \in \mathcal{M}_B, \tilde{\delta}(0) = \delta} \left\{ \sum_{\bar{q} \in \bar{\mathcal{Q}}_{k+1}(i, j)} \mathbb{P} \left(\mathbf{r}_{k+1}^{\bar{q}}(i) | j_1 = j \right) \|\Phi^R \left(k+1, \xi, i, \mathbf{r}_{k+1}^{\bar{q}}(i), \tilde{\delta} \right)\|^2 \right\} \\ & \leq \sup_{\tilde{\delta} \in \mathcal{M}_B, \tilde{\delta}(0) = \delta} \left\{ \sum_{q \in \mathcal{Q}_{k+1}(i)} \mathbb{P} \left(\mathbf{r}_{k+1}^q(i) \right) \|\Phi^R \left(k+1, \xi, i, \mathbf{r}_{k+1}^q(i), \tilde{\delta} \right)\|^2 \right\} \\ & \leq \sup_{\tilde{\delta} \in \mathcal{M}_B, \tilde{\delta}(0) = \delta} \left\{ \sum_{q \in \mathcal{Q}_{k+1}(i)} \mathbf{p}_{k+1}^q(i) \|\Phi^R \left(k+1, \xi, i, \mathbf{r}_{k+1}^q(i), \tilde{\delta} \right)\|^2 \right\} \\ & \leq \sup_{\tilde{\delta} \in \mathcal{M}_B} \left\{ \sum_{q \in \mathcal{Q}_{k+1}(i)} \mathbf{p}_{k+1}^q(i) \|\Phi^R \left(k+1, \xi, i, \mathbf{r}_{k+1}^q(i), \tilde{\delta} \right)\|^2 \right\} \\ & = \mathcal{J}(k+1, \xi, i). \end{aligned}$$

The proof of the lemma is complete.

Remark 52 The following lemma provides necessary Lyapunov conditions for REMSS property. This stage is different from the standard procedure adopted in the deterministic non switching and switching framework (see [113, 136, 225–227]). Indeed, such procedure makes use of Lyapunov characterization for the robust global asymptotic stability (see [113, Section 2.2]), while the procedure here presented makes use of the converse result for the robust exponential stability notion in the mean square sense (see Definition 19).

Lemma 14 Assume that the system described by (4.3) is REMSS, with ρ globally Lipschitz function of class \mathcal{K}_∞ , and positive reals $\mu \geq 1$, and $0 < \omega < 1$ as in Definition 19.

Then, there exist a function $V : \mathbb{R}^n \times \mathcal{S} \rightarrow \mathbb{R}^+$, positive real numbers $\alpha_l > 0$, $l = 1, 2, 3$ such that the following inequalities hold for any $i \in \mathcal{S}$, $\xi \in \mathbb{R}^n$, $\delta \in B_1^m$:

- a) $\alpha_1 \|\xi\|^2 \leq V(\xi, i) \leq \alpha_2 \|\xi\|^2$;
- b) $\mathcal{L}V(\xi, \rho(\|\xi\|^2)\delta, i) \leq -\alpha_3 \|\xi\|^2$.

Remark 53 Notice that it is not known whether these conditions are also sufficient for the REMSS. Indeed, in (68) the expected value is involved, which can well be different from the current solution. Therefore, condition (b) may well not hold for $\xi = x^R(k)$, $k \in \mathbb{N}$.

Proof 55 (Proof of Lemma 14) Assume that the system described by (4.3) is REMSS according to Definition 19, with constants $\mu \geq 1$, and $0 < \omega < 1$, as in (70). Let

$$V : \mathbb{R}^n \times \mathcal{S} \rightarrow \mathbb{R}^+$$

be the function defined, for $\xi \in \mathbb{R}^n$, $i \in \mathcal{S}$, as

$$V(\xi, i) = \sum_{k=0}^{\infty} \mathcal{J}(k, \xi, i), \quad (102)$$

where \mathcal{J} is defined in (94). Notice that, by Lemma 12, the sum in (102) is convergent. Since $\mathcal{J}(k, \xi, i) \geq 0$ for any $k \in \mathbb{N}$, and $\mathcal{J}(0, \xi, i) = \|\xi\|^2$, the inequality $\|\xi\|^2 \leq V(\xi, i)$ follows.

From Lemma 12, the following inequality is satisfied

$$V(\xi, i) \leq \sum_{k=0}^{\infty} \mu \omega^k \|\xi\|^2 = \mu \frac{1}{1-\omega} \|\xi\|^2.$$

Thus, condition (a) of the theorem is satisfied, with $\alpha_1 = 1$, and $\alpha_2 = \mu/(1-\omega)$.

Recalling that for any $j \notin \mathcal{S}_i^{\text{out}}$, $p_{ij} = 0$, we obtain the following equality:

$$\sum_{j \in \mathcal{S}} p_{ij} V(f_i(\xi, \rho(\|\xi\|^2)\delta), j) = \sum_{j \in \mathcal{S}_i^{\text{out}}} p_{ij} V(f_i(\xi, \rho(\|\xi\|^2)\delta), j) \quad (103)$$

$\delta \in B_1^m$.

From (103), by applying (102), we obtain the following equalities

$$\begin{aligned} \sum_{j \in \mathcal{S}} p_{ij} V(f_i(\xi, \rho(\|\xi\|^2)\delta), j) &= \sum_{j \in \mathcal{S}_i^{\text{out}}} p_{ij} \sum_{k=0}^{\infty} \mathcal{J}(k, f_i(\xi, \rho(\|\xi\|^2)\delta), j) \\ &= \sum_{k=0}^{\infty} \sum_{j \in \mathcal{S}_i^{\text{out}}} p_{ij} \mathcal{J}(k, f_i(\xi, \rho(\|\xi\|^2)\delta), j). \end{aligned} \quad (104)$$

From (104), by Lemma 13, the following inequality holds,

$$\sum_{k=0}^{\infty} \sum_{j \in \mathcal{S}_i^{\text{out}}} p_{ij} \mathcal{J}(k, f_i(\xi, \rho(\|\xi\|^2)\delta), j) \leq \sum_{k=0}^{\infty} \mathcal{J}(k+1, \xi, i). \quad (105)$$

From (104) and (105), by changing the variable of the sum in the right-hand side of (105), the following is obtained,

$$\sum_{j \in \mathcal{S}} p_{ij} V(f_i(\xi, \rho(\|\xi\|^2)\delta), j) \leq \sum_{k=1}^{\infty} \mathcal{J}(k, \xi, i). \quad (106)$$

Recalling that $\mathcal{J}(0, \xi, i) = \|\xi\|^2$ (see (95)), by adding and subtracting $\|\xi\|^2$ to the right-hand side of (106), we obtain

$$\sum_{j \in \mathcal{S}} p_{ij} V(f_i(\xi, \rho(\|\xi\|^2)\delta), j) \leq \sum_{k=0}^{\infty} \mathcal{J}(k, \xi, i) - \|\xi\|^2,$$

and recalling that

$$\sum_{k=0}^{\infty} \mathcal{J}(k, \xi, i) - \|\xi\|^2 = V(\xi, i) - \|\xi\|^2,$$

we get

$$\mathcal{L}V(\xi, \rho(\|\xi\|^2)\delta, i) \leq -\|\xi\|^2.$$

So, condition (b) of the theorem is satisfied with $\alpha_3 = 1$.

The proof of the lemma is complete.

Remark 54 The novelty in Lemma 14 is the existence of a Lyapunov function for REMSS of a discrete-time Markovian switching nonlinear system: the Markov property of the switching rule is exploited. Clearly, in the proof of the Lyapunov characterization of ISS for the deterministic discrete-time switching and non switching case the transition probabilities and the expected value are not considered in the robust global asymptotic stability characterization (see [136, Lemma 1] and [226, Lemma 3.8, Lemma 3.11]). The proposed methodology accounts for the transition probabilities (see (103)-(106)), as well as admissible transitions (see the definition of $\mathcal{S}_i^{\text{out}}$, for $i \in \mathcal{S}$).

Lemma 15 For a locally bounded function $V : \mathbb{R}^n \times \mathcal{S} \rightarrow \mathbb{R}^+$, satisfying, for any $i \in \mathcal{S}$, $V(0, i) = 0$ and $V(\cdot, i)$ continuous at zero for any $i \in \mathcal{S}$, the following conditions are equivalent.

- i) There exist a positive real number α , and a function ρ of class \mathcal{K}_∞ such that, for any $\xi \in \mathbb{R}^n$, $u \in \mathbb{R}^m$, satisfying $\|\xi\|^2 \geq \rho^{-1}(\|u\|)$, the following inequality holds, for any $i \in \mathcal{S}$,

$$\mathcal{L}V(\xi, u, i) \leq -\alpha\|\xi\|^2. \quad (107)$$

- ii) There exist a positive real number γ_1 , and a function γ_2 of class \mathcal{K}_∞ such that, for any $\xi \in \mathbb{R}^n$, $u \in \mathbb{R}^m$, the following inequality holds, for any $i \in \mathcal{S}$,

$$\mathcal{L}V(\xi, u, i) \leq -\gamma_1\|\xi\|^2 + \gamma_2(\|u\|). \quad (108)$$

Proof 56 (Proof of Lemma 15) Let us show that (i) implies (ii).

Pick $\gamma_1 = \alpha$, where α is the positive real involved in (107), and consider a function $\underline{\gamma}_2$ as follows,

$$\underline{\gamma}_2(s) = s + \sup \left\{ \mathcal{L}V(y, \mu, h) + \alpha\rho^{-1}(\|\mu\|), \right. \\ \left. \|\mu\| \leq s, \|y\|^2 \leq \rho^{-1}(\|\mu\|), y \in \mathbb{R}^n, \mu \in \mathbb{R}^m, h \in \mathcal{S} \right\}. \quad (109)$$

The supremum involved in the definition of $\underline{\gamma}_2(s)$ belongs to \mathbb{R}^+ . Indeed, $V : \mathbb{R}^n \times \mathcal{S} \rightarrow \mathbb{R}^+$ is a locally bounded function satisfying $V(0, h) = 0$, for any $h \in \mathcal{S}$, and the functions $f_h : \mathbb{R}^n \times \mathbb{R}^m \rightarrow \mathbb{R}^n$, $h \in \mathcal{S}$, are locally bounded.

Moreover, the supremum involved in (109) is evaluated for a finite number of times (recall that the cardinality of the set \mathcal{S} is finite). The function $\underline{\gamma}_2$ is strictly increasing.

Since f_h and $V(\cdot, h)$, $h \in \mathcal{S}$, are zero at zero and continuous at zero, the function $\underline{\gamma}_2$ is such that $\underline{\gamma}_2(0) = 0$, and $\lim_{s \rightarrow 0^+} \underline{\gamma}_2(s) = 0$. By [94, Lemma 2.4], there exists a \mathcal{K}_∞ function $\gamma_2 : \mathbb{R}^+ \rightarrow \mathbb{R}^+$, such that $\gamma_2(s) \geq \underline{\gamma}_2(s)$, for any $s \in \mathbb{R}^+$. For any given $\xi \in \mathbb{R}^n$, $u \in \mathbb{R}^m$, one of the following cases holds: $\|\xi\|^2 \leq \rho^{-1}(\|u\|)$ or $\|\xi\|^2 > \rho^{-1}(\|u\|)$.

In the first case, from (109) the following inequalities hold for all $i \in \mathcal{S}$, and $u \in \mathbb{R}^m$

$$\gamma_2(\|u\|) \geq \|u\| + \mathcal{L}V(\xi, u, i) + \alpha\|\xi\|^2 \geq \mathcal{L}V(\xi, u, i) + \alpha\|\xi\|^2. \quad (110)$$

Thus, if $\|\xi\|^2 \leq \rho^{-1}(\|u\|)$, from (110), the following inequality is satisfied,

$$\mathcal{L}V(\xi, u, i) \leq -\alpha\|\xi\|^2 + \gamma_2(\|u\|),$$

for any $i \in \mathcal{S}$. In the second case, that is $\|\xi\|^2 > \rho^{-1}(\|u\|)$, by condition (i), the following inequality holds,

$$\mathcal{L}V(\xi, u, i) \leq -\alpha\|\xi\|^2,$$

and thus, inequality (108) follows.

Let us prove now that condition (ii) implies condition (i). Assume that condition (ii) holds.

Pick

$$\rho(s) = \gamma_2^{-1} \left(\frac{1}{2} \gamma_1 s \right).$$

For $\|\xi\|^2 \geq \rho^{-1}(\|u\|)$,

$$\begin{aligned} \|u\| \leq \rho(\|\xi\|^2) &\implies \mathcal{L}V(\xi, u, i) \leq -\gamma_1\|\xi\|^2 + \gamma_2(\|u\|) \\ &\leq -\gamma_1\|\xi\|^2 + \gamma_2 \left(\gamma_2^{-1} \left(\frac{1}{2} \gamma_1 \|\xi\|^2 \right) \right) \\ &\leq -\frac{1}{2} \gamma_1 \|\xi\|^2. \end{aligned} \tag{111}$$

Pick

$$\alpha = \frac{1}{2} \gamma_1,$$

and so

$$\|u\| \leq \rho(\|\xi\|^2) \implies \mathcal{L}V(\xi, u, i) \leq -\alpha\|\xi\|^2.$$

The proof of the lemma is complete.

Proof 57 (Proof of Theorem 8) Let us prove first that (a) \implies (b). Assume that condition (a) holds. By Lemma 11, we obtain that system (4.3) is REMSS according to Definition 19. By applying Lemma 14 and Lemma 15, we obtain that condition (b) holds. Notice that $V(0, i) = 0$ for any $i \in \mathcal{S}$, and $V(\cdot, i)$ is continuous at zero, for any $i \in \mathcal{S}$, so Lemma 15 can be applied.

Let us prove now that (b) \implies (a). Assume that condition (b) holds. Assume that $u \in \mathcal{U}$ is bounded.

Let

$$v = \sup_{k \in \mathbb{N}} \|u(k)\|.$$

Consider, for $k \in \mathbb{N}$, $V(x(k), r(k))$.

By condition (b₂) computed in $(x(k), u(k), r(k))$, the following inequality is satisfied,

$$\mathcal{L}V(x(k), u(k), r(k)) \leq -\alpha_3 \|x(k)\|^2 + \alpha_4 (\|u(k)\|). \quad (112)$$

From (4.8), the following equality follows:

$$\mathcal{L}V(x(k), u(k), r(k)) = \sum_{r(k+1) \in \mathcal{S}} p_{r(k)r(k+1)} V(f_{r(k)}(x(k), u(k)), r(k+1)) - V(x(k), r(k)). \quad (113)$$

From (113), by applying the Markov property, and the definition of conditional expectation, it follows that:

$$\mathcal{L}V(x(k), u(k), r(k)) = \mathbb{E} \left[V(f_{r(k)}(x(k), u(k)), r(k+1)) | \mathcal{F}_k \right] - V(x(k), r(k)). \quad (114)$$

From (112), by applying the linearity of expectation, the following inequalities hold:

$$\begin{aligned} \mathbb{E} [\mathcal{L}V(x(k), u(k), r(k))] &\leq -\alpha_3 \mathbb{E} [\|x(k)\|^2] + \alpha_4 (\|u(k)\|) \\ &\leq -\alpha_3 \mathbb{E} [\|x(k)\|^2] + \alpha_4 (v). \end{aligned} \quad (115)$$

Furthermore, $V(x(k), r(k))$, $k \in \mathbb{N}$, is a random variable on $(\Omega, \mathcal{F}, \{\mathcal{F}_k\}_{k \in \mathbb{N}}, \mathbb{P})$.

By applying [141], Theorem 6.5.4],

$$\mathbb{E} \left[\mathbb{E} \left[V(f_{r(k)}(x(k), u(k)), r(k+1)) | \mathcal{F}_k \right] \right] = \mathbb{E} \left[V(f_{r(k)}(x(k), u(k)), r(k+1)) \right]. \quad (116)$$

Define

$$y(k) \triangleq \mathbb{E} [V(x(k), r(k))],$$

from equations (114)-(116), the following inequality is obtained:

$$y(k+1) - y(k) \leq -\alpha_3 \mathbb{E} [\|x(k)\|^2] + \alpha_4 (v). \quad (117)$$

Recalling condition (b₁), by the linearity of expectation,

$$\mathbb{E} [\|x(k)\|^2] \geq \frac{1}{\alpha_2} y(k).$$

Let

$$\alpha_5 \in \left(0, \min \left\{1, \frac{\alpha_3}{\alpha_2}\right\}\right).$$

From (117), it follows that

$$y(k+1) - y(k) \leq -\alpha_5 y(k) + \alpha_4(v),$$

and thus,

$$y(k+1) \leq (1 - \alpha_5) y(k) + \alpha_4(v). \quad (118)$$

Remark 55 Notice that inequalities

$$\mathbb{E} [\|x(k)\|^2] \geq \frac{1}{\alpha_2} y(k)$$

and

$$y(k+1) - y(k) \leq -\alpha_5 y(k) + \alpha_4(v)$$

hold even though

$$\alpha_3 \|\xi\|^2 < V(\xi, i),$$

for some $\xi \in \mathbb{R}^n$, $i \in \mathcal{S}$. Indeed, the inequality

$$\mathbb{E} [\|x(k)\|^2] \geq \frac{1}{\alpha_2} y(k)$$

follows from condition (b₁). Thus, if the following condition occurs,

$$\alpha_3 \|\xi\|^2 < V(\xi, i)$$

this fact does not perturb stability.

Actually, the situation

$$\alpha_3 \|\xi\|^2 \leq V(\xi, i)$$

occurs always, otherwise the inequality (b₂) in the Theorem would not hold for $u = 0$.

Let $\rho \in (0, 1)$. Let $j_0 \leq \infty$ be the minimum time such that

$$y(k) \leq \frac{1}{\alpha_5 \rho} \alpha_4(v). \quad (119)$$

We will prove later the following claim.

Claim 2 Assume that there is some $k_0 \in \mathbb{N}$, such that

$$y(k) \leq \frac{1}{\alpha_5 \rho} \alpha_4(v), \text{ for } k = k_0. \quad (120)$$

Then, (120) holds for all $k \geq k_0$.

By Claim 2, (119) holds for any $k \geq j_0$.

For all $k \in [0, j_0 - 1]$, the following inequality holds:

$$\rho \alpha_5 y(k) > \alpha_4(v). \quad (121)$$

By adding and subtracting the quantity $\rho \alpha_5 y(k)$ on the right-hand side of (118), the following inequality is obtained:

$$y(k+1) \leq [1 - (1 - \rho) \alpha_5] y(k). \quad (122)$$

Let

$$\zeta = 1 - (1 - \rho) \alpha_5.$$

Notice that $0 < \zeta < 1$.

From (122), it follows for any k in $[0, j_0 - 1]$:

$$y(k) \leq \zeta^k y(0). \quad (123)$$

Since the initial conditions $x(0) = \xi$ in \mathbb{R}^n and $r(0) = i$ in \mathcal{S} are given, the quantity $V(x(0), r(0))$ is deterministic.

Thus, $y(0) = V(x(0), r(0))$, and (123) can be written as

$$y(k) \leq \zeta^k V(x(0), r(0)). \quad (124)$$

Consider inequalities (124) and (119).

Let

$$\theta = \frac{\alpha_2}{\alpha_1} \geq 1, \quad \eta(s) = \frac{1}{\alpha_1 \alpha_5 \rho} (\alpha_4(s)), \quad s \in \mathbb{R}^+.$$

The function η is a function of class \mathcal{K} because α_4 is a function of class \mathcal{K} .

Applying condition (b_1) , the following inequality holds,

$$\mathbb{E} [\|x(k)\|^2] \leq \theta \zeta^k \|\xi\|^2 + \eta(v).$$

By causality arguments, the assumption on the boundedness of the input u can be removed and the following inequality is obtained,

$$\mathbb{E} [\|x(k)\|^2] \leq \theta \zeta^k \|\xi\|^2 + \eta \left(\sup_{s=0, \dots, k-1} \|u(s)\| \right).$$

It remains to prove Claim [2](#).

Proof 58 (Proof of Claim [2](#)) Assume that [\(120\)](#) holds for $k = k_0$.

Then, $\rho \alpha_5 y(k_0) \leq \alpha_4(v)$.

By [\(118\)](#), the following inequality holds for $k = k_0$:

$$y(k_0 + 1) \leq (1 - \alpha_5)y(k_0) + \alpha_4(v). \quad (125)$$

Let

$$b = \frac{1}{\alpha_5 \rho} \alpha_4(v).$$

Then, from [\(125\)](#), we get

$$y(k_0 + 1) \leq (1 - \alpha_5)b + \alpha_4(v). \quad (126)$$

By adding and subtracting $\rho \alpha_5 b$ in the right-hand side of inequality [\(126\)](#), we obtain:

$$y(k_0 + 1) \leq (1 - \alpha_5)b + \alpha_4(v) + \rho \alpha_5 b - \rho \alpha_5 b = -(1 - \rho)\alpha_5 b + b \leq b. \quad (127)$$

Therefore, by induction reasoning, it follows that

$$y(k_0 + l) \leq b,$$

for all $l \in \mathbb{N}$, i.e.,

$$y(k) \leq \frac{1}{\alpha_5 \rho} \alpha_4(v),$$

for all $k \geq k_0$. The claim is proved.

The implication $(b) \implies (a)$ in Theorem [8](#) is proved.

The proof of the theorem is complete.

Remark 56 The proof of implication $(b) \implies (a)$ follows the lines of reasoning used in [\[226\]](#). The novelty consists in evaluating the Lyapunov function on the random variables $x(k)$ and $r(k)$, and suitably dealing with its expectation, by applying the Markov property of the switching signal.

Proof of Theorem 9

This section reports the proof of Theorem 9 in the following.

Proof 59 (Proof of Theorem 9) Assume that conditions (a) and (b) of Theorem 9 are satisfied. Let us prove that the system described by (4.3) is p th moment ISS.

Let v be an arbitrary positive real. For any $u \in \mathcal{U}$, with $\|u(k)\| \leq v$, $k \in \mathbb{N}$, for any $r(k) \in \mathcal{S}$, $x(k) \in \mathbb{R}^n$, $k \in \mathbb{N}$, consider the inequality provided by condition (b) computed in $(x(k), u(k), r(k))$:

$$\mathcal{L}V(x(k), u(k), r(k)) \leq -\gamma(\|x(k)\|^p) + \delta(\|u(k)\|). \quad (128)$$

From (4.8), it follows that

$$\mathcal{L}V(x(k), u(k), r(k)) = \left[\sum_{r(k+1) \in \mathcal{S}} p_{r(k)r(k+1)} V(f_{r(k)}(x(k), u(k)), r(k+1)) \right] - V(x(k), r(k)).$$

Applying the Markov property, and the definition of conditional expectation, the following equation is satisfied

$$\mathcal{L}V(x(k), u(k), r(k)) = \mathbb{E} \left[V(f_{r(k)}(x(k), u(k)), r(k+1)) | \mathcal{F}_k \right] - V(x(k), r(k)). \quad (129)$$

By (128), applying the linearity of expectation, the following inequality holds,

$$\mathbb{E}[\mathcal{L}V(x(k), u(k), r(k))] \leq -\mathbb{E}[\gamma(\|x(k)\|^p)] + \mathbb{E}[\delta(\|u(k)\|)]. \quad (130)$$

Since γ is a convex function of class \mathcal{K}_∞ , by (141, Jensen's inequality), it follows that,

$$\mathbb{E}[\gamma(\|x(k)\|^p)] \geq \gamma(\mathbb{E}[\|x(k)\|^p]), \quad \forall k \in \mathbb{N}.$$

Moreover, the input u is such that

$$\|u(k)\| \leq v,$$

for any $k \in \mathbb{N}$, and δ is a function of class \mathcal{K} .

Consequently,

$$\mathbb{E}[\delta(\|u(k)\|)] \leq \mathbb{E}[\delta(v)],$$

for any $k \in \mathbb{N}$.

Since v is an arbitrary positive real, $\delta(v)$ is a number in \mathbb{R}^+ , and thus,

$$\mathbb{E}[\delta(v)] = \delta(v),$$

and the following holds

$$\mathbb{E}[\mathcal{L}V(x(k), u(k), r(k))] \leq -\gamma(\mathbb{E}[\|x(k)\|^p]) + \delta(v). \quad (131)$$

Furthermore, V is a function of the random variable $(x(k), r(k))$, defined on the probability space $(\Omega, \mathcal{F}, \{\mathcal{F}_k\}_{k \in \mathbb{N}}, \mathbb{P})$, therefore it is a random variable on $(\Omega, \mathcal{F}, \{\mathcal{F}_k\}_{k \in \mathbb{N}}, \mathbb{P})$.

By [141, Theorem 6.5.4], it follows that:

$$\mathbb{E}[\mathbb{E}[V(f_{r(k)}(x(k), u(k)), r(k+1)) | \mathcal{F}_k]] = \mathbb{E}[V(f_{r(k)}(x(k), u(k)), r(k+1))]. \quad (132)$$

Consider (129), (131), (132).

Let us apply the definition of $\mathcal{L}V$ operator, the following inequality is satisfied:

$$\mathbb{E}[V(x(k+1), r(k+1))] - \mathbb{E}[V(x(k), r(k))] \leq -\gamma(\mathbb{E}[\|x(k)\|^p]) + \delta(v). \quad (133)$$

Applying condition (a), by the linearity of expectation, inequality (134) holds,

$$\mathbb{E}[\|x(k)\|^p] \geq \frac{1}{\alpha_2} \mathbb{E}[V(x(k), r(k))] \quad (134)$$

Let us define the function

$$\alpha_4 \triangleq \gamma \circ \frac{1}{\alpha_2} I_d.$$

Particularly, α_4 is of class \mathcal{K}_∞ , because γ is a function of class \mathcal{K}_∞ and $\alpha_2 > 0$.

By the reasoning presented above, it follows that,

$$\mathbb{E}[V(x(k+1), r(k+1))] - \mathbb{E}[V(x(k), r(k))] \leq -\alpha_4(\mathbb{E}[V(x(k), r(k))]) + \delta(v). \quad (135)$$

Let us assume, without loss of generality, that

$$I_d - \alpha_4 \in \mathcal{K},$$

cf. [226, Lemma B.1].

Let us complete the Proof, by following the same reasoning in [226, Lemma 3.5].

Since V evaluated on $(x(k), r(k))$ is a random variable on the probability space $(\Omega, \mathcal{F}, \{\mathcal{F}_k\}_{k \in \mathbb{N}}, \mathbb{P})$, this proof focuses on the expectation of the function V .

This is the main difference between our approach and the one adopted in [226], where the function V is deterministic.

Let ρ be any \mathcal{K}_∞ function, such that $I_d - \rho \in \mathcal{K}_\infty$.

Let us define

$$b \triangleq \alpha_4^{-1} \circ \rho^{-1} \circ \delta(v).$$

Let us illustrate the following Claim that will be exploited to complete the proof.

Claim 3 Assume that there exists some $k_0 \in \mathbb{N}$, such that

$$\mathbb{E}[V(x(k_0), r(k_0))] \leq b.$$

Then,

$$\mathbb{E}[V(x(k), r(k))] \leq b,$$

for any $k \geq k_0$.

Proof 60 (Proof of Claim 3) Assume that

$$\mathbb{E}[V(x(k_0), r(k_0))] \leq b.$$

Then,

$$\rho \circ \alpha_4 (\mathbb{E}[V(x(k_0), r(k_0))]) \leq \delta(v).$$

By (135), inequality (136) holds,

$$\mathbb{E}[V(x(k_0 + 1), r(k_0 + 1))] \leq (I_d - \alpha_4) (\mathbb{E}[V(x(k_0), r(k_0))]) + \delta(v). \quad (136)$$

Let us recall that $\mathbb{E}[V(x(k_0), r(k_0))]$ is assumed to be such that $\mathbb{E}[V(x(k_0), r(k_0))] \leq b$.

Since $I_d - \alpha_4 \in \mathcal{K}$, inequality (137) holds:

$$\mathbb{E}[V(x(k_0 + 1), r(k_0 + 1))] \leq (I_d - \alpha_4) (b) + \delta(v). \quad (137)$$

By adding and subtracting $\rho \circ \alpha_4(b)$ on the right-hand side of inequality (137),

$$\begin{aligned} \mathbb{E}[V(x(k_0 + 1), r(k_0 + 1))] &\leq (I_d - \alpha_4) (b) + \delta(v) + \rho \circ \alpha_4(b) - \rho \circ \alpha_4(b) = \\ &= -(I_d - \rho) \circ \alpha_4(b) + b \leq b. \end{aligned}$$

Therefore, by induction arguments, it is proved that

$$\mathbb{E} [V (x(k_0 + l), r(k_0 + l))] \leq b,$$

for any $l \in \mathbb{N}$, that is,

$$\mathbb{E} [V (x(k), r(k))] \leq b$$

for any $k \geq k_0$.

The proof of the claim is complete.

Consider the time instant

$$j_0 = \inf \{k \in \mathbb{N} : \mathbb{E} [V (x(k), r(k))] \leq b\} \leq \infty.$$

By Claim [3](#), it follows that,

$$\mathbb{E}[V(x(k), r(k))] \leq \alpha_4^{-1} \circ \rho^{-1} \circ \delta(v), \quad (138)$$

for any $k \geq j_0$.

For $k \in \mathbb{N}_{[0, j_0-1]}$,

$$\rho \circ \alpha_4 (\mathbb{E} [V (x(k), r(k))]) > \delta(v).$$

Consider inequality [\(135\)](#).

By adding and subtracting the quantity $\rho \circ \alpha_4 (\mathbb{E} [V (x(k), r(k))])$ on the right-hand side of inequality [\(135\)](#), inequality [\(139\)](#) is obtained, as follows,

$$\mathbb{E} [V (x(k + 1), r(k + 1))] - \mathbb{E} [V (x(k), r(k))] \leq -(I_d - \rho) \circ \alpha_4 (\mathbb{E} [V (x(k), r(k))]), \quad (139)$$

for any $k \in \mathbb{N}_{[0, j_0-1]}$.

Let the function $y : \mathbb{N} \rightarrow \mathbb{R}^+$ be defined as follows,

$$y(k) = \mathbb{E} [V (x(k), r(k))].$$

Then, [\(139\)](#) can be written as follows,

$$y(k + 1) - y(k) \leq -(I_d - \rho) \circ \alpha_4 (y(k)), \quad (140)$$

for any $k \in \mathbb{N}_{[0, j_0-1]}$, where $(I_d - \rho) \circ \alpha_4$ is a function of class \mathcal{K}_∞ , since $(I_d - \rho)$ and α_4 are functions of class \mathcal{K}_∞ .

By [225, Lemma 4.3], there exists some \mathcal{KL} -function $\hat{\beta}$, such that :

$$y(k) \leq \hat{\beta}(y(0), k), \quad (141)$$

for any $k \in \mathbb{N}_{[0, j_0-1]}$.

Applying the definition of $y(k)$, inequality (141) becomes:

$$\mathbb{E}[V(x(k), r(k))] \leq \hat{\beta}(\mathbb{E}[V(x(0), r(0))], k), \forall k \in \mathbb{N}_{[0, j_0-1]}. \quad (142)$$

Considering both (138) and (142), applying condition (a), together with the linearity of the expected value, the following inequalities are satisfied for any $k \in \mathbb{N}$.

$$\begin{aligned} \alpha_1 \mathbb{E}[\|x(k)\|^p] &\leq \mathbb{E}[V(x(k), r(k))] \leq \\ &\leq \hat{\beta}(\mathbb{E}[V(x(0), r(0))], k) + \alpha_4^{-1} \circ \rho^{-1} \circ \delta(v) \leq \\ &\leq \hat{\beta}(\alpha_2 \mathbb{E}[\|x(0)\|^p], k) + \alpha_4^{-1} \circ \rho^{-1} \circ \delta(v) = \\ &= \hat{\beta}(\alpha_2 \|x_0\|^p, k) + \alpha_4^{-1} \circ \rho^{-1} \circ \delta(v). \end{aligned}$$

Let us define

$$\beta(s, t) \triangleq \frac{1}{\alpha_1} \hat{\beta}(\alpha_2 s, t), \quad s \in \mathbb{R}^+, \quad t \in \mathbb{R}^+.$$

The function β is a function of class \mathcal{KL} , since $\hat{\beta}$ is a function of class \mathcal{KL} and α_1, α_2 are positive real numbers.

Let us define

$$\eta(r) \triangleq \frac{1}{\alpha_1} \alpha_4^{-1} \circ \rho^{-1} \circ \delta(r), \quad r \in \mathbb{R}^+.$$

Note that the function η is of class \mathcal{K} . After these definitions,

$$\mathbb{E}[\|x(k)\|^p] \leq \beta(\|x_0\|^p, k) + \eta\left(\sup_{s \in \mathbb{N}_{[0, k-1]}} (\|u(s)\|)\right), \quad (143)$$

for any $k \in \mathbb{N}$.

Then, the system described by (4.3) is p th moment ISS, according to Definition 16.

Proof of Corollary [1](#)

This section shows the proof of Corollary [1](#).

Proof 61 (Proof of Corollary [1](#)) Let us define the function

$$\alpha_4(s) \triangleq \frac{\tilde{\gamma}}{\alpha_2} s,$$

with $s \in \mathbb{R}^+$.

By applying an analogous reasoning as the one presented in the Proof of Theorem [9](#), the following inequality is satisfied,

$$\mathbb{E} [V(x(k+1), r(k+1))] \leq (I_d - \alpha_4) (\mathbb{E} [V(x(k), r(k))]) + \delta(v). \quad (144)$$

Let us assume, without loss of generality,

$$0 < \frac{\tilde{\gamma}}{\alpha_2} < 1.$$

Let us define

$$\rho(s) \triangleq \tilde{\rho} s,$$

with $0 < \tilde{\rho} < 1$.

Let us consider $j_0 \leq \infty$. Let j_0 be the minimum time such that:

$$\mathbb{E} [V(x(k), r(k))] \leq \alpha_4^{-1} \circ \rho^{-1} \circ \delta(v). \quad (145)$$

Then, by Claim [3](#), [\(145\)](#) holds for any $k \geq j_0$.

For $k \in \mathbb{N}_{[0, j_0-1]}$, inequality [\(146\)](#) can be written as follows,

$$\rho \circ \alpha_4 (\mathbb{E} [V(x(k), r(k))]) > \delta(v). \quad (146)$$

By adding and subtracting the quantity

$$\rho \circ \alpha_4 (\mathbb{E} [V(x(k), r(k))])$$

on the right-hand side of inequality [\(144\)](#), the quantity $\mathbb{E} [V(x(k+1), r(k+1))]$ satisfies the following inequality,

$$\mathbb{E} [V(x(k+1), r(k+1))] \leq \left[1 - (1 - \tilde{\rho}) \frac{\tilde{\gamma}}{\alpha_2} \right] \mathbb{E} [V(x(k), r(k))]. \quad (147)$$

Let us define

$$\zeta \triangleq \left[1 - (1 - \tilde{\rho}) \frac{\tilde{\gamma}}{\alpha_2} \right].$$

Particularly, $0 < \zeta < 1$.

Applying recursively (147), inequality (148) follows,

$$\mathbb{E} [V(x(k), r(k))] \leq \zeta^k \mathbb{E} [V(x(0), r(0))], \quad (148)$$

for any $k \in \mathbb{N}_{[0, j_0-1]}$.

Consider both (145) and (148).

Let us define

$$\theta \triangleq \frac{\alpha_2}{\alpha_1} \geq 1, \quad \eta(r) \triangleq \frac{1}{\alpha_1} \alpha_4^{-1} \circ \rho^{-1} \circ \delta(r).$$

The function η is a function of class \mathcal{K} , since ρ and α_4 are functions of class \mathcal{K}_∞ and δ is a function of class \mathcal{K} .

Applying condition (a), the following inequality holds,

$$\mathbb{E} [\|x(k)\|^p] \leq \theta \zeta^k \|x_0\|^p + \eta \left(\sup_{s \in \mathbb{N}_{[0, k-1]}} \|u(s)\| \right).$$

Appendix D

Preliminary Results necessary for the Proofs of Theorem [10](#)

Let us introduce some technical results that are useful in the proof of Theorem [10](#). Consider the scalar function

$$V : \mathcal{C} \times D \rightarrow \mathbb{R}^+.$$

Let us define the operator $\widehat{\mathcal{L}V}$ as follows,

$$\widehat{\mathcal{L}V} : \mathcal{C} \times D \rightarrow \mathbb{R},$$

associated with the scalar function V defined above.

The operator $\widehat{\mathcal{L}V}$ is defined for $\Phi \in \mathcal{C}$, $H^{-1}(i) \in D$, $i \in \mathcal{S}$

$$\widehat{\mathcal{L}V}(\phi, H^{-1}(i)) \triangleq \sum_{j \in \mathcal{S}} p_{ij} V(F(\phi, H^{-1}(i)), H^{-1}(j)) - V(\phi, H^{-1}(i)). \quad (149)$$

The following Lemma provides a preliminary result for the Proof of Theorem [10](#).

Lemma 16 Let there exist a function

$$V : \mathcal{C} \times D \rightarrow \mathbb{R}^+,$$

real positive numbers α_i , $i = 1, 2, 3$, such that, for all $\phi \in \mathcal{C}$, for all $H^{-1}(i) \in D$, for all $i \in \mathcal{S}$, the following inequalities hold,

$$a_1) \quad \alpha_1 \|\phi(0)\|^2 \leq V(\phi, H^{-1}(i)) \leq \alpha_2 \|\phi\|_\infty^2,$$

$$a_2) \quad \widehat{\mathcal{L}V}(\phi, H^{-1}(i)) \leq -\alpha_3 \|\phi(0)\|^2,$$

with $\widehat{\mathcal{L}V}$ defined in (149).

Then, there exist a function

$$W : \mathcal{C} \times D \rightarrow \mathbb{R}^+,$$

real positive numbers β_i , $i = 1, 2, 3$, such that, for all $\phi \in \mathcal{C}$, for all $H^{-1}(i) \in D$, for all $i \in \mathcal{S}$, the following inequalities hold:

$$b_1) \beta_1 \|\phi(0)\|^2 \leq W(\phi, H^{-1}(i)) \leq \beta_2 \|\phi\|_\infty^2,$$

$$b_2) \mathcal{L}W(\phi, H^{-1}(i)) \triangleq \sum_{j \in \mathcal{S}} p_{ij} W(F(\phi, H^{-1}(i)), H^{-1}(j)) - W(\phi, H^{-1}(i)) \leq -\beta_3 \|\phi\|_\infty^2.$$

Proof 62 (Proof of Lemma 16) Let us consider the function

$$W : \mathcal{C} \times D \rightarrow \mathbb{R}^+,$$

defined, for $\phi \in \mathcal{C}$, $H^{-1}(i) \in D$ for all $i \in \mathcal{S}$, as

$$W(\phi, H^{-1}(i)) = V(\phi, H^{-1}(i)) + \max_{\theta=1,2,\dots,\Delta} e^{-\theta} \alpha_3 \|\phi(-\theta)\|^2.$$

Then, from condition (a₁), it follows that,

$$\beta_1 \|\phi(0)\|^2 \leq W(\phi, H^{-1}(i)) \leq \beta_2 \|\phi\|_\infty^2, \quad (150)$$

with

$$\beta_1 = \alpha_1, \quad \beta_2 = \alpha_2 + \alpha_3.$$

From (a₂), the following equalities/inequalities hold,

$$\begin{aligned} & \sum_{j \in \mathcal{S}} p_{ij} W(F(\phi, H^{-1}(i)), H^{-1}(j)) - W(\phi, H^{-1}(i)) \\ &= \sum_{j \in \mathcal{S}} p_{ij} V(F(\phi, H^{-1}(i)), H^{-1}(j)) - V(\phi, H^{-1}(i)) \\ &+ \max_{\theta=1,2,\dots,\Delta} e^{-\theta} \alpha_3 \|\phi(-\theta+1)\|^2 - \max_{\theta=1,2,\dots,\Delta} e^{-\theta} \alpha_3 \|\phi(-\theta)\|^2 \\ &\leq -\alpha_3 \|\phi(0)\|^2 + e^{-1} \max_{\theta=1,2,\dots,\Delta} e^{1-\theta} \alpha_3 \|\phi(-\theta+1)\|^2 - \max_{\theta=1,2,\dots,\Delta} e^{-\theta} \alpha_3 \|\phi(-\theta)\|^2 \\ &\leq -\alpha_3 \|\phi(0)\|^2 + e^{-1} \max_{\theta=0,1,\dots,\Delta-1} e^{-\theta} \alpha_3 \|\phi(-\theta)\|^2 - \max_{\theta=1,2,\dots,\Delta} e^{-\theta} \alpha_3 \|\phi(-\theta)\|^2 \\ &\leq -\alpha_3 \|\phi(0)\|^2 + e^{-1} \alpha_3 \|\phi(0)\|^2 + e^{-1} \max_{\theta=1,2,\dots,\Delta} e^{-\theta} \alpha_3 \|\phi(-\theta)\|^2 \\ &- \max_{\theta=1,2,\dots,\Delta} e^{-\theta} \alpha_3 \|\phi(-\theta)\|^2 \\ &\leq -(1-e^{-1}) \alpha_3 \|\phi(0)\|^2 - (1-e^{-1}) \alpha_3 e^{-\Delta} \max_{\theta=1,2,\dots,\Delta} \|\phi(-\theta)\|^2 \\ &\leq -(1-e^{-1}) \alpha_3 e^{-\Delta} \|\phi\|_\infty^2. \end{aligned}$$

Let us define

$$\beta_3 = (1 - e^{-1}) \alpha_3 e^{-\Delta}.$$

Then,

$$\sum_{j \in \mathcal{S}} p_{ij} W(F(\phi, H^{-1}(i)), H^{-1}(j)) - W(\phi, H^{-1}(i)) \leq -\beta_3 \|\phi\|_\infty^2,$$

and thus, the function W satisfies conditions (b_1) , (b_2) .

This completes the proof.

Theorem 11 Assume that there exist a function

$$V : \mathcal{C} \times D \rightarrow \mathbb{R}^+,$$

real positive numbers γ_i , $i = 1, 2, 3$ such that, for all $\phi \in \mathcal{C}$, for all $H^{-1}(i) \in D$, for all $i \in \mathcal{S}$, the following inequalities hold:

$$c_1) \quad \gamma_1 \|\phi(0)\|^2 \leq V(\phi, H^{-1}(i)) \leq \gamma_2 \|\phi\|_\infty^2,$$

$$c_2) \quad \widehat{\mathcal{L}}V(\phi, H^{-1}(i)) \leq -\gamma_3 \|\phi\|_\infty^2,$$

with $\widehat{\mathcal{L}}V$ defined in (149).

Then, the system described by (5.1) is EMSS.

Proof 63 (Proof of Theorem 11) From condition (c_2) , by evaluating $\widehat{\mathcal{L}}V$ in $x_k \in \mathcal{C}$, $H^{-1}(\eta(k)) \in D$, for all $\eta(k) \in \mathcal{S}$, $k \in \mathbb{N}$, it follows that,

$$\begin{aligned} \widehat{\mathcal{L}}V(x_k, H^{-1}(\eta(k))) &= \sum_{\eta(k+1) \in \mathcal{S}} p_{\eta(k)\eta(k+1)} V(x_{k+1}, H^{-1}(\eta(k+1))) - V(x_k, H^{-1}(\eta(k))) \\ &\leq -\gamma_3 \|x_k\|_\infty^2. \end{aligned} \quad (151)$$

From (151), by applying the Markov property, we obtain:

$$\mathbb{E} \left[(V(x_{k+1}, H^{-1}(\eta(k+1))) - V(x_k, H^{-1}(\eta(k)))) \middle| \mathcal{G}_k \right] \leq -\gamma_3 \|x_k\|_\infty^2. \quad (152)$$

From (152), applying the property of the expected value conditioned to a filtration, the following inequality holds:

$$\mathbb{E} \left[V(x_{k+1}, H^{-1}(\eta(k+1))) - V(x_k, H^{-1}(\eta(k))) \right] \leq -\gamma_3 \mathbb{E} \left[\|x_k\|_\infty^2 \right]. \quad (153)$$

Exploiting the linearity of the expected value, from (153), the following inequality is satisfied,

$$\mathbb{E} \left[V(x_{k+1}, H^{-1}(\eta(k+1))) \right] - \mathbb{E} \left[V(x_k, H^{-1}(\eta(k))) \right] \leq -\gamma_3 \mathbb{E} \left[\|x_k\|_\infty^2 \right]. \quad (154)$$

From (c₁), it follows that,

$$\mathbb{E} \left[\|x_k\|_\infty^2 \right] \geq \frac{1}{\gamma_2} \mathbb{E} \left[V(x_k, H^{-1}(\eta(k))) \right]. \quad (155)$$

From (154) and (155), the following inequality is obtained

$$\mathbb{E} \left[V(x_{k+1}, H^{-1}(\eta(k+1))) \right] - \mathbb{E} \left[V(x_k, H^{-1}(\eta(k))) \right] \leq -\frac{\gamma_3}{\gamma_2} \mathbb{E} \left[V(x_k, H^{-1}(\eta(k))) \right]. \quad (156)$$

Let us define γ_4 , as follows,

$$\gamma_4 \triangleq \frac{\gamma_3}{\gamma_2}.$$

Notice that $\gamma_4 > 0$, since $\gamma_3 > 0$, $\gamma_2 > 0$.

Without loss of generality, pick $\gamma_4 < 1$.

From (156), it follows that

$$\mathbb{E} \left[V(x_{k+1}, H^{-1}(\eta(k+1))) \right] \leq (1 - \gamma_4) \mathbb{E} \left[V(x_k, H^{-1}(\eta(k))) \right]. \quad (157)$$

By applying recursive arguments, from (157), it follows that,

$$\mathbb{E} \left[V(x_k, H^{-1}(\eta(k))) \right] \leq (1 - \gamma_4)^k \mathbb{E} \left[V(\xi_0, H^{-1}(\eta(0))) \right]. \quad (158)$$

From (c₁),

$$\begin{aligned} \gamma_1 \mathbb{E}[\|x(k)\|^2] &\leq \mathbb{E}[V(x_k, H^{-1}(\eta(k)))], \\ (1 - \gamma_4)^k \mathbb{E}[V(\xi_0, H^{-1}(\eta(0)))] &\leq (1 - \gamma_4)^k \gamma_2 \mathbb{E}[\|\xi_0\|_\infty^2]. \end{aligned} \quad (159)$$

From (158) and (159), it follows that

$$\gamma_1 \mathbb{E}[\|x(k)\|^2] \leq (1 - \gamma_4)^k \gamma_2 \mathbb{E}[\|\xi_0\|_\infty^2]. \quad (160)$$

From (160), the following inequalities hold

$$\begin{aligned} \mathbb{E}[\|x(k)\|^2] &\leq (1 - \gamma_4)^k \frac{\gamma_2}{\gamma_1} \mathbb{E}[\|\xi_0\|_\infty^2] \\ &\leq (1 - \gamma_4)^k \frac{\gamma_2}{\gamma_1} \|\xi_0\|_\infty^2. \end{aligned} \quad (161)$$

Let us define

$$M \triangleq \frac{\gamma_2}{\gamma_1} \geq 1, \quad q \triangleq (1 - \gamma_4),$$

with $0 < q < 1$, from (161),

$$\mathbb{E} [\|x(k)\|^2] \leq Mq^k (\|\xi_0\|_\infty)^2. \quad (162)$$

Thus, the system described by (5.1) EMSS.

Proof of Theorem 10

From (i)-(ii), by Lemma 16, it follows that there exist a function

$$V : \mathcal{C} \times D \rightarrow \mathbb{R}^+,$$

$\gamma_i \in \mathbb{R}^+, i = 1, 2, 3$, such that, for all $\phi \in \mathcal{C}$, for all $H^{-1}(i) \in D$, for all $i \in \mathcal{S}$, the following inequalities hold:

$$c_1) \quad \gamma_1 \|\phi(0)\|^2 \leq V(\phi, H^{-1}(i)) \leq \gamma_2 \|\phi\|_\infty^2,$$

$$c_2) \quad \widehat{\mathcal{L}}V(\phi, H^{-1}(i)) \leq -\gamma_3 \|\phi\|_\infty^2.$$

From Theorem 11, it follows that the systems described by (5.1) is EMSS.

References

- [1] P. Sadeghi, R. A. Kennedy, P. B. Rapajic, and R. Shams, “Finite-state Markov modeling of fading channels - a survey of principles and applications,” *IEEE Signal Process. Mag.*, vol. 25, no. 5, pp. 57–80, 2008.
- [2] P. Park, S. Coleri Ergen, C. Fischione, C. Lu, and K. H. Johansson, “Wireless network design for control systems: A survey,” *IEEE Communications Surveys & Tutorials*, vol. 20, no. 2, pp. 978–1013, 2018.
- [3] P. Patrinos, P. Sopasakis, H. Sarimveis, and A. Bemporad, “Stochastic model predictive control for constrained discrete-time Markovian switching systems,” *Automatica*, vol. 50, no. 10, pp. 2504–2514, 2014.
- [4] O. L. V. Costa, M. D. Fragoso, and R. P. Marques, “Discrete-time Markov jump linear systems,” Springer, New York, 2005.
- [5] P. Park, “Modeling, analysis, and design of wireless sensor network protocols,” Ph.D. dissertation, School Electrical Engineering, KTH Royal Institute Technology, Stockholm, Sweden, 2011.
- [6] J. Sztipanovits, X. Koutsoukos, G. Karsai, N. Kottenstette, P. Antsaklis, V. Gupta, B. Goodwine, J. Baras, and S. Wang, “Toward a Science of Cyber–Physical System Integration,” *Proceedings of the IEEE*, vol. 100, no. 1, pp. 29–44, 2012.
- [7] A. W. Al-Dabbagh and T. Chen, “Design Considerations for Wireless Networked Control Systems,” *IEEE Transactions on Industrial Electronics*, vol. 63, no. 9, pp. 5547–5557, 2016.
- [8] A. Goldsmith, *Wireless Communications*. Cambridge University Press, 2005.

- [9] W.-A. Zhang and L. Yu, “Modelling and control of networked control systems with both network-induced delay and packet-dropout,” *Automatica*, vol. 44, no. 12, pp. 3206–3210, 2008. [Online]. Available: <https://www.sciencedirect.com/science/article/pii/S0005109808003154>
- [10] A. Willig, “Recent and Emerging Topics in Wireless Industrial Communications: A Selection,” *IEEE Transactions on Industrial Informatics*, vol. 4, no. 2, pp. 102–124, 2008.
- [11] V. C. Gungor and G. P. Hancke, “Industrial Wireless Sensor Networks: Challenges, Design Principles, and Technical Approaches,” *IEEE Transactions on Industrial Electronics*, vol. 56, no. 10, pp. 4258–4265, 2009.
- [12] P. Park, C. Fischione, A. Bonivento, K. H. Johansson, and A. Sangiovanni-Vincent, “Breath: An Adaptive Protocol for Industrial Control Applications Using Wireless Sensor Networks,” *IEEE Transactions on Mobile Computing*, vol. 10, no. 6, pp. 821–838, 2011.
- [13] A. A. Kumar S., K. Ovsthus, and L. M. Kristensen., “An Industrial Perspective on Wireless Sensor Networks — A Survey of Requirements, Protocols, and Challenges,” *IEEE Communications Surveys & Tutorials*, vol. 16, no. 3, pp. 1391–1412, 2014.
- [14] Q. Wang and J. Jiang, “Comparative Examination on Architecture and Protocol of Industrial Wireless Sensor Network Standards,” *IEEE Communications Surveys & Tutorials*, vol. 18, no. 3, pp. 2197–2219, 2016.
- [15] E. Witrant, P. Di Marco, P. Park, and C. Briat, “Limitations and performances of robust control over WSN: UFAD control in intelligent buildings,” *IMA Journal of Mathematical Control and Information*, vol. 27, no. 4, pp. 527–543, 11 2010. [Online]. Available: <https://doi.org/10.1093/imamci/dnq017>
- [16] Y. Sadi and S. C. Ergen, “Optimal Power Control, Rate Adaptation, and Scheduling for UWB-Based Intravehicular Wireless Sensor Networks,” *IEEE Transactions on Vehicular Technology*, vol. 62, no. 1, pp. 219–234, 2013.
- [17] X. Yu and Y. Xue, “Smart grids: A cyber–physical systems perspective,” *Proceedings of the IEEE*, vol. 104, no. 5, pp. 1058–1070, 2016.

- [18] C. Lu, A. Saifullah, B. Li, M. Sha, H. Gonzalez, D. Gunatilaka, C. Wu, L. Nie, and Y. Chen, “Real-Time Wireless Sensor-Actuator Networks for Industrial Cyber-Physical Systems,” *Proceedings of the IEEE*, vol. 104, no. 5, pp. 1013–1024, 2016.
- [19] M. Pajic, J. Le Ny, S. Sundaram, G. J. Pappas, and R. Mangharam, “Closing the loop: A simple distributed method for control over wireless networks,” in *2012 ACM/IEEE 11th International Conference on Information Processing in Sensor Networks (IPSN)*, 2012, pp. 25–36.
- [20] M. Pajic, S. Sundaram, J. Le Ny, G. J. Pappas, and R. Mangharam, “The Wireless Control Network: Synthesis and robustness,” in *49th IEEE Conference on Decision and Control (CDC)*, 2010, pp. 7576–7581.
- [21] M. Pajic, S. Sundaram, G. J. Pappas, and R. Mangharam, “Topological conditions for wireless control networks,” in *2011 50th IEEE Conference on Decision and Control and European Control Conference*, 2011, pp. 2353–2360.
- [22] J. R. Moyne and D. M. Tilbury, “The Emergence of Industrial Control Networks for Manufacturing Control, Diagnostics, and Safety Data,” *Proceedings of the IEEE*, vol. 95, no. 1, pp. 29–47, 2007.
- [23] G. C. Goodwin, S. F. Graebe, and M. E. Salgado, *Control System Design*, 1st ed. USA: Prentice Hall PTR, 2000.
- [24] V. Gupta, A. F. Dana, J. P. Hespanha, R. M. Murray, and B. Hassibi, “Data transmission over networks for estimation and control,” *IEEE Transactions on Automatic Control*, vol. 54, no. 8, pp. 1807–1819, 2009.
- [25] B. Ding, “Stabilization of linear systems over networks with bounded packet loss and its use in model predictive control,” *Automatica*, vol. 47, no. 11, pp. 2526–2533, 2011.
- [26] J. P. Hespanha, P. Naghshtabrizi, and Y. Xu, “A Survey of Recent Results in Networked Control Systems,” *Proceedings IEEE*, vol. 95, no. 1, pp. 138–162, 2007.

- [27] M. Cloosterman, L. Hetel, N. van de Wouw, W. Heemels, J. Daafouz, and H. Nijmeijer, “Controller synthesis for networked control systems,” *Automatica*, vol. 46, no. 10, pp. 1584–1594, 2010. [Online]. Available: <https://www.sciencedirect.com/science/article/pii/S0005109810002670>
- [28] B. Sinopoli, L. Schenato, M. Franceschetti, K. Poolla, and S. Sastry, “Optimal control with unreliable communication: the TCP case,” in *Proceedings of the 2005, American Control Conference, 2005.*, 2005, pp. 3354–3359 vol. 5.
- [29] I. Tomić and J. A. McCann, “A Survey of Potential Security Issues in Existing Wireless Sensor Network Protocols,” *IEEE Internet of Things Journal*, vol. 4, no. 6, pp. 1910–1923, 2017.
- [30] D. E. Quevedo, A. Ahlen, and K. H. Johansson, “State Estimation Over Sensor Networks With Correlated Wireless Fading Channels,” *IEEE Transactions on Automatic Control*, vol. 58, no. 3, pp. 581–593, 2013.
- [31] J. Xiong and J. Lam, “Stabilization of Networked Control Systems With a Logic ZOH,” *IEEE Transactions on Automatic Control*, vol. 54, no. 2, pp. 358–363, 2009.
- [32] M. Branicky, S. Phillips, and W. Zhang, “Stability of networked control systems: explicit analysis of delay,” in *Proceedings of the 2000 American Control Conference. ACC (IEEE Cat. No.00CH36334)*, vol. 4, 2000, pp. 2352–2357 vol.4.
- [33] W.-A. Zhang and L. Yu, “A robust control approach to stabilization of networked control systems with time-varying delays,” *Automatica*, vol. 45, no. 10, pp. 2440–2445, 2009. [Online]. Available: <https://www.sciencedirect.com/science/article/pii/S0005109809002933>
- [34] A. S. Leong, D. E. Quevedo, and S. Dey, “State estimation over Markovian packet dropping links in the presence of an eavesdropper,” in *2017 IEEE 56th Annual Conference on Decision and Control (CDC)*, 2017, pp. 6616–6621.
- [35] M. S. Chong, H. Sandberg, and A. M. Teixeira, “A Tutorial Introduction to Security and Privacy for Cyber-Physical Systems,” in *2019 18th European Control Conference (ECC)*, 2019, pp. 968–978.

- [36] G. Fiore, Y. H. Chang, Q. Hu, M. D. Di Benedetto, and C. J. Tomlin, “Secure state estimation for Cyber Physical Systems with sparse malicious packet drops,” in *2017 American Control Conference (ACC)*, 2017, pp. 1898–1903.
- [37] A. Tsiamis, K. Gatsis, and G. J. Pappas, “State-Secrecy Codes for Networked Linear Systems,” *IEEE Transactions on Automatic Control*, vol. 65, no. 5, pp. 2001–2015, 2020.
- [38] —, “State Estimation with Secrecy against Eavesdroppers,” *IFAC-PapersOnLine*, vol. 50, no. 1, pp. 8385–8392, 2017.
- [39] A. B. Alexandru, A. Tsiamis, and G. J. Pappas, “Encrypted Distributed Lasso for Sparse Data Predictive Control,” in *60th IEEE Conference on Decision and Control*, 2021, pp. 4901–4906.
- [40] M. Schulze Darup, A. B. Alexandru, D. E. Quevedo, and G. J. Pappas, “Encrypted Control for Networked Systems: An Illustrative Introduction and Current Challenges,” *IEEE Control Systems Magazine*, vol. 41, no. 3, pp. 58–78, 2021.
- [41] A. B. Alexandru, K. Gatsis, Y. Shoukry, S. A. Seshia, P. Tabuada, and G. J. Pappas, “Cloud-Based Quadratic Optimization With Partially Homomorphic Encryption,” *IEEE Transactions on Automatic Control*, vol. 66, no. 5, pp. 2357–2364, 2021.
- [42] A. D’Innocenzo, M. D. Di Benedetto, and E. Serra, “Fault tolerant control of multi-hop control networks,” *IEEE Transactions on Automatic Control*, vol. 58, no. 6, pp. 1377–1389, 2013.
- [43] B. Sinopoli, L. Schenato, M. Franceschetti, K. Poolla, and S. Sastry, “Time varying optimal control with packet losses,” in *2004 43rd IEEE Conference on Decision and Control (CDC)*, vol. 2, 2004, pp. 1938–1943 Vol.2.
- [44] —, “Optimal Linear LQG Control Over Lossy Networks Without Packet Acknowledgment,” in *Proceedings of the 45th IEEE Conference on Decision and Control (CDC)*, 2006, pp. 392–397.
- [45] —, “An LQG Optimal Linear Controller for Control Systems with Packet Losses,” in *Proceedings of the 44th IEEE Conference on Decision and Control*, 2005, pp. 458–463.

- [46] W. P. M. H. Heemels, A. R. Teel, N. van de Wouw, and D. Nesic, “Networked control systems with communication constraints: Tradeoffs between transmission intervals, delays and performance,” *IEEE Transactions on Automatic Control*, vol. 55, no. 8, pp. 1781–1796, 2010.
- [47] J. Xiong and J. Lam, “Stabilization of linear systems over networks with bounded packet loss,” *Automatica*, vol. 43, no. 1, pp. 80–87, 2007.
- [48] L. Schenato, B. Sinopoli, M. Franceschetti, K. Poolla, and S. S. Sastry, “Foundations of Control and Estimation Over Lossy Networks,” *Proceedings IEEE*, vol. 95, no. 1, pp. 163–187, 2007.
- [49] B. Sinopoli, L. Schenato, M. Franceschetti, K. Poolla, M. Jordan, and S. Sastry, “Kalman filtering with intermittent observations,” *IEEE Transactions on Automatic Control*, vol. 49, no. 9, pp. 1453–1464, 2004.
- [50] M. Pajic, S. Sundaram, G. J. Pappas, and R. Mangharam, “The wireless control network: a new approach for control over networks,” *IEEE Transactions on Automatic Control*, vol. 56, no. 10, pp. 2305–2318, 2011.
- [51] K. Gatsis and G. J. Pappas, “Statistical learning for analysis of networked control systems over unknown channels,” *Automatica*, vol. 125, p. 109386, 2021. [Online]. Available: <https://www.sciencedirect.com/science/article/pii/S0005109820305884>
- [52] I. Matei, N. C. Martins, and J. S. Baras, “Optimal Linear Quadratic Regulator for Markovian Jump Linear Systems, in the presence of one time-step delayed mode observations,” *IFAC Proc.*, vol. 41, no. 2, pp. 8056–8061, 2008.
- [53] —, “Optimal state estimation for discrete-time Markovian Jump Linear Systems, in the presence of delayed mode observations,” in *2008 American Control Conference*, 2008, pp. 3560–3565.
- [54] R. Alur, A. D’Innocenzo, K. H. Johansson, G. J. Pappas, and G. Weiss, “Compositional Modeling and Analysis of Multi-Hop Control Networks,” *IEEE Transactions on Automatic Control*, vol. 56, no. 10, pp. 2345–2357, 2011.

- [55] A. P. C. Gonçalves, A. R. Fioravanti, and J. C. Geromel, "Markov jump linear systems and filtering through network transmitted measurements," *Signal Process.*, vol. 90, no. 10, pp. 2842–2850, 2010.
- [56] O. Costa and M. Fragoso, "Comments on "Stochastic stability of jump linear systems",", *IEEE Transactions on Automatic Control*, vol. 49, no. 8, pp. 1414–1416, 2004.
- [57] E. Costa, J. do Val, and M. Fragoso, "Weak detectability and the LQ problem of discrete-time infinite Markov jump linear systems," in *42nd IEEE International Conference on Decision and Control (IEEE Cat. No.03CH37475)*, vol. 6, 2003, pp. 5789–5794 Vol.6.
- [58] E. F. Costa, J. B. do Val, and M. D. Fragoso, "On a detectability concept of discrete-time infinite Markov jump linear systems," *IFAC Proceedings Volumes*, vol. 35, no. 1, pp. 437–442, 2002, 15th IFAC World Congress. [Online]. Available: <https://www.sciencedirect.com/science/article/pii/S1474667015395653>
- [59] O. Costa, E. Assumpção Filho, E. Boukas, and R. Marques, "Constrained quadratic state feedback control of discrete-time markovian jump linear systems," *Automatica*, vol. 35, no. 4, pp. 617–626, 1999.
- [60] C. Lutz, "Switched Markov jump linear systems: analysis and control synthesis," PhD Thesis, Virginia Polytechnic Institute and State University, 2014.
- [61] C. Luo, J. Ji, Q. Wang, X. Chen, and P. Li, "Channel state information prediction for 5G wireless communications: A deep learning approach," *IEEE Transactions on Network Science and Engineering*, vol. 7, no. 1, pp. 227–236, 2018.
- [62] Y. Zacchia Lun, C. Rinaldi, A. Alrish, A. D’Innocenzo, and F. Santucci, "On the impact of accurate radio link modeling on the performance of WirelessHART control networks," in *IEEE Conf. Comput. Commun. (INFOCOM)*, 2020, pp. 2430–2439.
- [63] Y. Zacchia Lun, "Stability and optimal control of polytopic time-inhomogeneous Markov jump linear systems," PhD Thesis, Gran Sasso Science Institute, 2017.

- [64] Y. Zacchia Lun, A. D’Innocenzo, and M. D. Di Benedetto, “Robust stability of time-inhomogeneous Markov Jump Linear Systems,” *IFAC-PapersOnLine*, vol. 50, no. 1, pp. 3418–3423, 2017.
- [65] Y. Zacchia Lun, A. D’Innocenzo, A. Abate, and M. D. Di Benedetto, “Optimal robust control and a separation principle for polytopic time-inhomogeneous markov jump linear systems,” *IEEE 56th Conf. Decis. Control*, pp. 6525–6530, 2017.
- [66] G. D. Di Girolamo and A. D’Innocenzo, “Codesign of controller, routing and scheduling in WirelessHART networked control systems,” *International Journal of Robust and Nonlinear Control*, vol. 29, no. 7, pp. 2171–2187, 2019.
- [67] Y. Zacchia Lun, A. D’Innocenzo, and M. D. Di Benedetto, “Robust stability of polytopic time-inhomogeneous Markov Jump Linear Systems,” *Automatica*, vol. 105, pp. 286–297, 2019.
- [68] D. Liberzon, “Switching in Systems and Control,” Birkhauser, Basel, Switzerland, 2003.
- [69] A. Girard and P. Mason, “Lyapunov Functions for Shuffle Asymptotic Stability of Discrete-Time Switched Systems,” *IEEE Control Systems Letters*, vol. 3, no. 3, pp. 499–504, 2019.
- [70] M. Fiacchini, M. Jungers, and A. Girard, “Stabilization and control Lyapunov functions for language constrained discrete-time switched linear systems,” *Automatica*, vol. 93, pp. 64–74, 2018. [Online]. Available: <https://www.sciencedirect.com/science/article/pii/S0005109818301262>
- [71] L. Etienne, A. Girard, and L. Greco, “Stability and stabilizability of discrete-time dual switching systems with application to sampled-data systems,” *Automatica*, vol. 100, pp. 388–395, 2019. [Online]. Available: <https://www.sciencedirect.com/science/article/pii/S0005109818305466>
- [72] H. Lin and P. J. Antsaklis, “Stability and Stabilizability of Switched Linear Systems: A Survey of Recent Results,” *IEEE Transactions on Automatic Control*, vol. 54, no. 2, pp. 308–322, 2009.

- [73] M. Yu, L. Wang, T. Chu, and G. Xie, “Stabilization of networked control systems with data packet dropout and network delays via switching system approach,” in *2004 43rd IEEE Conference on Decision and Control (CDC) (IEEE Cat. No.04CH37601)*, vol. 4, 2004, pp. 3539–3544 Vol.4.
- [74] A. F. Molish, *Wireless Communications*. IEEE PRESS, 2010.
- [75] P. Fuhrmann, “On some uses of factorizations in linear system theory,” *Annual Reviews in Control*, vol. 21, pp. 13–30, 1997. [Online]. Available: <https://www.sciencedirect.com/science/article/pii/S1367578897000321>
- [76] W.-A. Zhang and L. Yu, “Output Feedback Stabilization of Networked Control Systems With Packet Dropouts,” *IEEE Transactions on Automatic Control*, vol. 52, no. 9, pp. 1705–1710, 2007.
- [77] A. Impicciatore, Y. Zacchia Lun, P. Pepe, and A. D’Innocenzo, “Optimal output-feedback control over Markov wireless communication channels,” *IEEE Transactions on Automatic Control*. Under Review, 2022.
- [78] A. Mammadov and B. Abbasov, “A review of protocols related to enhancement of TCP performance in wireless and WLAN networks,” in *2014 IEEE 8th International Conference on Application of Information and Communication Technologies (AICT)*, 2014, pp. 1–4.
- [79] Y. Zacchia Lun and A. D’Innocenzo, “Stabilizability of Markov jump linear systems modeling wireless networked control scenarios,” in *IEEE Conference on Decision and Control (CDC)*, 2019, pp. 5766–5772.
- [80] H. Shousong and Z. Qixin, “Stochastic optimal control and analysis of stability of networked control systems with long delay,” *Automatica*, vol. 39, no. 11, pp. 1877–1884, 2003. [Online]. Available: <https://www.sciencedirect.com/science/article/pii/S0005109803001961>
- [81] A. Isidori, *Nonlinear Control Systems*. Springer London, 1995.
- [82] G. K. Pandey, D. S. Gurjar, H. H. Nguyen, and S. Yadav, “Security Threats and Mitigation Techniques in UAV Communications: A Comprehensive Survey,” *IEEE Access*, vol. 10, pp. 112 858–112 897, 2022.

- [83] Y. Hua and A. Maksud, “Unconditional secrecy and computational complexity against wireless eavesdropping,” in *2020 IEEE 21st International Workshop on Signal Processing Advances in Wireless Communications (SPAWC)*, 2020, pp. 1–5.
- [84] L. Wang, X. Cao, B. Sun, H. Zhang, and C. Sun, “Optimal Schedule of Secure Transmissions for Remote State Estimation Against Eavesdropping,” *IEEE Transactions on Industrial Informatics*, vol. 17, no. 3, pp. 1987–1997, 2021.
- [85] M. A. Arfaoui, M. D. Soltani, I. Tavakkolnia, A. Ghrayeb, M. Safari, C. M. Assi, and H. Haas, “Physical Layer Security for Visible Light Communication Systems: A Survey,” *IEEE Communications Surveys & Tutorials*, vol. 22, no. 3, pp. 1887–1908, 2020.
- [86] A. S. Leong, D. E. Quevedo, D. Dolz, and S. Dey, “Transmission Scheduling for Remote State Estimation Over Packet Dropping Links in the Presence of an Eavesdropper,” *IEEE Transactions on Automatic Control*, vol. 64, no. 9, pp. 3732–3739, 2019.
- [87] A. Impicciatore, A. Tsiamis, Y. Zacchia Lun, A. D’Innocenzo, and G. J. Pappas, “Secure state estimation over Markov wireless communication channels,” *IEEE 61st Conference on Decision Control*, 2022.
- [88] S. Battilotti, F. Cacace, M. d’Angelo, A. Germani, and B. Sinopoli, “Kalman-like filtering with intermittent observations and non-Gaussian noise,” *IFAC-PapersOnLine*, vol. 52, no. 20, pp. 61–66, 2019, 8th IFAC Workshop on Distributed Estimation and Control in Networked Systems NECSYS 2019. [Online]. Available: <https://www.sciencedirect.com/science/article/pii/S2405896319319676>
- [89] S. Battilotti, F. Cacace, M. D’Angelo, and A. Germani, “Distributed Kalman Filtering Over Sensor Networks With Unknown Random Link Failures,” *IEEE Control Systems Letters*, vol. 2, no. 4, pp. 587–592, 2018.
- [90] P. Bolzern and P. Colaneri, 2015.
- [91] A. Impicciatore, Y. Zacchia Lun, P. Pepe, and A. D’Innocenzo, “Optimal output-feedback control and separation principle for Markov jump linear systems

- modeling wireless networked control scenarios (extended version),” 2021. [Online]. Available: <https://arxiv.org/abs/2103.08992>
- [92] —, “Optimal output-feedback control and separation principle for Markov jump linear systems modeling wireless networked control scenarios,” in *American Control Conference (ACC)*, 2021, pp. 2700–2706.
- [93] H. Khalil, *Nonlinear systems*, A. Dworkin, Ed. Prentice Hall, 1996.
- [94] I. Karafyllis and Z.-P. Jiang, *Stability and Stabilization of Nonlinear Systems*, 2011.
- [95] S. Sastry, *Nonlinear Systems. Analysis, Stability, and Control*. Springer New York, NY, 1999.
- [96] M. Vidyasagar, *Nonlinear Systems Analysis: Second Edition*, ser. Classics in Applied Mathematics. Society for Industrial and Applied Mathematics, 2002. [Online]. Available: <https://books.google.it/books?id=PqIhcZAzI0oC>
- [97] A. Impicciatore, P. Pepe, and A. D’Innocenzo, “Lyapunov characterizations of exponential mean square input-to-state stability for discrete-time Markovian switching nonlinear systems,” *IEEE Transactions on Automatic Control*, pp. 1–16, 2022.
- [98] B. Wu, M. Cubuktepe, and U. Topcu, “Switched Linear Systems meet Markov Decision Processes: Stability Guaranteed Policy Synthesis,” in *Proceedings IEEE 58th Conf. Decis. Control (CDC)*, 2019, pp. 2509–2515.
- [99] M. Huang, “Stochastic Optimal Control with Markovian Lossy State Observations,” in *Proceedings IEEE 58th Conf. Decis. Control (CDC)*, 2019, pp. 678–683.
- [100] P. Sopasakis, D. Herceg, A. Bemporad, and P. Patrinos, “Risk-averse model predictive control,” *Automatica*, vol. 100, pp. 281–288, 2019.
- [101] L. Zhang, Y. Leng, and P. Colaneri, “Stability and Stabilization of Discrete-Time Semi-Markov Jump Linear Systems via Semi-Markov Kernel Approach,” *IEEE Transactions on Automatic Control*, vol. 61, no. 2, pp. 503–508, 2016.

- [102] A. N. Vargas, C. M. Agulhari, R. C. L. F. Oliveira, and V. M. Preciado, “Robust Stability Analysis of Linear Parameter-Varying Systems With Markov Jumps,” *IEEE Transactions on Automatic Control*, vol. 67, no. 11, pp. 6234–6239, 2022.
- [103] D. Nesic, A. Teel, and E. Sontag, “On stability and input-to-state stability Kl estimates of discrete-time and sampled-data nonlinear systems,” vol. 6, 1999, Conference paper, p. 3990 – 3994, cited by: 1. [Online]. Available: <https://www.scopus.com/inward/record.uri?eid=2-s2.0-0033285286&partnerID=40&md5=beba81518c71c4e012065e11e8fb0691>
- [104] E. Sontag, “Remarks on stabilization and input-to-state stability,” in *Proceedings of the 28th IEEE Conference on Decision and Control*, 1989, pp. 1376–1378 vol.2.
- [105] E. D. Sontag and Y. Wang, “New characterizations of input-to-state stability,” *IEEE Transactions on Automatic Control*, vol. 41, no. 9, pp. 1283–1294, 1996.
- [106] E. D. Sontag, *Mathematical Control Theory*. Springer-Verlag, 1990.
- [107] —, “Further facts about input to state stabilization,” *IEEE Transactions on Automatic Control*, vol. 35, no. 4, pp. 473–476, apr 1990.
- [108] M. Arcak, D. Angeli, and E. Sontag, “Stabilization of cascades using integral input-to-state stability,” in *Proceedings of the 40th IEEE Conference on Decision and Control (Cat. No.01CH37228)*, vol. 4, 2001, pp. 3814–3819 vol.4.
- [109] E. Sontag, “Notions of integral input-to-state stability,” in *Proceedings of the 1998 American Control Conference. ACC (IEEE Cat. No.98CH36207)*, vol. 5, 1998, pp. 3210–3214 vol.5.
- [110] D. Angeli, E. Sontag, and Y. Wang, “A remark on integral input to state stability,” in *Proceedings of the 37th IEEE Conference on Decision and Control (Cat. No.98CH36171)*, vol. 3, 1998, pp. 2491–2496 vol.3.
- [111] D. Angeli, E. D. Sontag, and Y. Wang, “A characterization of integral input-to-state stability,” *IEEE Transactions on Automatic Control*, vol. 45, no. 6, pp. 1082–1097, 2000.

- [112] E. Sontag and Y. Wang, “Notions equivalent to input-to-state stability,” vol. 4, 1994, Conference paper, p. 3438 – 3448, cited by: 5. [Online]. Available: <https://www.scopus.com/inward/record.uri?eid=2-s2.0-0028748865&partnerID=40&md5=4e28a7bc0b51eef8f960f97edebd5d25>
- [113] E. D. Sontag and Y. Wang, “On characterizations of the input-to-state stability property,” *Systems & Control Letters*, vol. 24, no. 5, pp. 351–359, 1995.
- [114] E. D. Sontag, “Comments on integral variants of ISS,” *Systems & Control Letters*, vol. 34, no. 1, pp. 93–100, 1998.
- [115] —, “Smooth stabilization implies coprime factorization,” *IEEE Transactions on Automatic Control*, vol. 34, no. 4, pp. 435–443, apr 1989.
- [116] Y. Lin, E. Sontag, and Y. Wang, “Various results concerning set input-to-state stability,” in *Proceedings of 1995 34th IEEE Conference on Decision and Control*, vol. 2, 1995, pp. 1330–1335 vol.2.
- [117] Y. Lin, E. D. Sontag, and Y. Wang, “Input to state stabilizability for parametrized families of systems,” *International Journal of Robust and Nonlinear Control*, vol. 5, no. 3, pp. 187–205, 1995. [Online]. Available: <https://onlinelibrary.wiley.com/doi/abs/10.1002/rnc.4590050304>
- [118] E. D. Sontag, “On the Input-to-State Stability Property,” *European Journal of Control*, vol. 1, no. 1, pp. 24–36, 1995. [Online]. Available: <https://www.sciencedirect.com/science/article/pii/S094735809570005X>
- [119] E. Sontag and Y. Wang, “Lyapunov Characterizations of Input to Output Stability,” *SIAM Journal on Control and Optimization*, vol. 39, no. 1, pp. 226–249, 2000.
- [120] L. Grüne, E. D. Sontag, and F. R. Wirth, “Asymptotic stability equals exponential stability, and ISS equals finite energy gain — if you twist your eyes,” *Systems & Control Letters*, vol. 38, no. 2, pp. 127–134, 1999.
- [121] D. Liberzon, E. D. Sontag, and Y. Wang, “On integral-input-to-state stabilization,” vol. 3, 1999, p. 1598 – 1602.

- [122] H. Ito, P. Pepe, and Z.-P. Jiang, “A small-gain condition for iISS of interconnected retarded systems based on Lyapunov–Krasovskii functionals,” *Automatica*, vol. 46, no. 10, pp. 1646–1656, 2010.
- [123] S. Peng and F. Deng, “New Criteria on p th Moment Input-to-State Stability of Impulsive Stochastic Delayed Differential Systems,” *IEEE Transactions on Automatic Control*, vol. 62, no. 7, pp. 3573–3579, 2017.
- [124] W. Hu, Q. Zhu, and H. R. Karimi, “On the p th moment integral input-to-state stability and input-to-state stability criteria for impulsive stochastic functional differential equations,” *International Journal of Robust and Nonlinear Control*, vol. 29, no. 16, pp. 5609–5620, 2019.
- [125] X. Wu and Y. Zhang, “ p th moment exponential input-to-state stability of nonlinear discrete-time impulsive stochastic delay systems,” *Int. J. Robust Nonlin*, vol. 28, no. 17, pp. 5590–5604, 2018.
- [126] H. Chen, P. Shi, and C.-C. Lim, “A new unified input-to-state stability criterion for impulsive stochastic delay systems with Markovian switching,” *International Journal of Robust and Nonlinear Control*, vol. 30, no. 1, pp. 159–181, 2020.
- [127] P. Pepe, I. Karafyllis, and Z. Jiang, “Lyapunov–Krasovskii characterization of the input-to-state stability for neutral systems in Hale’s form,” *Systems & Control Letters*, vol. 102, pp. 48–56, 2017. [Online]. Available: <https://www.sciencedirect.com/science/article/pii/S0167691117300129>
- [128] H. Ito, Z.-P. Jiang, and P. Pepe, “Construction of Lyapunov–Krasovskii functionals for networks of iISS retarded systems in small-gain formulation,” *Automatica*, vol. 49, no. 11, pp. 3246–3257, 2013.
- [129] H. Ito, P. Pepe, and Z.-P. Jiang, “Decentralized Robustification of Interconnected Time-Delay Systems Based on Integral Input-to-State Stability,” in *Delay Systems, From Theory to Numerics and Applications, Advances in Delays and Dynamics*, T. Vyhlídal, J.-F. Lafay, and R. Sipahi, Eds. Springer, 2014, vol. 1, pp. 199–213.
- [130] P. Pepe and H. Ito, “On Saturation, Discontinuities, and Delays, in iISS and ISS Feedback Control Redesign,” *IEEE Transactions on Automatic Control*, vol. 57, no. 5, pp. 1125–1140, 2012.

- [131] S. Dashkovskiy and A. Mironchenko, “Input-to-state stability of infinite-dimensional control systems,” *Mathematics of Control, Signals, and Systems*, vol. 25, no. 1, pp. 1–35, 2013.
- [132] A. Mironchenko, I. Karafyllis, and M. Krstic, “Monotonicity methods for input-to-state stability of nonlinear parabolic PDEs with boundary disturbances,” *SIAM Journal on Control and Optimization*, vol. 57, no. 1, pp. 510–532, 2019.
- [133] J. L. Mancilla-Aguilar and R. A. García, “A converse Lyapunov theorem for nonlinear switched systems,” *Systems & Control Letters*, vol. 41, no. 1, pp. 67–71, 2000. [Online]. Available: <https://www.sciencedirect.com/science/article/pii/S0167691100000402>
- [134] ———, “On converse Lyapunov theorems for ISS and iISS switched nonlinear systems,” *Systems & Control Letters*, vol. 42, no. 1, pp. 47–53, 2001.
- [135] J. L. Mancilla-Aguilar, R. García, E. Sontag, and Y. Wang, “Uniform stability properties of switched systems with switchings governed by digraphs,” *Nonlinear Analysis: Theory, Methods & Applications*, vol. 63, no. 3, pp. 472–490, 2005.
- [136] P. Pepe, “Converse Lyapunov Theorems for Discrete-Time Switching Systems with Given Switches Digraphs,” *IEEE Transactions on Automatic Control*, vol. 64, no. 6, pp. 2502–2508, 2019.
- [137] Z. Li, H. Xiao, and J. Song, “A converse Lyapunov theorem for the discrete switched system,” in *2011 Chinese Control and Decision Conference (CCDC)*, 2011, pp. 3947–3951.
- [138] L. Kleinrock, *Queueing Systems*. New York: John Wiley and Sons, 1976.
- [139] R. Goebel, “Discrete-Time Switching Systems as Difference Inclusions: Deducing Converse Lyapunov Results for the Former From Those for the Latter,” *IEEE Transactions on Automatic Control*, 2022. [Online]. Available: <https://doi.org/10.1109/TAC.2022.3192810>
- [140] P. Pepe, “On Lyapunov Methods for Nonlinear Discrete-Time Switching Systems With Dwell-Time Ranges,” *IEEE Transactions on Automatic Control*, vol. 67, no. 3, pp. 1574–1581, 2022.

- [141] R. B. Ash, *Real Analysis and Probability*, ser. Probability and Mathematical Statistics: A Series of Monographs and Textbooks. Academic Press, 1972.
- [142] A. Impicciatore, A. D’Innocenzo, and P. Pepe, “Sufficient Lyapunov conditions for p th moment ISS of discrete-time Markovian Switching Systems,” in *Proceedings IEEE 59th Conference on Decision Control (CDC)*. IEEE, Dec. 2020.
- [143] S. Peng and Y. Zhang, “Some New Criteria on p th Moment Stability of Stochastic Functional Differential Equations With Markovian Switching,” *IEEE Transactions on Automatic Control*, vol. 55, no. 12, pp. 2886–2890, 2010.
- [144] L. Huang and X. Mao, “On Input-to-State Stability of Stochastic Retarded Systems with Markovian Switching,” *IEEE Transactions on Automatic Control*, vol. 54, no. 8, pp. 1898–1902, 2009.
- [145] A. Tejada, O. R. González, and W. S. Gray, “On nonlinear discrete-time systems driven by Markov chains,” *Journal of the Franklin Institute*, vol. 347, no. 5, pp. 795–805, 2010.
- [146] W.-A. ZHANG and L. YU, “A robust control approach to stabilization of networked control systems with short time-varying delays,” *Acta Automatica Sinica*, vol. 36, no. 1, pp. 87–91, 2010. [Online]. Available: <https://www.sciencedirect.com/science/article/pii/S1874102909600069>
- [147] J. Nilsson, B. Bernhardsson, and B. Wittenmark, “Stochastic analysis and control of real-time systems with random time delays,” *Automatica*, vol. 34, no. 1, pp. 57–64, 1998. [Online]. Available: <https://www.sciencedirect.com/science/article/pii/S0005109897001702>
- [148] D. C. Bortolin, G. M. Gagliardi, and M. H. Terra, “Recursive Robust Regulator for Uncertain Linear Systems with Random State Delay Based on Markovian Jump Model,” *Proceedings of the IEEE Conference on Decision and Control*, vol. 2018-Decem, no. Cdc, pp. 6228–6233, 2019.
- [149] D. Nešić, A. Teel, and E. Sontag, “Formulas relating KL stability estimates of discrete-time and sampled-data nonlinear systems,” *Systems & Control Letters*, vol. 38, no. 1, pp. 49–60, 1999.

- [150] M. Di Ferdinando, “Sampled-Data Control of Nonlinear Time-Delay Systems,” PhD Thesis, University of L’Aquila, 2019.
- [151] E. Fridman, *Introduction to Time-Delay Systems: Analysis and Control*, ser. Systems & Control: Foundations & Applications. Springer International Publishing, 2014. [Online]. Available: <https://books.google.it/books?id=8i1nBAAAQBAJ>
- [152] F. Battista and P. Pepe, “Small-Gain Theorems for Nonlinear Discrete-Time Systems with Uncertain Time-Varying Delays,” in *2018 IEEE Conference on Decision and Control (CDC)*, 2018, pp. 2029–2034.
- [153] A. Germani and P. Pepe, “A State Observer for a Class of Nonlinear Systems with Multiple Discrete and Distributed Time Delays,” *European Journal of Control*, vol. 11, no. 3, pp. 196–205, 2005. [Online]. Available: <https://www.sciencedirect.com/science/article/pii/S0947358005710517>
- [154] P. Pepe, “On Control Lyapunov–Razumikhin Functions, Nonconstant Delays, Nonsmooth Feedbacks, and Nonlinear Sampled-Data Stabilization,” *IEEE Transactions on Automatic Control*, vol. 62, no. 11, pp. 5604–5619, 2017.
- [155] P. Pepe, G. Pola, and M. Di Benedetto, “On Lyapunov-Krasovskii characterizations of stability notions for discrete-time systems with unknown time-varying time-delays,” in *2016 IEEE 55th Conference on Decision and Control (CDC)*, 2016, pp. 447–452.
- [156] R. H. Gielen, M. Lazar, and S. V. Raković, “Necessary and sufficient Razumikhin-type conditions for stability of delay difference equations,” *IEEE Transactions on Automatic Control*, vol. 58, no. 10, pp. 2637–2642, 2013.
- [157] C. T. Baker, “Development and application of Halanay-type theory: Evolutionary differential and difference equations with time lag,” *Journal of computational and applied mathematics*, vol. 234, no. 9, pp. 2663–2682, 2010.
- [158] C. E. De Souza and D. Coutinho, *Local stabilization of Markov jump nonlinear quadratic systems*. IFAC, 2014, vol. 19, no. 3.

- [159] B. Liu and H. J. Marquez, “Razumikhin-type stability theorems for discrete delay systems,” *Automatica*, vol. 43, no. 7, pp. 1219–1225, 2007.
- [160] P. Pepe, G. Pola, and M. D. D. Benedetto, “On Lyapunov-Krasovskii Characterizations of Stability Notions for Discrete-Time Systems with Uncertain Time-Varying Time Delays,” *IEEE Transactions on Automatic Control*, vol. 63, no. 6, pp. 1603–1617, 2018.
- [161] “Bollobas modern graph theory,” 2021.
- [162] R. Diestel, “Graph theory,” 2013.
- [163] N. Athanasopoulos and M. Lazar, “Stability analysis of switched linear systems defined by graphs,” in *53rd IEEE Conference on Decision and Control*. IEEE, 2014, pp. 5451–5456.
- [164] V. B. Falchetto, M. Souza, A. R. Fioravanti, and R. N. Shorten, “ \mathcal{H}_2 and \mathcal{H}_∞ analysis and state feedback control design for discrete-time constrained switched linear systems,” *International Journal of Control*, vol. 94, no. 10, pp. 2834–2845, 2021. [Online]. Available: <https://doi.org/10.1080/00207179.2020.1737331>
- [165] M. Souza, A. R. Fioravanti, and R. N. Shorten, “On analysis and design of discrete-time constrained switched systems,” *International Journal of Control*, vol. 91, no. 2, pp. 437–452, 2018. [Online]. Available: <https://doi.org/10.1080/00207179.2017.1285053>
- [166] N. Athanasopoulos, K. Smpoukis, and R. M. Jungers, “Safety and invariance for constrained switching systems,” in *2016 IEEE 55th Conference on Decision and Control (CDC)*, 2016, pp. 6362–6367.
- [167] —, “Invariant sets analysis for constrained switching systems,” *IEEE Control Systems Letters*, vol. 1, no. 2, pp. 256–261, 2017.
- [168] A. Kundu and D. Chatterjee, “A graph theoretic approach to input-to-state stability of switched systems,” *European Journal of Control*, vol. 29, pp. 44–50, 2016.

- [169] P. Pepe, “Discrete-Time Systems with Constrained Time Delays and Delay-Dependent Lyapunov Functions,” *IEEE Transactions on Automatic Control*, vol. 65, no. 4, pp. 1724–1730, 2020.
- [170] M. T. Grifa and P. Pepe, “On stability analysis of discrete-time systems with constrained time-delays via nonlinear Halanay-type inequality,” *IEEE Control Systems Letters*, vol. 5, no. 3, pp. 869–874, 2020.
- [171] C. de Souza, V. J. Leite, L. F. Silva, and E. B. Castelan, “ISS robust stabilization of state-delayed discrete-time systems with bounded delay variation and saturating actuators,” *IEEE Transactions on Automatic Control*, vol. 64, no. 9, pp. 3913–3919, 2018.
- [172] J. Zhang, P. Shi, and W. Lin, “Extended sliding mode observer based control for Markovian jump linear systems with disturbances,” *Automatica*, vol. 70, pp. 140–147, 2016. [Online]. Available: <http://dx.doi.org/10.1016/j.automatica.2016.03.020>
- [173] A. Impicciatore, M. T. Grifa, P. Pepe, and A. D’Innocenzo, “Sufficient lyapunov conditions for exponential mean square stability of discrete-time systems with markovian delays,” in *2021 29th Mediterranean Conference on Control and Automation (MED)*, 2021, pp. 1305–1310.
- [174] A. N. Vargas, L. Acho, G. Pujol, E. F. Costa, J. Y. Hishihara, and J. B. R. do Val, “Output feedback of Markov jump linear systems with no mode observation: An automotive throttle application,” *Int. J. Robust Nonlinear Control*, vol. 26, pp. 1980–1993, 2016.
- [175] H. J. Chizeck, A. S. Willsky, and D. Castañón, “Discrete-time Markovian-jump linear quadratic optimal control,” *International Journal of Control*, vol. 43, no. 1, pp. 213–231, 1986.
- [176] Y. Mo, E. Garone, and B. Sinopoli, “LQG control with Markovian packet loss,” in *European Control Conference (ECC)*, 2013, pp. 2380–2385.
- [177] R. Bucy, R. Kalman, and I. Selin, “Comment on “The Kalman filter and nonlinear estimates of multivariate normal processes”,” *IEEE Transactions on Automatic Control*, vol. 10, no. 1, pp. 118–119, 1965.

- [178] A. De Santis, A. Germani, and C. Scoglio, “Kalman filter approach to solution of rational expectations models,” *Computers & Mathematics with Applications*, vol. 25, no. 12, pp. 39–47, 1993. [Online]. Available: <https://www.sciencedirect.com/science/article/pii/089812219390184W>
- [179] L. Shi, M. Epstein, and R. M. Murray, “Kalman Filtering Over a Packet-Dropping Network: A Probabilistic Perspective,” *IEEE Transactions on Automatic Control*, vol. 55, no. 3, pp. 594–604, 2010.
- [180] Y. Ji and H. J. Chizeck, “Jump linear quadratic Gaussian control : Steady-state solution and testable conditions,” 1990.
- [181] G. F. Franklin, M. L. Workman, and D. Powell, *Digital Control of Dynamic Systems*, 3rd ed. Addison-Wesley, 1997.
- [182] A. Ruberti and A. Isidori, *Teoria dei Sistemi*. Bollati Boringhieri, 1985.
- [183] V. De Iuliis, A. D’Innocenzo, A. Germani, and C. Manes, “Stability conditions for linear discrete-time switched systems in block companion form,” *IET Control Theory & Applications*, vol. 14, no. 19, pp. 3107–3115, 2020.
- [184] V. De Iuliis, A. D’Innocenzo, A. Germani, and C. Manes, “On the stability of discrete-time linear switched systems in block companion form,” *IFAC-PapersOnLine*, vol. 53, no. 2, pp. 2033–2038, 2020.
- [185] V. De Iuliis, C. Manes, and A. D’Innocenzo, “First-moment stability of Markov Jump Linear Systems with homogeneous and inhomogeneous transition probabilities,” in *2022 IEEE 61st Conference on Decision and Control (CDC)*. IEEE, 2022.
- [186] R. E. Megginson, *An Introduction to Banach Space Theory*, ser. Graduate Texts in Mathematics. Springer, 1998, vol. 183.
- [187] J. W. Brewer, “Kronecker products and matrix calculus in system theory,” *IEEE Trans. Circuits Syst.*, vol. 25, no. 9, pp. 772–781, 1978.
- [188] A. Ahlen, J. Akerberg, M. Eriksson, A. J. Isaksson, T. Iwaki, K. H. Johansson, S. Knorn, T. Lindh, and H. Sandberg, “Toward Wireless Control in Industrial

- Process Automation: A Case Study at a Paper Mill,” *IEEE Control Systems Magazine*, vol. 39, no. 5, pp. 36–57, 2019.
- [189] T. Iwaki, J. Wu, Y. Wu, H. Sandberg, and K. H. Johansson, “Multi-hop sensor network scheduling for optimal remote estimation,” *Automatica*, vol. 127, p. 109498, 2021. [Online]. Available: <https://www.sciencedirect.com/science/article/pii/S0005109821000182>
- [190] C. Iskander and P. Mathiopoulos, “Fast simulation of diversity Nakagami fading channels using finite-state Markov models,” *IEEE Transactions on Broadcasting*, vol. 49, no. 3, pp. 269–277, 2003.
- [191] Q. Zhang and S. Kassam, “Finite-state Markov model for Rayleigh fading channels,” *IEEE Transactions on Communications*, vol. 47, no. 11, pp. 1688–1692, 1999.
- [192] C. Pimentel, T. Falk, and L. Lisboa, “Finite-state Markov modeling of correlated Rician-fading channels,” *IEEE Transactions on Vehicular Technology*, vol. 53, no. 5, pp. 1491–1501, 2004.
- [193] C. E. Shannon, “Certain results in coding theory for noisy channels,” *Information and Control*, vol. 1, no. 1, pp. 6–25, 1957. [Online]. Available: <https://www.sciencedirect.com/science/article/pii/S0019995857900396>
- [194] D. Blackwell, L. Breiman, and A. J. Thomasian, “Proof of Shannon’s Transmission Theorem for Finite-State Indecomposable Channels,” *The Annals of Mathematical Statistics*, vol. 29, no. 4, pp. 1209 – 1220, 1958. [Online]. Available: <https://doi.org/10.1214/aoms/1177706452>
- [195] E. Gilbert, “Capacity of a Burst-Noise Channel,” *Bell System Technical Journal*, vol. 39, no. 5, p. 1253 – 1265, 1960.
- [196] E. O. Elliott, “Estimates of error rates for codes on burst-noise channels,” *The Bell System Technical Journal*, vol. 42, no. 5, pp. 1977–1997, 1963.
- [197] R. H. McCullough, “The binary regenerative channel,” *The Bell System Technical Journal*, vol. 47, no. 8, pp. 1713–1735, 1968.

- [198] B. Fritchman, “A binary channel characterization using partitioned Markov chains,” *IEEE Transactions on Information Theory*, vol. 13, no. 2, pp. 221–227, 1967.
- [199] R. Gallager, *Information Theory and Reliable Communication*. New York: Wiley, 1968.
- [200] J. G. Proakis, *Digital Communications*. New York: McGraw-Hill, 2000.
- [201] A. Goldsmith and P. Varaiya, “Capacity, mutual information, and coding for finite-state Markov channels,” *IEEE Transactions on Information Theory*, vol. 42, no. 3, pp. 868–886, 1996.
- [202] A. Semmar, M. Lecours, J.-Y. Chouinard, and J. Ahern, “Characterization of error sequences in UHF digital mobile radio channels,” *IEEE Transactions on Vehicular Technology*, vol. 40, no. 4, pp. 769–776, 1991.
- [203] B. Vucetic, “An adaptive coding scheme for time-varying channels,” *IEEE Transactions on Communications*, vol. 39, no. 5, pp. 653–663, 1991.
- [204] S. Sivaprakasam and K. Shanmugan, “An equivalent Markov model for burst errors in digital channels,” *IEEE Transactions on Communications*, vol. 43, no. 2/3/4, pp. 1347–1355, 1995.
- [205] L. R. Rabiner, “A Tutorial on Hidden Markov Models and Selected Applications in Speech Recognition,” *Proceedings of the IEEE*, vol. 77, no. 2, p. 257 – 286, 1989.
- [206] H. S. Wang and N. Moayeri, “Finite-State Markov Channel—A Useful Model for Radio Communication Channels,” *IEEE Transactions on Vehicular Technology*, vol. 44, no. 1, p. 163 – 171, 1995.
- [207] R. H. Clarke, “A statistical theory of mobile-radio reception,” *The Bell System Technical Journal*, vol. 47, no. 6, pp. 957–1000, 1968.
- [208] M. Mushkin and I. Bar-David, “Capacity and coding for the Gilbert-Elliott channels,” *IEEE Transactions on Information Theory*, vol. 35, no. 6, pp. 1277–1290, 1989.

- [209] M. Zorzi, R. Rao, and L. Milstein, “ARQ error control for fading mobile radio channels,” *IEEE Transactions on Vehicular Technology*, vol. 46, no. 2, pp. 445–455, 1997.
- [210] A. Chockalingam, M. Zorzi, L. Milstein, and P. Venkataram, “Performance of a wireless access protocol on correlated rayleigh-fading channels with capture,” *IEEE Transactions on Communications*, vol. 46, no. 5, pp. 644–655, 1998.
- [211] M. Chu, D. Goeckel, and W. Stark, “On the design of Markov models for fading channels,” in *Gateway to 21st Century Communications Village. VTC 1999-Fall. IEEE VTS 50th Vehicular Technology Conference (Cat. No.99CH36324)*, vol. 4, 1999, pp. 2372–2376 vol.4.
- [212] F. Babich, O. Kelly, and G. Lombardi, “Generalized Markov modeling for flat fading,” *IEEE Transactions on Communications*, vol. 48, no. 4, pp. 547–551, 2000.
- [213] H. Kong and E. Shwedyk, “Sequence detection and channel state estimation over finite state Markov channels,” *IEEE Transactions on Vehicular Technology*, vol. 48, no. 3, pp. 833–839, 1999.
- [214] C. Komminakis and R. Wesel, “Joint iterative channel estimation and decoding in flat correlated Rayleigh fading,” *IEEE Journal on Selected Areas in Communications*, vol. 19, no. 9, pp. 1706–1717, 2001.
- [215] S. Aberkane, “Stochastic stabilization of a class of nonhomogeneous Markovian jump linear systems,” *Systems & Control Letters*, vol. 60, no. 3, p. 156 – 160, 2011.
- [216] P. Bolzern, P. Colaneri, and G. De Nicolao, “Markov Jump Linear Systems with switching transition rates: Mean square stability with dwell-time,” *Automatica*, vol. 46, no. 6, pp. 1081–1088, 2010. [Online]. Available: <https://www.sciencedirect.com/science/article/pii/S0005109810001263>
- [217] N. Guglielmi, F. Wirth, and M. Zennaro, “Complex Polytope Extremality Results for Families of Matrices,” *SIAM Journal on Matrix Analysis and Applications*, vol. 27, no. 3, pp. 721–743, 2005.

- [218] R. M. Jungers, A. Cicone, and N. Guglielmi, “Lifted Polytope Methods for Computing the Joint Spectral Radius,” *SIAM Journal on Matrix Analysis and Applications*, vol. 35, no. 2, pp. 391–410, 2014.
- [219] M. Karan, P. Shi, and C. Y. Kaya, “Transition probability bounds for the stochastic stability robustness of continuous- and discrete-time markovian jump linear systems,” *Automatica*, vol. 42, no. 12, pp. 2159–2168, 2006. [Online]. Available: <https://www.sciencedirect.com/science/article/pii/S0005109806002810>
- [220] C. C. Lutz and D. J. Stilwell, “Stability and Disturbance Attenuation for Markov Jump Linear Systems with Time-Varying Transition Probabilities,” *IEEE Transactions on Automatic Control*, vol. 61, no. 5, pp. 1413–1418, 2016.
- [221] B. Ding, “Stabilization of linear systems over networks with bounded packet loss and its use in model predictive control,” *Automatica*, vol. 47, no. 11, pp. 2526–2533, 2011.
- [222] S. Boyd and L. Vandenberghe, *Convex optimization*. Cambridge University Press, 2004.
- [223] M. Z. Chen, L. Zhang, H. Su, and G. Chen, “Stabilizing solution and parameter dependence of modified algebraic Riccati equation with application to discrete-time network synchronization,” *IEEE Transactions on Automatic Control*, vol. 61, no. 1, pp. 228–233, 2016.
- [224] G. F. Franklin, J. D. Powell, and A. Emami-Naeini, *Feedback control of dynamic systems*, 6th ed. Prentice Hall, 2009.
- [225] Z. P. Jiang and Y. Wang, “A converse Lyapunov theorem for discrete-time systems with disturbances,” *Systems & Control Letters*, vol. 45, no. 1, pp. 49–58, 2002.
- [226] Z.-P. Jiang and Y. Wang, “Input-to-state stability for discrete-time nonlinear systems,” *Automatica*, vol. 37, no. 6, pp. 857–869, 2001.
- [227] Y. Lin, E. D. Sontag, and Y. Wang, “A smooth converse Lyapunov theorem for robust stability,” *SIAM Journal on Control and Optimization*, vol. 34, no. 1, pp. 124–160, 1996.

- [228] L. Zhou, H. Ding, and X. Xiao, “Input-to-state stability of discrete-time switched nonlinear systems with generalized switching signals,” *Applied Mathematics and Computation*, vol. 392, no. 201908320096, p. 125727, 2021. [Online]. Available: <https://doi.org/10.1016/j.amc.2020.125727>
- [229] W. H. Young, “On classes of summable functions and their fourier series,” *Proceedings of the Royal Society of London. Series A, Containing Papers of a Mathematical and Physical Character*, vol. 87, no. 594, pp. 225–229, 1912.
- [230] C. S. Kubrusly, *Elements of operator theory*. Birkhäuser, 2001.
- [231] R. A. Horn and C. R. Johnson, *Matrix analysis*, 2nd ed. CUP, 2012.
- [232] A. W. Naylor and G. R. Sell, *Linear operator theory in engineering and science*, ser. Appl. Math. Sci. Springer, 2000, vol. 40.
- [233] Joachim Weidmann and Joseph Szücs, *Linear Operators in Hilbert Spaces*. Springer-Verlag, 1980.
- [234] I. Karafyllis, P. Pepe, and Z. P. Jiang, “Input-to-output stability for systems described by retarded functional differential equations,” *European Journal of Control*, vol. 14, no. 6, pp. 539–555, 2008.